TECTONIC GEOMORPHOLOGY AND PALEOSEISMICITY OF THE NORTHERN ESK FAULT, NORTH CANTERBURY, NEW ZEALAND

A thesis submitted in partial fulfilment of

the requirements for the degree of

Master of Science in Geology

at the

University of Canterbury

by

Duncan Paul Noble

University of Canterbury

2011

ABSTRACT

Geomorphic, structural and chronological data are used to establish the late Quaternary paleoseismicity of the active dextral-oblique Northern Esk Fault in North Canterbury, New Zealand.

Detailed field mapping of the preserved c. 35 km of surface traces between the Hurunui River and Ashley Head reveals variations in strike ranging from 005° to 057°. Along with kinematic data collected from fault plane striae and offset geomorphic markers along the length of the fault these variations are used to distinguish six structural subsections of the main trace, four dextral-reverse and two dextral-normal.

Displacements of geomorphic markers such as minor streams and ridges are measured using differential GPS and rangefinder equipment to reveal lateral offsets ranging from 3.4 to 23.7 m and vertical offsets ranging from < 1 to 13.5 m. Characteristic single event displacements of c. 5 m and c. 2 m have been calculated for strike-slip and reverse sections respectively. The use of fault scaling relationships reveals an anomalously high displacement to surface rupture length ratio when compared to global data sets. Fault scaling relationships based on width limited ruptures and magnitude probabilities from point measurements of displacement imply earthquake magnitudes of M_w 7.0 to 7.5.

Optically Stimulated Luminescence (OSL) ages from displaced Holocene alluvial terraces at the northern extent of the active trace along with OSL and radiocarbon samples of the central sections constrain the timing of the last two surface rupturing events (11.15 ±1.65 and 3.5 ± 2.8 ka) and suggest a recurrence interval of c. 5612 ± 445 years and late Quaternary reverse and dextral slip rates of c. 0.31 mm/yr and 0.82 mm/yr respectively.

The results of this study show that the Northern Esk Fault accommodates an important component of the c. 0.7 – 2 mm/yr of unresolved strain across the plate boundary within the North Canterbury region and affirm the Esk Fault as a source of potentially damaging ground shaking in the Canterbury region.

TABLE OF CONTENTS

LIST OF FIGURES

Chapter 1

Chapter 2

Chapter 3

Chapter 4

Attached Map

LIST OF TABLES

Chapter 2

Chapter 4

CHAPTER 1
INTRODUCTION

1.1 BACKGROUND AND RELEVENCE OF STUDY

New Zealand's position within a plate boundary setting and the relatively short historical records of permanent strain on structures accommodating plate boundary motion have made geomorphic and paleoseismic studies a vital part of active tectonic and hazard research in New Zealand. Fault specific studies are important for recognising and quantifying hazards associated with these structures and modelling the style of deformation occurring across the plate boundary.

Constraints on the timing and scale of pre historic surface rupturing events have been useful in estimating slip rates, recurrence intervals, coseismic displacements and magnitudes for many of the large strike-slip faults accommodating slip through the upper South Island and the Southern Alps (e.g. Benson et al. (2001), Howard (2005), Langridge & Berryman (2005), Van Dissen & Nicol (2009)). As a result of studies such as these the distribution and style of strain across the plate boundary in the South Island is generally well constrained for the major strike slip faults in the area but little is known about the nature of the numerous smaller or less active faults that lie between the more significant block boundaries (Wallace et al. (2007, In review). North Canterbury in particular is identified by Wallace et al. (2007, In review) as an area in which some strain must be accommodated on as yet unstudied structures. Active faults in the area such as the Esk, Waitohi and Poulter Faults are likely to account for much of the strain currently missing from the geologic data. As a part of this wider zone of deformation associated with the New Zealand plate boundary, the Northern Esk Fault provides an opportunity to quantify the style and scale of deformation outside of the major structures of the Marlborough and Porters Pass-Amberley fault zones. Knowledge

gained from the study of a relatively structurally immature fault system will improve our understanding of young fault segmentation and linkage, interactions between faults and topography and the distribution of strain across the plate margin.

Several studies have estimated the Esk Fault's recurrence interval for the purpose of assessing the potential for damaging earthquakes in Canterbury (e.g. (Pettinga 2001), (Van Dissen et al. 2003), (Stirling et al. 2008)). To date, all attempts to quantify slip rates, recurrence intervals or magnitude for the Esk Fault have come from the use of fault-scaling relationships or from direct comparisons with superficially similar but better studied faults. A paleoseismic and geomorphic study of the Esk Fault will provide insight into the temporal distribution and physical characteristics of late Quaternary ruptures in an area where relatively little quantitative data is currently available.

Due to the proximity of the Esk Fault to towns and cities along the South Islands east coast and northern high country, including the city of Christchurch (population c. 400,000) which lies c. 60 km to the south-east, a direct study of the Esk Fault is an important step in assessing the hazard posed by fault rupture and the temporal and kinematic variability of Esk Fault earthquakes.

1.2 AIMS AND METHODOLOGY

As outlined above, the principle aims of this study are to build an understanding of the characteristic behaviour of the Northern Esk Fault (NEF) during the late Quaternary and to use this information to better understand fault behaviour in North Canterbury. Outcomes will include a revised understanding of the hazards associated with the NEF and the structure's role in accommodating regional strain. The methods used to undertake these tasks are

outlined below. Additional detail on the methods used is provided throughout the rest of the thesis.

Research methods used in this study include:

1. Analysis of aerial photographs and subsequent detailed field mapping of tectonic geomorphological features within the study area to locate active fault traces and related surface features.

2. Examination and measurement of fault plane exposures as well as laterally and vertically offset features such as stream banks, ridges, terrace surfaces and hill slopes along the length of the fault to determine single event and cumulative displacements. Displacements and separations were measured using a combination of differential Global Positioning System (GPS) data, hand-held laser rangefinder and tape measures.

3. Dating of displaced terrace surfaces using Optically Stimulated Luminescence (OSL) to constrain the timing of the most recent surface rupturing events and to calculate average slip rates and recurrence interval over the last c. 30,000 years.

4. Radiocarbon (^{14}C) dating of charcoal samples within and overlaying a coseismic colluvial deposit to further constrain the timing of the most recent surface rupture.

5. A seismic reflection survey along the Waitohi Valley to investigate a possible connection between eastern and western sections beneath the relatively young and unfaulted terraces.

6. Analysis and interpretation of geomorphic, kinematic and chronologic data to determine slip rates, recurrence intervals, average single event displacements and magnitudes of previous surface rupturing earthquakes.

7. Use of new data and interpretations to update the likely seismic hazard posed by the Esk Fault for the Canterbury region.

1.3 GEOLOGICAL SETTING

1.3.1 PLATE BOUNDARY TECTONICS

The Southern Alps owe their existence to their position straddling the boundary between the Australian and Pacific plates. As a result, the South Island experiences a relatively high rate of strain and deformation associated with the oblique convergence between these two plates.

Convergence rates are highest to the north where the Pacific Plate is subducted beneath the overriding Australian Plate along the North Islands east coast and Northernmost South Island (Figure 1.1). Further south, through the central South Island the plates converge obliquely at c. 39 mm yr^{-1} (DeMets et al. 1990; DeMets et al. 1994) and the majority of the plate motion is transferred from the subduction interface through the Marlborough Fault System (MFS), a series of east-north-east west-south-west striking dextral strike-slip faults, to the Alpine Fault, which accommodates 70 - 75% of the plate boundary deformation (Norris & Cooper 2001; Sutherland et al. 2006) (Figure 1.1). The MFS consists of four major faults, the Wairau, Awatere, Clarence and Hope Faults, each splaying from the Alpine Fault and striking sub-parallel to the plate motion vector. The Hope Fault, the southernmost and most active component of the MFS marks a strain partitioning boundary between laterally dominated oblique-dextral faulting in the MFS and what are believed to be predominantly thrust-

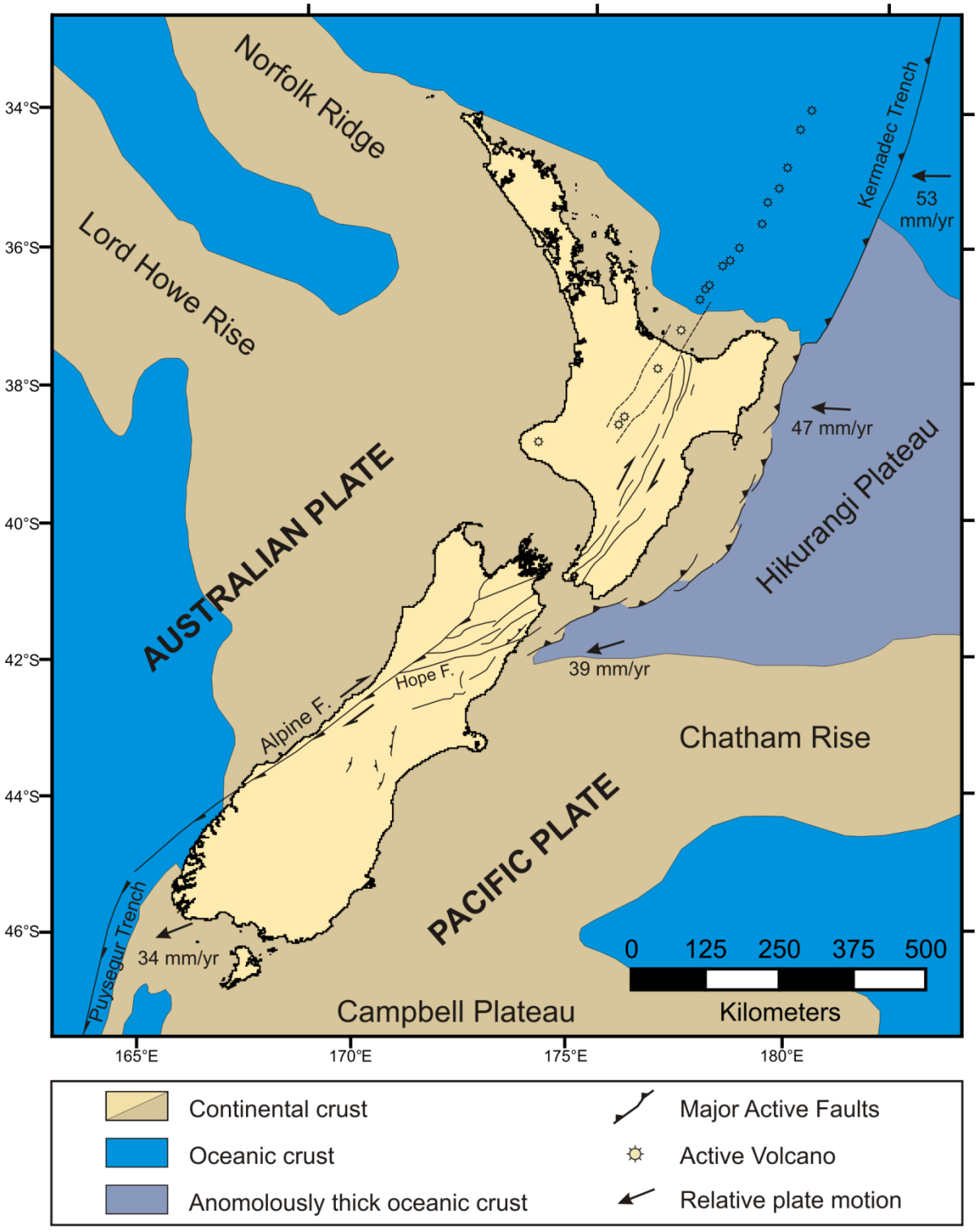

Figure 1.1. Map of the tectonic setting of New Zealand with major active structural features. (F): fault. Relative plate motions from De Mets et al. (1990, 1994). Modified from Pettinga et al. (1998)

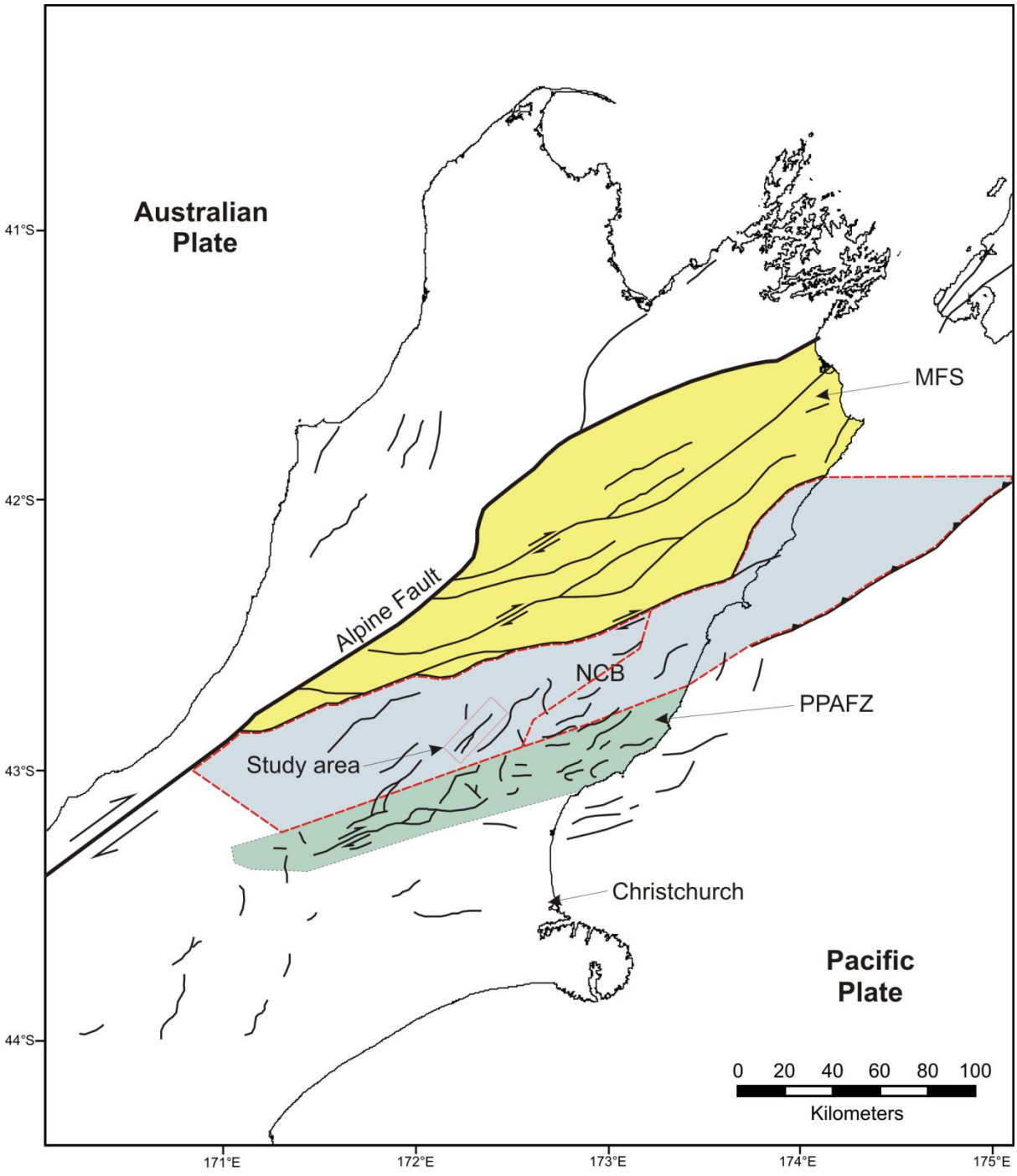

Figure 1.2. Map of the central and northern South Island showing the location of the MFS (yellow), PPAFZ (green) and the North Canterbury Block (grey) of Wallace et al. (2007 and In review).The red dashed line divides the North Canterbury block into that used by Wallace et al (2007) (entire grey area) and that used by Wallace et al. (In review) (south-western portion). Active faults in and around Canterbury are shown in black and the NEF study area is shown in red.

dominated structures to the south and west, through North Canterbury (Eusden et al. 2000; Pettinga 2001). Further to the south lies the Porters Pass – Amberley Fault Zone (PPAFZ) a series of dominantly strike-slip fault segments extending from the Canterbury foothills up towards Amberley and Waipara in the northeast (Figure 1.2). The PPAFZ is relatively young structure and although it does not yet have a direct link to the Alpine Fault it is considered to be the latest addition to the major plate boundary-defining faults linking the Alpine fault to the Hikurangi subduction zone in the north (Cowan 1992). This process is part of the southward migration of the MFS (Furlong & Kamp 2009).

It is between the major strike-slip structures of the MFS and PPAFZ that the NEF field area is found (Figure 1.2). The numerous NE-trending fault segments between the PPAFZ in the south and the Hope Fault to the north have been termed a "thrust wedge" by Pettinga et al. (2001) and interpreted as a series of back-thrusts off the Alpine Fault Zone to the west. The major active faults within the area, including the Esk Fault, are thought to mark the range-front of a narrower plate boundary zone during the Early Pleistocene. Subsequently the range front has continued to step out to the east, towards the coast with further folding and thrust faulting associated with the Hikurangi Subduction Zone occurring offshore.

1.3.2 GEOLOGY OF NORTH CANTERBURY

The geology of the North Canterbury region is dominated by Mesozoic greywacke of the Torlesse Supergroup. Throughout the western Hurunui area where this study was conducted, the Torlesse consists of thick, poorly bedded sandstone, mudstone, broken formation and Melange. Included within the Torlesse is the Esk Head Belt, first described by Bradshaw (1973), the Esk Head Belt is a southeast trending zone of deformed sandstone and mudstone with blocks of red and green mudstone, limestone and basalt commonly as broken formation or melange (Rattenbury et al. 2006).

Between the northeast trending folds and faults lie several basins containing remnants of Cretaceous-Tertiary cover sequence, often capped by extensive Quaternary fluvial deposits (Mould 1992). The largest of these, the Culverden Basin lies directly east of the field area and is bound on the east and west by east-dipping and west-dipping faults respectively. The trend of these basins and their bounding faults outline the general structure of the active components of the North Canterbury Region. As no remnants of Tertiary cover are found within the study area they are not discussed further.

1.4 PREVIOUS WORK

Geological surveys of the North Canterbury region date back to the 1860's (Buchanan 1868) and structural work was carried out in and around the Culverden and Waikari Basins by Speight (1918), Gregg (1964) and Mason (1949). Few studies relating to active deformation in the Hurunui region, south of the hope fault were conducted until Powers' (1962) study of warped terraces in the Hurunui River Valley. Powers (1962) gave no indication of the subtle warping and faulting of the Sheep Yard Basin terraces described in this thesis but attempted to put an approximate age on the surfaces by relating them to the Sisters Stream, Lake Sumner and Three Trees Moraines up stream.

Bradshaw (1972) included the Esk Fault as a late stage structure where it crosses Mt Noble (Therein called the Mt Noble Fault) but did not recognise the faulting of Hurunui River Terraces, instead terminating the fault at Lake Sumner Road. Bradshaw's (1972) mapping also included structural fabric in the Northern Waitohi Valley and descriptions of lithologies in the local Torlesse Bedrock as well as large scale mapping of other northeast-southwest trending faults to the west of Culverden Basin.

Botsford's (1983) thesis on the Esk Head Melange includes the Esk fault in the southern Waitohi Valley and also references several active fault exposures in and around the Okuku River. Nicol (1991) defined structural styles and kinematics of the Waipara region in his PhD Thesis but did not work as far north as the Culverden Basin.

Cowan (1992) worked on the structure and tectonics of the Porters Pass – Amberley Fault Zone to the southeast of the Esk Fault but included the NEF field area in his 1990 microearthquake survey to define the kinematics of crustal deformation in North Canterbury.

The most detailed structural and kinematic work in the region to date is that of Mould (1992) on the western margin of the Culverden Basin. His thesis provides insight into the style of deformation occurring to the east of the Esk Fault as well as data on the local strain axes and maximum rates of deformation inferred from weathering rind dating of terrace surfaces.

Pettinga et al. (2001) reviewed work relating to active faulting in Canterbury with limited additional fieldwork and aerial photograph interpretations. They note that the Esk Fault has not been studied in detail and its exact extent and location are not well defined.

The most detailed mapping of the Northern Esk Fault prior to this study was that conducted by Rattenbury et al. (2006). Their mapping, conducted both in the field and from aerial photography, projects the NEF through the Waitohi Valley and across the Hurunui River terraces. They also include structural fabric of the basement rock throughout the field area.

1.5 LOCATION AND CHARACTERISTICS OF STUDY AREA

The NEF study area lies just north of the Waimakariri – Hurunui district boundary in North Canterbury (Figure 1.2). The majority of field work was conducted in the Waitohi and

Figure1.3. Location of study area and surrounding structures. Red lines indicate active faults. NEF = Northern Esk Fault, WDF = Waitohi Downs Fault, LVF = Lees Valley Fault, MAF = Mount Arden Fault. Base map is from the Topo250 series Murchison map sheet in the area of Topo50 maps BV22-24. Active fault data from Mould (1992), GNS Active Faults Database (http://maps.gns.cri.nz/website/af/viewer.htm), Rattenbury et al. (2006) and this study.


Study Area
PUKETERAKI RANGE
PANCAKE RANGE
OKUKU RANGE
DAMPIER RANGE
RANGE
THE HOOLIGAN
NEF
WDF
LVF
MAF
Lake Taylor
Hurunui River
South Branch
North Esk River
Esk River
Crossley Stm
Kennedy Stm
Homestead Stm
Sisters Stm
Cherry Tree Hill
Rough Stm
Dozy Stm
Devils Creek
Robyns
Ben Cliberack
Mt Miza
Mt Roderick
Dampier Knob
Beau Saddle
Mt Catherine
Jacks Saddle
Jacks Stm
Mt Selfe
Coppers Knob
Waitohi Downs
Waitohi Peaks
Hurunui Peak
Green Hill
The Peaks
Balmoral
Waitohi River
Medbury
Horsley Down
Washpen Stream
Mt Oval
Mt Noble
Mt Mason
Esk Head
Woolshed Stm
Valley Stm
Bridge Stm
Trumper Stm
Anderson Stm
Fossil Stm
Fooks Stream
Lucy Stream
Crossley Stm
Ant Stream
Anna Stream
Grant Stream
Pig Spur Stream
Virginia Peak
Virginia
Mt Meehan
Haydon Downs
Waipara R North Br
Bridge Ck
Waitohi River
Mt Whatno
Madrid Hill
Gola Peak
Block Hill
Little Den
The Brothers
Cabin Stm
Parkhill
Mt Hilton
Mallockvale
Mount Hilton
Mt Lance
Tommys Stm
Manilla Stream
Waipara R Middle Br
Mt Arden
Blue Mountain
Lees Pass
Punanui Stream
Waipara River South Br
Mt MacDonald
Pyramid Valley
Mason Flat
Hawarden
Waikari
Timpendean
Weka Pass
Weka Creek
North Dean
South Dean
Waipara River
Waipara
Mt Brown
Silver Stm
Castle
Mt Dor
Okuku Saddle
Okuku River
Okuku Hill
Retreat Hill
Okuku R South Br
Mt Karetu
Mt Grey / Maukatere
Grey River
Duck Creek
Broom Stm
Island Hill
Kingsdown
Whistler River
Lilburne River
Ashley R / Rakahuri
Pancake Stream
Spring Hill
Lilburne Hill
Puketeraki
Mt Pember
Burn
Hut
Study Area
0
10
Kilometres

Hurunui valleys with access being via Virginia and Lake Sumner Roads respectively (Figure 1.3).

The topography of the region generally increases in height and relief to the west with the ranges bounding the Waitohi Valley being the first significant step up to over 1200 m from elevations of 400 – 800 m to the west of Culverden Basin. Further west the Puketeraki Range regularly reaches heights in excess of 1700 m (Figure 1.3).

The slopes within the Waitohi Valley are generally quite steep but vegetated, unlike the western slopes of the Mt Noble range which are exposed to the prevailing westerly winds and in places are bare scree slopes. The study area within the Hurunui Valley covers a wide basin of abandoned Quaternary gravels between Maori Gorge to the west and narrow, steep-sided river valley to the east.

The majority of the land within the study area is used for year-round sheep and cattle grazing though pockets of beach forest and other native bush are scattered across the slopes. Dense native bush including Matagouri makes access to some higher areas slow and difficult.

The locations of figures throughout the thesis are shown in Figure 1.4.

1.6 THESIS ORGANISATION

Chapter 1 gives the background to the study and a brief outline of the aims, expected outcomes and the methods used. The study area is introduced and described in the context of the wider tectonic setting and previous structural and geomorphic studies in the area are briefly reviewed.

Chapter 2 describes the geometry and geomorphic expression of fault traces in the study area as well as dividing the NEF into sections based on changes in along-strike surface expression. Additional faults within a few kilometres of the study area are briefly described.

In Chapter 3 measurements of lateral and vertical displacements along the fault are presented and analysed to characterise single event displacements. Principle strain axes are derived from kinematic data on the NEF and compared with regional seismological data and the results of previous studies in North Canterbury. The structure of the NEF and possible rupture segments are explored.

Chapter 4 presents the results of paleoseismic work conducted on the NEF to constrain the timing of prehistoric surface rupturing events and calculate late Quaternary slip rates and recurrence intervals. Magnitudes of paleoearthquakes are also estimated from fault scaling relationships. The hazard associated with the NEF is reviewed in terms of recurrence intervals and the likely timeframe of future events.

Chapter 5 summarises the findings of all aspect of the study and the conclusions draw in each chapter.

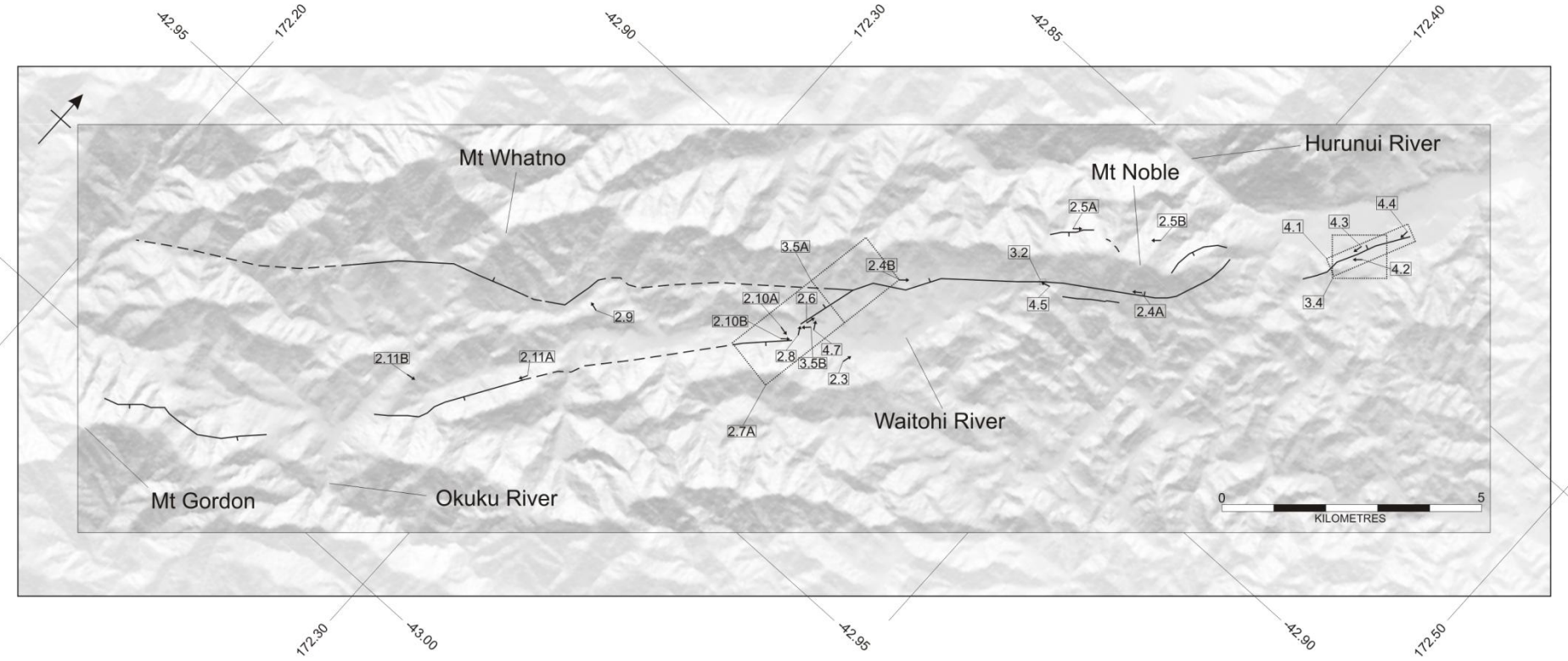

Figure 1.4. Map of the NEF (black) with the locations of figures presented throughout the thesis. Dashed boxes show mapped areas.

CHAPTER 2
SURFACE RUPTURE GEOMETRY AND GEOMORPHOLOGY

2.1. OVERVIEW

The northern segment of the Esk Fault consists of a series of fault sections stretching across c. 25 km of steep farmland and river valleys in the North Canterbury High Country. On average, the surface trace strikes at c. 045° but varies between 005° and 057°. Where exposed along the northern and central sections, the fault dips at approximately 45° to the west but in the far north dips as shallowly as 32°.

Detailed field mapping reveals significant changes in fault strike, dip and dip direction at several locations along the fault. These changes are, in many places, coincident with changes in the slope and height of the adjacent hillsides and the position of topographic highs relative to the surface trace.

Based on changes in the sense of slip and style of deformation associated with surface rupture, the NEF is divided into a series of distinct structural sections (Figure 2.1) that are outlined below. These sections, in turn, are grouped into the east-dipping sections and west-dipping sections, divided by the Waitohi River.

2.2. WESTERN FAULT SECTIONS

2.2.1. HURUNUI RIVER SECTION

The Hurunui River Section is the northernmost extent of the preserved scarps. This 2 km long dextral-reverse section strikes at c. 027° across a 100 m thick sequence of Holocene alluvial terraces of the Hurunui River. Discernable surface deformation is limited to vertical

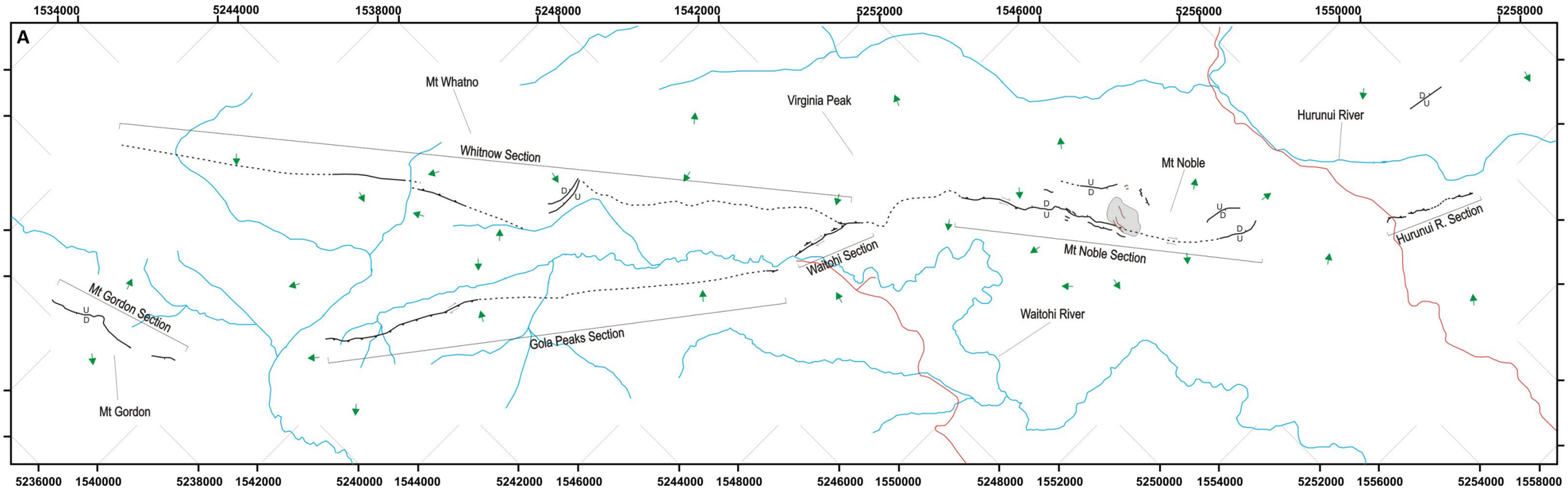

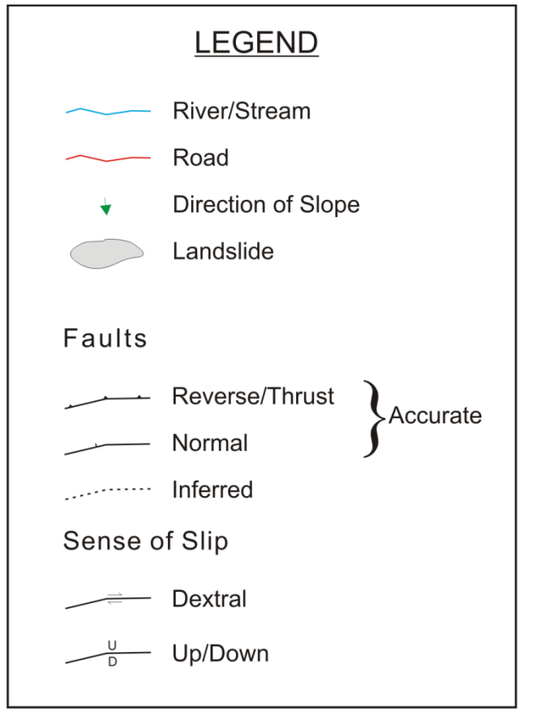

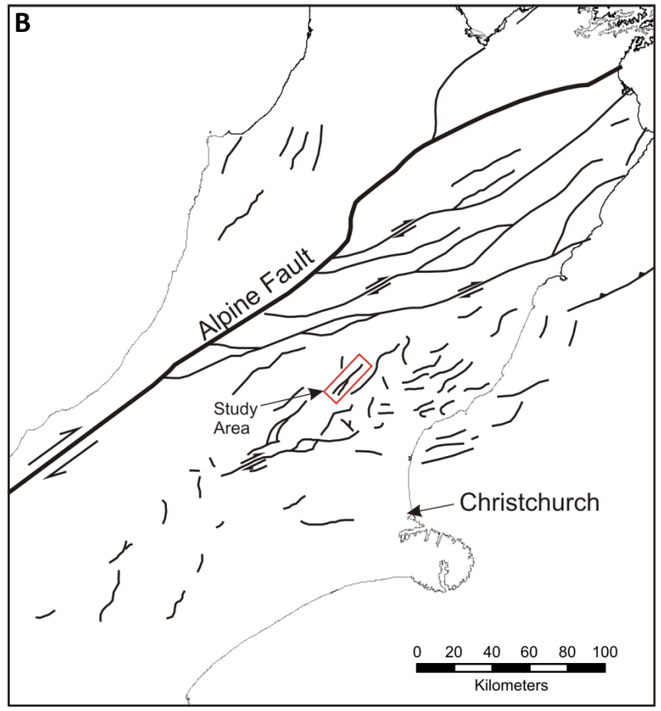

0 1 2 4 6 8 10
Kilometers

Figure 2.1. A) Simplified map of the study area showing mapped and inferred fault traces. The Fault is divided into six sections based on changes in strike, dip and sense of movement. See Attached Map for detailed geological map. B) location of study area and significant faults in North Canterbury. Coordinates are in NZTM.

separation of the terrace surfaces across a narrow fault zone (c. 5 – 10 m wide) with very little off-fault folding or tilting of the wider terrace surface other than at the very northern end, where vertical separation diminishes into a gentle anticline in the hanging wall before disappearing completely to the north (see Figure 4.1). With a single c. 700 m long uphill-facing scarp on Mt Miza being the only active surface deformation mapped within 8 km of the section tip (Figure 1.3), the northern extent of the Hurunui River Section is interpreted to represent the northern termination of typical late Quaternary surface ruptures along the NEF (see Section 3.5).

The fault scarp is most prominent on the higher terraces to the south where scarp height peaks at c. 4m (Figure 2.2A). 120 m to the north, on terrace T5 (Figure 2.2A), the vertical separation varies little and averages 2.1 m along its 400 m length. Further north, along terrace T6, the separation decreases along the 300 m long section, from c. 2 m to 0 m where the active trace terminates.

Dextral displacement is apparent at the T3-T4 terrace riser but the errors caused by the rounding of riser edges due to weathering, cattle movement and the formation and use of a farm track along the scarp mean that it is challenging to interpret. Dextral displacement of the T2-T3 riser is complicated by a bend in the trend of the trace at this point from 057° in the south to 026° in the north and by the shallow angle at which the fault intersects the terrace riser, producing errors of ±75%. No other preserved lateral displacements have been observed on the Hurunui River Section.

A jog in the surface trace across a steep terrace riser between T3 and T5 can be used to calculate a near surface dip for the Hurunui River Section of 28 to 36° W.

Figure 2.2. A) View of the higher Hurunui River terraces showing vertical separations of terraces treads T2 and T5 across the NEF. Fault trace marked by arrows and dotted line. The location of Photo B is marked on the lower faulted terrace. B) Looking north along the c. 2 m fault scarp on T5. Evidence of Ponding drainage is seen on the downthrown side of the sinuous scarp. Very little deformation is apparent outside of the 5 to 10 m wide fault scarp.


T6
B
T5
T3
T2

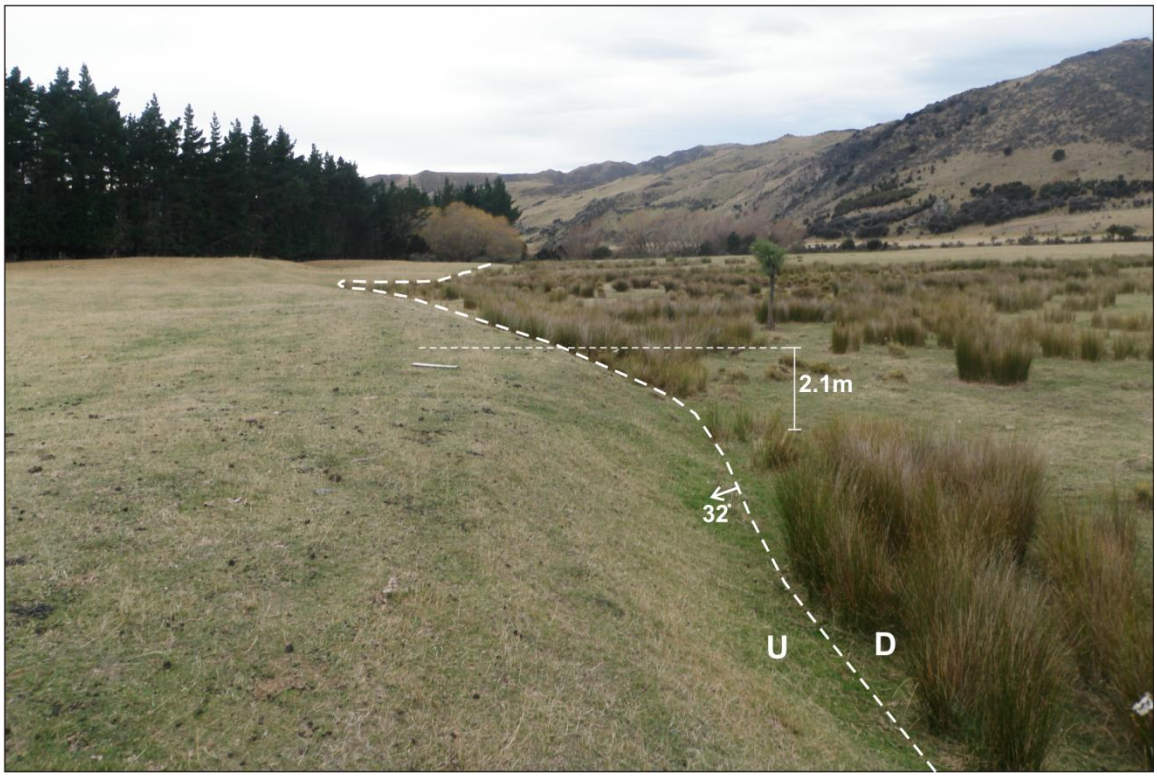
2.1m
32
U
D

2.2.2. MOUNT NOBLE SECTION

The Mt Noble Section is the most prominent section of the Northern Esk Fault. It stretches for 5.7 km from the north-eastern face of Mt Noble to the northern edge of Virginia Peak in the south. For most of its length this section is a normal scarp forming a broad bench or uphill-facing scarp. The trace ranges in elevation from over 1000 m in the north to less than 700 m in the south (Figure 2.3).

The mapped trace is almost uninterrupted for the entire length of the section apart from a 1.5 km gap through Big Bush Forest where it is obscured from view in aerial photographs and inaccessible on the ground (see Figure 1.3 for location). The trace is visible just south of the forest but does not appear again until the wide bench resumes 700 m north of the northern edge of the forest.

South of Big Bush Forest the scarp is at its most prominent with up to 16 m horizontal separation of the hillside, normal to the slope direction. For much of the length of the scarp additional smaller normal scarps can be seen above and below the main trace. These traces are up to 500 m long and preserve lateral offsets of up to 10 m (see Figure 2.1). Towards the southern end of the section the deformation becomes progressively more dispersed with many discontinuous traces making up a >30 m wide zone of diffuse uphill-facing scarps and eventually merging to a subtle, broad change in slope. At the southern-most extent of the preserved scarp the vertical component appears to be up to the west for c. 500m, implying a switch from the dextral-normal faulting in the north to dextral-reverse faulting in the south before the scarp dies out completely (Figure 2.4B).

Along the length of the section, dextrally offset streams, stream banks and ridges are common and range in lateral displacement from c. 4 to 24 m (see Section 3.3). Approximately 3.6 km

Figure 2.3. View of the southern Mt Noble Section looking northwest from the Waitohi Valley. Arrows mark the visible extent of the fault trace. The Mt Noble landslide is outlined in white. Locations A and B refer to parts A and B of Figure 2.4.

Figure 2.4. A) View looking southwest along the dextral-normal Mt Noble Section (arrows). B) View looking northeast along the Mt Noble Section. Arrows mark the visible extent of the fault trace. Notice the change in fault morphology from west side up in the foreground to east side up at the northern end of the scarp. Normal displacement increases with increasing elevation of the ridgeline to the north. See figure 2.3 for photo locations.


A


B

Figure 2.5. A) A small uphill-facing scarp on the western slope of Mt Noble. Soil and vegetation accumulated in the trench have been undercut by the scree slope below leaving a line of over-hanging soil and roots. B) A series of overlapping normal scarps on the western slope of Mt Noble viewed from the north. The scarp on the left crosses the main ridge to the left of view. See Figure 1.4 for locations.


A
U
D


B

from the northern end of the section a natural exposure of the fault plane reveals a dip of 45° west (see Section 4.2.2.). This dip is used to calculate vertical separations of the hill slope where normal faulting is apparent. Calculated vertical separations range from c. 2.5 m to 5.7 m (see Section 3.3).

Where the main trace crosses the highest and steepest eastern slopes of Mt Noble, opposing uphill-facing scarps can often be found on the western slopes (Figure 2.5). These scarps preserve much less vertical displacement than their eastern counterparts and have no obvious lateral offsets across them. The most prominent of these western scarps protrudes up to 3 m out from the hillslope and is almost 1 km long. In places there are multiple, overlapping scarps like those on the eastern face and step-overs are common between short (<100m) sections. Occasionally the scarps are defined only by a line of vegetation and soil which has been undercut by lower scree slopes eroding the foot wall (Figure 2.5A). Further scarps are also found cutting across the main ridge to the north of the highest peak (Figure 2.5B). Like all other scarps on Mt Noble the displacement is normal with the uphill side downthrown.

Another significant geomorphologic feature of Mt Noble is the Mt Noble landslide. The landslide consists of a c. 250,000 square metre area to the east of the highest peak that has slumped, largely intact, more than 60 m down towards the south-east (Figures 2.1, 2.3 and Attached Map). Rents are common near the toe of the landslide where it crosses and obscures the active main trace and the upper surface forms a very broad, flat area below the summit of Mt Noble. The landslide is not cut by the Esk Fault and therefore must either be coseismic or post-date the most recent surface rupture.

2.2.3. WAITOHI SECTION

The Waitohi Section is a dextral-reverse scarp extending over 1.6 km from Virginia Peak to the western bank of the Waitohi River. The northern limit of this section is visible in the field

as a broad rise on the eastern slope of Virginia Peak. Several subtle, discontinuous benches extend northwards, high on Virginia Peak towards the Mt Noble section and are highlighted by increased vegetation growth where water emerges from the fault zone as is common along the Mt Noble section. Individual rents between the two sections are no longer than a few tens of metres.

Where the surface trace is defined by a continuous reverse scarp trending at 012°, the morphology of the scarp is in places suggestive of a pressure ridge over a listric fault producing a relatively high apparent separation (Kelson et al. 2001) (Figure 2.6A and B), while elsewhere the scarp crest is level with the surface of the hanging wall, suggesting a simple hanging wall collapse scarp (Figure 2.6A and C). A road cutting through the scarp at the southern end reveals tensional cracks in the crest of the scarp related to the collapse of the overhanging fault plane soon after formation. These short wavelength variations in near surface structural style and scarp morphology are consistent with features observed from historic surface ruptures on other reverse faults (e.g. the 1999 Chi-Chi earthquake (Kelson et al. 2001) and 1988 Armenian earthquake (Philip et al. 1992)).

Scarp height generally increases towards the south but fluctuates depending on the aspect and steepness of the hillslope it crosses. Where the fault trends straight up a hill side, on the south-facing slopes, the scarp is better preserved and the vertical separation of the hillslope averages from 2.3m at the northern end to 3.8 m in the south (Figure 2.7B and C). On the northern slopes the scarp trends obliquely across the hill sides leading to the collapse of the unsupported hanging-wall down-slope and a lower, more diffuse scarp (Figure 2.7B and E). This process limits the use of hillslope separation in quantifying the amount of dextral displacement along this section as the expected increase in preserved scarp height on northern faces is diminished by the increased rate of erosion. Two of the larger southern hillslopes

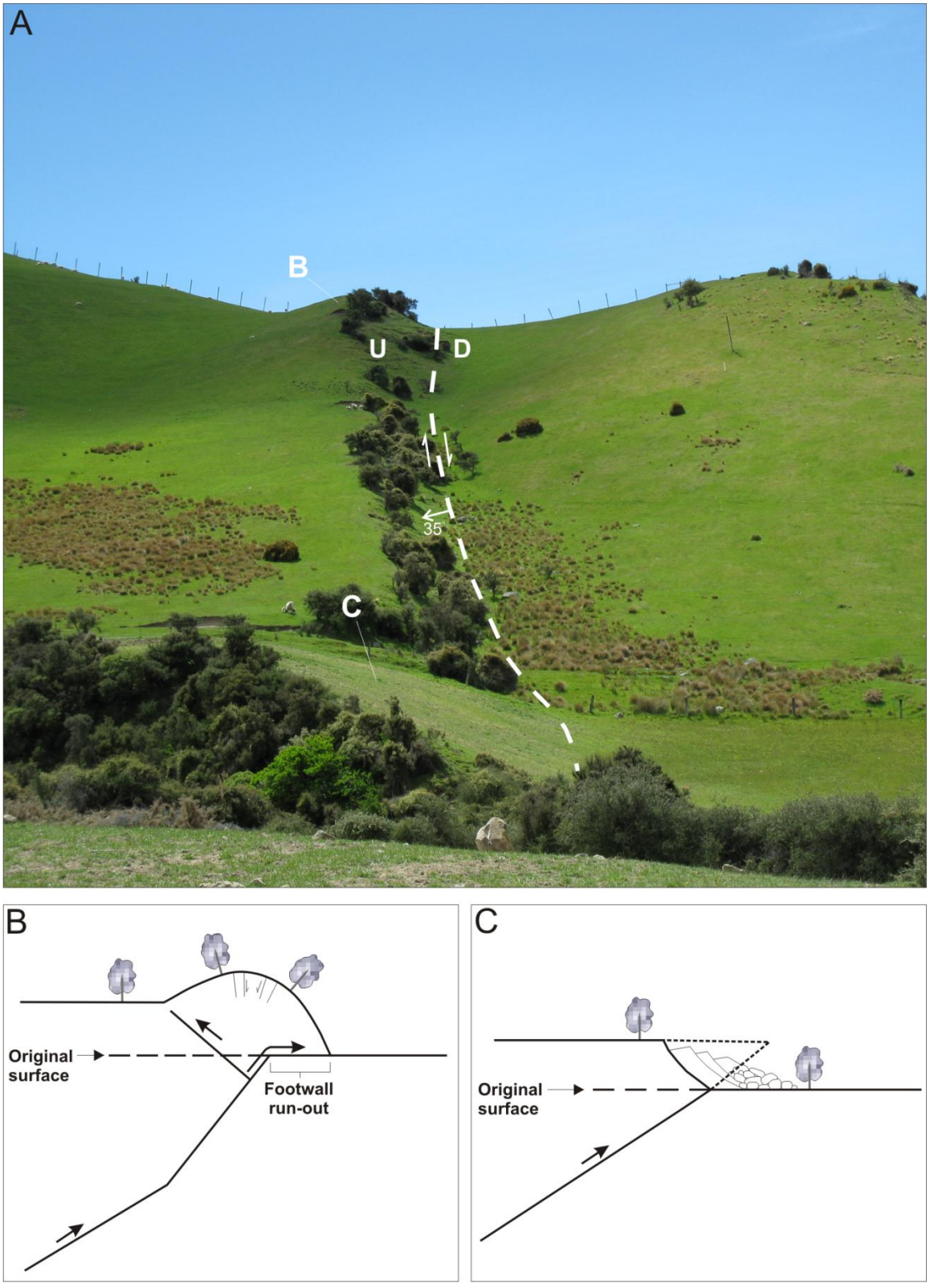

Figure 2.6. A) A prominent reverse scarp over a west dipping fault on the Waitohi section displaces a bedrock hill slope and terrace surface. Pressure ridging is apparent at the top of the hill while the displaced terrace tread is not discernibly tilted or folded. Vertical separation of the terrace tread is c. 9.5 m. Labels B and C refer to diagrams B and C. B) The development of a pressure ridge over a listric fault. C) A simple hangingwall collapse scarp. Photo by Mark Quigley. Diagrams modified from Kelson et al. (2001)

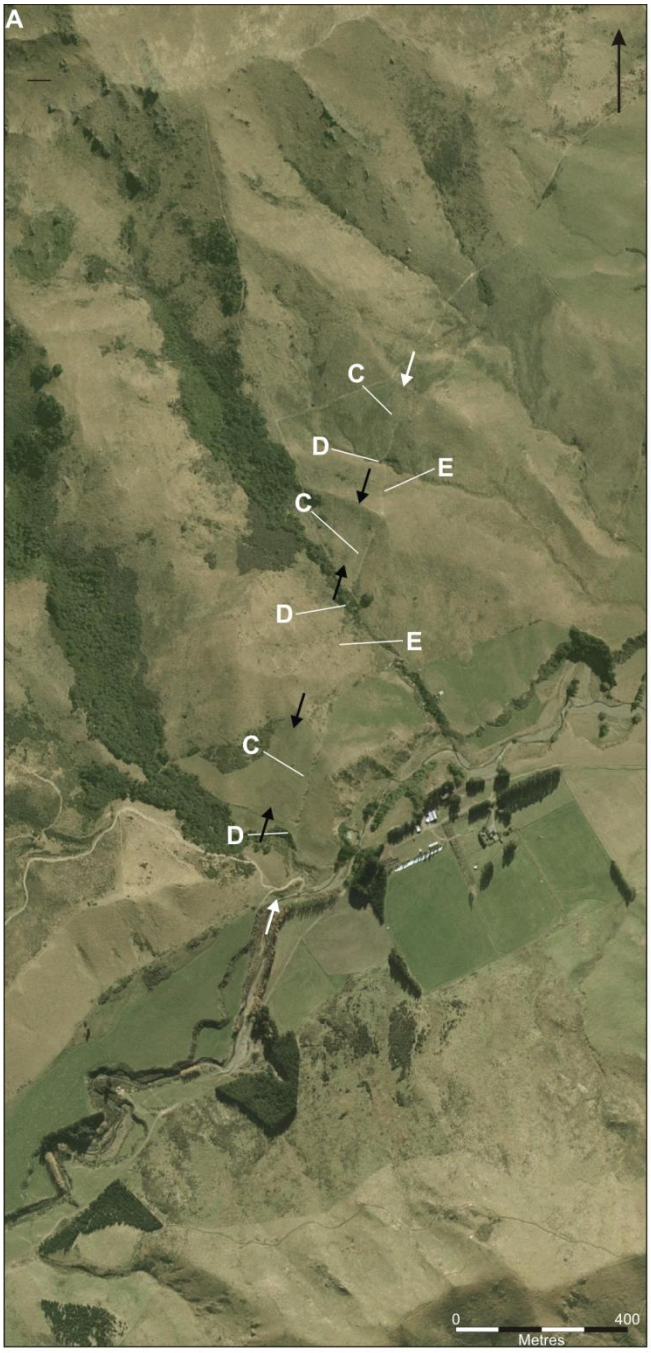

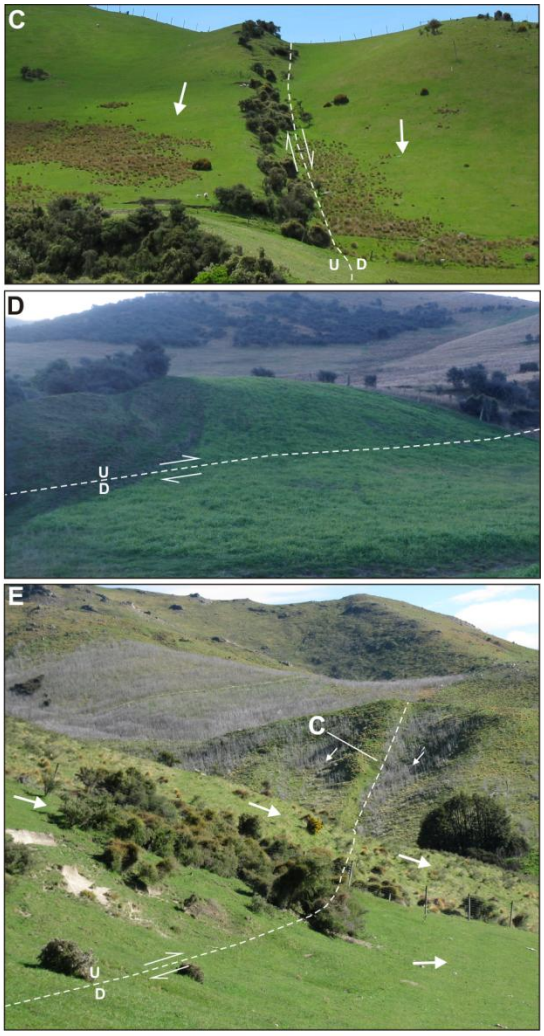

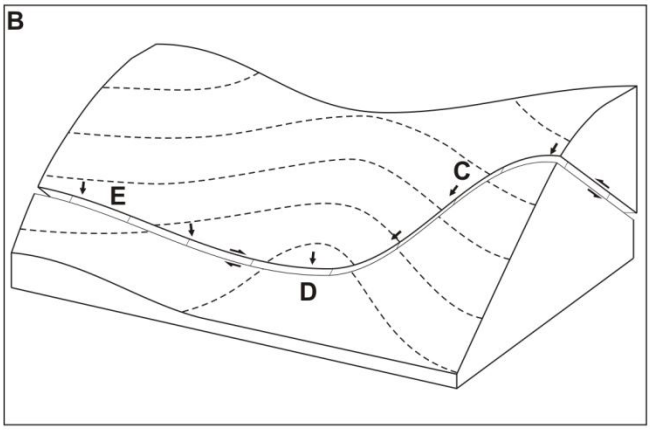

Figure 2.7. A) Aerial Photograph of the Waitohi Section showing the main trace (white arrows) trending across three spurs above the Waitohi River. Labels refer to locations where the slope aspect is similar to those in photographs C, D and E and the corresponding labels in diagram B. Black arrows indicate locations of secondary traces that do not displace the late Quaternary terraces. B) Block diagram showing the three ways the slope aspect and fault trend interact on the Waitohi Section. C) The scarp trends straight up the hillslope, reducing the tendency for the scarp to collapse downhill. D) The fault scarp is preserved on level terrace surfaces. E) The scarp in the foreground trends across the slope and has quickly collapsed downhill. The collapse of scarps on north-facing slopes inhibits the use of hillslope separation to quantify the dextral component of slip. Arrows in B, C and D indicate the slope direction.

have also preserved diffuse fault scarps running parallel to the main active trace (Figure 2.7A). These scarps, which both appear for lengths of c. 150 m on the eastern side of the active trace, are more affected by erosion of the crest and deposition at the toe, producing a broader scarp face and increasing the difficulty of accurate measurement. While the active scarp can be traced across all alluvial surfaces in the valleys that it crosses, neither of the two parallel scarp sections displace Quaternary deposits and are instead truncated by them at the valley sides indicating that they have not been active since the surfaces were abandoned.

Vertical displacement on the main active trace is greatest at the southern end of the section where an abandoned Waitohi River terrace surface is displaced by c. 9.5 m (Figure 2.6). To the south the fault enters the valley floor where the modern river bed and flood plains have removed any evidence of faulting across the valley floor and exposed the west dipping fault plane in the valley side. The exposure reveals Torlesse greywacke thrust over Quaternary river gravels on a west-dipping fault plane (Figure 2.8). Bedrock is not seen in the footwall at this site but separation of the bedrock surface measured from the modern riverbed reveals a minimum vertical separation of 7 m. The c. 1 m thick zone of shearing above the fault plane yielded numerous striations which are used to determine the components of dextral and reverse slip on the Waitohi Section (see Section 3.6.2)

A small tributary to the Waitohi River crosses the fault just west of the Whitnow homestead and appears to be displaced in a dextral sense across the fault (Figure 2.7A). However, the bend in the stream begins c. 40 m west of the fault scarp suggesting that much of the apparent offset may be an unrelated meander in the original stream bed. The stream flows south along the fault trace for c. 40 m before resuming its course east. It is likely that a significant proportion of the apparent offset is in fact due to faulting but without a more precise piercing point, quantifying the dextral offset at this location is not possible.

Figure 2.8. Photo and interpretation of an exposure of the fault plane on the Waitohi Section. Mesozoic sandstone is thrust over Quaternary gravels of the Waitohi River. Bedrock is not visible in the footwall but a minimum of 7 m vertical separation has occurred. Colluvial deposits are visible overlying alluvial deposits in the footwall. Fault dip = 35°W. A thin band of Iron staining emerging from the fault plane (orange line) indicates that the fault is a conduit for fluid flow. Fault marked by White arrows.

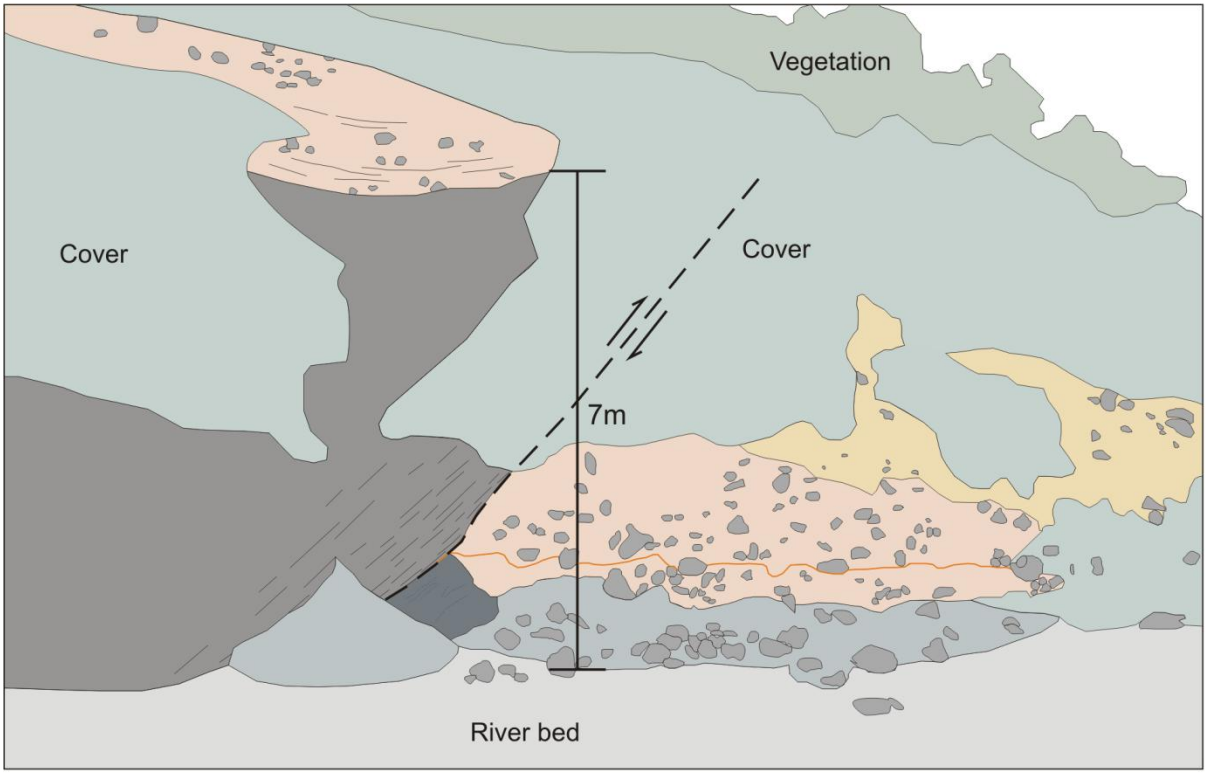

Bedrock (Torlesse sandstone)
Alluvial gravels
Colluvial wedge
Active colluvial deposits
Fault gouge

2.2.4. WHITNOW SECTION

Approximately 600 m from its northern terminus the Waitohi scarp is intercepted by the Whitnow Section, forming a fork in the surface trace. While the Waitohi Section heads south towards the river, the Whitnow section branches off to the southeast as a diffuse reverse scarp. In the field, the northern Whitnow scarp is only traceable for c. 150m and from the fork is inferred to traverses the western slopes of the Waitohi valley for over 7 km before crossing the Okuku River and disappearing below Ashley Head (Figure 2.1). South of the Waitohi Valley the trace is only inferred through aerial photo interpretation and the total length of the section is estimated to be c. 14 km.

The Whitnow Section consists of both reverse scarps where it intersects the Waitohi Section and on the slopes of Mt Whatno and a normal, uphill-facing scarp above Whistling Creek. In between the prominent scarps at either end of the Waitohi Valley, the trace is difficult to follow in the field but is inferred to cut through a series of saddles in the eastern spurs of the main ridgeline. Many parallel linear features are visible in aerial photographs and satellite imagery on Google Earth traversing the lower slopes north of the normal scarp in Whistling Creek but no evidence is seen in the field. These features may simply be an expression of the structural grain of the bedrock (see Attached Map).

The northern reverse scarp can be traced for about 200 m south of its intersection with the Waitohi Section and a dextral component is obvious where a small ephemeral stream crosses the fault and is offset by c. 4.5 m. To the north, two parallel traces are visible striking at c. 005° across the lower slopes of Mt Whatno (Figure 2.9). The lower and more prominent of the two preserves up to 10 m of slope-normal separation of the hill side. The same trace offsets a small stream and ridge by c. 3.4 m in a left-lateral sense. The upper trace is less well preserved and forms a diffuse break in slope of approximately 2 to 5 m wide. From here the

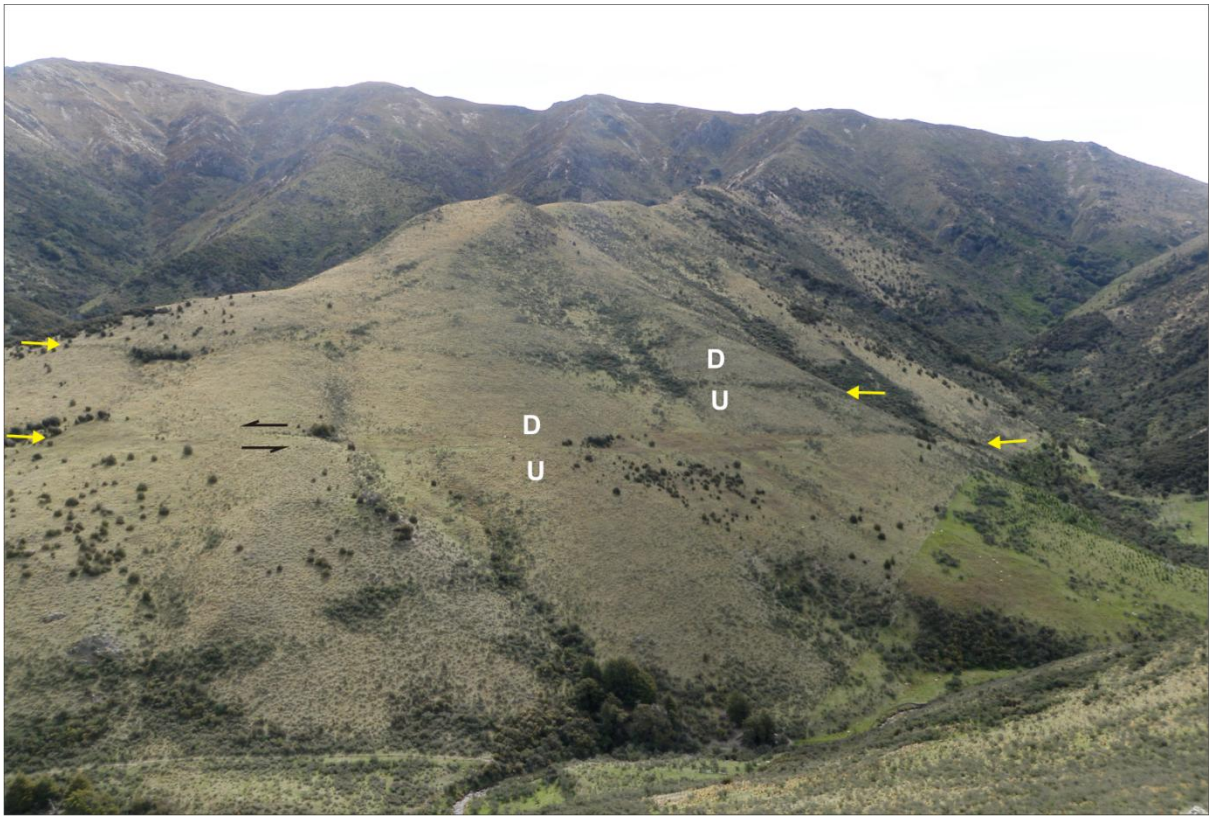

Figure 2.9. Normal, uphill-facing scarps of the Whitnow Section above Whistling Creek. Arrows mark the visible extent of two parallel fault traces. A sinistrally offset stream can be seen at centre-left of the photo on the lower, more prominent fault.

trace again dies out for several hundred metres before picking up again on the slopes of Mt Whatno where a discontinuous line of stream heads and waterfalls coincident with a brief steepening of the hill slope mark the surface expression of a southwest trending reverse fault. To the south the trace can be followed in aerial photographs as a near straight line trending c. 232° for c. 3.5 km.

2.3. EASTERN FAULT SECTIONS

2.3.1. GOLA PEAKS SECTION

The Gola Peaks Section is a c. 8 km long dextral-reverse section consisting of several discontinuous scarps traversing the eastern slopes of the Waitohi Valley.

The northern boundary of this section is marked by an exposure at the Waitohi River where Torlesse bedrock is thrust over Quaternary alluvial deposits (Figure 2.10). The fault plane at this point dips towards the east, the opposite direction to the dip of the Waitohi section, just 400 m to the north. The vertical separation of the bedrock surface at this site is c. 16 m (Figure 2.10A). River gravels and alluvial fan deposits are cut by the fault and deposits in the hanging wall are tilted to the west across the folded bedrock while beds directly beneath the fault have been dragged up the fault plane (Figure 2.10A and B).Within the hanging wall anticline, tensional fractures and small-scale normal faulting (< 0.5 m displacement) is seen in the bedrock.

Stratigraphic logs of the hanging wall and footwall at the eastern Waitohi River exposure are shown in Figure 2.12. The base of both logs is marked by Torlesse sandstones, the local bedrock. Lying unconformably above the bedrock surface is a unit of sub-rounded to sub-angular cobbles and boulders interbedded with finer sandy pebble layers (Unit A Figure 2.12). Unit A is generally well stratified with individual beds of <0.1 to c. 1.5 m thick. The

lower beds pinch out to the south where they onlap the gently rising bedrock surface (Figure 2.10A). Angularity of the larger clast sizes increases up the stratigraphic column and clast size within the thicker beds becomes less regular. All cobble and boulder dominated beds in Unit A are imbricated with flow to the north, down the Waitohi River. Above Unit A, angular to sub-angular cobble-supported layers dominate and are interbedded with layers of angular coarse sand and pebbles which also include occasional cobbles (Unit B Figure 2.12). Unit B continues to the top of both columns and in places contains decimetre thick, well stratified beds of medium sand to granule and pebble sized clasts with little or no cobbles. All clasts in units A and B are composed of sandstones of the Torlesse Supergroup.

The major difference between units A and B in the footwall and hanging wall is their thicknesses (Figure 2.12). Both units are thinner in the hanging wall, making the full column c. 8 m thinner. The difference in thickness of unit B is explained by erosion of uplifted deposits in the hanging wall after each surface rupture. A colluvial wedge at the surface is evidence of this process (Figure 2.10A and B). The difference in thickness of unit A may be the result of the bedrock surface being higher in the hanging wall at the time of deposition. This could have been due to pre-existing separation of the bedrock surface or a result of the natural channel shape of the valley side, with the hanging wall being closer to the valley wall and therefore higher than the footwall (Figure 2.11). As a result, individual beds cannot be correlated between units A and B and the apparent offset of the bedrock surface may be greater than the actual offset; However, the upper contact of unit A can be correlated between the hanging and footwalls and, being a fluvial deposit, is known to have been a level surface across both the hanging and footwall before faulting. The resulting vertical offset is 13.5 ± 1.5 m (Section 3.3).

Figure 2.10. A) A spectacular exposure at the northern end of the Gola Peaks Section. Mesozoic sandstone is thrust over Quaternary alluvial deposits. The bedrock surface (dotted black line) shows c. 16 m of vertical separation. Dotted white lines mark bedding, which is sub-horizontal in the footwall and folded and tilted up-dip above and directly below the fault plane. A colluvial wedge is visible where the fault cuts the upper alluvial deposits. B) Close up of the fault plane looking north. Tilted deposits can be seen in the hangingwall. The colluvial wedge can be seen in the background, outlined by iron staining.


A
Colluvium
Torlesse
U
D

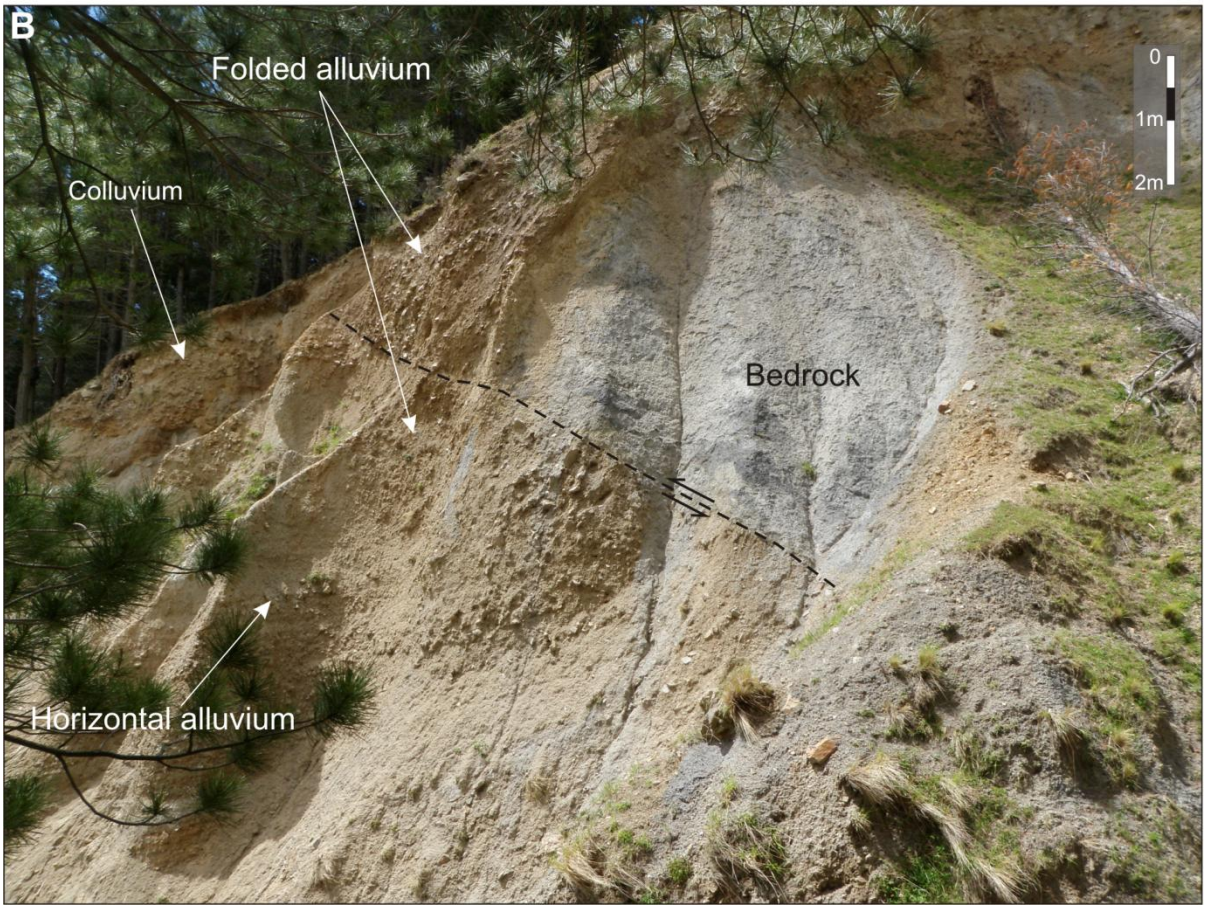
B
Folded alluvium
Colluvium
0
1m
2m
Bedrock
Horizontal alluvium

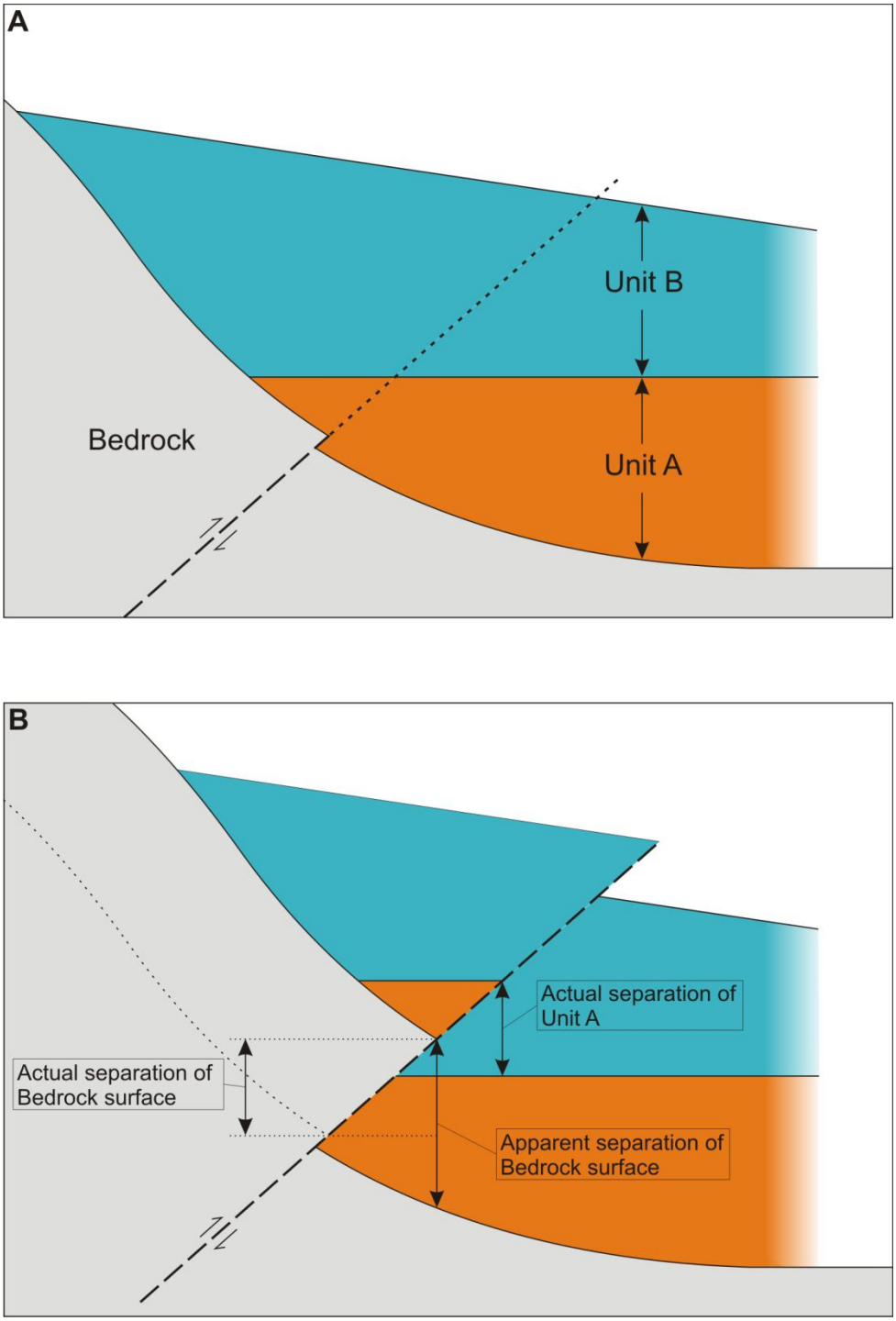

Figure 2.11. Schematic cross sections showing the potential for over estimating the vertical separation of the bedrock surface at the Gola Peaks exposure. A) After deposition of Unit A (see Figure 2.12) but before subsequent faulting. B) After faulting of units A and B. Apparent separation may result from the original upward slope of the bedrock surface at the hillside. The top of Unit A was deposited as a flat surface so preserves a true vertical separation.

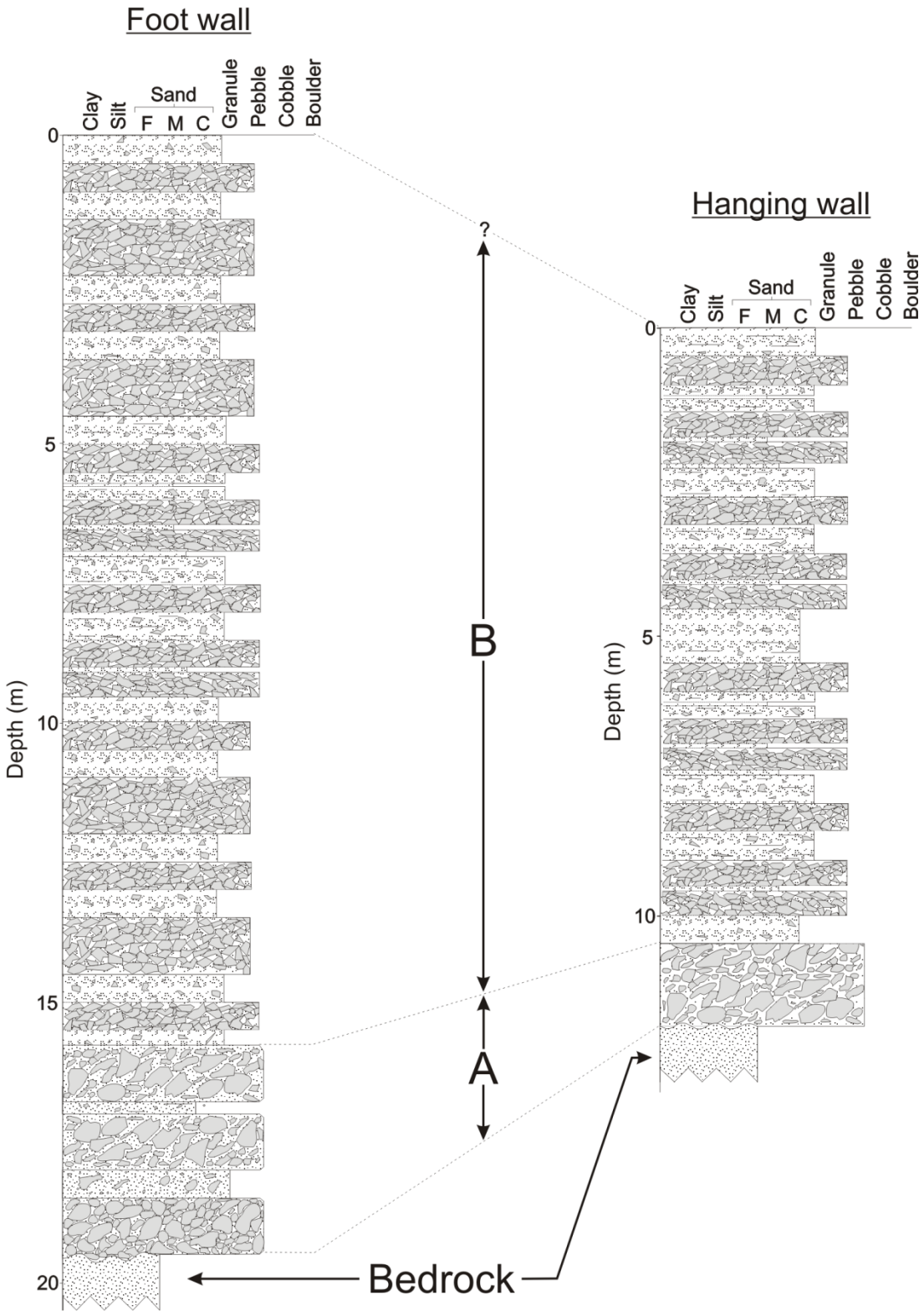

Figure 2.12. Simplified stratigraphic columns of the hanging wall and foot wall at the Gola Peaks exposure (see Figure 2.10). Two distinct units have been identified in both columns. Unit A consists of interbedded sub-rounded cobble and boulder supported conglomerates and coarse pebbly sands. Unit B consists of sub-angular coarse alluvial deposits interbedded with finer sandy beds. Thicknesses of beds are schematic and not representative of individual beds in the outcrop. Unit thicknesses are accurate.

Above the exposure, the fault does not offset the steep, forested hillslope but the trace can be followed for 100 m to the south by a series of obscured faulted contacts and exposed tensional structures in the anticlinal fold of the hanging wall.

No fault scarp or exposures are visible for 5.5 km south of the northern exposures but the trace picks up again south of Retreat Creek where the valley side trends in a more southerly direction. Here the fault is seen as a reverse scarp trending at 035°, c. 100m above the valley floor. As the scarp crosses much steeper hillsides here than at the Waitohi section, the scarp is more degraded and defined by a steepening of the hill slope and numerous small slumps (Figure 2.13). The scarp lies above an east dipping fault, thrusting the hilltops to the west, for 2.2 km along the eastern valley side before dying out as it crosses the saddle into the Okuku River valley at the southernmost extent of the preserved fault section. Dextral offsets of streams and ridges are apparent along this section and offset geomorphic markers by up to 20 m (Section 3.3).

2.3.2. MOUNT GORDON SECTION

The Mt Gordon Fault Section is a continuous normal scarp that trends across the high north-western slopes of Mt Gordon, south of the Okuku River. The fault is previously unmapped and unnamed but is clearly visible in 1:40,000 aerial photographs. The orientation of the Mt Gordon Fault, at c. 079°, and its position to the south of, but not obviously connected to the NEF and the Waitohi Downs Fault at the surface make its connection to the local fault system somewhat ambiguous. The possibility of the Mount Gordon Fault rupturing as a part of the NEF segment is discussed in Chapter Three.

Figure 2.13. A) The view looking east towards the southern extent of the Gola Peaks Section. The fault trace is visible as a change in slope along which a series of shallow slumps have occurred. 'B' marks the location of photo B. B) Looking south along the fault scarp. Dotted line shows approximate location of fault plane at the surface. Several small slumps can be seen along the steep scarp face.

2.4. ADIITIONAL STRUCTURES IN THE AREA

Several other active faults traces are visible within 15 km of the NEF, some of which appear to converge towards the southern end of, and may have a significant structural connection to the NEF (Figure 1.3). Many of these fault segments have not been studied in great detail and some have only been mapped from aerial photographs and limited fieldwork (e.g. Mould (1992), Rattenbury et al. (2006)). The more conspicuous of these include:

1. The *Waitohi Downs Fault* – Mapped in detail by Mould (1992) the Waitohi Downs Fault stretches for over 35 km sub-parallel to the Esk fault at an average trend of c. 042°. Listed as part of the West Culverden Fault Zone by Pettinga et al. (2001) the fault is a west dipping reverse fault skirting the western edge of the Culverden Basin at its northern end and stretching inland towards Gola Peaks and the southernmost section of the NEF to the south. In the field the fault is visible as a 2-3 m high reverse scarp crossing Virginia Rd and Quaternary terraces of the Waitohi River at its midpoint and again as a normal, uphill-facing scarp trending across Block Hill to the south. Van Dissen et al. (2003) estimate a recurrence interval for the "West Culverden Fault" from fault scaling relationships of 5000 – 10,000 years.

2. The *Leasemen Stream Fault* – The Leasemen Stream Fault is a previously unnamed fault that has a prominent 6 km surface trace though Leasemen Stream and south to where it crosses the Okuku River, below the Waitohi Downs Fault. The Leasemen Stream Fault has been mapped by Rattenbury et al. (2006) as a south-dipping structure and surface trace interactions with topography support this. No obvious signs of lateral displacement are visible in aerial photographs. For its entire surface expression The Leasemen Stream Fault appears to be a

normal, uphill-facing scarp. No estimates have been made of its recurrence interval though it may be considered part of the West Culverden Fault zone as described by Pettinga et al. (2001).

Several other small, active fault segments have been mapped to the east of the NEF, between the Waitohi Downs Fault and the Culverden Basin as well as short sections to the northwest (Figure 1.3).

2.5. SUMMARY

- Detailed field mapping of the NEF has reveals a series of distinct fault sections trending at 005 - 057° from the Hurunui River in the north to Ashley Head in the south.

- Changes in fault strike, dip, dip direction and sense of slip occur at several key locations along the preserved trace and distinguish six fault sections, four dominantly dextral-reverse and two dextral-normal.

- Surface expressions range from > 9 m high reverse scarps to subtle changes in hill-slope to broad, uphill-facing normal scarps.

- A number of previously unmapped fault traces have been identified to the south and east of the NEF.

CHAPTER 3
KINEMATICS AND STRUCTURE

3.1. INTRODUCTION

Both offset geomorphic markers and slip vector data obtained directly from fault planes provide useful insight into the kinematics of fault rupture. Whilst some environments may accurately preserve vertical displacement (e.g. terrace treads) others such as the steep slopes of the Waitohi Valley may not. The opposite may be true for steep hill slopes where streams and ridges preserve lateral displacement but vertical movement is quickly disguised by erosion. As a result a combination of methods and measurements including measured offsets, fault plane striations and historic seismicity used across the field area are needed to accurately resolve and explain the kinematics of surface rupturing events.

Additionally, cumulative and single event displacements of geomorphic features can provide invaluable information on long term slip-rates, coseismic slip, magnitude and other characteristics of prehistoric surface rupturing earthquakes, the combination of which aids in more accurate assessment of the seismic hazard posed by the NEF.

3.2. METHODOLOGY

Several different techniques have been employed to measure the separation of geomorphic markers across the fault trace. Each method has its advantages and disadvantages in terms of ease of use, portability and accuracy.

The first method is measurement by tape measure. This method was used at several of the sites that had small and geometrically simple displacements that did not require nor warrant the use of more complicated methods. Errors involved in these measurements reflect the

uncertainty involved in pin pointing the exact intersection of a rounded and possibly eroded feature, such as a stream bank, with the fault trace.

The second method is measurement by laser rangefinder. This method is particularly useful where steep or uneven terrain or dense scrub make the accurate use of a tape measure near impossible. The range finder also proved useful in measuring vertical separations without the additional errors involved in calculating vertical distances by tape measure and trigonometry. The accuracy of the particular rangefinder used in this study is quoted by the manufacturer as ± 0.3m and this is added to other uncertainties when calculating errors.

The third method is measurement by differential GPS profiling. This method involves the use of GPS to outline or profile features in the field which are then analysed and measured in the lab on Pathfinder software. Advantages of this method include the ability to collect a lot of data over a large area relatively quickly, enabling the detection of more subtle features and diffuse deformation that would be near impossible to measure by hand. The accuracy of processed data ranged from ± 0.1 m to ± 1 m. These errors were added to other uncertainties.

The fourth method is by topographic contouring of the ground surface using differential GPS. This method was utilised at three significant sites along the fault trace where large features such as broad ridges or streams are offset. This method provides more accurate location of piercing points that would not be possible in the field as well as creating a large data set from which profiles across the fault trace can be constructed.

3.3. DISPLACEMENTS

3.3.1. OVERVIEW AND DATA

A total of 20 offset geomorphic and stratigraphic features were measured along the NEF producing 15 vertical and 12 horizontal separations. The locations of measured offsets are

shown in Figure 3.1 and data obtained from these sites is displayed in Table 3.1. The majority of lateral offset sites were along the eastern slopes of Mt Noble where streams and ridges are offset by between 4 and 24 m. Two sinistral offsets were also measured, one on the Waitohi Section and one on the Whitnow Section.

Vertical offsets are both reverse and normal. All reverse separations with the exception of one at the northern tip of the fault and one at the Gola Peaks exposure were measured on terrace treads where scarp height is believed to be representative of actual slip on the fault plane with discrete displacement at the surface and no pressure ridging or longer wavelength folding. Measurements of reverse separation of the bedrock hill slope along the Gola Peaks and Waitohi sections have not been included as dextral movement as well as an unknown amount of erosion make the vertical offsets unreliable (Section 2.2.3.). Both laser rangefinder and GPS profiling were used to measure reverse separations.

Normal separations were calculated from horizontal scarp widths measured normal to the fault trace. By projecting the fault dip measured at site C (Figure 3.1) of 45°W along the full length of the Mt Noble section the hill slope and scarp width can be used to estimate vertical separation where more precise piercing points cannot be found. When using this method relatively straight sections of fault scarp and ridge crests give the best results as they will not be affected by the dextral movement along the same fault plane. Results from these calculations are presented as minimum separations as an unknown amount of erosion of the fault scarp makes projection of the scarp edge difficult in the field. The projected dip of 45° is also likely to be a minimum as the section is dominantly strike-slip and steeper fault dips are likely at depth.

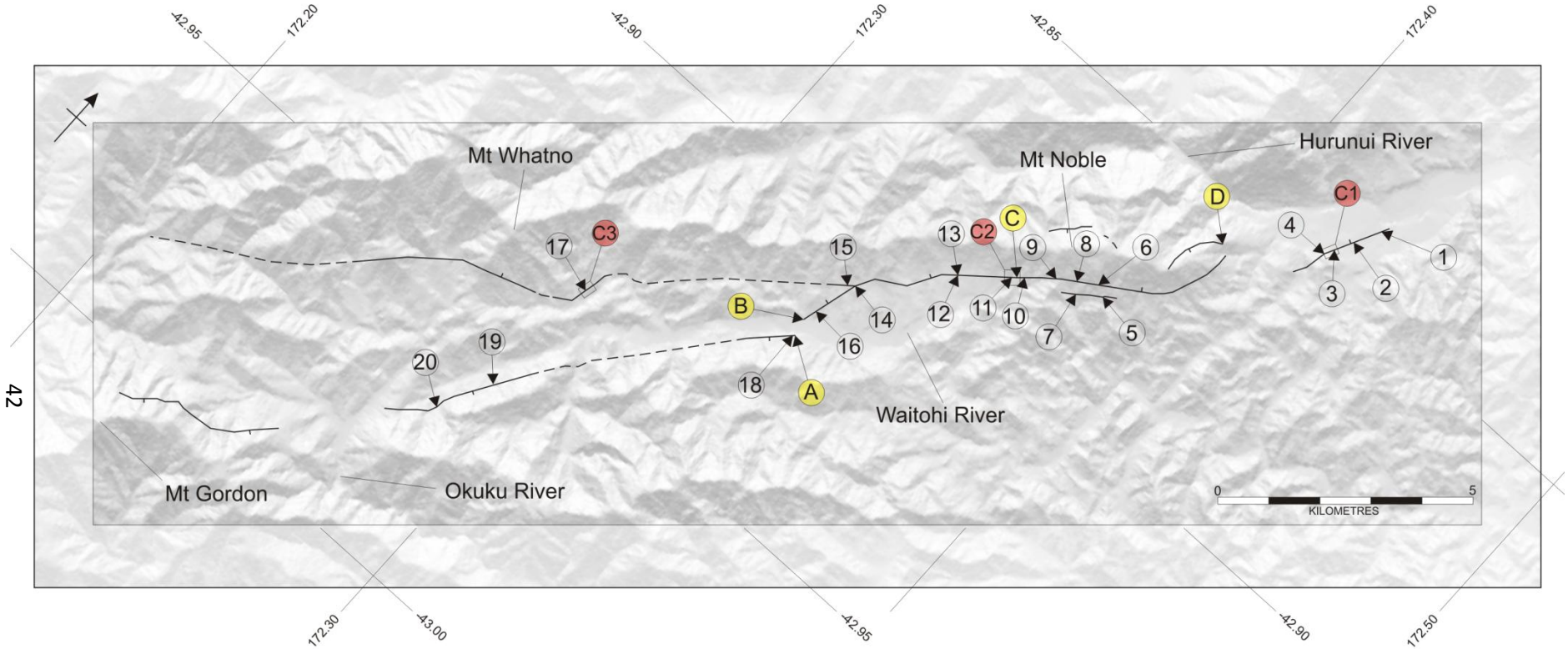

Figure 3.1. Map of the Northern Esk Fault showing locations of all measured vertical and horizontal separations (Hollow circles), Fault plane exposures (Yellow circles) and contour maps produced from differential GPS data (Red circles). Numbers refer to measurements in Table 3.1.

Number	Section	Distance along fault (km)*	Horizontal Displacement (m)	Horizontal Error +/-	Vertical Displacement (m)	Vertical Error +/-	Horiz/Vert Ratio	Side up	Dextral/Sinistral	Normal/Reverse	Offset Feature	Fault Strike	Fault Dip	Azimuth Slip Vector (E)	Plunge of Slip Vector	P-axes	T-axes
1	Hurunui	0.3			1	0.3		W			T6 Terrace tread	027	32W				
2	Hurunui	1.2			2.1	0.3	4.05	W			T5 Terrace tread	027	32W	79 - 39.44	26.2 - 7.6	092.9/16.7 - 064.5/30.4	224.8/65.8 - 188.9/43.9
3	Hurunui	1.3	8.5	6				W			T3-T4 Terrace riser	027	32W				
4	Hurunui	1.4			3.7	0.3		W			T2 Terrace Tread	050	32W				
5	Mt Noble**	6.8			2.5†	0.6		E			Hillslope	057					
6	Mt Noble	6.9	20	4	5.7†	3	3.51	E			Stream bank	057	45W	41.09	-15.32	082.5/43.4	190.7/18.2
7	Mt Noble**	6.9	10	3	2.5†	0.6	4.00	E			Gully Wall	057	45W	42.96	-13.88	083.6/41.8	192.0/19.5
8	Mt Noble	7.2	21	5	5.2†	0.9	4.20	E			Gully Wall	057	45W	43.09	-13.52	083.6/41.7	192.1/19.6
9	Mt Noble	7.2	4	1	5.2†	0.9	0.80	E			Stream	057	45W				
10	Mt Noble	7.3			5.4†	1.0					Hillslope						
11	Mt Noble	7.4	23.7	3.2	5.3†	2.1	3.57	E			Ridge	057	45W	44.39	-12.32	085/40	193/20
12	Mt Noble	7.5			3.9†	0.6					Hillslope						
13	Mt Noble	8.4	15.5	3				E			Gully Wall	057	45W				
14	Waitohi	11.6	11	1	4.1	0.3	2.68	w			Stream bank	015	35W				
15	Whitnow	11.6	4.5	0.5				W			Stream bank	040	35W				
16	Waitohi Scarp	12.4			9.5	0.6		W			Terrace surface	012	35W				
17	Whitnow	16.8	3.4	1	2.7†	0.5	1.26	E			Ridge and Stream	005	45W	219.6	-34.1	063.8/8.9	168.2/57.7
18	Gola Peaks	13.5			13.5	1.5		E			Alluvial deposits	045	35E				
19	Gola Peaks	19.2	3.5	1				E			Stream bank	027	E				
20	Gola Peaks	20.2	19	3							Stream Bank	027	E				

*From northern of Hurunui River Section

† Estimate based on Fault dip of 45° W

**Not the main active trace

Dextral / Normal

Sinistral / Reverse

Table 3.1. All measured offsets of geomorphic features along the Northern Esk Fault with kinematic data where available. See Figure 3.1 for offset locations.

3.3.2 TOPOGRAPHIC CONTOURING BY DIFFERANTIAL GPS

Three sites along the eastern section of the NEF were chosen for detailed topographic contour mapping using a Trimble GeoXH GPS differentially corrected using the Land Information New Zealand's (LINZ) Lake Taylor and Kaikoura GPS sites as base stations. Data was collected along a roughly 5 m by 5 m grid across areas of up to 52,000 square metres with additional data collected near important features.

The three sites surveyed by this method were 1) a section of dextral-reverse fault scarp displacing terrace treads and risers of the Hurunui River, 2) an offset ridge along a normal-dextral section of the fault on Mt Noble and 3) a normal-sinistral section displacing a ridge and stream above Whistling Creek on the Whitnow Section (Figure 3.1 sites C1, C2 and C3 respectively). Figure 3.2 shows the Mt Noble site with errors projected up the ridge line to the fault plane where dextral separation is measured at 23.7 ± 3.2 m. Errors involved in the projection of the ridge line stem from the roundness of the ridge, particularly above the fault and the apparent bend of the ridge in the footwall towards the ridge in the hanging wall. This perceived bend is the result of erosion of the once sharp scarp edge below the fault plane. The trend of the fault scarp does change slightly below the fault and this also adds to the errors. Projection of the footwall ridge line at both the angle of the ridge in the hanging wall and in the footwall, from the point at which the ridge begins to curve, produces a triangle within which the actual ridge must once have existed directly below the fault plane (e.g. Little et al. (1998)). This allows the dextral displacement to be measured with high confidence that the actual separation is within the error given.

The above methods were also applied to the two other sites and the data and resulting contour maps are presented in Appendix A.

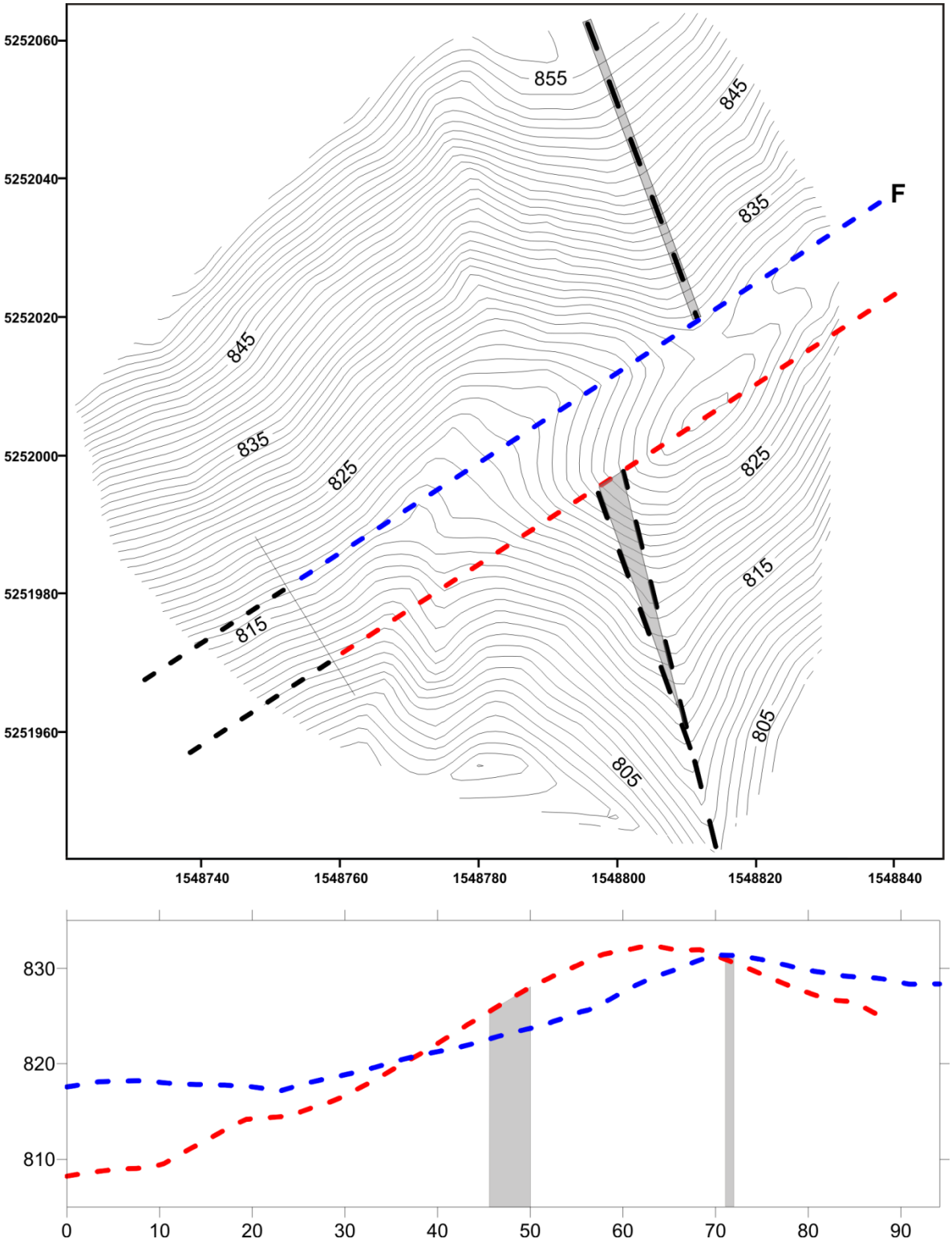

Figure 3.2. A) Contour map of an offset ridge and stream on the Mt Noble Section produced from differential GPS data. Blue line shows intersection of the fault with the hill slope. Red line marks the intersection of the scarp edge with the ridgeline parallel to the fault. Grey area show the errors associated with locating the ridgeline. B) Cross sections along lines in 'A' showing the 23.7 ± 3.2 m offset at this site.

3.4. SINGLE EVENT DISPLACEMENT

3.4.1. LATERAL DISPLACEMENT

Right-lateral displacements along the length of the NEF range from 3.5 ± 1 to 23.7 ± 3 m while two sinistral displacements were also recorded at 3.4 ± 1 and 11 ± 1 m. All cumulative dextral displacements identified on the western sections cluster around multiples of 5 m with no displacements being more than 1.3 m higher or lower than a multiple of 5 m (Figure 3.3). These observations permit an average lateral displacement for the Mt Noble section of c. 5 m/event in a characteristic slip model, with the largest displacement of 23.7 ± 3 m implying five preserved surface rupturing events.

Of the dextral displacements on the Mt Noble and Waitohi sections the two smallest are 4.0 ± 1 and 4.5 ± 0.5 m. Both of these measurements are of small ephemeral streams and, as they are the smallest displacements found on the western sections and also fit the c. 5 m/event characteristic slip model, are considered to be single event displacements of features formed during the last interseismic period.

The one possible exception to this model is a measurement of 8.5 ± 6 m. This separation was measured at the Hurunui Terraces site along the terrace 3 – terrace 4 (T3 and T4, Figure 3.4) riser (see contour map in Appendix A). The high uncertainty in this measurement reflects the difficulty in defining the terrace edge as a result of dense vegetation of the riser on the hanging wall and modification of the scarp and terrace riser in the footwall for use as a farm track. The angle at which the terrace crosses the scarp is also quite acute, increasing the errors associated with projecting the terrace riser edge to the fault plane. Based on the displacement data collected along the Mt Noble section the actual separation at this site is likely to be less than 5 m as the scarp here is known to preserve only the latest surface rupturing event (see

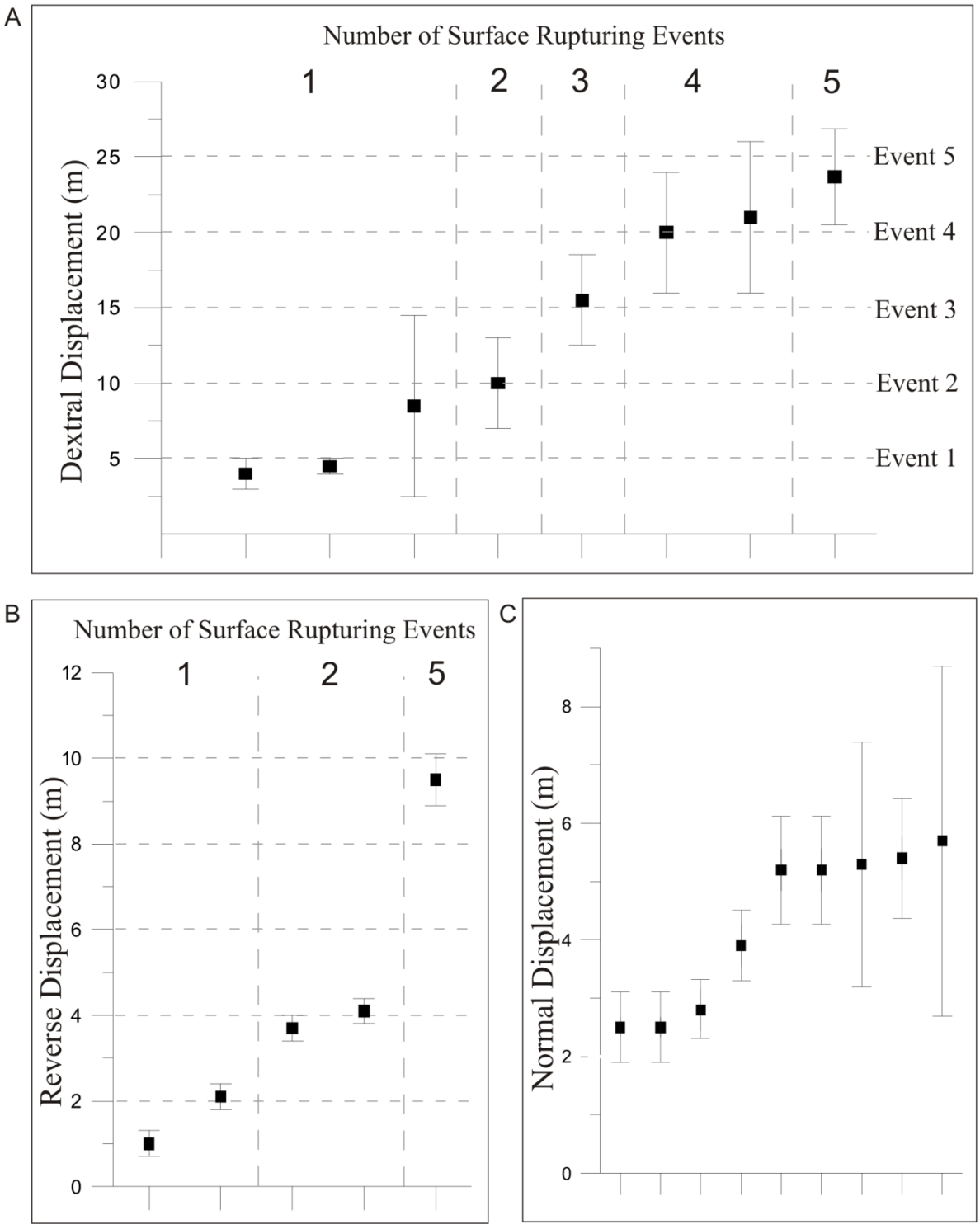

Figure 3.3. Measured offsets along the western sections in ascending order. A) Dextral, B) Reverse, C) Normal. A & B show expected cumulative offsets for the last 5 events based on a characteristic earthquake model (horizontal dashed lines) and assign a likely number of preserved events to each offset.

Section 3.4.2. below), is nearer to the fault tip and also accommodates a significant amount of reverse slip.

3.4.2. VERTICAL DISPLACEMENT

Both normal and reverse dip-slip movement is preserved along the NEF with sense of displacement dependant on the strike of the fault and the relief of the surrounding topography. Normal and reverse separations recorded along the full length of the NEF are shown in Table 3.1.

The faulted terraces of the Hurunui River provide an excellent opportunity to characterise single event vertical separations for the more northerly striking, dextral-reverse sections of the fault. The terraces preserve two distinctly different scarp heights across 4 terrace surfaces (Figures 3.4 and 2.2). The highest faulted terrace tread, T2, preserves an average vertical separation of 3.7 ± 0.3 m along the 200 m long scarp. The scarp is then truncated by the T2 – T3 riser and appears on the T3 and T5 terrace treads a sinuous scarp averaging 2.1 ± 0.3 m vertical separation for c. 500 m. Further north the scarp dies out into a gentle fold on T6. T4 is not present between T3 and T5 at the point at which the fault trace would cut it, resulting in a 20 m vertical drop across the T3-T5 terrace riser.

The measured vertical separation on T2 is considered a minimum estimate of the actual vertical movement on the fault plane as the intersection angle of the fault trace and the T2-T3 terrace riser is very acute producing a narrow ridge just 10 to 30 m wide between the bottom of the scarp face on T2 and the bottom of the T2-T3 terrace riser (Figure 3.4). This leaves little to no flat T2 surface in the hanging wall towards the northern end of the scarp but increasing width and absolute scarp height towards the south where the T2-T3 riser curves away from the fault trace. Unfortunately, colluvium deposited on T2 at the bottom of the adjacent bedrock slope makes measuring the separation of the terrace tread at the southern

Figure 3.4. Map of the Northern Esk Fault crossing terraces 2 - 5 of the Hurunui River Section. The scarp marked ‘A’ preserves 2 surface rupturing events while the scarp marked ‘B’ preserves a single event. See text for explanation. The jog in the fault trace across the T3 – T5 riser is used to calculate a near surface fault dip of 28 - 35°. See Figure 1.4 for location.

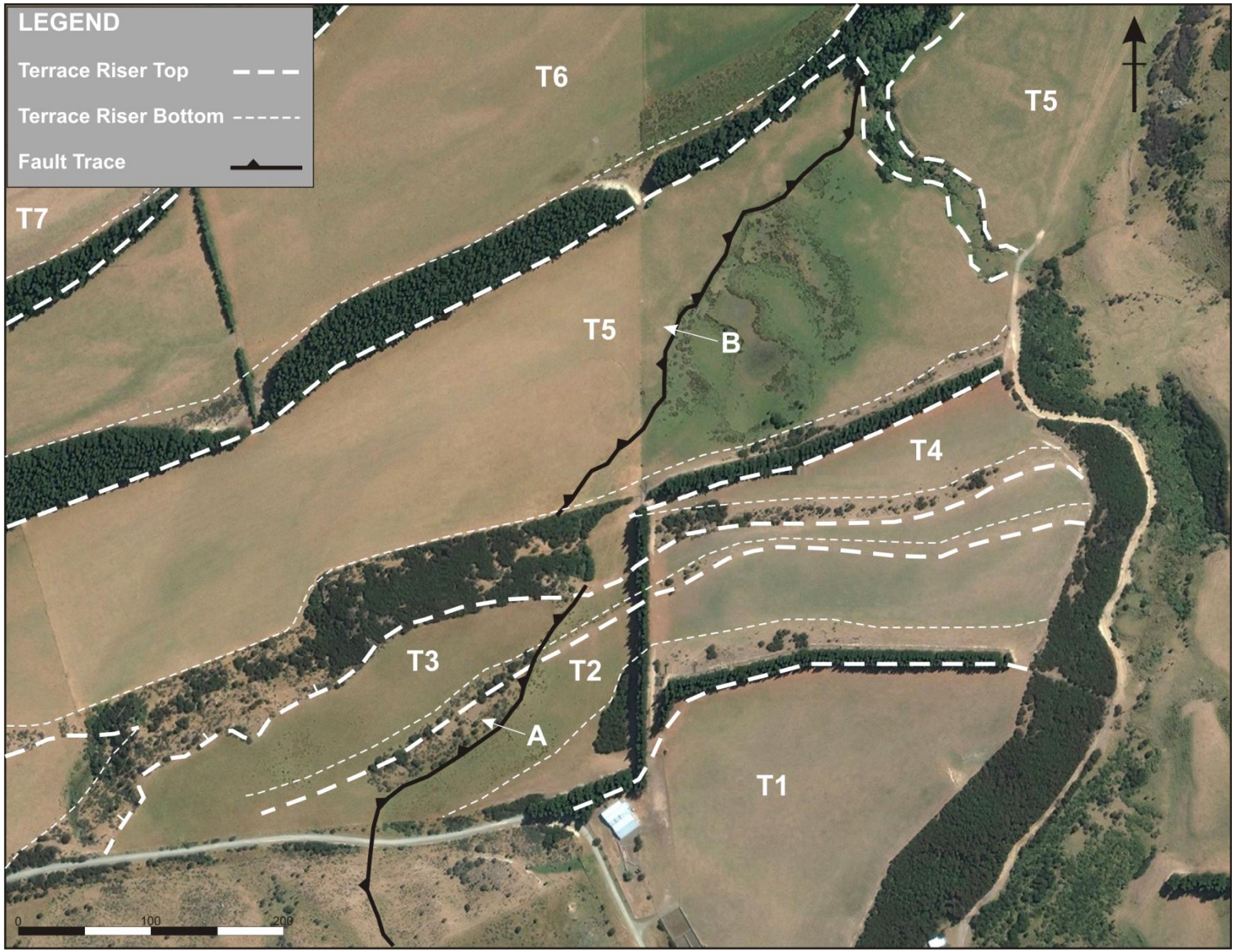
LEGEND
Terrace Riser Top
Terrace Riser Bottom
Fault Trace
T7
T6
T5
T5
B
T4
T3
T2
A
T1
0
100
200

end difficult. Additionally, the terrace is active agricultural land grazed by sheep and cattle which only works to increase erosion from the top of the scarp slope. A steepening of the scarp-face down-slope of the midpoint is indicative of the overriding of a colluvial deposit (McCalpin 2009), a feature not seen along the lower scarp on T3 – T6.

The two distinct and consistent scarp heights on T2 and T3 – T5 reflect the preservation of a single event on the lower faulted terraces and two events on the higher, older T2. From this it is evident that single event displacements on this section of the NEF must be on the order of 1.7 – 2.4 m. Given the consistency of the measured scarp height of 2.1 m on T5 and the likelihood that the actual separation on T2 is somewhat greater than the 3.7 m average, an average vertical displacement of c. 2 m per event is likely for surface ruptures of the Hurunui River Section.

The other major dextral reverse section of the NEF that has preserved vertical separation is the Waitohi Section. The Waitohi Section scarp crosses several spurs and intervening terrace surfaces as it trends at c. 192° for over 1 km south towards its intersection with the Waitohi River. Along this section the vertical separation of the terrace tread can be measured with useful accuracy in two locations. The first is the 9.5 ± 0.6 m high scarp that cross the terrace surface directly above the Waitohi River at the southern end of the preserved scarp. The errors quoted for this calculation take into account the modification of the terrace tread in the footwall by the digging of drainage channels for agricultural use as well as the errors in the processed differential GPS data.

The second measured separation is of a 4.1 ± 0.3 m high scarp 1 km to the north where the fault trace crosses a high terraced surface occupied by a minor tributary of the Waitohi River. This area is relatively unmodified by agricultural use so the errors mainly reflect those of the GPS data.

The scarp height of 4.1 ± 0.3 m on the Waitohi Section fits well with the estimated c. 2 m/event of purely vertical movement seen on the Hurunui Section, with the inference being that the terrace surface has preserved the vertical movement of the same two surface rupturing events that displace T2 on the Hurunui Section. The 9.5 ± 0.6 m offset at the southern end of the Waitohi Section also fits this model with the 8.9 – 10.1 m of separation implying the preservation of five surface rupturing events of c. 1.8 - 2 m/event.

Normal separations calculated from the dextral-normal central Mt Noble section are shown in Figure 3.3. Two modes are apparent, one at c. 2.5 m and one at c. 5.2 – 5.7 m. Ratios of horizontal to vertical separation for sites where both are believed to be accurately preserved give a range of 3.51 – 4.20 (Table 3.1), emphasising the dominance of dextral slip on this section. By using the number of repeated c. 5 m single-event lateral displacements preserved at each of these sites, it is inferred that the single-event normal displacement for the Mt Noble Section is c. 1 – 1.5 m/event.

3.4.3. CHARACTERISTIC DISPLACEMENTS

The use of cumulative displacements along the NEF to estimate the average displacement per event is based on the important assumption that offset geomorphic markers measured along the fault preserve co-seismic displacement associated with surface-rupturing earthquakes and negligible interseismic slip/creep, an assumption that many historical observations of New Zealand faults have shown to be reasonable (Yetton 2000; Howard 2005; Wallace et al. 2007; McCalpin 2009).

The characteristic earthquake model of Schwartz and Coppersmith (1984) suggests that successive surface rupturing earthquakes produce the same amount of surface displacement with little variability of displacement for any given point at which cumulative offsets are measured. This assumption has been used widely in paleoseismic studies but is more difficult

to justify as data on repeated historic surface ruptures of the same fault does not exist in New Zealand and is extremely limited elsewhere. Because of this, the data on which this model is based is primarily from paleoseismic studies of other dominantly strike-slip faults. One recent study by Liu-Zeang et al. (2006) on the San Andreas Fault found that dextral displacements at a single site over the last six surface rupturing events varied from 5.2 ± 0.6 m to 8.0 ± 0.5 m with a the exception of a single 1.4 ± 0.5 m displacement. They describe the common occurrence of 7 to 8 m offsets as remarkably regular, but not strictly uniform, slip behaviour. Another recent paleoseismic study conducted on the Wellington Fault by Little et al. (2010) also found consistent slip per event for a single site over the last four earthquakes with a mean displacement of 5.0 ± 0.24 m and a root mean square scatter of slips about the mean of just 1.5 m (Little et al. 2010). Several other paleoseismic studies also reveal characteristic fault behaviour (e.g. the Awatere Fault (Benson et al. 2001) and the Emerson Fault (Rubin & Sieh 1997)) and studies of global data sets also indicate consistency in slip at a single point over repeated surface ruptures (Hecker, 2002, 2004). These studies give credit to the common simplification of assuming reasonably consistent slip per event over several earthquake cycles for any given site along a fault.

The consistency of dextral offsets measured to a multiple of c. 5 m on the NEF strongly suggests a consistent characteristic displacement for surface rupturing events along the Mt Noble Section in the absence of interseismic creep. The vertical separations measured for two distinct events at the Hurunui River Section and the consistency of cumulative displacements across the Waitohi Section strengthen the idea of characteristic displacements along the length of the NEF over a series of repeated surface rupturing events, a hypothesis that is also consistent with slip-rates and dated seismic events on these sections (see Section 4.3). As a result, any future surface ruptures could be expected to produce approximately 5 m of right-

lateral displacement along NE striking sections and c. 2 m of vertical displacement along the more northerly striking Hurunui River and Waitohi Sections.

3.5. STRUCTURE AND SEGMENTATION

The structural relationship between the eastern and western sections of the NEF has important implications for the kinematics of faulting as well as rupture length and therefore magnitude of surface rupturing events.

When projected across the late Quaternary gravels of the Waitohi Valley, the remarkably straight Waitohi Section strikes directly into the northern-most extent of the Gola Peaks Section (Figures 2.1A and 3.5). With the Waitohi section preserving over 9 metres of late Quaternary vertical displacement just 100 m north of the valley floor and a minimum of 7 m uplift of the bedrock surface at the riverside exposure (Figure 2.8), the possibility of the trace simply terminating within the c. 300 m width of the valley floor is considered very improbable. The modern river bed at this location turns to flow directly along the projected strike of the Waitohi section, towards the Gola Peaks exposure, hinting at a possible tectonic control on the location of the stream bed (Figures 2.1A and 2.7A). Bedrock is visible on both sides of the valley to the south of the Waitohi and Gola Peaks sections but is not exposed to the north, within the Waitohi Section's footwall. Additionally, the Gola Peaks Section cannot be traced further north in the field and its absence is marked by a drop in topography from over 1200 m at Gola Peak to c. 600 – 800 m in the north-east (Figure 1.3).

Given the substantial late Quaternary displacement on both the Waitohi and Gola Peaks sections, neither trace is likely to terminate within several hundred metres of their preserved traces. This leaves two basic geometries possible through the central NEF. The first is a direct link between the two sections, across the valley floor. The second is a significant change in

strike of the Waitohi Section towards the south-west, separating the fault sections into distinct eastern and western fault segments.

3.5.1. THROUGH-GOING WESTERN SEGMENT

The possibility of a link between the Waitohi and Gola Peaks sections raises interesting questions about the kinematics of the NEF and the relationships between topography, near surface fault geometry and the nature of faulting at depth. While the dip of the dextral-reverse Waitohi Section at the valley side is approximately 35°W, the dip measured at the Gola Peaks exposure is c. 35° to the east, implying a reversal of dip direction and relative displacement between the two sections, within the valley floor. Along the full length of the NEF all fault traces consistently dip towards the topographic highs, regardless of their sense of slip (Figure 2.1). The relationship between topography and surface expression is most obvious on the Mt Noble Section where a west-dipping reverse fault quickly develops into a west-dipping normal fault as it approaches the relatively high topography of Mt Noble (see Section 3.8).

The influence of topography on near surface fault dip has been investigated by a number of authors (e.g. Berrill (1988), Miller & Dunne (1996), Tibaldi (1998), Howard (2001)). Numerical and physical modelling of the basic interactions between fault traces and topography is in agreement with field observations of dominantly strike-slip faults such as the Porter-Pass Fault, which exhibits changes in dip direction and sense of slip at several locations where the position of topographic highs relative to the fault trace is reversed over a fault length of only a few hundred metres (Howard 2001). This effect is the result of increased shear strength of rock under topographic loading. Fault rupture will tend to take the path of least resistance, bending it away from the strengthened region, towards the valley (Berrill 1988) (Figure 3.7). Although this effect is relatively well understood for strike-slip

faults, the influence of strike-parallel topography on the surface expression of reverse faults has not been examined in detail.

The change in sense of slip between a true west thrusting section and a true east thrusting section across the Waitohi Valley would require extremely complicated fault geometry at depth and is not considered plausible. A more likely scenario would involve a near-vertical, dominantly strike-slip fault at depth being affected by topographically enhanced regional compression in the near-surface. In this case, topographic influences similar to those reported by Howard (2001) on the Porters-Pass Fault (Figure 3.7) would force the near-vertical fault plane away from the topographic highs in the near surface and thrust faulting may occur within the valley due to the amplification of regional compression as a result of the surrounding topography (Miller & Dunne 1996).

To assess the possibility of a direct link between western and eastern sections a seismic investigation was planned to search for evidence of faulting beneath the unfaulted river gravels at the ends of both the eastern and western sections. The original survey plan was to conduct two seismic reflection lines of approximately 400 m length, one on each side of the valley. The lines would be centred on top of the projected fault connecting the exposures on either side of the river with the distance between the lines being roughly equal to the distance from each line to the valley side (Figure 3.5A). Unfortunately, as a result of equipment and processing delays due to the Darfield and Christchurch earthquakes, only one line was able to be completed.

The seismic reflection survey was completed using a 48 channel seismometer with 5 m geophone spacing along the 425 m line. A sledge hammer and plate were used as a seismic source with a shot point spacing of 2.5 m (Figure 3.5B). The results of the seismic survey reveal several significant faults displacing bedrock beneath the valley floor. Figure 3.6 shows

Figure 3.5. A) Aerial photograph showing the location of the seismic reflection survey that was conducted in the Waitohi valley (solid yellow line). The proposed second line is also marked (dotted yellow line). See Figure 3.6 for the processed line. Location B refers to photo B. B) Looking south across the seismic line (dashed line). The seismograph set up can be seen in the foreground while a sledge hammer is used as a seismic source in the background. The location of the Gola Peaks exposure is marked to the left (GPE). The Waitohi River follows the line of poplar trees between the Waitohi and Gola Peaks Sections (refer to photo A).

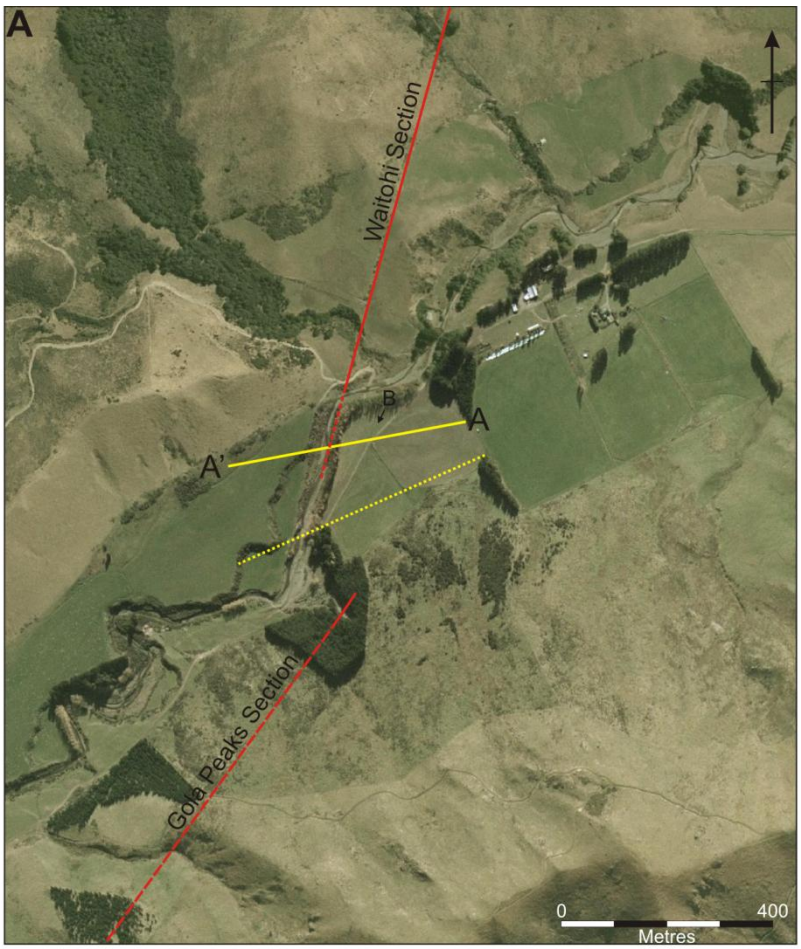
A
Waitohi Section
B
A
A'
Gora Peaks Section
0
400
Metres


B
GPE
Southern Geophysical Ltd

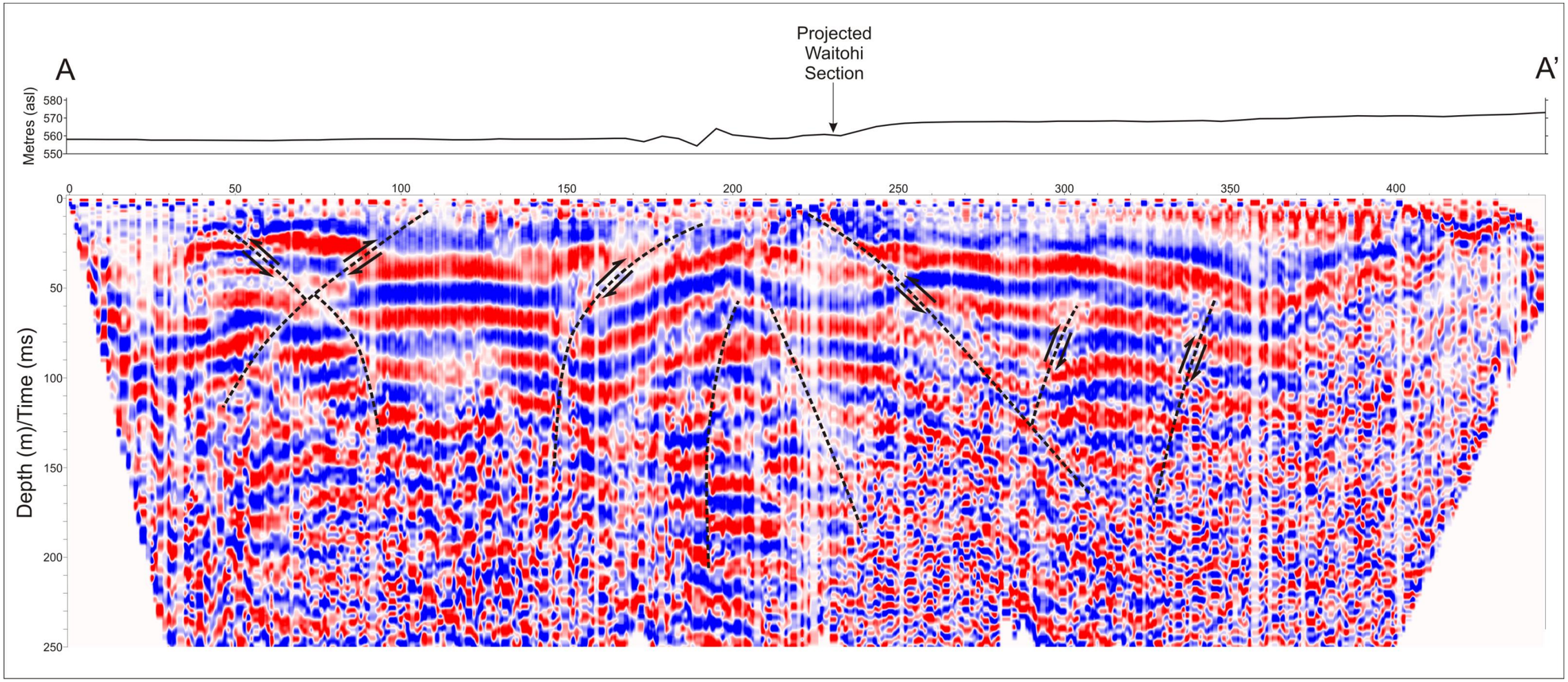

Figure 3.6. The processed seismic reflection survey conducted in the Waitohi Valley. Several faults are visible displacing strata of the Mesozoic bedrock. The position of the projected Waitohi Section is shown on the topographic profile above the seismic line. The west dipping reverse fault reaching the surface at c. 225 m is the hidden extension of the western Waitohi Section. Other structures in the profile have no known surface expression and may be inherited structures. Depth converted using 2000 m/s.See Figure 3.5 for section location.

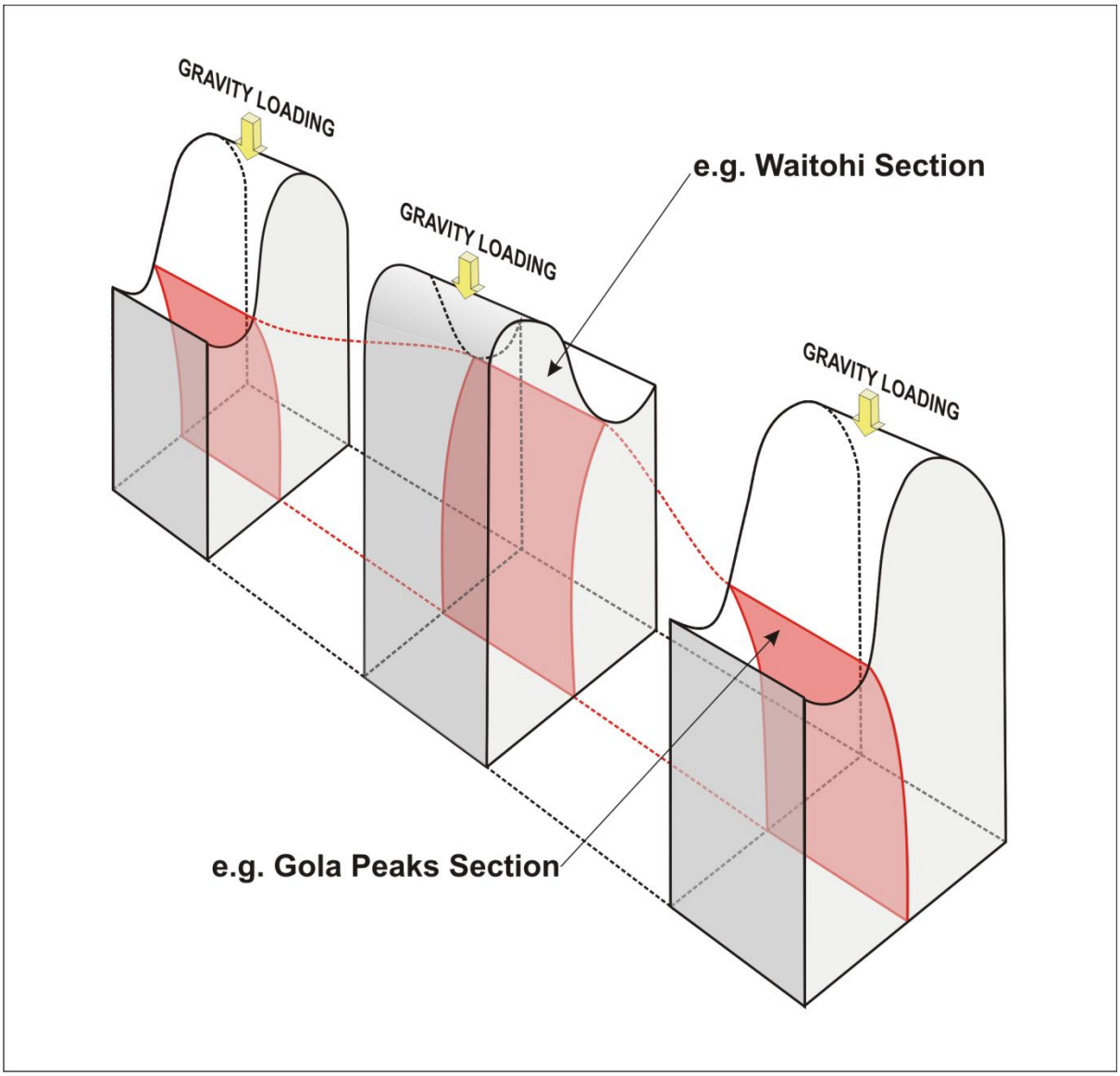

Figure 3.7. A schematic block diagram showing the affect of topographic loading on the near-surface dip of a vertical fault. Gravity loading increases the shear strength beneath high topography causing the fault to bend in towards the valleys. Modified from Howard (2001).

the processed seismic section with interpreted structure and the topographic profile along the line. The projected line of the Waitohi Section coincides with a west dipping thrust seen in the seismic section, confirming the continuation of the fault along strike for at least 100 m into the valley floor. At this point vertical displacement across the fault appears to be approximately 15 m though an unknown amount of erosion of the hanging wall means that the actual displacement could be much greater. Three significant east-dipping reverse faults extend to the near surface east of the Waitohi Section and may be associated with the east-dipping Gola Peaks Section. None of the east dipping fault seen in the seismic profile have any obvious surface expression in the valley floor.

3.5.2. SEPARATE EASTERN AND WESTERN SEGMENTS

The alternative geometry to a near-vertical through-going fault is that of structurally separate eastern and western fault segments. In this scenario the east-dipping Gola Peaks segment is likely to be a back-thrust off one of the west-dipping imbricate reverse faults that dominate the region (Pettinga et al. 2001), most likely the Waitohi Downs Fault, which breaks the surface < 10 km east of the Waitohi Valley.

The east-dipping reverse faults seen in the seismic reflection survey along the Waitohi valley represent a zone of complex compressional deformation where the opposing fault segments meet. This geometry is similar to that seen along the Harper Fault where opposing thrust faults converge across the Hamilton Creek to Cass River area (Chamberlain 1996). In the field the Gola Peaks Segment cannot be traced any further to the north and is inferred to continue along strike down the valley floor where evidence of late Quaternary displacement is quickly disguised by the Waitohi river.

The higher topography around and to the east of Mt Noble alludes to increased uplift to the north of the Gola Peaks Segment forcing the Waitohi River to cut a steeply sided, winding

Figure 3.8. Schematic block diagram of the Waitohi Valley and bounding ranges through Mt Whitnow Station showing possible fault geometry. The eastern and western sections of the NEF are split into separate faults with the east-dipping Gola Peaks Section depicted as a back thrust off the west dipping Waitohi Downs Fault. Fault splays branch off the Gola Peaks Section into the Waitohi Valley where they are overridden by the

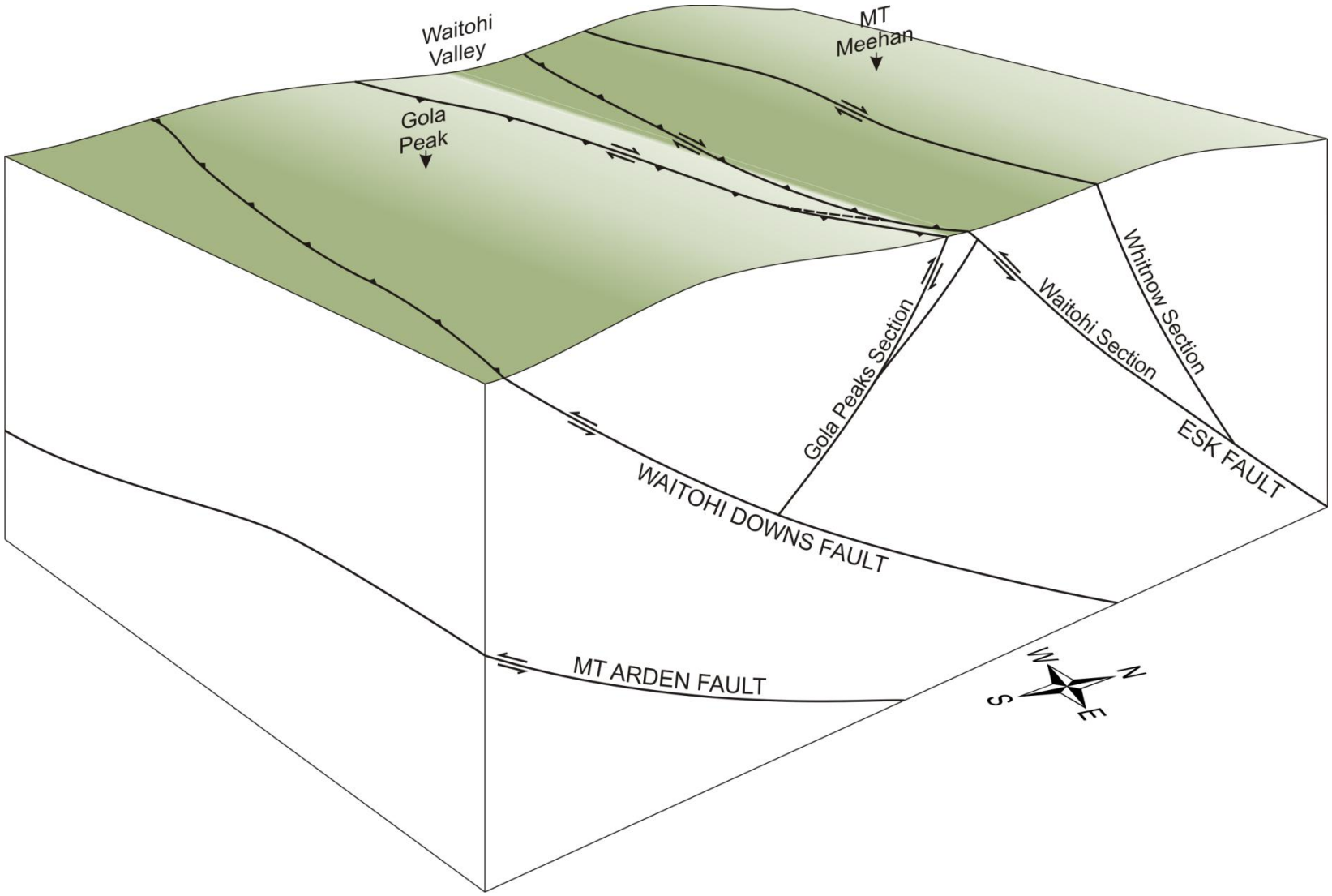
Waitohi
Valley
MT
Meehan
Gola
Peak
Gola Peaks Section
Waitohi Section
Whitnow Section
ESK FAULT
WAITOHI DOWNS FAULT
MT ARDEN FAULT
W
N
S
E

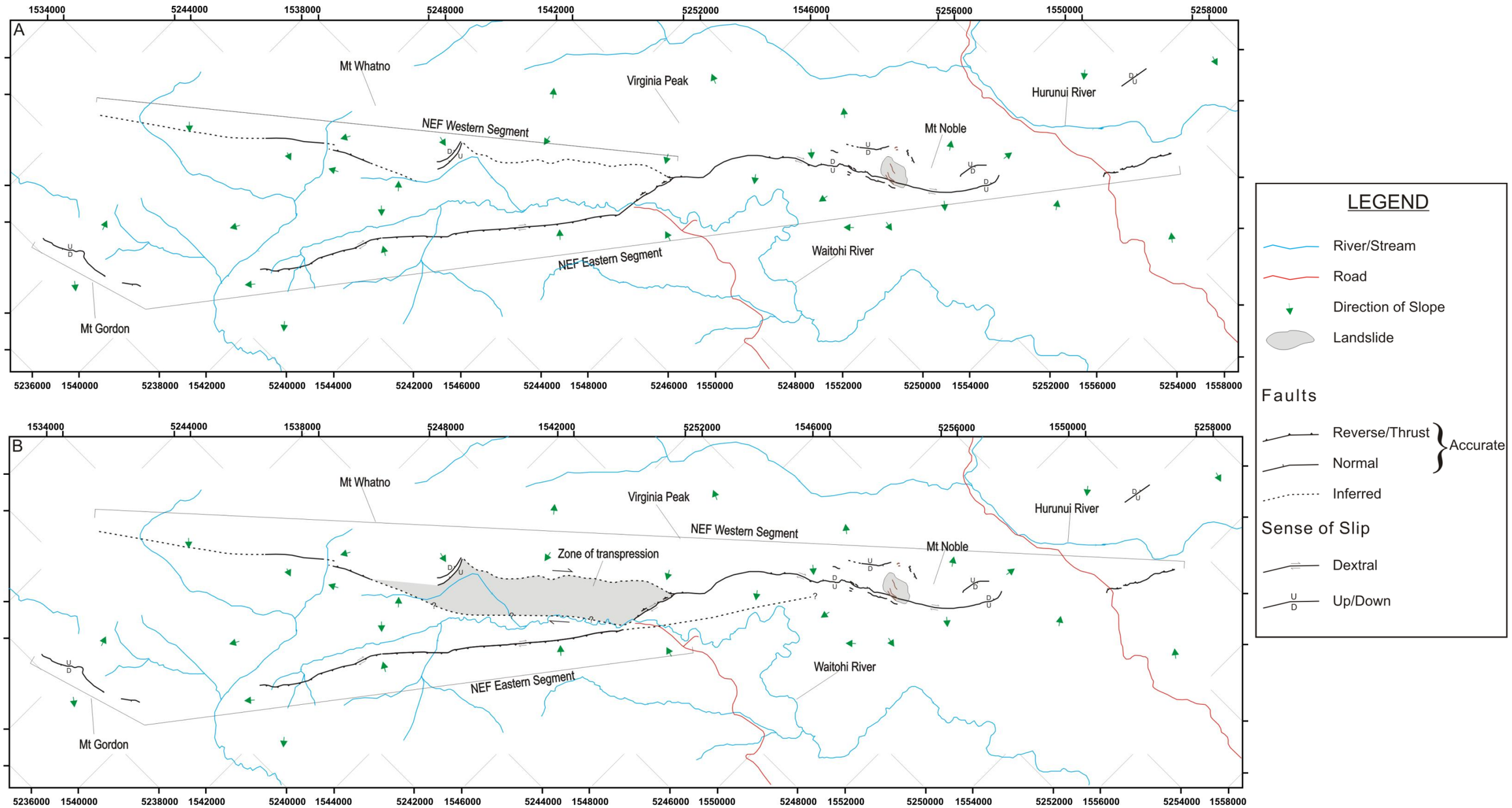

Figure 3.9. A) Map showing the NEF divided into a major eastern segment and shorter western segment. This model requires the fault plane to switch dip direction and sense of slip across the Waitohi Valley. This may be achieved by topographic loading over a near vertical fault plane similar to that seen on the Porters Pass Fault (Figure 3.7). B) Map showing the NEF divided into a major western segment and shorter eastern segment. This model requires a continuation of the Waitohi Section up the river valley, parallel to the Whitnow Section, creating a zone of transpressional deformation along the range front. East-dipping reverse faults seen in the seismic reflection survey are attributed to deformation in a zone of intense compression between the eastern and western segments with the eastern section being progressively overrun by the western Segment. See Figure 3.8 schematic block diagram across the Waitohi Valley and bounding ranges. Coordinates in NZTM.

gully out of the valley to arrive on the plains of the Culverden Basin. Interactions between back-thrusts associated with the Waitohi Downs Fault and possibly directly linked to the Gola Peaks Segment may be responsible for the relatively high elevation of Mt Noble as the NEF encroaches on and overrides the existing east-dipping fault segments (Figure 3.8).

The Waitohi Section is likely to change strike within the valley and continue southward along the western valley side, parallel to the dominantly dextral Whitnow Section, creating a wide zone of faulting along the western range front (Figure 3.9B). This proposed zone of faulting and rotation may explain the short sinistral traces observed along the Whitnow Section and the dispersed nature of faulting visible in aerial photography between the Waitohi and Whitnow Sections north of Mt Whatno. Strain partitioning between the Waitohi and Whitnow sections is also consistent with the lack of reverse separation seen in the Whitnow Section north of Mt Whatno and the c. 4 m of dextral slip preserved on the same section near the fork with the Waitohi Section. Slip partitioning on this scale is described by King et al. (2005) on the Kunlun Fault in Tibet and the mechanisms responsible for slip partitioning on oblique reverse faults are explained by Bowman et al. (2003).

The western NEF segment and eastern back-thrust model is considered the more likely of the two geometries presented here due to its relative simplicity and similarity to other known fault geometries in Canterbury such as the Harper and Bruce faults (Chamberlain 1996).

3.5.3. SURFACE RUPTURE LENGTH

In either segmentation scenario, the preserved rupture length of a single segment is c. 23 – 25 km. These estimates are based on a full rupture from the Hurunui River to Ashley Head on the western sections, or from the Hurunui River to Mt Gordon on the northern and eastern sections (Figure 3.9). The preserved rupture length is likely to be significantly shorter than the actual surface rupture (Wells & Coppersmith 1994; Stirling et al. 2002). With steep,

densely vegetated terrain to the south, identifying a degrading fault that may be thousands of years old becomes difficult. In the North, the Hurunui River Section dies out along the T6 terrace surface (see Figure 4.1). The absence of any preserved fault trace on the relatively subdued topography within 8 km of the Hurunui River Section, aside from a 700 m long uphill-facing scarp on Mt Miza, is a strong indication (Wesnousky 2008) that late Quaternary ruptures on the NEF have terminated within the Hurunui River valley.

3.6. KINEMATICS

Resolving the kinematics of fault rupture is important for understanding the way strain is accommodated across the NEF. Comparisons of NEF derived principle strain axes and slip vectors with local historic seismicity, previous structural studies in the area and the wider plate boundary setting allow qualitative and quantitative resolution of the NEFs role in accommodating unaccounted for strain in North Canterbury. In this study these important parameters are obtained through net displacement data, fault plane striations and historic seismicity.

3.6.2. NET DISPLACEMENT

Net displacement on any fault is a function of fault dip, vertical separation and lateral separation. For the NEF all of these parameters vary widely along the preserved fault trace. Both normal and reverse scarps, dextral and sinistral offsets and east and west dipping fault planes are present.

Where fault dip and strike are known, offset geomorphic markers can be used to determine the net displacements and slip vector for that section of the fault. Along the NEF this is possible at one location on the Hurunui terraces, one location on the Whitnow Section and

Figure 3.10. Slip vectors obtained from fault plane striations (1 & 2) and offset geomorphic markers (3 – 6). Arrows show the azimuth of hanging wall movement and plunge is shown for each vector (negative numbers = down, positive numbers = up). Fault plane solutions correspond to locations on map. The Pacific Plate motion vector relative to the Australian Plate is shown at top right (DeMets. 1990, 1994). NEF = Northern Esk Fault, WDF = Waitohi Downs Fault.

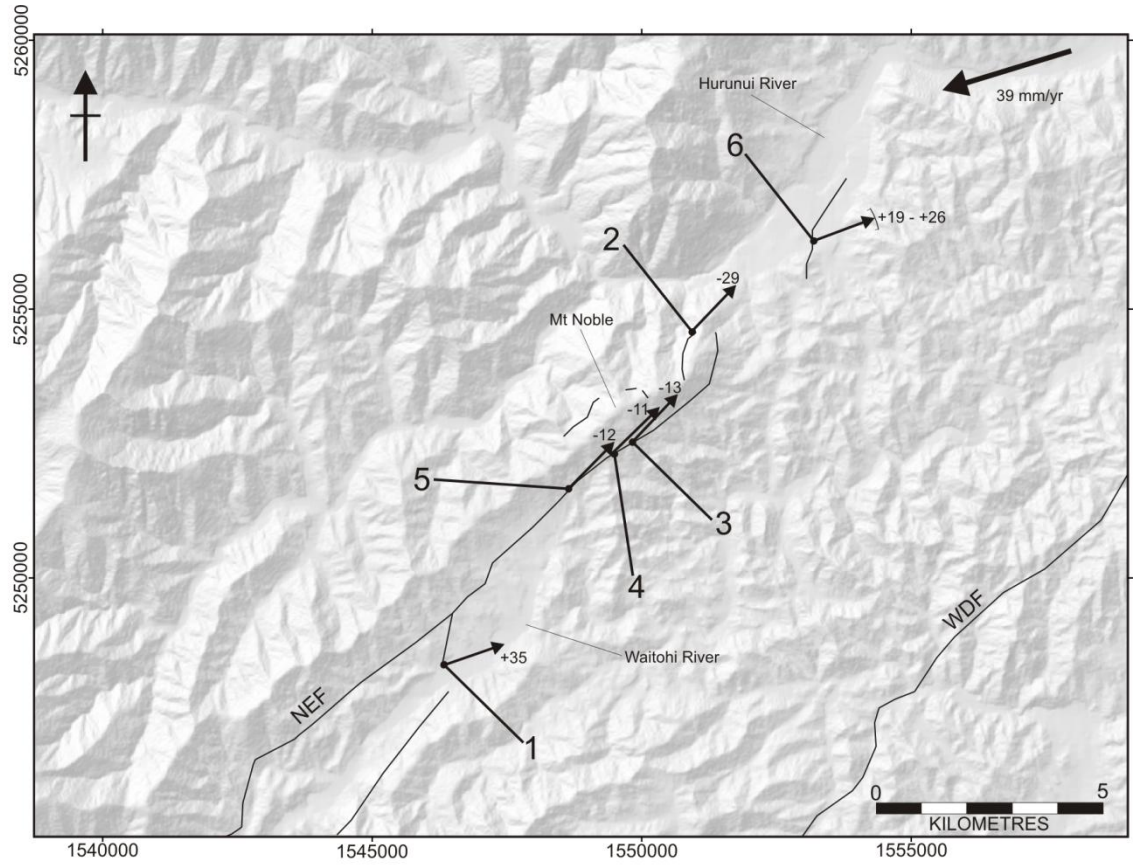
5260000
5255000
5250000
1540000
1545000
1550000
1555000
Hurunui River
39 mm/yr
6
+19 - +26
2
-29
Mt Noble
-13
-11
-12
5
3
4
+35
Waitohi River
NEF
WDF
1
0
5
KILOMETRES

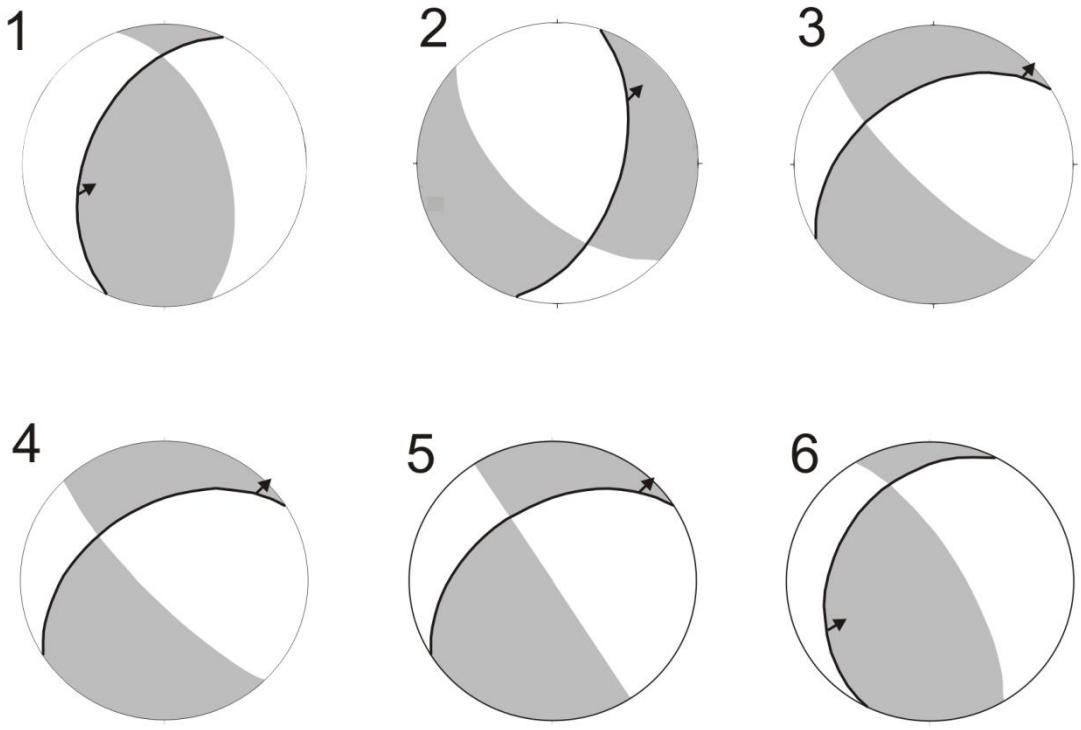
1
2
3
4
5
6

Figure 3.11. P and T axes obtained from fault plane striations (1 & 2) and offset geomorphic markers (3 – 6). Bars show the orientation of the P-axes for each solution while double headed arrows represent the T-axes. Plunges are shown for each axis (negative numbers = down, positive numbers = up). Fault plane solutions correspond to locations on map. Red points are P-axes, blue point T-axes. For simplicity, locations 3 and 4 in Figure 3.10 have been combined as location 3. NEF = Northern Esk Fault, WDF = Waitohi Downs Fault.

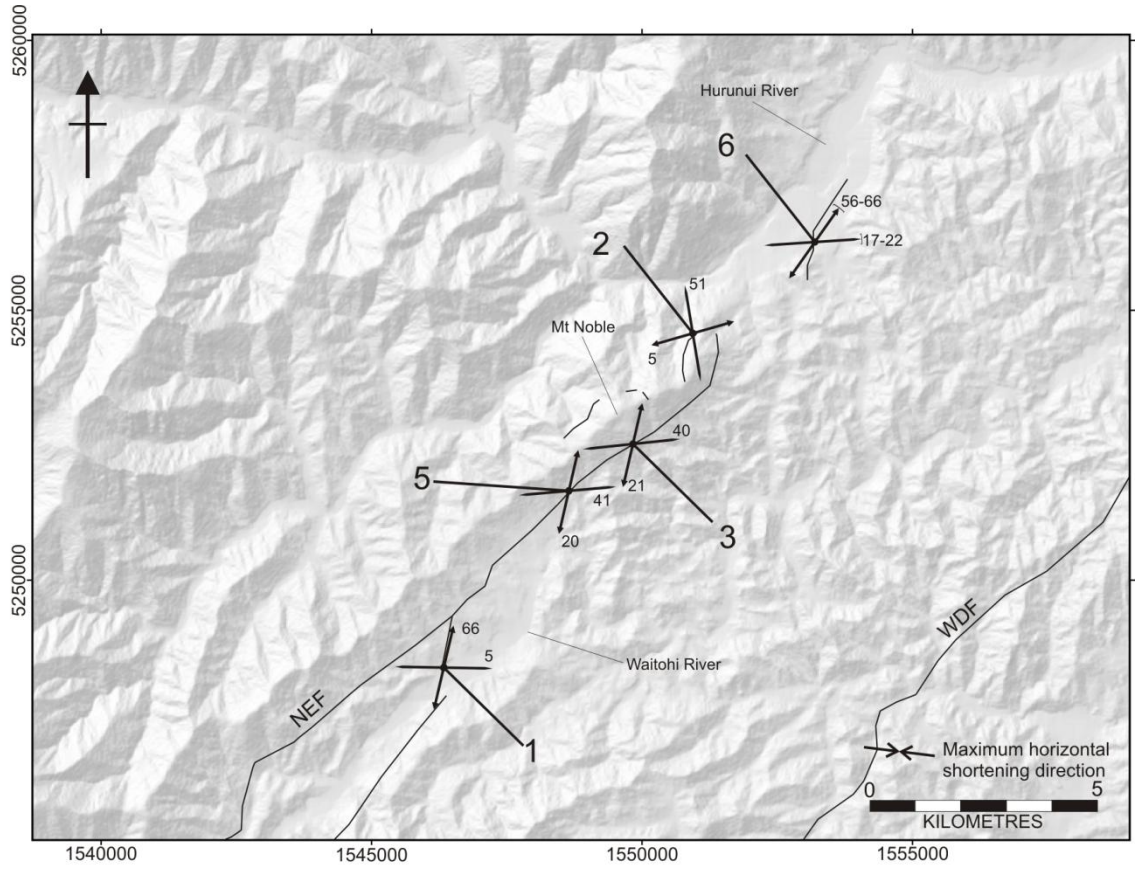
5260000
5255000
5250000
1540000
1545000
1550000
1555000
Hurunui River
6
56-66
17-22
2
51
5
Mt Noble
40
5
41
21
20
3
66
5
Waitohi River
1
NEF
WDF
Maximum horizontal
shortening direction
0
5
KILOMETRES

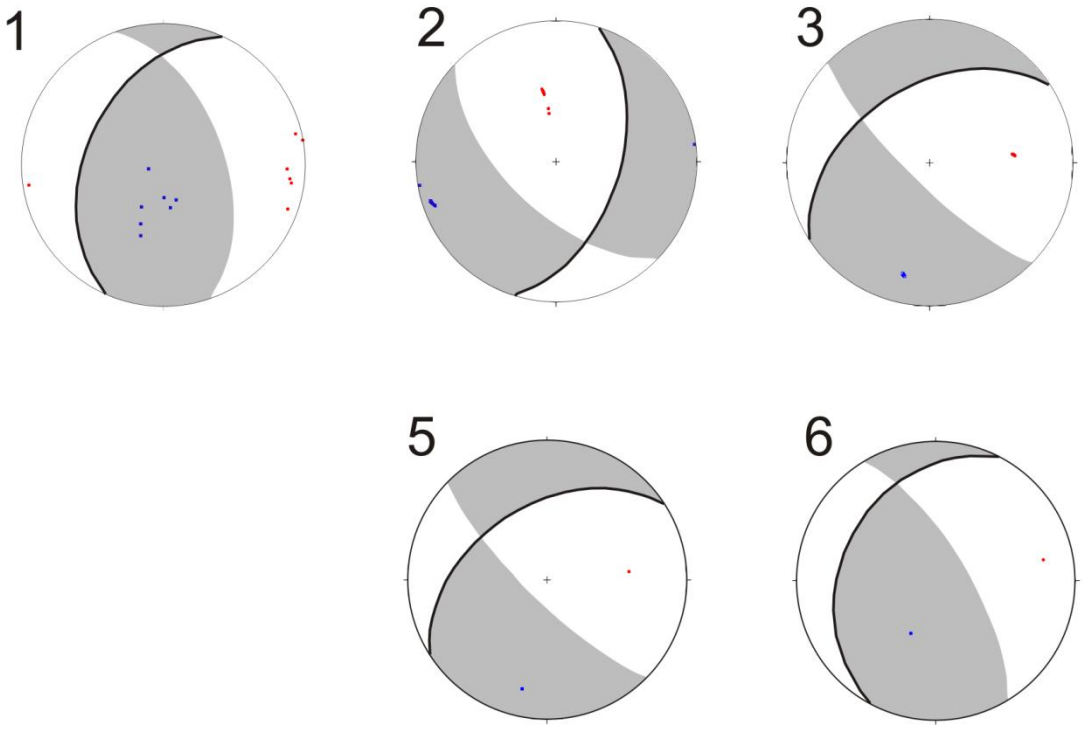
1
2
3
5
6

three locations on the Mt Noble Section. At all other locations where separations were measured net slip calculations were not possible due to either only having a vertical or horizontal separation or because the vertically and horizontally offset features are not believed to preserve the same number of events.

The slip vectors derived from offset geomorphic features are displayed in Figure 3.10 (numbers 3 – 6). The data shows a significant difference in the azimuth of hanging wall movement between the two available sections of the fault, changing from c. 044° on the Mt Noble Section to c. 070° on the Hurunui River Section. The Mt Noble Section alone has a very tight range of 044° - 046° over the three measured sites.

The errors involved in measuring a lateral separation at the Hurunui River site have been included in net slip calculations and the range of possible azimuths for dextral slip of less than 5 m are shown in Figure 3.10. Errors have not been included for the Mt Noble sites as they are deemed too small to be relevant at this scale (on the order of c. 5°).

Assuming a single event lateral displacement of ≤ 5 m, the slip vector range produced for the Hurunui Section is reduced to 060 - 079°. This range encompasses the regional plate motion vector of 073° (reciprocal of 253°) (DeMets et al. 1990; DeMets et al. 1994). As a result of the normal component of displacement, the Mt Noble Section slip vectors differ from the plate motion vector by 27 - 29°W.

From the slip vectors we can calculate the axes of maximum compression and maximum tension (P-axis and T-axis respectively). These axes are displayed in Figure 3.11 for the Mt Noble and Hurunui River sites. The P-axes show a WNW – ESE trend and differ by only a few degrees in the horizontal between the Mt Noble and Hurunui sections. The T axes consistently trend NNE – SSW and differ by c. 23° between fault sections.

3.6.3. FAULT PLANE STRIATIONS

Striations were found and measured at two fault plane exposures along the NEF and are inferred to reflect the slip vector of characteristic fault ruptures for individual fault sections.

The two exposures were found on the dextral-reverse Waitohi Section and an antithetic sinistral-normal scarp on the north-western slope of Mt Noble (see Figure 3.1 for locations). At each exposure the strike and dip of the fault plane and the trend and plunge of any striations were recorded. Slip vectors produced from these measurements are shown in Figure 3.10 and P and T axes are shown in Figure 3.11 (numbers 1 & 2). The slip vector for the Waitohi Section exposure is consistent with that derived from net displacement on the Hurunui River Section, trending c. 071°, just 2° from the plate motion vector. The slip vector derived for the sinistral northwest Mt Noble exposure also trends northeast but at a higher angle (29°) to the plate motion vector.

The P and T axes of the Waitohi Section striations are also highly consistent with those calculated for the Hurunui Section, differing in the horizontal plane by just c. 4° and c. 22° respectively while the plunge of the axes differ by 10 - 17°. These results are also comparable to previous studies in North Canterbury, which have found predominantly W-NW oriented compression. The consistent kinematic results for two geomorphically similar fault sections reinforce the validity of earlier comparisons between the two scarps when calculating single event displacements.

The P and T axes derived from the sinistral-normal northwest Mt Noble exposure differ significantly from all other net displacement and striation derived axes. The P-axis trends NNW while the T axis trends ENE. These inconsistencies suggest gravity driven movement on this minor fault trace.

3.7. HISTORIC SEISMICITY

The kinematics of historic seismicity in close proximity to known surface faults can give an indication of local stress orientations and slip vectors where historic surface ruptures do not exist. In North Canterbury the New Zealand National Seismograph Network is dense enough to allow the resolution of first-motion focal mechanisms for selected shallow earthquakes of local magnitude (M_L) greater than c. 3.2.

For the purpose of this study all recorded earthquakes within 15 km of the preserved surface trace of the NEF since January 2004 were manually examined to find first-motion focal mechanisms and slip vectors for each one. Many of the earthquakes were not able to be resolved or were resolved too poorly to be reputable due to too few seismographs picking up the event or the first motions being lost in the background noise. Of the 153 recorded earthquakes of M_w> 1.6 just 9 were able to be resolved to a reasonable standard. Each of these solutions involved the use of first motions from at least 6 individual seismometers and produced P and T axis scatter over less than one quadrant of the lower hemisphere projection (see Appendix B for focal solutions). Additionally, two earthquakes reported by Cowan (1992) from his 1990 North Canterbury Microearthquake Network study lie within the NEF study area and are also used here. The resulting focal mechanisms and P and T axes of all 11 earthquakes are shown in Figures 3.12 and 3.13. Of the 11 mechanisms produced two lie in a position which may place them on the NEF at depth (#2263205 and #2274769 Figure 3.12), though the depth of these events (c. 6 – 10 km) and their close proximity to the surface trace mean that they probably lie underneath the west-dipping fault plane, within the footwall.

In each solution two nodal planes are found, one of which must give the correct orientation of the actual fault plane. Nine of the 11 solutions involve a NE striking dextral fault and a SW striking sinistral fault, each with varying amounts of dip-slip. Due to the northeast trend of

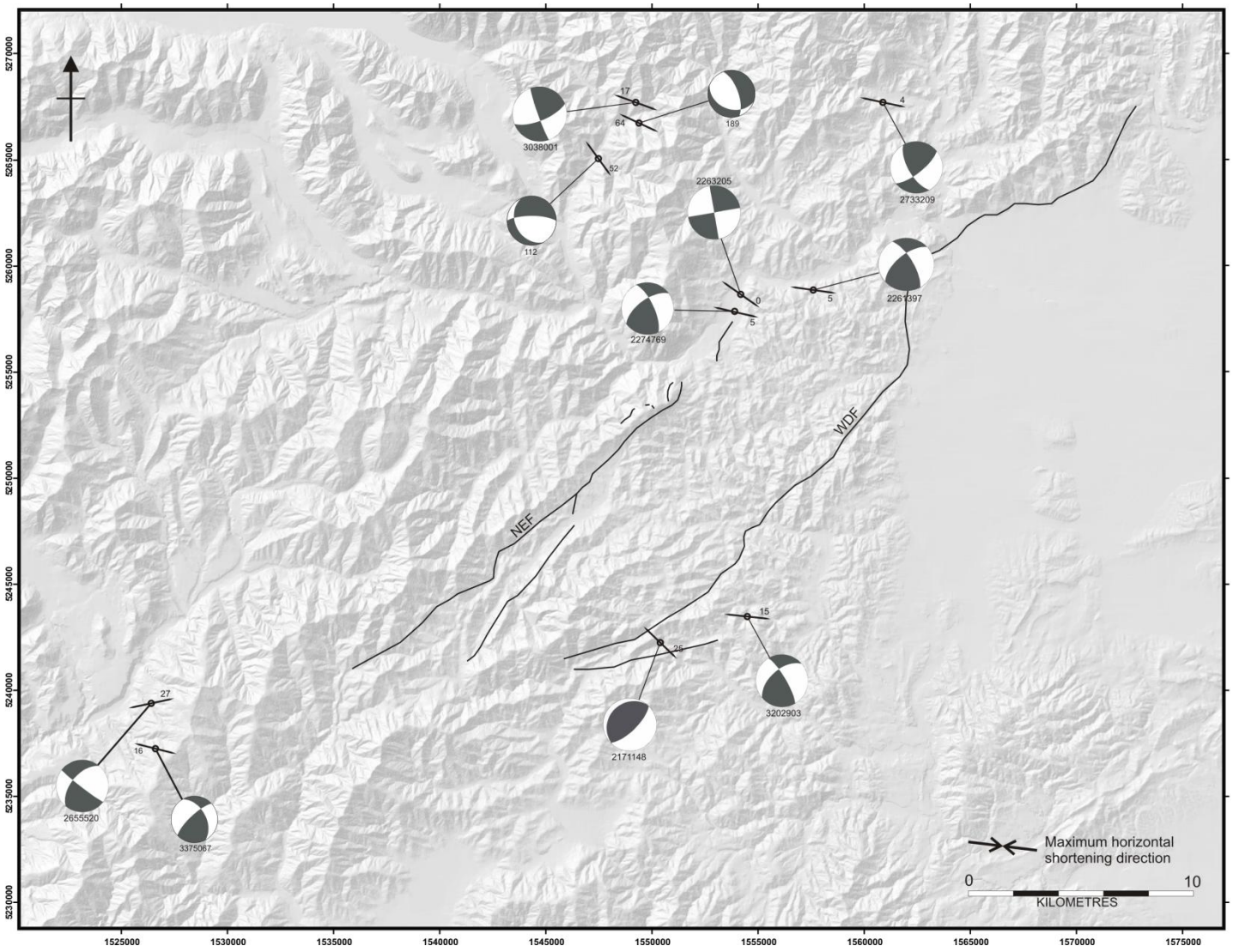

Figure 3.12. Map of focal mechanisms and related P-axes for resolved earthquakes occurring between January 2004 and March 2011 with 2 additional events recorded by Cowan (1992). Bars show the P-axis for each event. Plunge is shown next to each axis. Focal mechanisms are lower hemisphere projections. NEF = Northern Esk Fault, WDF = Waitohi Downs Fault. Maximum horizontal shortening direction from Wallace et al. (2007).

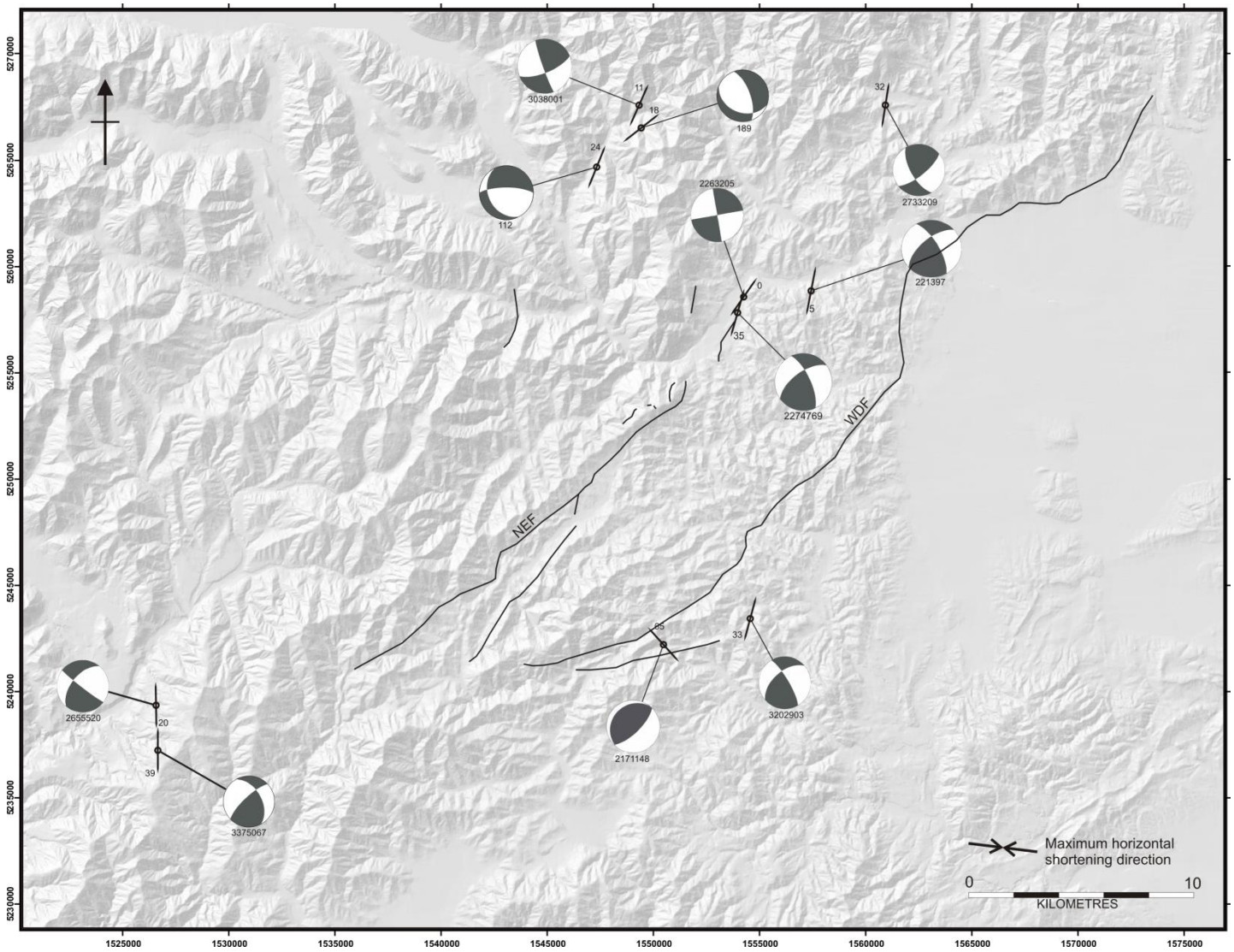

Figure 3.13. Map of focal mechanisms and related T-axes for resolved earthquakes occurring between January 2004 and March 2011 with 2 additional events recorded by Cowan (1992). Bars show the T-axis for each event. Plunge is shown next to each axis. Focal mechanisms are lower hemisphere projections. NEF = Northern Esk Fault, WDF = Waitohi Downs Fault. Maximum horizontal shortening direction from Wallace et al. (2007).

the major surface faults such as the northern and southern Esk Faults, the Waitohi Downs Fault and numerous smaller faults in the area, the ENE trend of the major Marlborough faults to the north and Porters Pass – Amberley fault zone to the south as well as dominantly dextral nature of all of these faults, it is likely that in most cases the northeast striking fault is likely to be the actual fault plane for each of these solutions; However, with sinistral displacements measured within the field area, the SW striking, sinistral nodal planes cannot be ruled out completely.

The P and T axes derived from historic seismicity are fairly consistent with all but one P axis trending W to NW and all but three T axes trending NE – SW. P-axes are generally sub-horizontal, while most T-axes dip moderately NE or SW.

3.8. DISCUSSION

The historic seismicity data over the preceding seven year period shows a highly consistent stress field across the North Canterbury study area. Not only is the data internally consistent but also fits well with the data collected directly from the NEF in the form of net displacement and fault plane striations. Although the majority of resolved earthquakes did not occur on the NEF, the results give a good overview of the stress regime in which the NEF lies.

Several other structural and seismic studies in North Canterbury have found similar stress field results. These include the microearthquake study of Cowan (1992) who found that with few exceptions, contractional strain axes (P-axes) for shallow events in the Porters Pass-Amberley Fault Zone and wider Canterbury foothills region were uniformly orientated WNW-NW, as are eight of the additional nine earthquakes used in this study.

In two recent studies conducted by Wallace et al. (2007, In review), principal strain rates through North Canterbury were modelled using a combination of geologic data and GPS site velocities. The two studies use largely the same data for the upper South Island but produce quite different results for North Canterbury. Wallace et al. (2007) report contractional and extensional strain axes of ε_1 = 097° ± 8° and ε_2 = 187 ± 8° respectively. Wallace et al. (In review) report contractional axes orientated at ε_1 = 77.98° ± 20.07° and ε_2 = 167° ± 20.07°. The ε_2 axis of Wallace et al. (In review) is reported as an axis of contractional strain within the NCB. This hypothesis is in contrast to the results obtained from both the Waitohi and Mt Noble sections of the NEF (Figure 3.11) and the historic seismicity in the study area (Figure 3.12, 3.13). The full range of orientations of ε_2 provided by Wallace et al. (In review) fits entirely within the tensional segment of the offset-derived Mt Noble Section focal mechanism (Figure 3.14). When compared to the striation-derived Waitohi Section focal mechanism, the range of ε_2 orientations fits mostly within the tensional segment but could be contractional if the axes trend is more towards the NW end of the range. In contrast, the contractional and extensional strain axes proposed by Wallace et al. (2007) both fit neatly within the appropriate segments of the Mt Noble and Waitohi Section focal mechanisms (Figure 3.14) and as a result have a close fit to the maximum stress axes derived from the NEF and from historic seismicity. The findings of Wallace et al. (2007) are also in agreement with the geologic and seismic studies of Cowan (1992), Cowan (1990) and McMorran (1991), which all found predominantly NNW – WNW contraction with NNE-NE oriented extension in North Canterbury.

Extensional axes in the NEF study area are also consistent with the NE – SW trend described by Cowan (1990, 1992) and McMorran (1991). Syme (1991) and Mould (1992), however, report contraction orientated both NW-SE and to a lesser degree NE-SW as well as localised

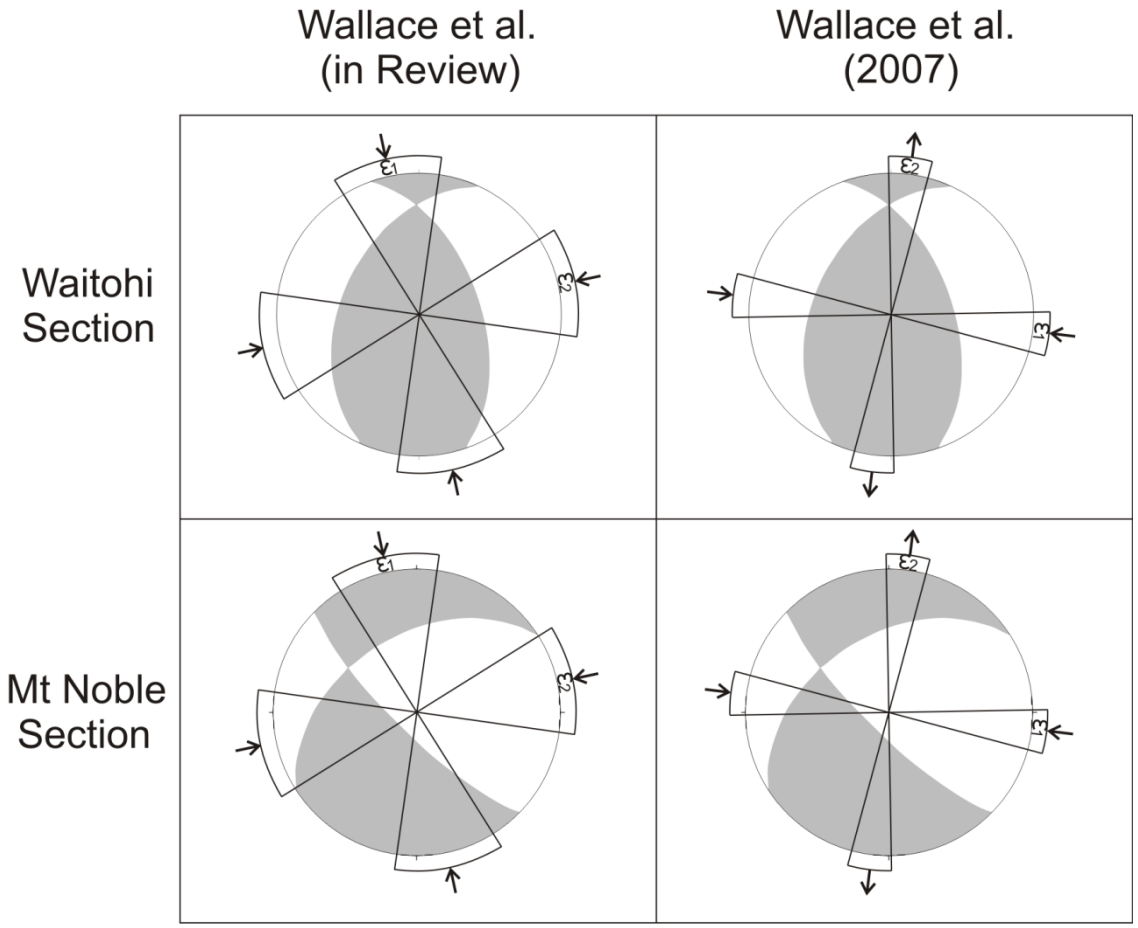

Figure 3.14. Comparison of the horizontal stress axes reported in the studies of Wallace et al. (In review) and Wallace et al. (2007) (ε_1 and ε_2) with the stress fields derived from kinematic analysis of the Waitohi and Mt Noble Sections (beach balls). The horizontal stresses derived from the NEF coincide with those reported by Wallace et al. (2007) while the contractional ε_1 axis of Wallace (In review) lays mostly within the extensional sector of the NEF derived stress fields at the horizontal.

near vertical extension. These latter two studies are more in keeping with the dual horizontal contraction axes of Wallace et al. (In review).

The two models of Wallace et al. (2007, In review) appear to reflect localised strain partitioning within the NCB across very short distances (Mould. 1992, Syme. 1991, Nicol. 1991). Within the NEF study area, minor faulting recorded between 2004 and 2011 reflects the style of deformation observed along the NEF itself. This spatial relationship between small scale faulting and the more significant faults such as the Esk or Waitohi Downs faults was also noted by Mould (1992) along the western margin of the Culverden Basin, just a few kilometres from the NEF and within the historic seismicity study area. As a result, the stress field within which the NEF lies is consistent with the dominant NW-SE compression found in all seismic and geological studies in North Canterbury over the last c. 20 years with an additional gently inclined to sub-horizontal extensional axis oriented NNW, consistent with the findings of Cowan (1990, 1992), McMorran (1991) and Wallace et al. (2007).

The dextral-normal Mt Noble section, however, does show a slight deviation from the general W-NW trend of P-axes within the study area. On the Mt Noble main trace the P-axes trend slightly to the WSW and dip moderately steeply to the east. Slip vectors produced for this section consistently trend c. 30° north of the plate motion vector, a more northerly trend than all but one of the historic earthquake slip vectors. The differences are even greater for the antithetic normal-sinistral scarp on the north-western slope of Mt Noble (#2, Figure 3.11) where the P and T axes are reversed.

These apparent local changes in the regional stress field are likely to be the result of gravitational tectonic processes along this dominantly dextral section of the main trace. The change in strike from 012 - 027° on the dextral-reverse section to c. 057° on the Mt Noble section is consistent with a change from reverse dominated slip to dextrally dominated slip

but given the regional stress field and the slip vectors of 60 - 79° found for other sections of the fault, a minor component of reverse slip could be expected along this section. Preserved normal separation on the Mt Noble section increases to the north with increasing elevation of the ridgeline. This change also coincides with an area of sub-parallel trending structural grain of the bedrock, which is at a higher angle to the fault along most other sections (Nathan 2002; Rattenbury et al. 2006; Forsyth et al. 2008) (see Attached Map). This relationship suggests a topographic influence on the vertical component of slip. Added to this is the presence of a series of discontinuous east-dipping normal faults on the western side of Mt Noble sub-parallel to the main trace (Figure 2.1 and Attached Map). These uphill facing scarps reveal an inward collapse of the Mt Noble ridgeline along a c. 2 km section encompassing the highest peak, in a fashion similar to that described by Beck (1968). In a study of topographic affects on regional stress, Miller & Dunne (1996) demonstrate that high regional compression combined with high topography can cause tension at ridge tops and increased compression within valleys. This is consistent with the normal component of slip of Mt Noble being a local topographic effect within a wider region of NW-SE compression (Figure 3.15). Given all these factors it is evident that although the apparent surface deformation along this section of the NEF is dextral-normal the wider deformation across the range is likely to be compressional and may manifest as broad folding of the range or small-scale slip on distributed faults within the hanging wall (Nicol & Van Dissen 2002). These processes work against the gravitational collapse of Mt Noble to maintain the obvious increase in mountain-top elevation west of the Waitohi River.

The anomalous stress axes (Figure 3.11) and slip vector (Figure 3.10) derived from a well striated exposure of north-western Mt Noble also point to gravitational tectonic stresses. The wedge of hillside bound by the northern tip of the Mt Noble main trace to the east and a significant east dipping normal-sinistral fault to the west is slipping down and away from Mt

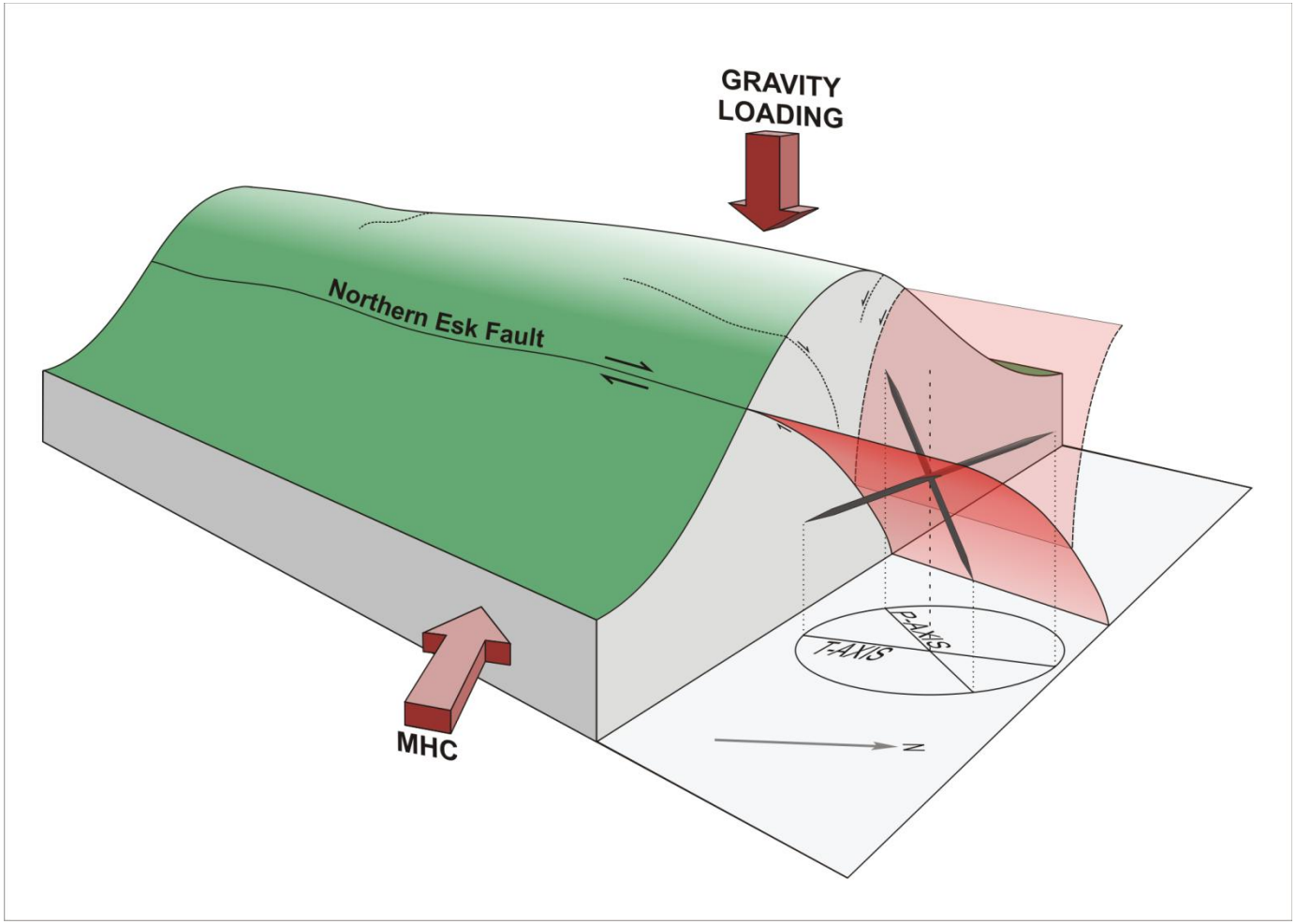

Figure 3.15. Schematic block diagram of Mt Noble showing the inward collapse of the ridge top. The WNW trending axis of Maximum Horizontal Compression (MHC) combined with the topographic loading around the peak of Mt Noble force the P-Axis to plunge at approximately 40° to the east resulting in normal movement on the west-dipping Mt Noble Section. Numerous small, discontinuous, normal faults on the western slopes help to accommodate vertical contraction.

Noble towards the northeast. Although substantially driven by gravity, the movement of this block is likely to be coseismic as it is bound by the main trace to the east.

3.9. SUMMARY

- Tape measure, laser rangefinder and differential GPS measurements across 20 offset geomorphic and stratigraphic markers reveal lateral and vertical separations of up to 23.7 ± 3 and 13.5 ± 1.5 m respectively.

- Single and double event vertical displacements identified on the Hurunui Terraces and cumulative displacements on the Waitohi Section indicate a characteristic vertical displacement of c. 2 m/event.

- The smallest lateral offsets identified on the eastern sections are no less than 4 m and cumulative lateral displacements consistently cluster around multiples of c. 5 m, consistent with a characteristic lateral displacement of c. 5 m/event.

- A seismic reflection survey confirms the continuation of the Waitohi Section into the valley floor and the presence of several east dipping reverse faults to the northeast. Due to the complicated geometry required for a through-going fault, the preferred model is that of two opposing thrust segments with the Gola Peaks Segment likely to be a back-thrust associated with the west-dipping Waitohi Downs Fault.

- Consistent strain axes derived from striations and offset data on the Waitohi and Hurunui River Sections indicate that a similar style of deformation is occurring on similarly striking fault sections.

- Historic seismicity within 15 km of the NEF has been used to assess the regional stress field. The results show dominant WNW – NW oriented compression and SE

extension, consistent with the deformation seen at the surface and with numerous kinematic and seismological studies in North Canterbury.

- Deviations in stress axes on normal sections of the NEF coincide with high topography and imply a gravitational influence on surface faulting in these areas.

CHAPTER 4
PALEOSEISMICITY

4.1. OVERVIEW

While geomorphic and kinematic studies provide insight into the style of deformation occurring on the NEF, a more detailed study of paleoearthquakes is needed to quantify the strain accommodated by the NEF and accurately assess the hazard posed to the region by future surface rupturing events.

In this study Optically Stimulated Luminescence (OSL) and radiocarbon (^{14}C) dating techniques are employed at three sites along the eastern sections of the NEF to constrain the timing of the two most recent surface ruptures and to calculate average late Quaternary slip-rates and recurrence intervals. Together with the kinematic analysis and estimates of probable paleoearthquake magnitudes through fault scaling relationships, this study aims to resolve some of the so far unaccounted-for strain occurring outside of the major strike slip faults of the Marlborough and Porters Pass fault systems and revise the current understanding of the NEF as a hazard in North Canterbury.

4.2. TIMING OF EARTHQUAKES

Constraining the timing of paleoearthquakes is an important step towards assessing the probability of a surface rupturing earthquake on the NEF in the near future. Two sites were chosen for dating the two most recent surface rupturing events using OSL and ^{14}C dating techniques.

4.2.1. HURUNUI TERRACES

The faulted terraces of the Hurunui River Section provide an excellent opportunity to constrain the timing of the two most recent surface ruptures. As described in section 3.4.2., two individual events can be distinguished by a reduction in vertical separation of the terrace treads from the second highest terrace (T2 Figure 4.1) to the third, fifth and sixth highest terraces (T3 - T6 Figure 4.1) of the Hurunui River at Sheep Yard Basin.

By dating the abandonment ages of the T2, T3 and T6 terrace treads we can constrain the timing of these two most recent events. Because vertical displacement of the terrace tread is being used we know that any preserved separation of the terrace surface must have occurred after the surface was abandoned, avoiding the ambiguity that can arise from using lateral displacements of terrace risers, which may have been trimmed after faulting (Gold et al. 2009). Using this principle, the penultimate surface rupturing event (from here on referred to as Event 2) must have occurred after the abandonment of T2 but before the abandonment of T3. The latest event (Event 1) must have occurred after the abandonment of T6.

The fault trace dies out within T6 and there is very little deformation outside of the c. 5 to 10 m wide fault zone along the majority of the section. As a result, it is very difficult to determine whether any of the lower, younger terraces were abandoned before or after Event 1. Differential GPS profiles across T8 and T6, perpendicular to faulting on T5 do not reveal any obvious warping or tilting of the terraces that would help to indicate their presence during one or both surface rupturing events. Because of this, only a maximum age of rupture for Event 1 can be obtained from this site, by dating T6.

Optically Stimulated Luminescence dating was used on each of the three useful faulted terraces (T2, T3 and T6). OSL was chosen over radiocarbon dating at this site for two main reasons. Firstly, not all terrace treads contained suitable organic material for ^{14}C dating within

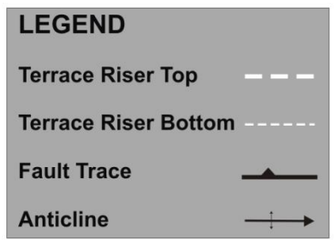

Figure 4.1. Aerial photograph mosaic of the Hurunui River Section. Terrace surfaces are labelled from the highest terrace (T1) to the lowest terrace in the image (T11). The locations of OSL sample sites are marked on terraces T2, T3 and T6. At the northern extent of the fault trace a broad anticline has developed adjacent to the diminishing scarp before both die out to the north, within T6. Ponded drainage can be seen on the downthrown side of terraces T5 and T6. The apparent jog in the surface trace between T3 and T5 has been used to calculate a likely near surface dip of c. 32°.

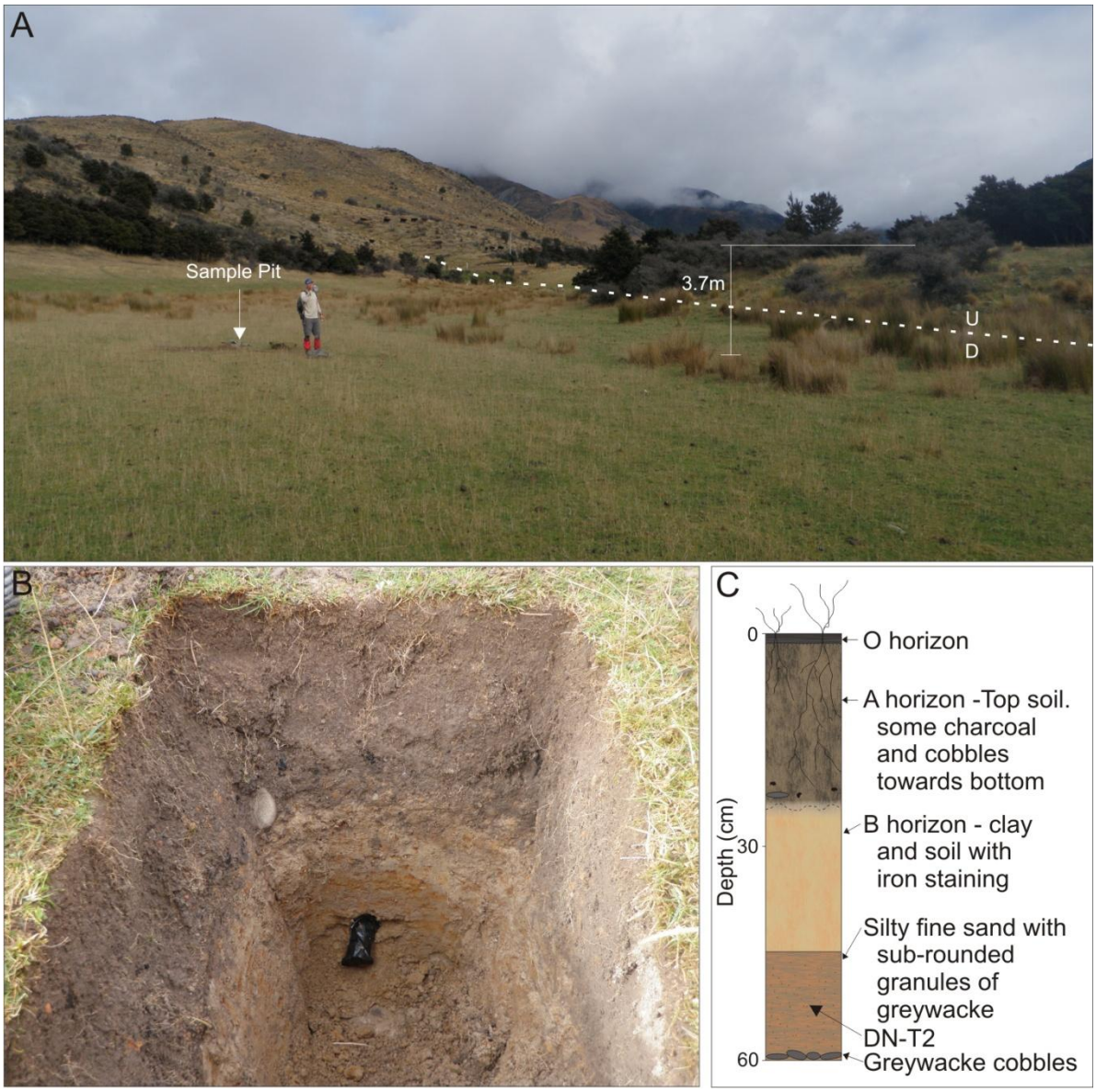

Figure 4.2. A) The site at which OSL sample DN-T2 was collected. The two event-preserving scarp can be seen in the background and the fault trace is marked at the base of the scarp (dashed line). B) The sample pit with DN-T2 still in position. Charcoal can be seen near the bottom of the A-horizon. C) A simple stratigraphic column of the soils and alluvial units on T2. See Figure 4.1 for location.

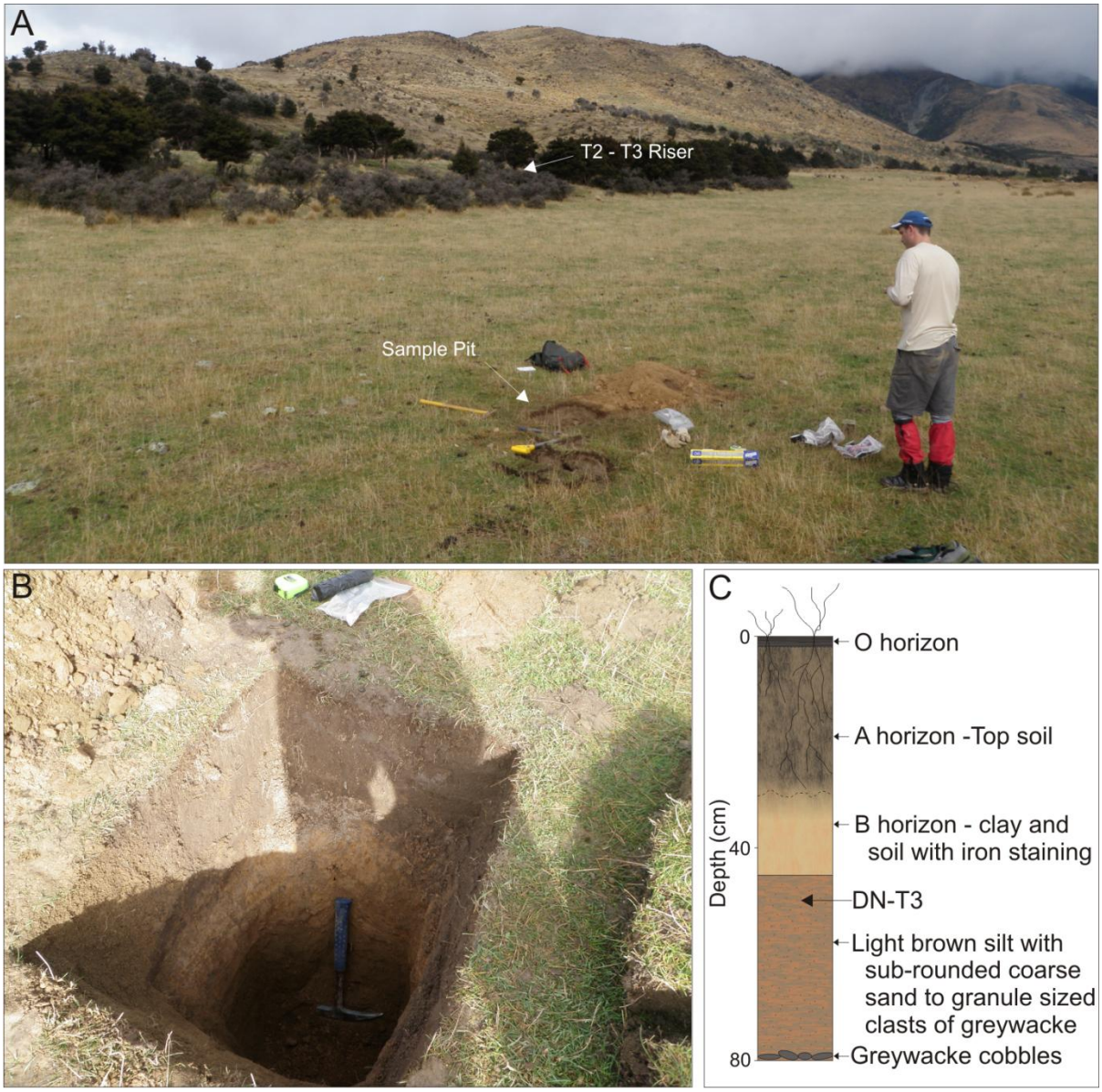

Figure 4.3. A) The view to the south at the collection site of OSL sample DN-T3. The T2-T3 terrace riser can be seen in the background. The fault trace is to the left of view. Mt Noble is visible at top-right, shrouded in cloud. B) The sample pit from which DN-T3 was collected. C) A simple stratigraphic column of the soils and alluvial units on T3. See Figure 4.1 for location.

Figure 4.4. A) The view to the south at the collection site of OSL sample DN-T6. The fault trace can be seen cutting across the T6 surface (dashed line). Ponded drainage is apparent on the downthrown side. B) The sample pit from which DN-T6 was collected. C) A simple stratigraphic column of the soils and alluvial units on T6 from the test pit and auger holes. See Figure 4.1 for location.

the overbank deposits. All terrace surfaces at the Hurunui River site contained a cap of silty overbank deposits which were deposited during high flow events shortly before the surface was completely abandoned. These deposits are well suited to OSL dating (Lian & Roberts 2006) and mean that the desired surfaces can be dated without the need for organic material. Secondly, assuming that all dated deposits are sufficiently exposed to sunlight during transport, the OSL technique removes the possibility of reworked material being used as a proxy for depositional age by dating the deposit directly.

OSL samples were collected by digging a small whole into the terrace surface at the desired location (see Figure 4.1 for sample locations) and driving a light-tight aluminium tube into the silty deposits below the soil horizons. All three samples were collected from 46 to 53 cm below the surface and consisted of silty, fine sand with varying amounts of sub-rounded coarse sand to granule sized clasts (see Figures 4.2 to 4.4 for sample descriptions).

Samples were processed using the fine grain preparation technique and paleodoses were evaluated by the Multiple Aliquot Additive Dose (MAAD) method based on measurements of blue luminescence from the fine grained (4-11µm) feldspar produced during infrared radiation. The results are shown in table 4.1. OSL reports are presented in appendix x.

4.2.2. MT NOBLE SECTION

A natural exposure of the normal-dextral fault scarp on the Mt Noble Section provides another opportunity to further constrain the timing of Event 1 and to affirm the results obtained from the Hurunui River site using radiocarbon dating.

The sample site, 2 km southwest of Mt Noble, exposes the fault in the wall of a small gully. Loose soil and colluvium deposited against the cutting were removed to expose the fault plane, bedrock hill slope and several distinct sedimentary deposits within and mantling the uphill-facing scarp (Figure 4.5).

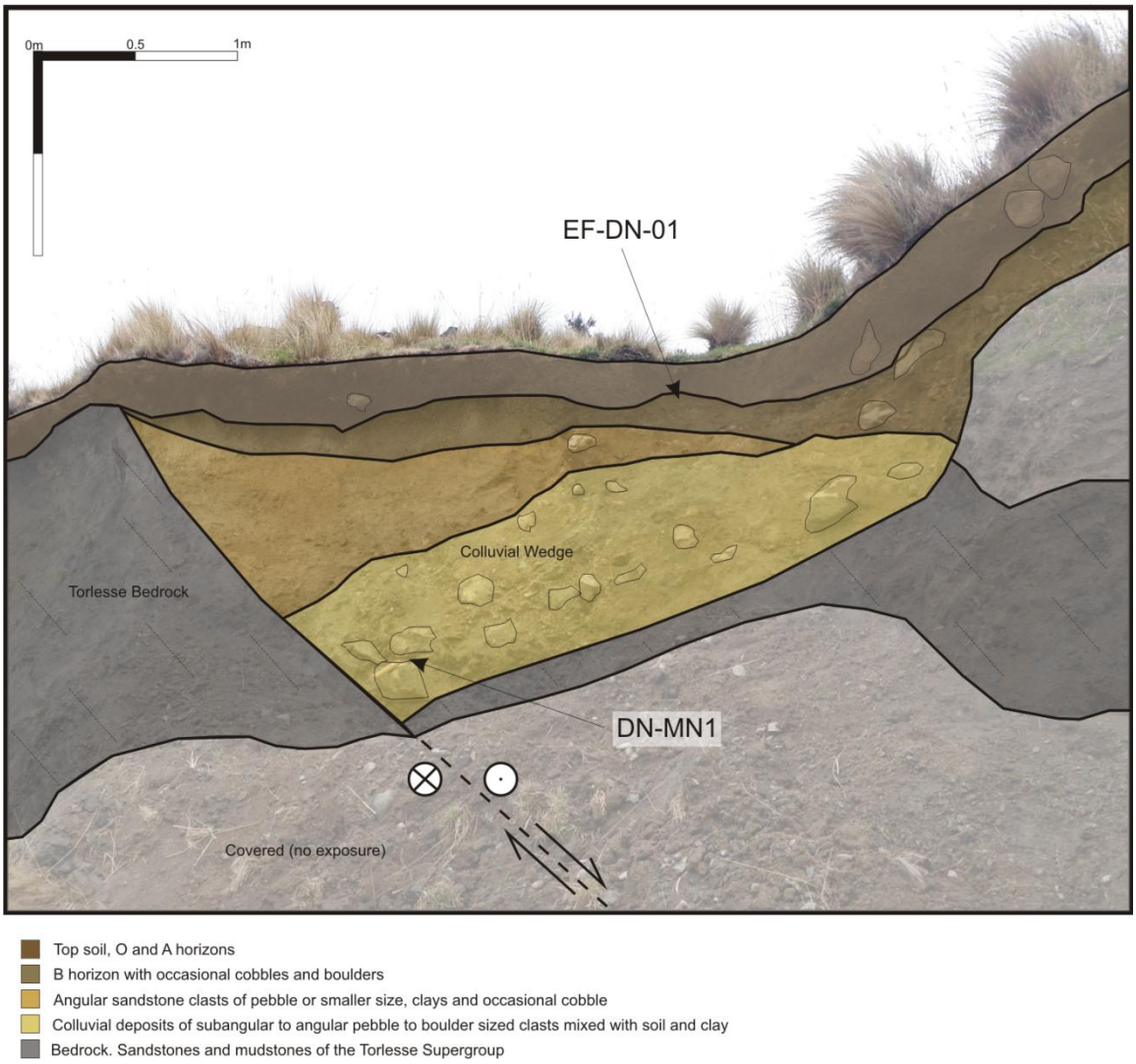

Figure 4.5. A natural exposure of the dextral-normal uphill facing scarp on Mt Noble. The scarp face has been in-filled with colluvium and slope-wash. A c. 50 cm thick soil profile has developed above the coluvial wedge. A fault dip of 45° was measured at this site. Locations of samples DN-MN1 and EF-DN-01 are shown. See figure 1.4 for location.

Figure 4.6. A) Sample EF-DN-01. Charcoal within the B horizon above a coseismic coluvial wedge on the Mt Noble Section. The charcoal has formed by burning of in situ roots and still holds the shape of the original root structure. B) Sample DN-MN1. Charcoal within a coluvial wedge on Mt Noble.


A


B
Charcoal
NIWASHI

Sample DN-MN1 was collected from a 1.3 m thick deposit of coarse, clast-supported colluvium consisting of angular pebble to boulder sized clasts of greywacke deposited directly on top of the bedrock surfaces of the fault plane and adjacent hill slope. The sample consisted of black charcoal found near the bottom of the deposit, wedged between two boulders (Figure 4.6B). Directly above the colluvial wedge lies a deposit of angular coarse sand to cobble sized greywacke clasts. This deposit is interpreted as weathered slope wash and debris shed off the fault scarp and hill slope shortly after fault rupture, before any significant soil cover had developed. This deposit then grades into the B soil horizon which also incorporates some angular cobbles and boulders. It is within this B-horizon that sample EF-DN-01 was collected. EF-DN-01 consisted of black charcoal which could be found intermittently across the B-horizon and was collected from c. 25cm below the ground surface (Figure 4.5 and 4.6A).

The position of sample DN-MN1, within the colluvial wedge implies deposition during or very shortly after the development of the scarp. It is considered very unlikely that the charcoal developed in situ from tree roots penetrating the colluvium as the charcoal was isolated and fragmented and no other roots or charcoal are found within the deposits below the B-horizon. As a result, the sample must predate the colluvial deposits and therefore the age derived from this sample gives a maximum age of surface rupture for Event 1, the most recent surface rupturing event.

The position, form and abundance of charcoal in the B-horizon strongly suggest in situ burning of tree roots (Tuttle & Schweig 1995), (Santos et al. 2000). Charcoal samples within the B-horizon are elongate and still hold the form of branching roots (Figure 4.6A). As this charcoal developed in situ within the soil horizon it must postdate the development of the colluvial deposits within the scarp and therefore sample EF-DN-01 gives a minimum age for

Event 1. The radiocarbon ages of both Mt Noble samples are shown in Table 4.1. AMS laboratory reports are presented in Appendix C.

4.2.3. RESULTS

The results of both the OSL and ^{14}C samples provide some constraint on the timing of the two most recent surface rupturing events. The age of the penultimate event (Event 2) is constrained by the abandonment ages of T2 and T3. OSL samples of these surfaces reveal an age of rupture between 12.8 and 9.5 ka. These ages are considerably younger than the estimates of Rattenbury et al. (2006), who portray these higher terraces as c. 59 – 71 ka, and those of Powers (1962) who suggested that they were formed along with the Sisters Stream Moraines, contemporaneous with the Otarama or Blackwater advances in the Waimakariri Valley to the south (> 20 ka (Berger et al. 1996)) .

Event 1, the most recent surface rupturing event, is constrained to the last 6.3 ka by the OSL age returned from T6. Because a minimum age of rupture could not be confirmed at the Hurunui Terraces site, the Mt Noble radiocarbon samples were dated to constrain the timing of Event 1 more precisely. Radiocarbon results quoted as 'cal BP' are calibrated ages BP at the 95% confidence interval while those simply quoted 'BP' are in calendar years before 2011 AD for easy comparison with OSL ages.

Sample DN-MN1, collected to provide a maximum age of rupture, returned a calibrated age of 6131 ± 132.5 cal BP. This result fits well with the OSL age of T6 (5.9 ± 0.4 ka) and further constrains the maximum age of Event 1 to 6325 BP.

Sample EF-DN-01, collected to provide a minimum age of rupture for Event 1 returned a calibrated age of 686 ± 30 cal BP. This result constrains the timing of Event 1 to 6325 – 717 BP.

4.3. SLIP-RATES AND RECURRENCE INTERVAL

4.3.1. WESTERN SECTIONS

In order to calculate average late Quaternary recurrence intervals and slip-rates for the western sections of the NEF a single OSL sample was taken from a faulted alluvial terrace in the Waitohi valley (Sample DN-WW1, Figure 4.7). The terrace surface is vertically displaced by 9.5 ± 0.6 m along the dextral-reverse Waitohi Section. The OSL sample consisted of coarse sand with sub-rounded granule to pebble sized clasts of greywacke collected from 60 cm below the terrace surface at the terrace edge (Figure 4.7).The sample was processed using the techniques described in section 4.2.1 and returned an age of 30.5 ± 2.2 ka.

Given the average c. 2 m vertical displacement per event demonstrated on the Hurunui River and Waitohi Sections (section 3.4.2.) and assuming a characteristic displacement model (see Section 3.4.3), the 9.5 m vertical separation of the dated terrace tread suggests approximately five surface rupturing events. With the minimum age of rupture constrained by ^{14}C sample EF-DN-01, the period of 29.8 ±2.2 ka since the Waitohi terrace was abandoned gives an average recurrence interval of 5511 - 6403 years.

Given the age and cumulative displacement data obtained from the Hurunui River, Mt Noble and Waitohi Sections, maximum and minimum average recurrence interval ranges can be calculated for four different periods of time, each encompassing between two and five events (Figure 4.8A). The results (displayed in Figure 4.8B) give a full range of possible late Quaternary recurrence intervals of 4200 - 6403 years. All estimates overlap for the period of 5511 – 5800 with at least three estimates overlapping for the period of 5167 – 6057 years. Due to the consistency of results of between 5167 to 6057 years, the latter estimate is considered the most likely to encompass the true average late Quaternary recurrence interval of the NEF.

Figure 4.7. A) The collection site of OSL sample DN-WW1. The sample was taken from 60 cm below the surface of an abandoned terrace of the Waitohi River. The Waitohi Section fault can be seen in the background (dashed line and arrows) displacing the terrace surface vertically by c. 9.5 m. See figure 1.4 for location. B) A simple stratigraphic column showing the soils and alluvial units in the top 80 cm of the terrace surface.

Table 4.1. Radiocarbon AMS results. See Appendix C for lab reports.

Sample ID	Sample Location	Sample Material	^{14}C Age Conventional Years B.P.	^{14}C Age Calibrated Years B.P.	^{14}C Age Calibrated Calander Years
DN-MN1-2010	Mt Noble	Charcoal	5399 ± 20	6131.5 ± 132.5	44315 - 4050 BC
EF-DN-01	Mt Noble	Charcoal	778 ± 15	686 ± 30	1294 - 1234 AD

Table 4.2. Optically Stimulated Luminescence results. See Appendix C for lab report.

Sample ID	Sample Location	Sample Material	Paleodose (Gy)	Dose Rate (Gy/Ka)	Age (ka)
DN-T2-2010	Hurunui Terraces	Silty Fine Sand	42.97 ± 4.92	3.78 ± 0.17	11.4 ± 1.4
DN-T3-2010	Hurunui Terraces	Silty Fine Sand	38.70 ± 3.52	3.67 ± 0.13	10.5 ± 1.0
DN-T6-2010	Hurunui Terraces	Silty Fine Sand	23.78 ± 1.48	4.00 ± 0.11	5.9 ± 0.4
DN-WW1-2010	Waitohi Section	Coarse Sand	121.43 ± 6.32	3.99 ± 0.20	30.5 ± 2.2
DN-WE1-2010	Gola Peaks Section	Silty Fine Sand	225.72 ± 15.57	4.03 ± 0.16	56.0 ± 4.4

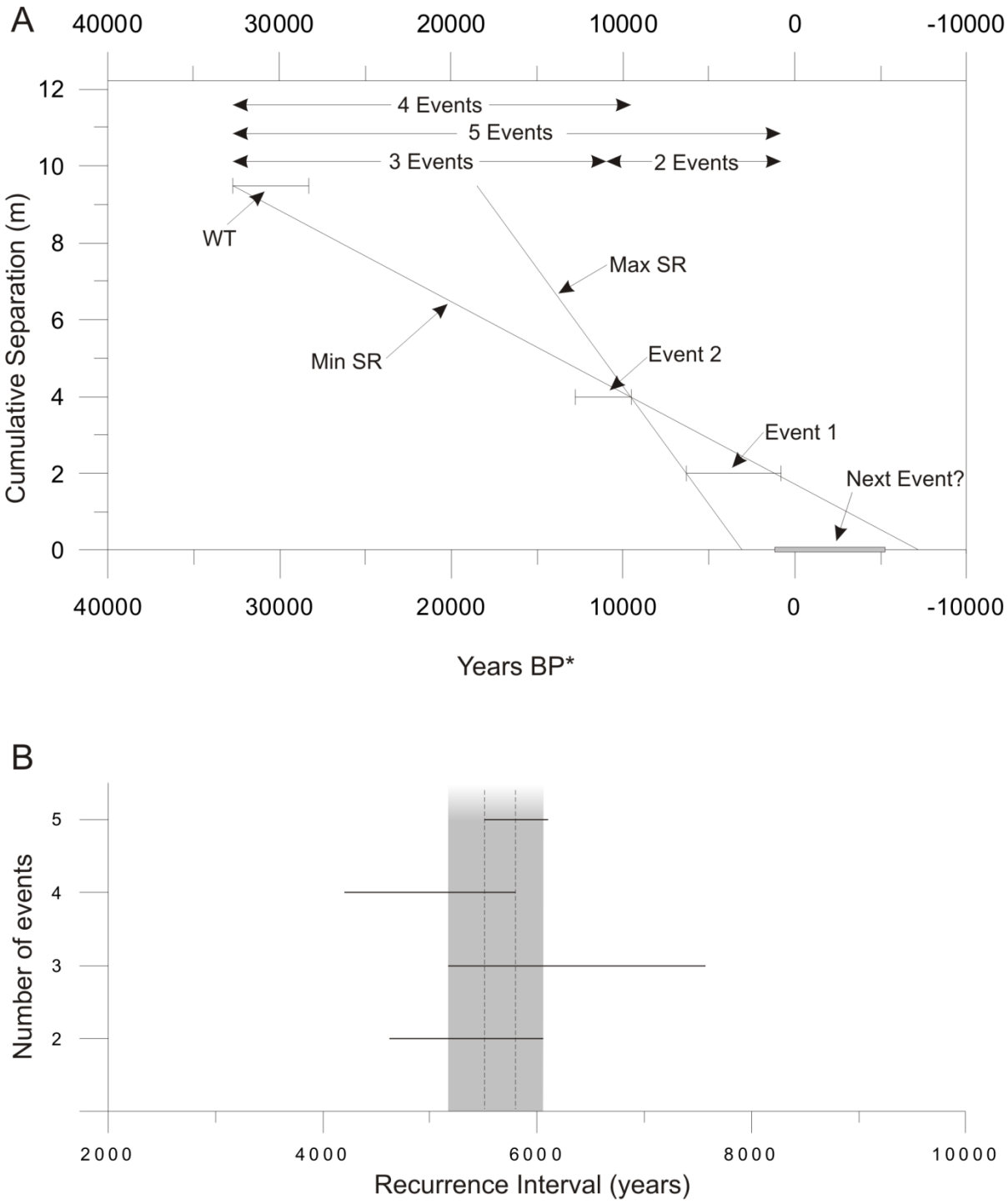

Figure 4.8. A) Cumulative vertical separation vs. time for western sections of the NEF. Maximum and minimum vertical slip-rates fitting all age data are shown (Max SR and Min SR). Event 1 and Event 2 are constrained by OSL and ^{14}C dating on the Hurunui River and Mt Noble sections. WT is the age of abandonment of the displaced Waitohi Section terrace (OSL sample DN-WW1). Time periods known to span between 2 and 5 events are shown at top of graph. Period labelled 'next event' is calculated from the max and min recurrence Intervals (RIs) and the max and min age of Event 1. *BP = before 2011. B) The range of RIs calculated for each of the time periods shown in A. Grey shaded box shows range covered by at least three of the four estimates. Dotted lines encompass the area in which all estimates overlap.

The Waitohi terrace vertical separation and abandonment age is also used to calculate an average separation-rate for the dextral-reverse Waitohi and Hurunui River sections. The resulting range of 0.31 ± 0.06 mm yr^{-1} fits well with the displacement data and abandonment ages derived from the Hurunui River Section where an average vertical slip-rate of 0.37 ± 0.06 mm yr^{-1} is calculated for the c. 4 m vertical separation of T2. When the known fault dips of c. 35° and 32° are included for the Waitohi and Hurunui River sections respectively, the resulting dip-slip rates are 0.54 ± 0.10 mm yr^{-1} and 0.69 ± 0.11 mm $yr^{-1}$and convergence rates across the fault sections are 0.44 ± 0.08 mm $yr^{-1}$and 0.58 ± 0.09 mm yr^{-1}. Viewed in light of the c. 2 m of separation known to have accumulated on T2 between 12,800 BP and 9,500 BP, these slip rates support the identification of single and double-event scarps on the Hurunui River Section. Maximum and minimum vertical slip-rates fitting all dated surfaces and events are shown in Figure 4.8.

Using the slip vector data obtained from striations at the Waitohi Section exposure (Section 3.6.2), a total net slip of c. 16.4 ± 1 m is calculated for the c. 30 ka since the Waitohi Terrace was abandoned. This equates to a net slip rate of 0.68 ± 0.07 mm yr^{-1} at a lateral to vertical slip ratio of 0.6.

Given the age of the five event-preserving terrace of the Waitohi Section we can obtain a late Quaternary slip-rate for the Mt Noble section based on the average single event lateral displacement of 5 m (Section 3.4.1.).

The maximum dextral separation measured is that of a 23.7 ± 3.2 m offset ridge on Mt Noble. Given a characteristic displacement of 5 m/event (section 3.4.1), this offset suggests the preservation of five surface rupturing events of c. 5 metres/event, the same five events that displace the dated terrace surface of the Waitohi Section. Using the terrace age of 30.5 ± 2.2

ka the average lateral slip-rate for the Mt Noble Section of the NEF equates to 0.82 ± 0.06 mm yr^{-1}.

4.3.2. EASTERN SECTIONS

The Gola Peaks exposure provides an opportunity to calculate a late Quaternary vertical slip-rate for the eastern section. As described in Section 2.3.1, the exposure reveals Mesozoic greywacke thrust over alluvial deposits of the Waitohi River. Correlation between the upper limit of a unit of river gravels in both the foot wall and hanging wall allows a vertical separation of 13.5 ± 1.5 m to be calculated.

A single OSL sample was collected from unit B in the hanging wall (see Figure 2.12) to provide a minimum age of the underlying unit A, which is to coarse for OSL dating techniques (see Figure 4.9 for sample location). Many of the beds within unit B are also too coarse for OSL dating. As a result, a sample could only be taken from c. 9 m up-section of the A-B contact. The sample returned an age of 56 ± 4.4 ka. This produces a vertical separation rate of 0.25 ± 0.05 mm yr^{-1}. At a dip angle of 35° this equates to a dip-slip rate of 0.44 ± 0.09 mm yr^{-1} and a convergence rate across the fault of 0.36 ± 0.07 mm yr^{-1}. Because the age is considered a minimum age of unit A, these slip-rates must be considered maximums.

These slip-rates are comparable with the slip rates calculated for the Waitohi and Hurunui River Sections. Although the vertical rate is slightly lower than those calculated on the western sections, this could be expected due to the more NE strike of the Gola Peaks Section, which likely favours oblique slip (see Section 3.6). Although dextral displacements of up to 19 m were measured on the Gola Peaks Section, too few offsets could be identified to estimate a single event lateral displacement and as a result no lateral slip-rate or recurrence

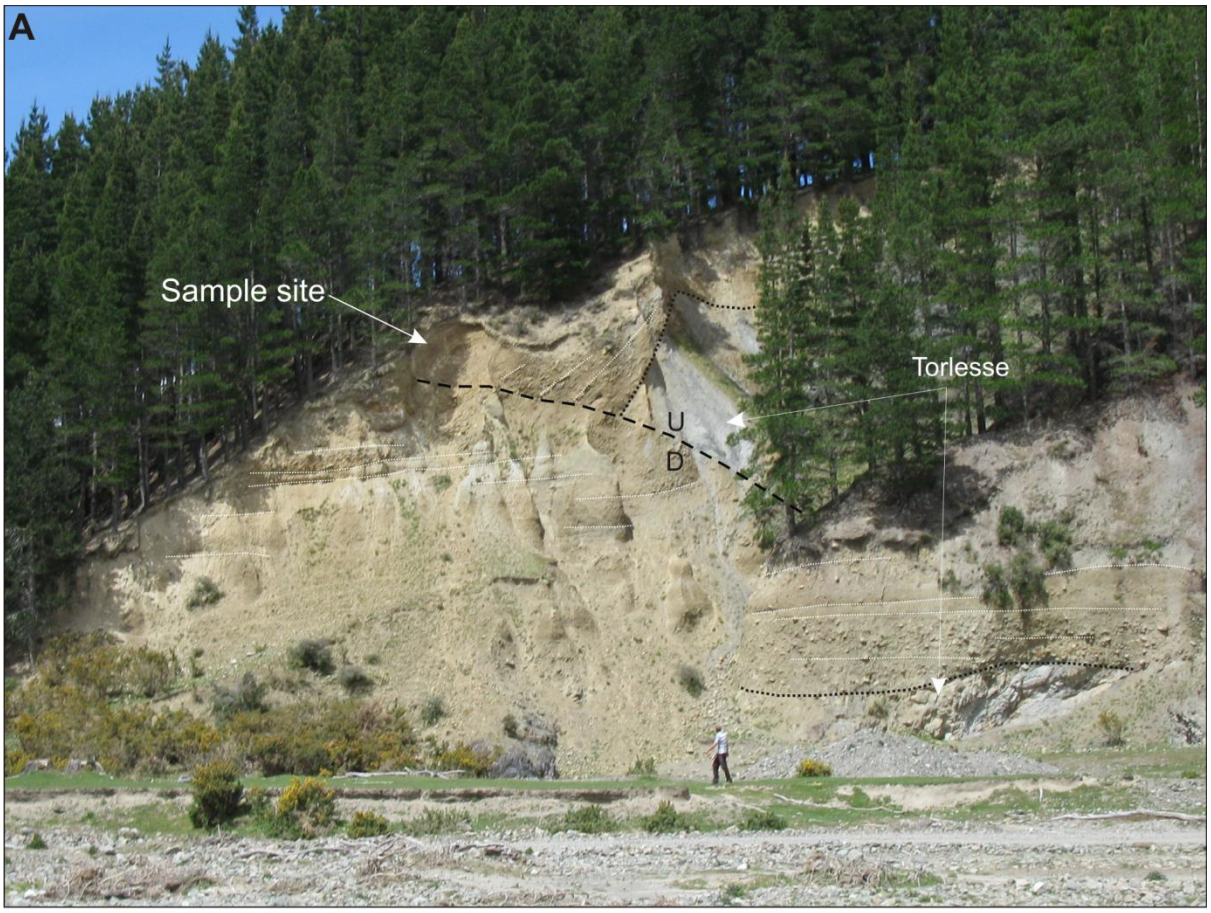

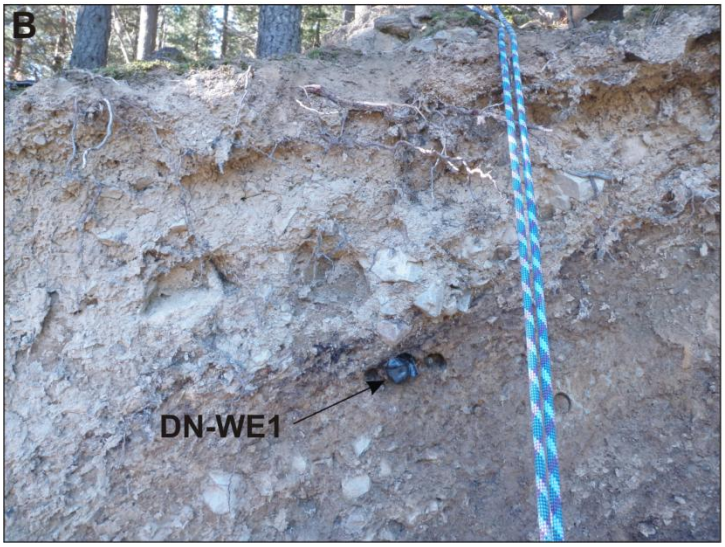

Figure 4.9. A) The Gola Peaks exposure with OSL sample site labelled. The beds in the hanging wall have been tilted and folded over the bedrock as it thrust up the fault plane. B) OSL sample DN-WE1 collection site. Sample consisted of brown silt and sand with angular granule and pebble sized greywacke clasts. See Figure 2.11 for stratigraphic columns of hanging and foot walls.

intervals can be determined. However, given the consistency of maximum stress axes derived both from the NEF and historic seismicity in the area, net slip can be estimated based on the strike of the Gola Peaks Section within the regional stress field. Using the strike and dip of 045/35° obtained from the Gola Peaks exposure and stress axes obtained from the Waitohi Section (see Section 3.6.2.) the Gola Peaks Section could be expected to have accommodated c. 39.8 ± 3.4 m of dextral slip at the exposure site since the deposition of Unit A. This equates to c. 46.1 ± 4.4 m of net slip over 56 ± 4.4 ka at an average slip-rate of 0.72 ± 0.06 mm yr^{-1}.

4.3.3. THE NEF'S ROLE IN ACCOMODATING REGIONAL STRAIN

The majority of plate motion across the South island is passed through the Marlborough Fault System and accumulated as both lateral and vertical displacement on the Alpine Fault (Norris & Cooper 2001; Sutherland et al. 2006; Langridge et al. 2010). Much of the remaining slip is dispersed among the many smaller, slower slipping faults in the wider plate boundary zone of the Southern Alps and Canterbury.

While strain on the fast-slipping faults of the MFZ and PPAFZ is reasonably well studied the deformation occurring between these major block boundaries is still poorly constrained. In a study comparing GPS derived strain rates over a 10 year period with geologically derived slip rates across the South Island, Wallace et al. (2007) report on strain occurring within the North Canterbury Block (NCB), defined by the Hope Fault to the north, the PPAFZ to the southeast and the Rakia River and Alpine Fault to the south and west (Figure 1.2). When compared with their model, constructed from GPS derived site velocities and geological data, the lack of geologically derived slip-rates within the NCB results in a residual strain rate across North Canterbury of ε_1 = 8.8 ± 3.1 nstrain/year of contraction and ε_2 = 19.7 ± 8.1 nstrain/year extension along axes of 097 ± 8° and 187 ± 8° respectively. Across block widths of 90 - 145 km and 68 - 70 km (for contraction and extension respectively), these strain rates equate to

0.51 – 1.73 mm yr^{-1} and 0.79 – 2.14 mm yr^{-1} within the NCB. A more recent study by Wallace et al. (In review) uses additional GPS data and new model parameters to establish residual strain rates for a redefined NCB (Figure 1.2) of ε_1 = 59.03 ± 12.97 and ε_2 = 30.36 ± 9.41 nstrain/year of contraction along axes of 167.98 ± 20.07 and 77.98 ± 20.07 respectively. Across block widths of 56 – 60 km and 120 – 200 km, these strain rates equate to ε_1 = 2.58 – 4.32 mm yr^{-1} and ε_2 = 2.15 – 7.94 mm yr^{-1}. This residual strain must be accommodated either by internal aseismic deformation, permanent coseismic deformation or by the build up of elastic strain on structures for which, as of 2011, no reliable geological estimates of strain rate have been made.

The slip-rates calculated for the NEF account for some of this unresolved internal deformation of the NCB. Including the full range of slip-rates calculated for both the Mt Noble and Waitohi sections, the NEF horizontal strain rates along the principle strain axes of Wallace et al. (2007) equate to 0.46 – 0.82 mm yr^{-1} contraction and 0.17 – 0.72 mm yr^{-1} extension orientated ~ 097° and ~ 187° respectively. These strain rates account for 27 – 161% of residual shortening and 8 – 91% of residual extension within the NCB.

When compared with the residual strain rates of Wallace et al. (In review), the horizontal strain-rates calculated for the Mt Noble and Waitohi Sections of the NEF account for 0.49 – 0.97 mm yr^{-1} of contraction along ε_1 and 0.64 mm yr^{-1} extension to 0.15 mm yr^{-1} contraction along ε_2. These strain rate account for -0.4 to 25% of residual contraction along ε_1 and 6 - 45% contraction along ε_2. As discussed in section 3.8, the principal strain axes of Wallace et al. (2007) are a better approximation to strain occurring around the NEF and western Culverden Basin area than those of Wallace et al. (In review).

However, several other significant faults preserving late Quaternary displacements have been mapped within the NCB. These include the Waitohi Downs, Craigiburn, Torlesse, Poulter,

Hurunui Bluff and Lees Valley Faults as well as the Southern segment of the Esk Fault and the Gola Peaks Segment. Only one of these structures, the Poulter Fault, has ruptured historically (Berryman & Villamor 2004) and all are believed to have recurrence intervals in excess of 2000 years (Van Dissen et al. 2003). Surveys in the Arthurs Pass region prior to 1995 were not used in Wallace et al. (2007) study in order to exclude the deformation associated with the 1994 Arthurs Pass and 1995 Cass earthquakes. As no evidence of aseismic creep has been found on faults within the South Island (Wallace et al. 2007, In review) and no earthquakes of magnitude ≥ 6 occurred within the NCB during the sample period, the vast majority of additional strain within the NCB is likely to be accumulated as elastic strain across the faults mentioned above that is transformed episodically into permanent strain via faulting. Some additional strain is also likely to be accumulated across un-mapped and subsurface structures such as the faults that ruptured during the M_w 6.7 Arthurs Pass earthquake of 1994.

4.4. MAGNITUDE

4.4.1. FAULT SCALING RELATIONSHIPS

Relationships between surface rupture length (SRL), average and maximum surface displacement (AD and MD respectively), moment magnitude (M_w) and rupture area (RA) are often used to estimate the magnitude of prehistoric fault ruptures (e.g. Howard (2005), McCalpin (1996), Van Dissen & Nicol (2009)). The most commonly used regressions are those of Wells & Coppersmith (1994). Several authors have noted discrepancies between magnitudes of measured historic South Island surface ruptures and those predicted for the same rupture length by Wells & Coppersmiths regressions (eg Berryman (2002), Howard (2005), Stirling et al. (2002), Quigley et al. (2010, 2012)) and those of other authors. A

recurring problem for New Zealand faults in particular is the under-estimation of M_w for a given SRL or over-estimation of SRL and M_w for a given AD.

The issue of high AD to SRL ratios was noted by Campbell et al. (1994) in the active north and western margins of the Canterbury plains and has also been highlighted by the recent M_w 7.1 Greendale Fault rupture in Canterbury which produced a surface trace c. 29 km long and lateral offsets averaging c. 2.5 m (maximum c. 5 m) (Quigley 2010, 2012). Using the average displacement of this event with Wells & Coppersmiths' regressions yields a rupture length of 87 km, three times longer than the observed trace. A similar result is produced from the 1929 M_w 7.0 Poulter Fault rupture which produced a surface trace < 36 km long and possibly as short as 16 km with lateral displacements of up to 4.4 m(Berryman & Villamor 2004). Results of well studied prehistoric ruptures of the Porters Pass Fault (Howard 2005) and possibly sections of the Awatere (McCalpin 1996) and Clarence faults (Van Dissen & Nicol 2009) also suggest relatively short SRLs for the measured single event AD. Similarly, underestimations of magnitude are obtained from the surface rupture lengths of the 1929 Arthurs Pass (Berryman & Villamor 2004), 1888 North Canterbury (Cowan 1991), and 1848 Marlborough (Benson et al. 2001) earthquakes when compared with reported shaking intensities or recorded magnitudes.

Another important point to note is that the regressions derived for AD:M_w, MD:M_w, SRL:MD and SRL:AD on reverse faults by Wells & Coppersmith (1994) are not statistically significant at the 95% confidence interval and AD:Mw regressions also do not include data for events producing more than 1.5 m AD. Conversely, the data used by Leonard (2010) is mostly of dip-slip earthquakes and may not be applicable to large (>45 – 100 km SRL) strike-slip earthquakes. The study of Stirling et al. (2002) does not differentiate between dip-slip and strike-slip faulting implying the use of their regressions for all fault types. The fault scaling

Figure 4.10. Empirically derived relationships between average coseismic displacement and surface rupture length. A) Strike-slip faulting relationships. Historic South Island ruptures are shown for comparison. B) Reverse faulting relationships. NEF = Northern Esk Fault, GF = Greendale Fault, AF = Awatere Fault, HF = Hope Fault.

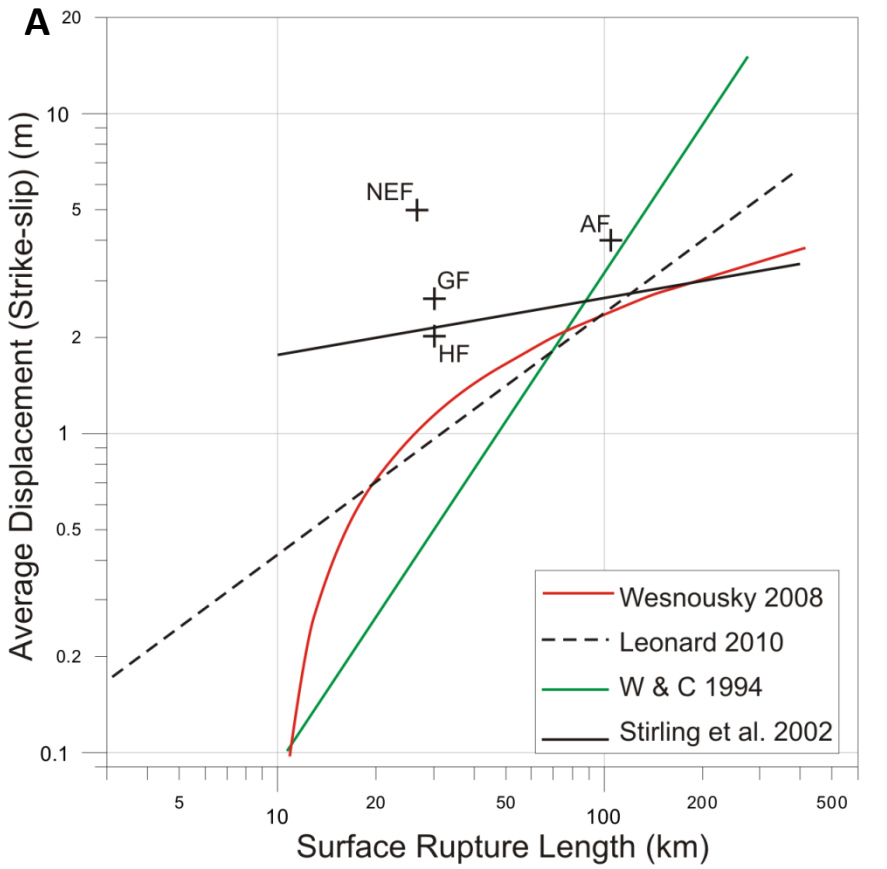
A
Average Displacement (Strike-slip) (m)
20
10
5
2
1
0.5
0.2
0.1
NEF
AF
GF
HF
Wesnousky 2008
Leonard 2010
W & C 1994
Stirling et al. 2002
5
10
20
50
100
200
500
Surface Rupture Length (km)

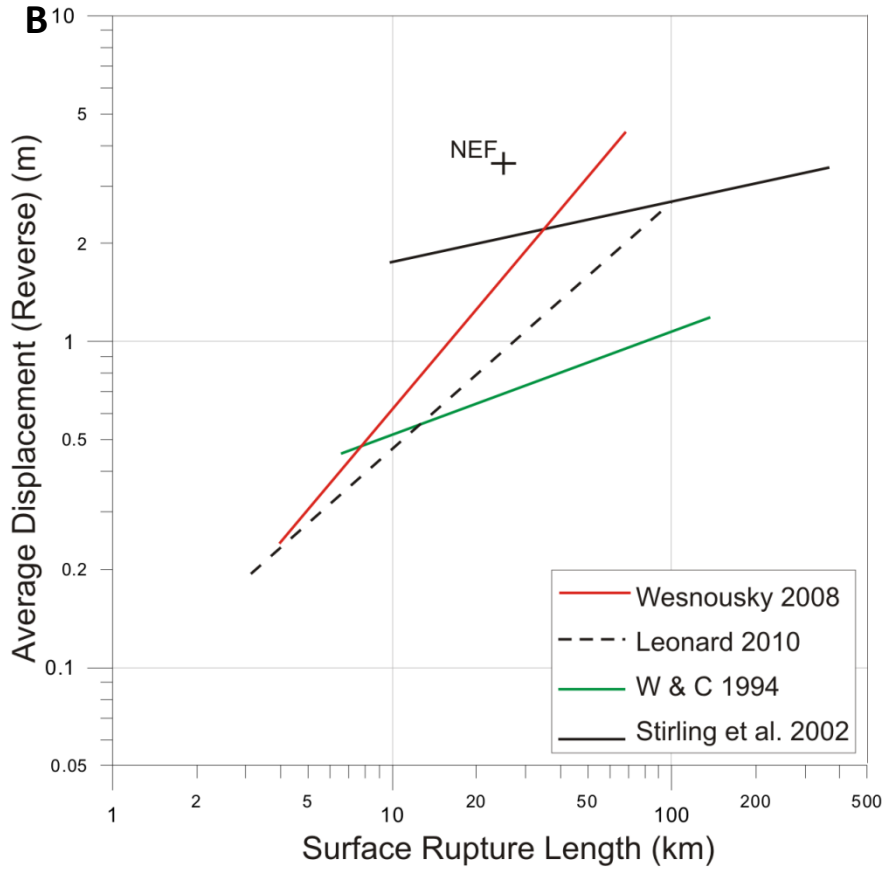
B
Average Displacement (Reverse) (m)
10
5
2
1
0.5
0.2
0.1
0.05
NEF
Wesnousky 2008
Leonard 2010
W & C 1994
Stirling et al. 2002
1
2
5
10
20
50
100
200
500
Surface Rupture Length (km)

Figure 4.11. Empirically derived relationships between average coseismic displacement and moment magnitude. Lateral and vertical single event displacements for the NEF are shown (dashed line). A) Strike-slip faulting relationships. Historic South Island ruptures are shown for comparison. B) Reverse faulting relationships. GF = Greendale Fault, AF = Awatere Fault, HF = Hope Fault.

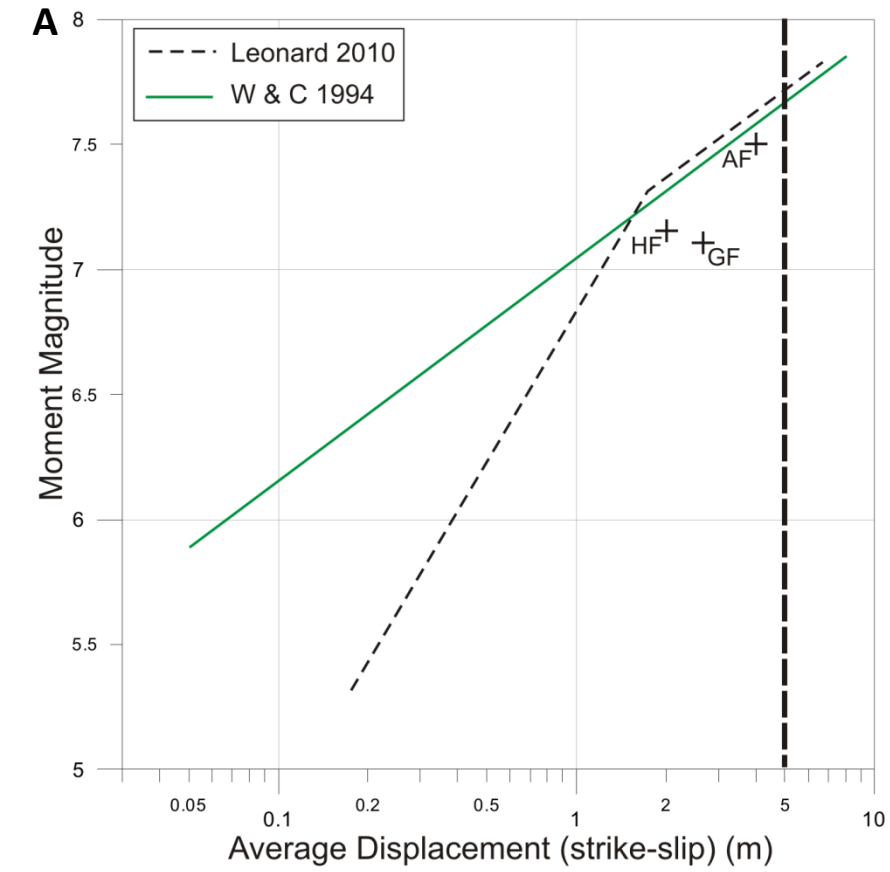
A
Leonard 2010
W & C 1994
AF
HF
GF
Moment Magnitude
8
7.5
7
6.5
6
5.5
5
0.05
0.1
0.2
0.5
1
2
5
10
Average Displacement (strike-slip) (m)

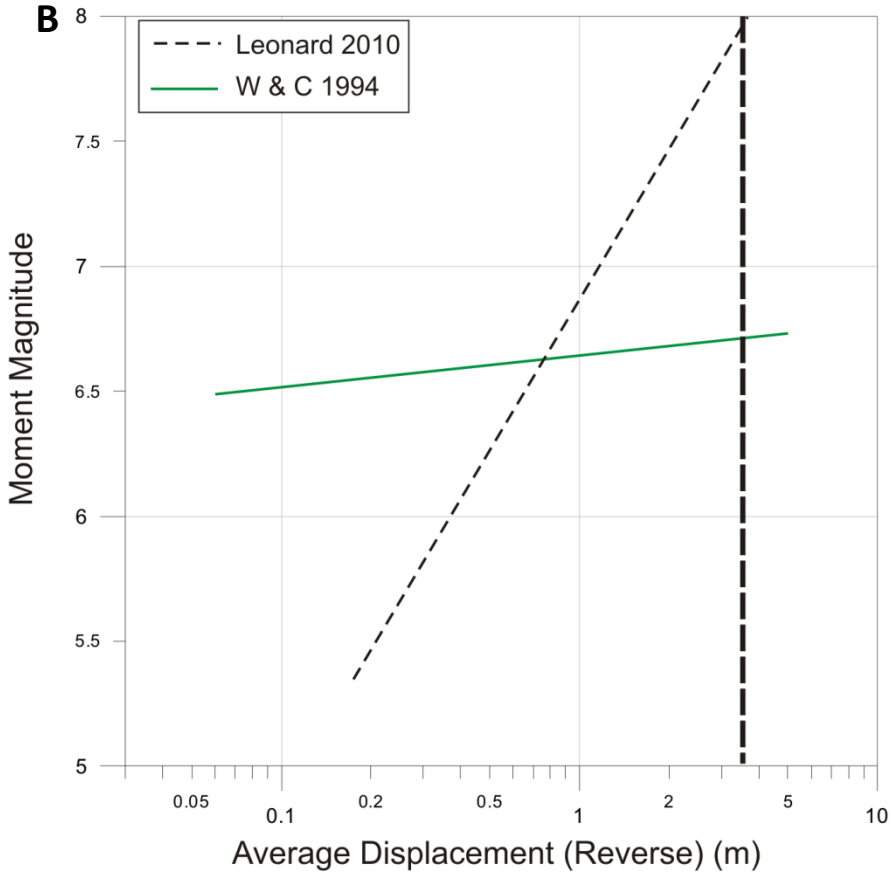
B
Leonard 2010
W & C 1994
Moment Magnitude
8
7.5
7
6.5
6
5.5
5
0.05
0.1
0.2
0.5
1
2
5
10
Average Displacement (Reverse) (m)

Figure 4.12. Empirically derived relationships between maximum coseismic displacement, surface rupture length and moment magnitude. A) Maximum displacement vs. moment magnitude for strike-slip and reverse faults. Historic South Island ruptures are shown for comparison. Single event displacements of 3.5 m vertical, and 5 m lateral on the NEF are shown (dashed lines). B) Maximum displacement vs. surface rupture length for strike-slip and reverse faults. Historic South Island ruptures are shown for comparison (cross = strike-slip fault, X = reverse fault). NEF = Northern Esk Fault, GF = Greendale Fault, AF = Awatere Fault, HF = Hope Fault.

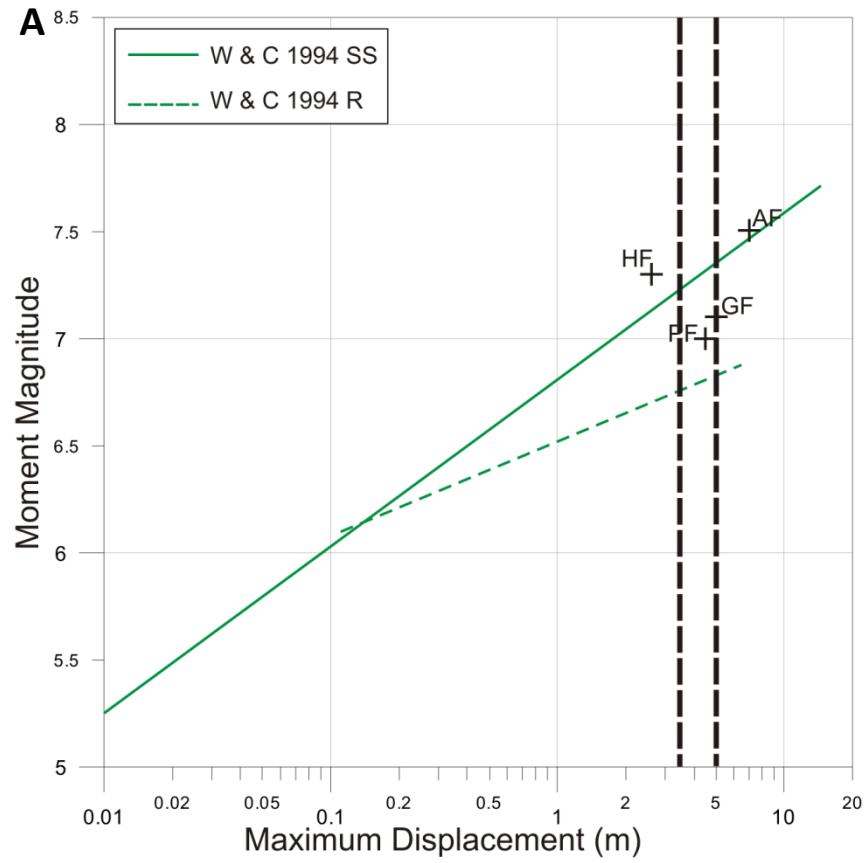
A
W & C 1994 SS
W & C 1994 R
AF
HF
GF
PF
Moment Magnitude
Maximum Displacement (m)
8.5
8
7.5
7
6.5
6
5.5
5
0.01
0.02
0.05
0.1
0.2
0.5
1
2
5
10
20

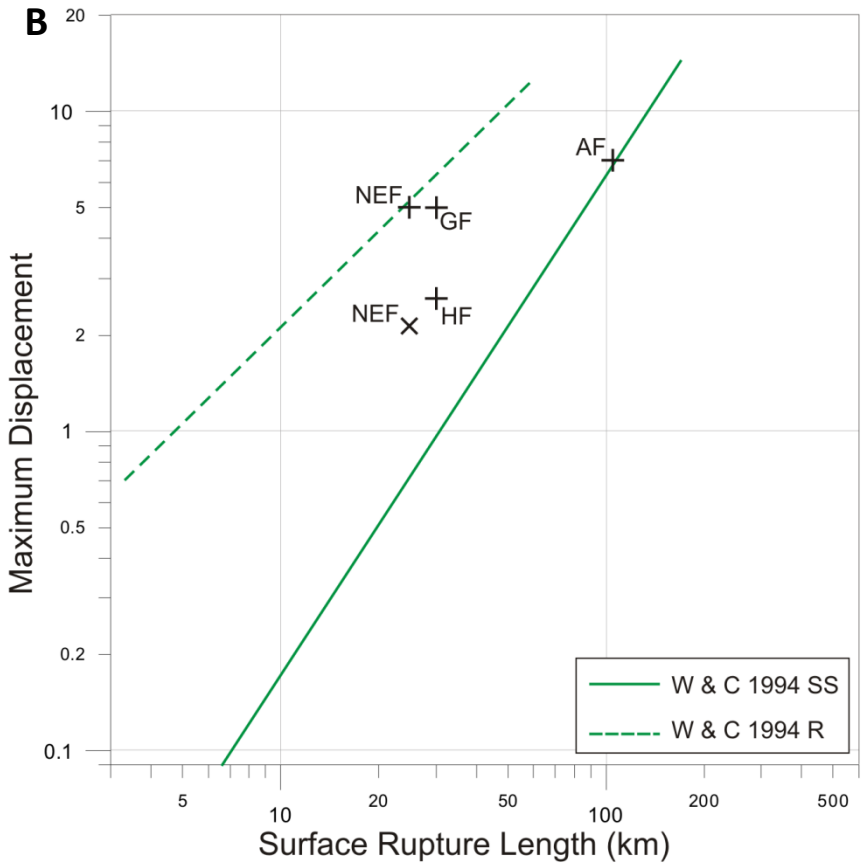
B
AF
NEF
GF
NEF
HF
W & C 1994 SS
W & C 1994 R
Maximum Displacement
Surface Rupture Length (km)
20
10
5
2
1
0.5
0.2
0.1
5
10
20
50
100
200
500

Figure 4.13. Empirically derived relationships between moment magnitude and surface rupture length. The 25 km length of the NEF is shown (dashed line). A) Strike-slip faulting relationships. Historic South Island ruptures are shown for comparison. B) Reverse faulting relationships. NEF = Northern Esk Fault, GF = Greendale Fault, AF = Awatere Fault, HF = Hope Fault.

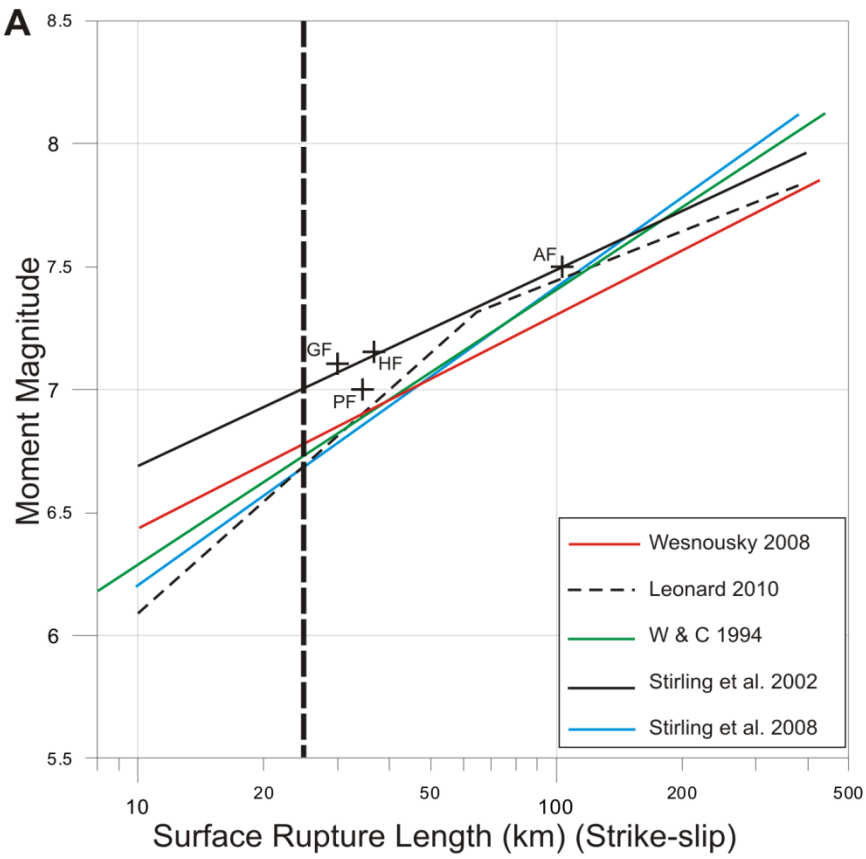
A
8.5
8
7.5
7
6.5
6
5.5
Moment Magnitude
AF
GF
HF
PF
Wesnousky 2008
Leonard 2010
W & C 1994
Stirling et al. 2002
Stirling et al. 2008
10
20
50
100
200
500
Surface Rupture Length (km) (Strike-slip)

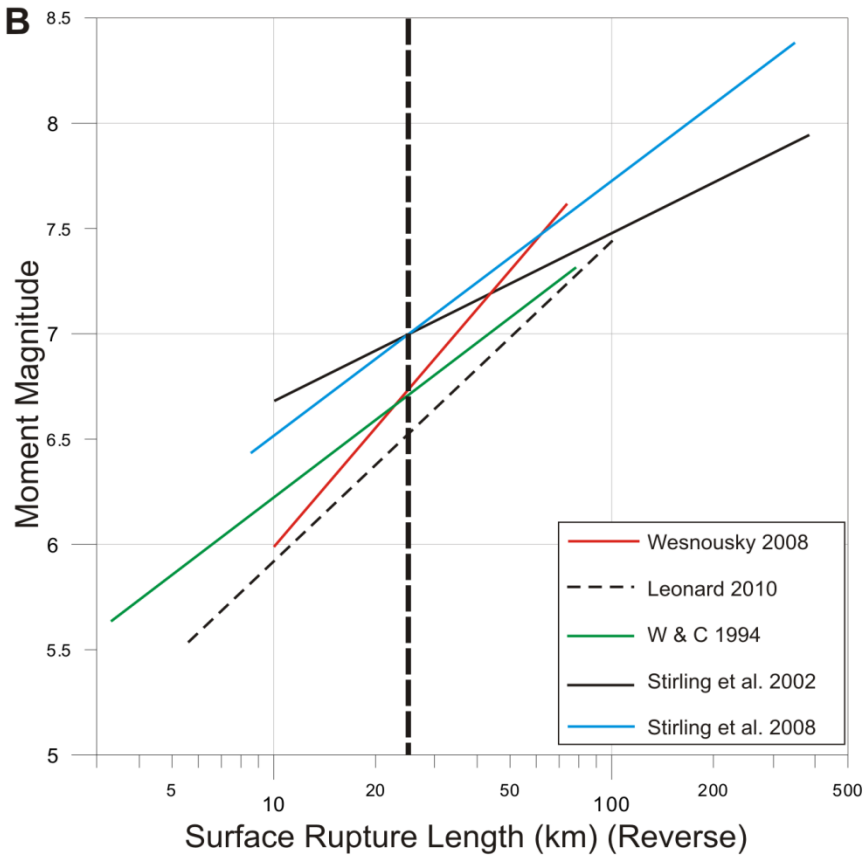
B
8.5
8
7.5
7
6.5
6
5.5
5
Moment Magnitude
Wesnousky 2008
Leonard 2010
W & C 1994
Stirling et al. 2002
Stirling et al. 2008
5
10
20
50
100
200
500
Surface Rupture Length (km) (Reverse)

Figure 4.14. Empirically derived relationships between rupture area and moment magnitude. The calculated NEF rupture area of 300 km^2 is shown (dashed line) A) Strike-slip faulting relationships B) Reverse faulting relationships.

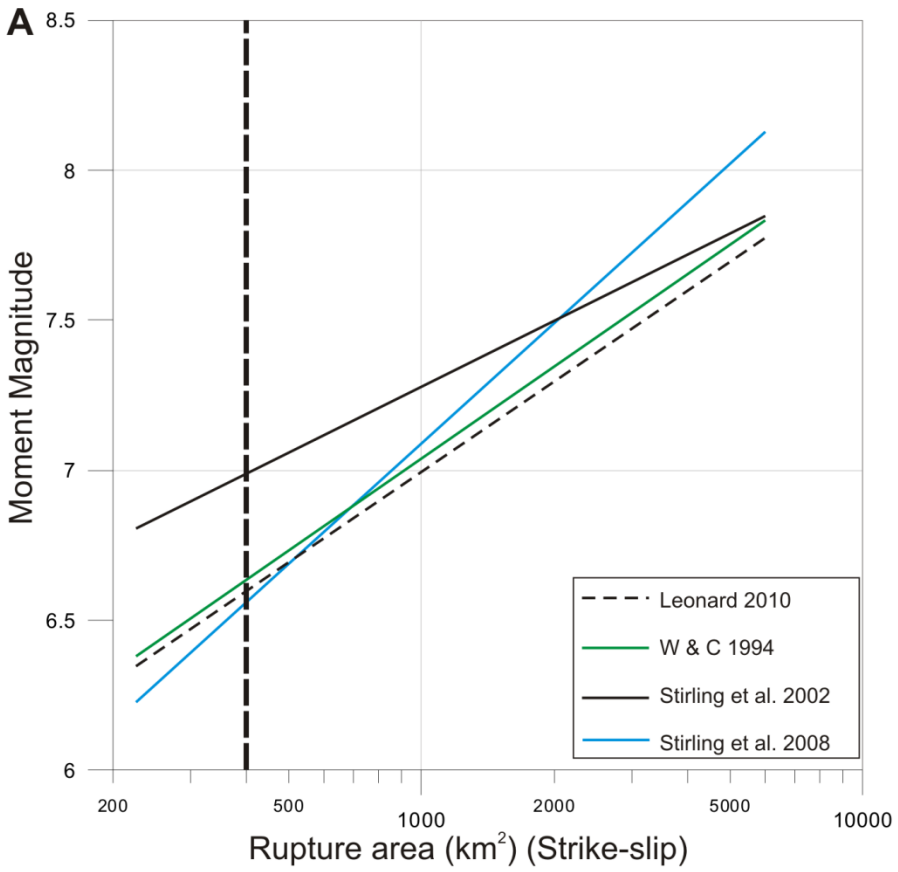
A
8.5
8
7.5
7
6.5
6
Moment Magnitude
200
500
1000
2000
5000
10000
Rupture area (km^2) (Strike-slip)
Leonard 2010
W & C 1994
Stirling et al. 2002
Stirling et al. 2008

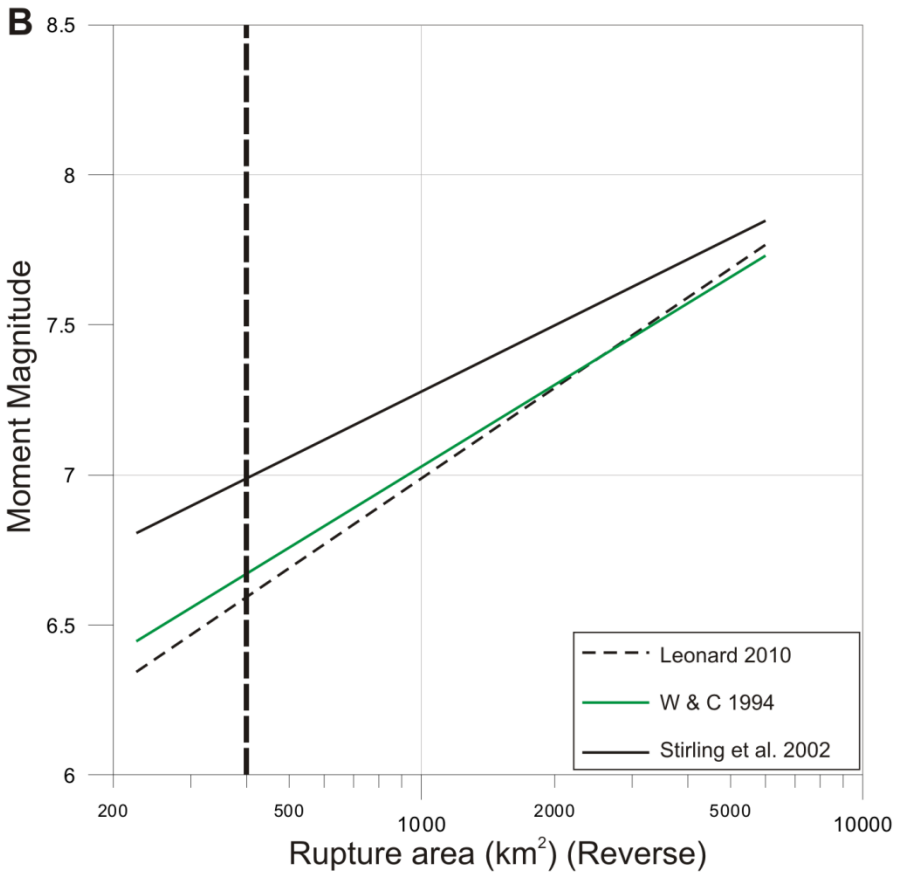
B
8.5
8
7.5
7
6.5
6
Moment Magnitude
200
500
1000
2000
5000
10000
Rupture area (km^2) (Reverse)
Leonard 2010
W & C 1994
Stirling et al. 2002

Author	Moment Magnitude								
	AD Strike-Slip (5 m)	AD Dip-Slip (3.5 m)	MD Strike-Slip (5 m)	MD Dip-Slip (3.5 m)	SRL Strike-Slip (25 km)	SRL Reverse (25 km)	RA Strike-Slip (375 km^2)†	RA Dip-Slip (375 km^2)†	Range
Wells & Coppersmith (1994)	7.7	6.7*	7.4	6.6*	6.7	6.7	6.6	6.7	6.6 - 7.7
Stirling et al. (2002)	-	-			7.0	7.0	7.0	7.0	7.0
Wesnousky (2008)	-	-			6.8	6.7			6.7 - 6.8
Stirling et al. (2008)†	-	-			6.7	7.0	6.6		6.6 - 7.0
Leonard (2010)	7.7	7.9			6.7	6.7	6.6	6.6	6.6 - 7.9
Range	7.7	6.7* - 7.9	7.4	6.6*	6.6 - 7.0	6.7 - 7.0	6.6 - 7.0	6.6 - 7.0	**6.6 - 7.9**

*Not statistically significant at 95% confidence interval

† Calculated with a fault width of 16 km. SRL to subsurface rupture length ratio after Leonard (2010)

Table 4.3. Estimates of paleoearthquake magnitude for the NEF Western Segment based on fault Scaling relationships. AD=Average Displacement, MD=Maximum Displacement, SRL=Surface Rupture Length, RA=Rupture Area

regressions among SRL, AD, MD, RA and M_w proposed by several authors (Wells & Coppersmith 1994: Stirling et al. 2002: Stirling et al. 2008: Wesnousky 2008: Leonard 2010) are shown in Figures 4.10 to 4.14. Plotted with these regressions are the average displacements (3.5 m dip-slip and 5 m strike-slip) and surface rupture length (c. 25 km) measured on the NEF Western Segment, however, this SRL is consistent with both segmentation models presented in Chapter Three so the resulting estimates of M_w may apply to either scenario. The 3.5 m dip-slip value is calculated from a single event vertical displacement of 2 m on a fault plane dipping 35°, the dip measured at the Waitohi Section exposure and within the likely range of 28 – 36° calculated for the Hurunui River Section. Stirling et al. (2002, 2008) and Wesnousky (2008) and do not provide regressions directly relating AD, MD or RA to M_w so are not included in those plots. Leonard (2010) also does not include regressions for AD or MD to M_w but since his regressions are self-consistent a comparison between AD and M_w can be derived by relating both parameters to fault length.

The equations presented in Stirling et al. (2008) require a fault width to be estimated. Given the known SRL of the NEF of c. 25 km it is very likely that surface rupturing earthquakes rupture the full width of the seismogenic zone. Estimates of the seismogenic zone in Canterbury are approximately 12 – 14 km (Cowan 1992; Gledhill et al. 2011). With the NEF being predominantly strike-slip for most of its length, the dip at depth is likely to be relatively steep, for these reasons my estimates of magnitude derived from Stirling et al. (2008) are based on an average fault dip of >60° and seismogenic zone of 13 ± 1 km, producing a fault width of 14 ± 2 km. The difference in estimates of magnitude based on a width of 12 and those based on a width of 16 km is negligible (c. 0.08). As a result, all magnitudes calculated from the regressions of Stirling et al. (2008) are based on a rupture width of 16 km and may be considered maximum estimates. All M_w estimates based on RA of the NEF are also

calculated for a width of 16 km and may be considered maximums estimates for a 25 km SRL.

The SRL to M_w regressions of Leonard (2010) and Stirling et al. (2002) are calculated using the SRL to subsurface rupture length (L) relationship SRL = 1.1logL-0.275 proposed by Leonard (2010). This relationship was chosen over that of Wells & Coppersmith (1994) because it is a better fit to the data set as a whole than their SRL = 0.75L relationship, which slightly underestimates SRL for larger ruptures (Wells & Coppersmith 1994, Leonard 2010).

As no single event displacement measured on the NEF was greater than the inferred characteristic displacements (see Section 3.4), the same values have been used for AD and MD regressions (5 m for strike-slip, 3.5 m for reverse). The use of AD vs. MD is discussed in section 4.4.3.

4.4.2. MAGNITUDES FROM POINT MEASUREMENTS OF DISPLACEMENT

Because the SRL of the NEF is not well constrained, measurements of single-event co-seismic displacement may be a better indicator of paleoearthquake magnitude.

The study of Biasi & Weldon (2006) describes a method of finding the probability of a chosen magnitude range given a single displacement measured in the field. This method scales the normalised displacements of a set of 13 historic surface ruptures to a chosen magnitude using the AD to SRL regression of Wells & Coppersmith (1994). The frequency of individual displacements along a rupture is related to the magnitude of the earthquake but the variability of displacements is not (Hemphill-Haley & Weldon 1999; Biasi & Weldon 2006). As a result, the probability of a particular displacement being sampled within a particular rupture profile is also a function of magnitude. Using the Bayesian inverse probability distribution functions, the probability of a particular magnitude can be estimated from a single surface displacement (Figure 4.15). This inversion is based on the observation.

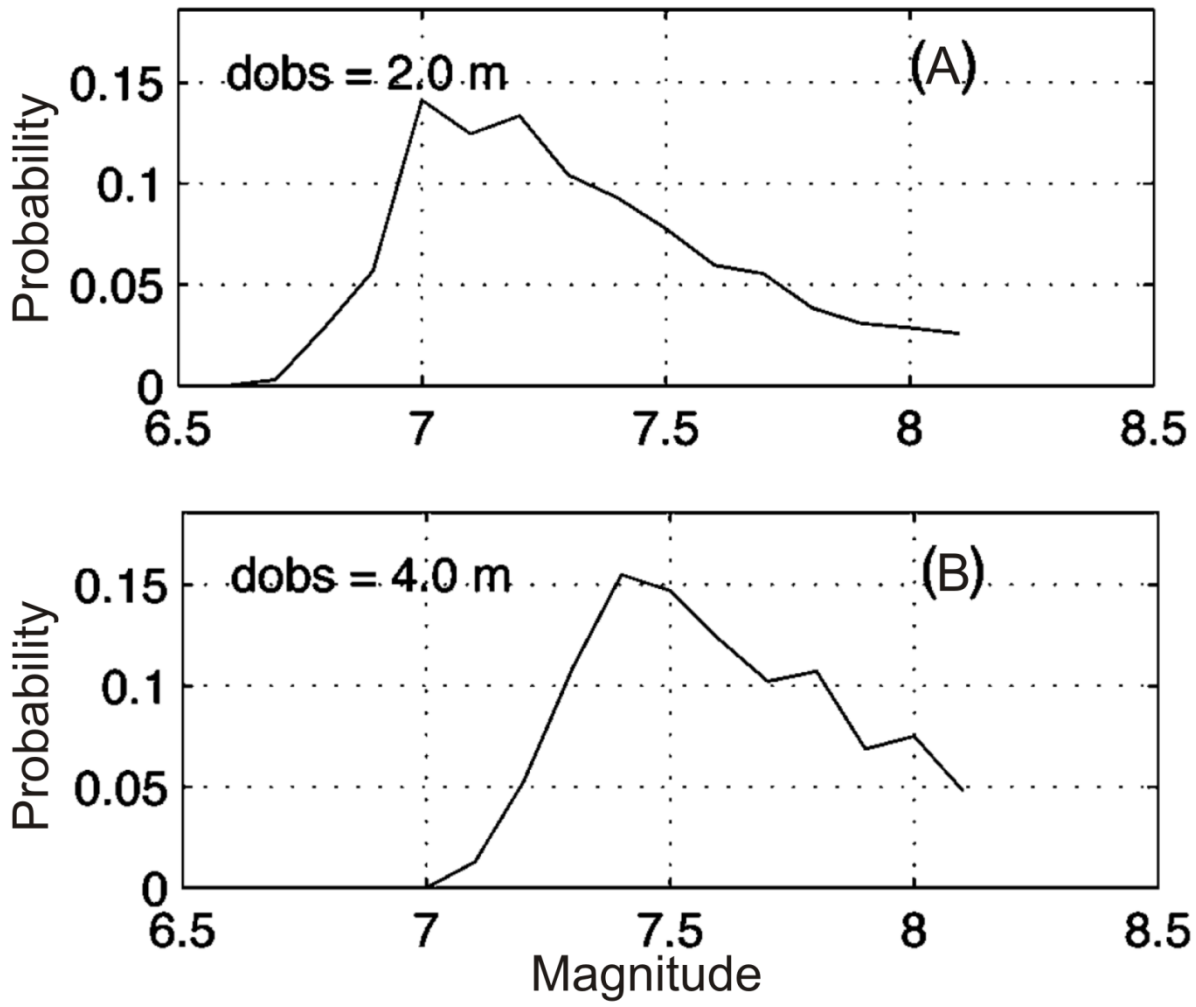

Figure 4.15. A) Probability distribution function for earthquake magnitude given an observed displacement of 2 m. The observed displacement is most likely to have been caused by an earthquake of M_w 7.0 to 7.2. B) Same as (A) but for an observed displacement of 4 m. The observed displacement is most likely to have been caused by an earthquake of M_w 7.3 to 7.5. Modified from Biasi & Weldon (2006).

that sampling from a random point on a histogram of slip measurements is the same as sampling from a random location along the corresponding fault rupture (Biasi & Weldon 2006). For the NEF, single event vertical and horizontal displacements of 2 m and 4 m are considered the most appropriate for magnitude probability analysis. The value of 2 m is derived from the measurements of single event terrace tread displacement on the Hurunui River Section (Table 3.1) (see Section 3.4.2.) while the 4 m displacement is of a small stream on Mt Noble and is the only observed displacement considered to represent the preservation of a single event on the Mt Noble Section (see Section 3.4.1).

4.4.3. RESULTS

The AD and MD to SRL ratios for the NEF are significantly above the relationships proposed by all included authors for strike-slip faults (Figure 4.10A, 4.12A). The historic ruptures of three other faults in Canterbury and Marlborough (the 2010 Greendale, 1888 Hope and 1848 Awatere Fault ruptures) also plot higher than most regressions with the 2010 and 1888 ruptures encompassing the AD regression of Stirling et al. (2002) and the 1848 rupture above all regressions but closest to that of Wells & Coppersmith (1994). A similarly poor fit for the NEF is produced from the reverse faulting AD to SRL regressions (Figure 4.10B) with Wesnousky (2008) and Stirling et al. (2002) providing the closest approximations to the NEF data.

The regressions relating AD, MD, SRL and RA to M_w are displayed in Figures 4.11, 4.12A, 4.13 and 4.14 and resulting magnitude estimates are displayed in Table 4.3. The estimated magnitude of surface rupturing events on the NEF ranges from M_w 6.5 to 7.0 for a surface rupture length of 25 km while the vertical and lateral displacements imply M_w 6.4 – 7.9 and M_w 7.0 – 7.7 respectively. M_w results for both dip-slip and strike-slip fault rupture areas range from 6.6 to 7.0.

The results of the single point displacement analysis show a probability of greater than 0.5 for earthquakes of M_w 7.0 – 7.5 with M_w 7.0 and 7.4 having the highest probabilities for 2 m and 4 m displacements respectively (Figure 4.15).

4.4.4. DISCUSSION

Although the data set for historic surface ruptures in Canterbury is small, the consistently high ratios of magnitude to surface rupture length and average and maximum displacement to surface rupture length suggest a regional variation from the global datasets used to construct most of the common scaling relationships. Paleoseismic studies of prehistoric surface ruptures in Canterbury also appear to be consistent with historic events in the region, showing relatively high displacements for the preserved rupture lengths.

Because the displacement across a surface trace will inevitably reduce to zero towards the fault tips, erosion of prehistoric fault scarps will tend to reduce the preserved SRL over time, increasing the apparent AD to SRL ratio. This is likely to explain in part the anomalously high AD to SRL ratio of the NEF. Higher and steeper terrain to the south-west of the NEF where displacements are likely to be below average are also likely to erode faster than the slopes and gravels of the Waitohi Valley, reducing the likelihood of any prehistoric displacement being preserved. This process also works to increase the average displacement on the preserved fault scarp with the area of highest slip most likely to be preserved and subsequently measured. These effects were the topic of a study by Stirling et al. (2002) who concluded that although the underestimation of SRL and overestimation of AD can account for some of the observed differences between the instrumental era-derived regressions of Wells & Coppersmith (1994) and their own pre-instrumental regressions, the overall difference requires another explanation. They suggest a difference in scaling between large earthquakes, which rupture the entire seismogenic zone, and smaller earthquakes, which are

able to propagate both along strike and down dip. This may explain the difference between regressions derived only from large historic earthquakes or from preserved, and therefore most likely large, pre-instrumental earthquakes and regressions such as those of Wells & Coppersmith that include data from surface rupturing earthquakes of all sizes.

One implication of the possible difference in scaling relations for moderate and large earthquakes is that linear regressions based on all historic data will likely underestimate the magnitude of large to great sized earthquakes and possibly overestimate magnitudes for especially long or short rupture lengths.

The regressions of Leonard (2010) take into account the possible difference in scaling by implementing different constants for earthquakes above and below 65 km SRL and by fitting a log-linear curve to the data. This addition brings the regression closer that of Stirling et al. (2002) for longer SRLs and closer to Wells & Coppersmiths (1994) for shorter SRLs. By taking into account these scaling differences the regressions of Stirling et al. (2002) and Leonard (2010) also fit the historic New Zealand data more closely than the global regressions of Wesnousky (2008), Stirling et al. (2008) and Wells & Coppersmith (1994).

Other possible factors contributing to the discrepancies between historic rupture characteristics and those predicted by fault scaling relationships include tectonic setting and local geology. These possibilities are raised by Leonard (2010) who suggests that "It is likely that these variables [the empirically derived constants used in his regressions] differ between tectonic environments..." but also notes that data sets are too small to resolve for these differences. Manighetti et al. (2007) propose differences in MD to SRL ratios for young and mature faults with younger, more strongly segmented faults tending to produce greater displacements for a short rupture length. This may help to explain high AD and MD on the

NEF but may not account for the displacements associated with historic ruptures of the more structurally mature MFS.

The magnitude estimates for the NEF based on AD of reverse ruptures are much wider ranging than those based on strike-slip faults, possibly due to the smaller dip-slip data set used by Wells & Coppersmith (1994). The AD regressions in general also produce significantly higher magnitudes than the SRL regressions. This is a reflection of the anomalously high AD to SRL ratio of the preserved NEF and, due to the nature of erosive processes discussed above, the AD derived magnitude estimates are likely to be overestimations while SRL derived magnitudes are likely to be underestimations. The AD derived estimate of M_w 7.9 from Leonard's (2010) regression in particular is considered improbably high as it would require an unfeasibly long fault length (c. 200 km). As a result, using characteristic coseismic lateral displacements on the NEF with MD regressions may give a more realistic result than those based on AD. The characteristic lateral displacement of 5 m/ event is based on inferred single event and cumulative displacements on the Mt Noble and Whitnow Sections (see Section 3.4.). The consistency of measured displacements of multiples of c. 5 m and the lack of displacements less than 4 m or within c. 7 km of the fault tips strongly suggests a bias towards the MD, which generally occurs within the central third of the surface rupture (Biasi & Weldon 2006; Wesnousky 2008). Conversely, the characteristic vertical displacement is derived primarily from measurements of remarkably consistent separations of c. 2 m measured within 2 km of the northern fault tip. These measurements are consistent with vertical separations and slip-rates measured on the central sections and appear to represent a consistent AD across all similarly NNW striking segments. As a result the MD regressions are favoured for characteristic lateral displacements while AD regressions are favoured for the characteristic dip-slip displacement. However, the lateral MD results may be viewed as a minimum estimate due to the likelihood that displacement at some

point along the fault will exceed the average displacement of the Mt Noble Section while the AD estimate should be viewed as a maximum as diminishing scarp height at the tips of the fault scarp have not been accounted for.

The SRL to M_w regressions of Stirling et al. (2002) are derived from censored instrumental data meaning that only mid to large-sized earthquakes were used, preventing smaller earthquakes from influencing the regression relationship. The historic Canterbury ruptures fit quite tightly to this regression. As a result of this and because the SRL of the NEF is likely to be longer than the preserved c. 25 km, the regression of Stirling et al (2002) is considered to be the most appropriate of the M_w to SRL and RA regressions in estimating a maximum likely magnitude for a 25 km surface rupture of the NEF.

The preferred regressions outlined above result in best M_w estimates for the NEF of 7.0 for AD to M_w, RA to Mw and SRL to M_w and 7.4 for MD to M_w All of these are considered minimum estimates for their respective parameters

These results are consistent with the single point displacement analysis, which indicates a high probability of magnitudes between 7.0 and 7.5 for 2 to 4 metres of displacement (Biasi & Weldon 2006) (Figure 4.15). The methods used by Biasi & Weldon (2006) involve scaling slip value frequencies to an AD calculated from the M_w to AD regression of Wells & Coppersmith (1994). As a result of the regional variance from the global data set discussed above, the use of Wells and Coppersmith's regressions is likely to underestimate AD for the chosen M_w range resulting in a shift of the displacement distribution towards smaller displacements and a slight overestimation of higher M_w probabilities. However, as this method produces probabilities for a broad range of magnitudes rather than a single M_w value, any regional variation is considered to have little effect on the overall result.

Considering all of the methods used, late Quaternary ruptures on the NEF are likely to have been of approximately M_w 7.0 to 7.5.

4.5. SEISMIC HAZARD

Being just c. 60 km northwest of the city of Christchurch, a rupture of the NEF would likely have a significant impact on a population in excess of 400,000 people. As a result, assessing the likelihood of future large earthquakes on the NEF is an important step towards mitigating seismic hazards in Canterbury.

A full assessment of the likely distribution, intensity and implications of ground accelerations accompanying fault rupture is beyond the scope of this thesis but the physical effects are likely to be significant for the North Canterbury region with landsliding, liquefaction and ground shaking all potential hazards.

4.5.1 TIMING OF FUTURE EVENTS

Previous estimates of recurrence interval for the purpose of surface rupture mitigation have classed the NEF as a 5,000 to 10,000 year risk (Van Dissen et al. 2003). The results of this paleoseismic investigation indicate a return period of c. 5612 ± 445 years for surface rupturing events of M_w 7.0 – 7.5 on the NEF. These results agree with previous estimates and therefore have no effect on the fault avoidance recurrence interval assigned by Van Dissen et al. (2003); however, with new constraints on the timing of the two most recent ruptures, estimates of the likely timing of future events can be made.

The last two events on the NEF have been constrained to 11150 ± 1650 and 3509 ± 2792 BP. The maximum age of rupture for Event 1 is derived from charcoal entrained in a colluvial wedge on Mt Noble. This age is considered likely to be closer to the actual age of fault rupture than the minimum age of 717 BP derived from in situ burnt roots within the soil

overlying the colluvium. This assertion is based on the fact that the charcoal was found at c. 25 cm below the surface in a c. 50 cm thick soil profile. Because the charcoal was in situ (Figure 4.6A), assuming that soil development rates have not changed considerably over the last 6000 years, the top 25 cm of soil must have accumulated in an absolute minimum of 717 years, as the soil at 25 cm depth had to have already been deposited by 717 BP. Therefore it is a reasonable assumption that the entire thickness of the soil layer must have taken a minimum of 1400 years to accumulate above the colluvial wedge.

Assuming time predictable behaviour, this inference is consistent with the minimum time interval between the two most recent events. With an average recurrence interval of 5612 ± 445 years and a minimum age of rupture for Event 2 of 9500 BP, Event 1 could be expected to have occurred by 3443 BP. Event 1 occurring any later than 3000 BP would imply an interseismic period outside the range of all four maximum estimates over the last c. 30 ka (see Section 4.3.).

As a result, it is likely that the NEF is in the latter half of its current interseismic period and the current risk associated with the NEF could be viewed as the equivalent of a Ia or Ib class fault (RI $\leq$ 3500 years) (Van Dissen et al. 2003).

As the Gola Peaks Section is likely to be a distinct rupture segment it also poses its own risk to the north Canterbury region. Unfortunately displacement data is too scarce and the SRL is too poorly constrained to be useful for estimating the magnitude potential of this fault. However, given the known combined minimum SRL of the Gola Peaks and Mt Gordon Sections of 14 km a rupture of the Eastern Segment is likely to be of $M_w > 6.2$ (See Figure 4.13).

4.5.2 GROUND ACCELERATION

The most significant factor in assessing the likely impact of a NEF earthquake on any off-fault location in Canterbury is the peak ground accelerations at the site in question. Campbell & Bozorgnia (1994) use accelerogram data from historic earthquakes to produce a relationship between M_w, distance from the fault rupture in kilometres (R) and Peak Horizontal Acceleration (PHA) at a given site. Their relationship,

$$\ln PHA\ (gals) = 3.512 + 0.904Mw - 1.328ln\sqrt{R^2 + (0.149\exp(0.647Mw))^2} + (1.125 - 0.112lnR - 0.0957Mw)$$

produces PHAs of 0.07 to 0.10 g in central Christchurch for a M_w 7.0 – 7.5 earthquake on the NEF (R = 65). Using the Modified Mercalli Intensity (MMI) correlation formula of Trifunac & Brady (1975),

$$\log PHA\ (gal) = 0.014 + 0.3MMI$$

these PHAs result in MMIs of VI to VII. The same magnitude range results in PHAs of over 0.23 g and MMIs ≥ VIII for the towns of Waikari and Hawarden, less than 30 km from the NEF. Ground accelerations of this magnitude are enough to cause damage to unreinforced masonry buildings in Christchurch but are likely to be just below the threshold for liquefaction in vulnerable areas of the city (Quigley personal commun) while significant structural damage to unreinforced buildings and houses not properly secured to their foundations is likely to occur within 30 km of the NEF.

4.6. SUMMARY

- OSL and ^{14}C dating on the Hurunui River Terraces and Mt Noble uphill-facing scarp respectively constrain the timing of the two most recent surface rupturing events on the western NEF to 12800 – 9500 and 6324 – 716 years BP.

- OSL dating of a terrace tread offset by five surface rupturing events reveals an average late Quaternary recurrence interval for the western NEF of 5612 ± 445 years and a late Quaternary vertical slip rate for the dextral-reverse Waitohi and Hurunui River sections of 0.31 ± 0.06 mm yr^{-1}.

- Cumulative displacements of stream banks on the Mt Noble Section allow a late Quaternary lateral slip rate of 0.82 ± 0.06 mm yr^{-1} to be calculated for the Mt Noble Section.

- The strain accommodated by the NEF can account for 8 to > 100% of the residual strain found to be unaccounted for in North Canterbury by Wallace et al. (2007).

- The average displacement to surface rupture length ratio of the NEF is anomalously high when compared to empirically derived regressions due to likely erosion of the fault tips and a possible regional departure of fault scaling relationships in Canterbury from the global average.

- Fault scaling relationships produce a preferred moment magnitude range for characteristic surface rupturing events on the NEF of 7.0 – 7.4. These estimates fit well with the magnitude probability estimates obtained from single point displacements by Biasi & Weldon (2006), producing a preferred range of M_w 7.0 – 7.5 for characteristic surface rupturing events.

- Based on average late Quaternary recurrence intervals and temporal constrains on the two most recent events, the NEF is likely to be within the latter half of its current interseismic period and as such, should be considered a greater hazard than the c. 5,600 year recurrence interval would imply.

CHAPTER 5
CONCLUSIONS

5.1. FAULT GEOMETRY AND DISPLACEMENTS

Detailed field mapping of the NEF has revealed a series of distinct, discontinuous fault sections stretching across c. 25 kilometres of steep farmland in the North Canterbury High Country. Changes in strike and the surrounding topography are accompanied by changes in the style of deformation seen along the surface trace. Based on these changes, the NEF is divided into six fault sections, four dominantly dextral-reverse (the Hurunui River, Waitohi, Whitnow and Gola Peaks Sections) and two dextral-normal (the Mt Noble and Mt Gordon Sections) (Figure 2.1). With all fault traces dipping towards the topographic highs, the faults on the eastern and western slopes can be grouped into two major sections of east-dipping and west-dipping fault traces, separated by the Waitohi River.

Defining distinct rupture segments on the NEF is complicated by the ambiguity of the relationship between the Waitohi and Gola Peaks Sections, which appear to strike directly towards each other from opposite sides of the Waitohi valley. Although geomorphic clues such as the straightening of the river along the projected strike, the reduction in topographic relief to the north of the Gola Peaks Section and the apparently undisturbed terraces to the south of the Waitohi Section give credit to the idea of a link across the valley floor, the complex geometry required to link the two oppositely dipping thrust faults makes this scenario structurally improbable. The preferred model is that of two opposing thrust segments converging on the valley floor. As a result, the Gola Peaks Segment is inferred to be a back-thrust off of the west-dipping Waitohi Downs Fault to the east (Figure 3.8 and 3.9).

Measurements along the western sections yield maximum lateral and vertical offsets of c. 24 m and c. 9.5 m respectively. The consistency of dextral offsets measured to a multiple of c. 5 m on the NEF strongly suggests a consistent characteristic displacement for surface rupturing events along the Mt Noble Section in the absence of interseismic creep. The vertical separations measured for two distinct events at the Hurunui River Section and the consistency of cumulative displacements across the Waitohi Section strengthen the idea of characteristic displacements along the length of the NEF over a series of repeated surface rupturing events. As a result, any future surface ruptures could be expected to produce approximately 5 m of right-lateral displacement along central NE striking sections and c. 2 m of vertical displacement along the more northerly striking Hurunui River and Waitohi Sections.

5.2. KINEMATICS AND REGIONAL STRAIN

The kinematics of fault rupture on the NEF were analysed through net displacements and striations measured directly from exposed fault planes. Additionally, seismicity within 15 km of the NEF over the last 7 years was analysed to assess the regional stress field in North Canterbury.

The results of kinematic analysis of the NEF are in agreement with the regional stress field derived from historic seismicity. W to NW oriented compression and moderately plunging NE/SW extension dominate the area, a conclusion in keeping with the findings of numerous other North Canterbury studies (e.g. {Cowan, 1992 #95}, {Cowan, 1990 #124}, {Nicol, 1991 #86}, {Mould, 1992 #84}, {McMorran, 1991 #123}, {Wallace, 2007 #121}). Local variations in the lesser stress fields among these authors are indicative of some level of strain partitioning within North Canterbury. Variations in the orientation of principal stress axes between the Mt Noble Section and the Hurunui River and Waitohi Sections reflect the inward gravitational collapse of Mt Noble. Gravity driven faulting is also evident on the north

western slope of Mt Noble where a local reversal in P and T axes reflects the downward sliding of a 300, 000 m^2 fault-bound block towards the Hurunui River Valley.

5.3. PALEOSEISMICITY

Paleoseismic investigations conducted along the central and northern sections of the NEF uncover its late Quaternary surface rupture history. Using a combination of long-term slip-rates and individually dated events we have improved our understanding of the characteristic temporal behaviour of the NEF as well as quantifying the strain accommodated by the structure.

OSL samples collected from the faulted terraces of the Hurunui River combined with ^{14}C dating of colluvial deposits on Mt Noble constrain the timing of the last two surface rupturing events to 12,800 – 9,500 and 6,324 – 716 BP. Dating of a displaced terrace tread on the Waitohi section reveals average late Quaternary recurrence intervals of 5,612 ± 445 years and vertical and lateral slip-rates of 0.31 ± 0.06 and 0.82 ± 0.06 mm yr^{-1} respectively.

The consistency of average recurrence interval estimates for time periods spanning between 2 and 5 events is suggestive of a time dependent rupture sequence over the last c. 30 ka. These results, combined with the consistent characteristic offsets measured along the western sections, are evidence of characteristic earthquake behaviour analogous to that described by {Schwartz, 1984 #100}.

When viewed in light of the GPS and geologically derived elastic block models of Wallace et al. (2007, In review) the NEF is found to be responsible for a significant portion of the previously unaccounted-for strain across North Canterbury. The orientation of stress axes in the 2007 model appear to be a better fit to the stress field within the NEF study area and the observed deformation on the NEF itself accounts for 27 to >100% of residual WNW-ENE

oriented shortening and 8 to 91% of residual NNE-SSW extension reported by Wallace et al. (2007).

5.4. MAGNITUDE AND HAZARD OF SURFACE RUPUTRE

A comparison of numerous published fault scaling relationships with data from historic South Island surface ruptures and paleoseismic studies reveals a regional deviation from the global datasets. Surface ruptures within the South Island generally have anomalously high AD, MD and M_w to SRL ratios as well as very high ADs and MDs for a known M_w.

The magnitude of paleoearthquakes on the NEF was assessed by using the fault scaling relationships proposed by several empirical studies to relate magnitude to surface rupture length, average and maximum displacement and rupture area. The results give a range of potential magnitudes of between 6.5 and 7.9. The large range is partly due to the anomalously high AD to SRL ratio of the NEF and partly due to variations in the different regressions proposed by each author. As a result, a preferred range of values of M_w 7.0 – 7.4 is calculated based on the best fitting regressions to historic South Island ruptures and the parameters that were able to be most accurately measured on the NEF. These estimates are consistent with magnitude probabilities derived from single point measurements on the Mt Noble and Hurunui River Sections, resulting in a likely paleoearthquake magnitude range of 7.0 – 7.5.

Being just c. 60 km northwest of the city of Christchurch, a rupture of the NEF would likely have a significant impact on a population in excess of 400,000 people. Analysis of the temporal data produced in this study agrees with the fault avoidance recurrence interval assigned by Van Dissen et al (2003) of 5000 – 10,000 years but also indicates that the NEF is likely to be in the latter half of the characteristic earthquake cycle. As a result the current hazard associated with the NEF should be viewed as the equivalent of a Ia or Ib class fault

(RI ≤ 3500 years) (Van Dissen et al. 2003). Peak horizontal ground accelerations associated with an earthquake of M_w 7.0 – 7.5 could be as high as 0.1 g in Christchurch city resulting in damage to unreinforced masonry.

ACKNOWLEDGMENTS

Thank you to Mark Quigley for his enthusiastic and encouraging supervision during a period that has been both extremely exciting and extremely difficult for all of us. Also, to Joc Campbell, Jarg Pettinga, the technical and administrative staff and many others in the department, thank you for discussions guidance and assistance throughout the past two years.

Seismic work and OSL sampling would not have been possible without the help of Mike Finnemore, Matt Cockcroft, Cristian Vasquez, Carolyn Phillips and Eva Hartung. Input and assistance from Andy Nicol, John Ristau, Kevin Fenaughty and others at GNS is gratefully acknowledged.

I wish to thank all of the land owners who allowed me free rein on their property, including Bob and Burnadette Frame of Mt Noble, Jerry and Ginny Kennedy and Simon of Mt Whitnow, Mark Rutherford of Gola Peaks, Graeme and Nancy Inch of Seven Hills and in particular Malcolm and Keri Spencer of Mt Virginia who also provided field accommodation.

REFERENCES

Beck AC 1968. Gravity faulting as a mechanism of topographic adjustment. New Zealand Journal of Geology and Geophysics 11(1): 191–199.

Benson AM, Little TA, Van Dissen RJ, Hill N, Townsend DB 2001. Late Quaternary paleoseismic history and surface rupture characteristics of the eastern Awatere strike-slip fault, New Zealand. Geological Society of America Bulletin 113(8): 1079.

Berger GW, Tonkin PJ, Pillans BJ 1996. Thermoluminescence ages of Post-Glacial loess, Rakaia River, South Island, New Zealand. Quaternary International 34-36: 177-181.

Berrill JB 1988. Diversion of faulting by hills. Quarterly Journal of Engineering Geology & Hydrogeology 21(4): 371.

Berryman K, Villamor P 2004. Surface rupture of the Poulter Fault in the 1929 March 9 Arthur's Pass earthquake, and redefinition of the Kakapo Fault, New Zealand. New Zealand Journal of Geology and Geophysics 47: 341-351.

Berryman K, Webb, T., Hill, N., Rhoades, D., Beavan, J. and Darby, D. 2002. Seismic loads on dams - Waitaki system: Earthquake source characterisation. Institute of Geological & Nuclear Sciences client report.

Biasi GP, Weldon RJ 2006. Estimating surface rupture length and magnitude of paleoearthquakes from point measurements of rupture displacement. Bulletin of the Seismological Society of America 96(5): 1612.

Botsford JW 1983. The Esk Head melange in the Esk Head/Okuku area, North Canterbury : a thesis submitted in partial fulfilment of the requirements for the degree of Master of Science in Geology in the University of Canterbury. Unpublished Thesis (M Sc) thesis, University of Canterbury, 1983. xi, 249 leaves (some folded) p.

Bowman D, King G, Tapponnier P 2003. Slip partitioning by elastoplastic propagation of oblique slip at depth. Science 300(5622): 1121.

Bradshaw JD 1972. Stratigraphy and structure of the Torlesse Supergroup (Triassic-Jurassic) in the foothills of the Southern Alps near Hawarden (S60-61), Canterbury. New Zealand Journal of Geology and Geophysics 15: 71-87.

Bradshaw JD 1973. Allocthonous Mesozoic fossil localities in melange within the Torlesse rocks of North Canterbury. Journal of the Royal Society of New Zealand 3(2): 161–167.

Buchanan J 1868. Kaikoura district. New Zealand Geological Survey report of geological explorations 4: 34-41.

Campbell J, Cowan, HA., Nicol, A., Pettinga, JR. 1994. Interpreting paleoseismic data in areas of structural complexity. International Association of Seismology and Physics of the Earth s Interior, 27th General Assembly, Wellington, New Zealand Abstracts(W99.4).

Campbell KW, Bozorgnia Y 1994. Near-source attenuation of peak horizontal acceleration from worldwide accelerograms recorded from 1957 to 1993. Pp. 10-14.

Chamberlain CG 1996. Seismic Hazard from Cross-Faulting in North Canterbury. Unpublished thesis, University of Canterbury, Christchurch.

Cowan H 1992. Structure, Seismicity and Tectonics of the Porter's Pass-Amberly Fault Zone, North Canterbury, New Zealand. Unpublished thesis, University of Canterbury, Christchurch.

Cowan HA 1990. Late Quaternary displacements on the Hope Fault at Glynn Wye, North Canterbury. New Zealand Journal of Geology and Geophysics 33(2): 285-293.

Cowan HA 1991. The North Canterbury earthquake of September 1, 1888. Journal of the Royal Society of New Zealand 21(1): 1–12.

DeMets C, Gordon RG, Argus DF, Stein S 1990. Current plate motions. Geophysical Journal International 101(2): 425-478.

DeMets C, Gordon RG, Angus DF, Stein S 1994. Effect of recent revisions to the geomagnetic reversal time scale on estimates of current plate motions.

Eusden JD, Pettinga JR, Campbell JK 2000. Structural evolution and landscape development of a collapsed transpressive duplex on the Hope Fault, North Canterbury, New Zealand. New Zealand Journal of Geology and Geophysics 43(3): 391-404.

Forsyth PJ, Jongens R, Barrell DJA 2008. Geology of the Christchurch area, Lower Hutt, Institute of Geological and Nuclear Sciences.

Furlong KP, Kamp PJJ 2009. The lithospheric geodynamics of plate boundary transpression in New Zealand: Initiating and emplacing subduction along the Hikurangi margin, and the tectonic evolution of the Alpine Fault system. Tectonophysics 474(3-4): 449-462.

Gledhill K, Ristau J, Reyners M, Fry B, Holden C 2011. The Darfield (Canterbury, New Zealand) Mw 7.1 Earthquake of September 2010: A Preliminary Seismological Report. Seismological Research Letters 82(3): 378.

Gold RD, Cowgill E, Arrowsmith JR, Gosse J, Chen X, Wang XF 2009. Riser diachroneity, lateral erosion, and uncertainty in rates of strike slip faulting: A case study from Tuzidun along the Altyn Tagh Fault, NW China. Journal of Geophysical Research 114(B4): B04401.

Gregg DR 1964. Sheet 18 Hurunui Geological Map of New Zealand 1: 250,000. NZ Department of Scientific and Industrial Research, Wellington.

Hecker S, Abrahamson N 2002. Characteristic fault rupture: implications for fault rupture hazard analysis, paper presented at the Pacific Earthquake Engineering Research Centre (PEER) Lifelines Research Meeting, Oakland, California., 24 June.

Hecker SaA, N. S. 2004. Low slip-at-a-point variability: Implications for earthquake size distribution, fault rupture hazard, and ground-motion modeling. paper presented at Basin and Range Province Seismic Hazard Summit II, West. States Seismic Policy Council, Reno, Nevada.

Hemphill-Haley MA, Weldon RJ 1999. Estimating prehistoric earthquake magnitude from point measurements of surface rupture. Bulletin of the Seismological Society of America 89(5): 1264.

Howard ME 2001. Holocene surface-faulting earthquakes along the Porters Pass fault : a thesis submitted in partial fulfilment of the requirements for the degree of Master of Science in Engineering Geology at the University of Canterbury. Unpublished Thesis (M Sc) thesis, University of Canterbury, 2001. xii, 165 leaves (4 folded) p.

Howard MN, A; Campbell, J; Pettinga, J 2005. Holocene paleoearthquakes on the strike-slip Porters Pass Fault, Canterbury, New Zealand. New Zealand Journal of Geology and Geophysics 48(1): 59-74.

Kelson KI, Kang KH, Page WD, Lee CT, Cluff LS 2001. Representative styles of deformation along the Chelungpu fault from the 1999 Chi-Chi (Taiwan) earthquake: geomorphic characteristics and responses of man-made structures. Bulletin of the Seismological Society of America 91(5): 930.

King G, Klinger Y, Bowman D, Tapponnier P 2005. Slip-partitioned surface breaks for the Mw 7.8 2001 Kokoxili earthquake, China. Bulletin of the Seismological Society of America 95(2): 731.

Langridge RM, Berryman KR 2005. Morphology and slip rate of the Hurunui section of the Hope Fault, South Island, New Zealand. New Zealand Journal of Geology and Geophysics 48(1): 43-57.

Langridge RM, Villamor P, Basili R, Almond P, Martinez-Diaz JJ, Canora C 2010. Revised slip rates for the Alpine fault at Inchbonnie: Implications for plate boundary kinematics of South Island, New Zealand. Lithosphere 2(3): 139.

Leonard M 2010. Earthquake Fault Scaling: Self-Consistent Relating of Rupture Length, Width, Average Displacement, and Moment Release. Bulletin of the Seismological Society of America 100(5A): 1971.

Lian OB, Roberts RG 2006. Dating the Quaternary: progress in luminescence dating of sediments. Quaternary Science Reviews 25(19-20): 2449-2468.

Little TA, Grapes R, Berger GW 1998. Late Quaternary strike slip on the eastern part of the Awatere fault, South Island, New Zealand. Geological Society of America Bulletin 110(2): 127.

Little TA, Van Dissen R, Rieser U, Smith EGC, Langridge RM 2010. Coseismic strike slip at a point during the last four earthquakes on the Wellington fault near Wellington, New Zealand. Journal of Geophysical Research 115(B5): B05403.

Liu-Zeng J, Klinger Y, Sieh K, Rubin C, Seitz G 2006. 2 Serial ruptures of the San Andreas fault, Carrizo Plain, 3 California, revealed by three-dimensional excavations.

Manighetti I, Campillo M, Bouley S, Cotton F 2007. Earthquake scaling, fault segmentation, and structural maturity. Earth and Planetary Science Letters 253(3-4): 429-438.

Mason BH 1949. The geology of the Mandamus-Pahau District, North Canterbury. Transactions of the Royal Society of New Zealand 77: 403-428.

McCalpin J 2009. Paleoseismology, Academic Pr.

McCalpin JP 1996. Tectonic geomorphology and Holocene paleoseismicity of the Molesworth section of the Awatere fault, South Island, New Zealand. New Zealand Journal of Geology and Geophysics 39: 33-50.

McMorran T 1991. The Hope Fault at Hossack Station east of Hanmer Basin, North Canterbury. Unpublished thesis, University of Canterbury, Christchurch.

Miller DJ, Dunne T 1996. Topographic perturbations of regional stresses and consequent bedrock fracturing. Journal of Geophysical Research 101(B11): 25523.

Mould R 1992. Structure and Kinematics of Late Cenozoic Deformation Along the Western Margin of the Culverden Basin, North Canterbury, New Zealand: A Thesis Submitted in Partial Fulfillment of the Requirements for the Degree of Master of Science in Geology in the University of Canterbury. Unpublished thesis, University of Canterbury.

Nathan S, Rattenbury, M.S., Suggate, R.P. 2002. Geology of the Greymouth area, Lower Hutt, Institute of Geological and Nuclear Sciences. 1 sheet + 58 p p.

Nicol A 1991. Structural styles and kinematics of deformation on the edge of the New Zealand plate boundary zone, mid-Waipara region, North Canterbury. Unpublished thesis, University of Canterbury, Christchurch.

Nicol A, Van Dissen R 2002. Up-dip partitioning of displacement components on the oblique-slip Clarence Fault, New Zealand. Journal of Structural Geology 24(9): 1521-1535.

Norris RJ, Cooper AF 2001. Late Quaternary slip rates and slip partitioning on the Alpine Fault, New Zealand. Journal of Structural Geology 23(2-3): 507-520.

Pettinga JR, Yetton, M.D., Van Dissen, R.J., Downes, G.L. 2001. Earthquake source identification and characterisation for the Canterbury region, South Island, New Zealand. Bulletin of the New Zealand Society for Earthquake Engineering 34(4): 282-317.

Philip H, Rogozhin E, Cisternas A, Bousquet JC, Borisov B, Karakhanian A 1992. The Armenian earthquake of 1988 December 7: faulting and folding, neotectonics and palaeoseismicity. Geophysical Journal International 110(1): 141-158.

Powers WE 1962. Terraces of the Hurunui River, New Zealand, Northwestern University.

Quigley M, Van Dissen, R., Litchfield, N., Villamor, P., Duffy, B., Barrell, D., Furlong, K., Stahl, T., Bilderback, E., Noble, D. 2012. Surface rupture during the 2010 Mw 7.1 Darfield (Canterbury, New Zealand) earthquake: implications for fault rupture dynamics and seismic-hazard analysis. Geology 40(1): 4.

Quigley M, Van Dissen, R., Villamor, P., Litchfield, N., Barrell, D., Furlong, K., Stahl, T., Duffy, B., Bilderback, E., Noble, D., Townsend, D., Begg, J., Jongens, R., Ries, W., Claridge, J., Klahn, A., Mackenzie, H., Smith, A., Hornblow, S., Nicol, R., Cox, S., Langridge, R., Pedley. K. 2010. Surface Rupture of the Greendale Fault during the Mw 7.1 Darfield (Canterbury) Earthquake, New Zealand: Initial Findings. Bulletin of the New Zealand Society for Earthquake Engineering 43(4): 1 - 7.

Rattenbury MS, Townsend DB, Johnston MR 2006. Geology of the Kaikoura area, Lower Hutt, Institute of Geological and Nuclear Sciences. 1 map+ 70p p.

Rubin CM, Sieh K 1997. Long dormancy, low slip rate, and similar slip-per-event for the Emerson fault, eastern California shear zone. J. geophys. Res 102: 15,319–15,333.

Santos GM, Gomes PRS, Anjos RM, Cordeiro RC, Turcq BJ, Sifeddine A, Di Tada ML, Cresswell RG, Fifield LK 2000. 14C AMS dating of fires in the central Amazon rain forest. Nuclear Instruments and Methods in Physics Research Section B: Beam Interactions with Materials and Atoms 172(1-4): 761-766.

Schwartz DP, Coppersmith KJ 1984. Fault behavior and characteristic earthquakes: examples from the Wasatch and San Andreas fault zones. Journal of Geophysical Research 89(B7): 5681-5698.

Shimazaki K, Nakata, T. 1980. Time-predictable recurrence model for large earthquakes. Geophysical research letters 7.

Speight R 1918. Structure and Glacial Features of the Hurunui Valley. Transactions of the New Zealand Institute 50: 93-105.

Stirling M, Rhoades D, Berryman K 2002. Comparison of Earthquake Scaling Relations Derived from Data of the Instrumental and Preinstrumental Era. Bulletin of the Seismological Society of America 92(2): 812-830.

Stirling M, Gerstenberger M, Litchfield N, McVerry G, Smith W, Pettinga J, Barnes P 2008. Seismic hazard of the Canterbury region, New Zealand: New earthquake source model and methodology. Bulletin of the New Zealand Society for Earthquake Engineering 41: 51–67.

Sutherland R, Berryman K, Norris R 2006. Quaternary slip rate and geomorphology of the Alpine fault: Implications for kinematics and seismic hazard in southwest New Zealand. Geological Society of America Bulletin 118(3-4): 464.

Syme AR 1991. Structural Analysis of the Deformation of the Marble Point Outlier, Waiau River, North Canterbury. Unpublished thesis, University of Canterbury, Christchurch.

Tibaldi A 1998. Effects of topography on surface fault geometry and kinematics: examples from the Alps, Italy and Tien Shan, Kazakstan. Geomorphology 24(2-3): 225-243.

Trifunac MD, Brady AG 1975. On the correlation of seismic intensity scales with the peaks of recorded strong ground motion. Bulletin of the Seismological Society of America 65(1): 139.

Tuttle MP, Schweig ES 1995. Archeological and pedological evidence for large prehistoric earthquakes in the New Madrid seismic zone, central United States. Geology 23(3): 253.

Van Dissen R, Nicol A 2009. Mid-late Holocene paleoseismicity of the eastern Clarence Fault, Marlborough, New Zealand. New Zealand Journal of Geology and Geophysics 52(3): 195-208.

Van Dissen RJ, Berryman K, Webb T, Stirling M, Villamor P, Wood PR, Nathan S, Nicol A, Begg J, Barrell D 2003. An interim classification of New Zealand's active faults for the mitigation of surface rupture hazards.

Wallace LM, Beavan J, McCaffrey R, Berryman K, Denys P 2007. Balancing the plate motion budget in the South Island, New Zealand using GPS, geological and seismological data. Geophysical Journal International 168(1): 332-352.

Wallace LM, Barnes, P., Beaven, J., Van Dissen, R., Litchfield, N., Mountjoy, J., Lamarche, G., Pondard, N. In review. The Kinematics of a Transition from Subduction to Strike-Slip: an example from the central New Zealand plate boundary.

Wells DL, Coppersmith KJ 1994. New empirical relationships among magnitude, rupture length, rupture width, rupture area, and surface displacement. Bulletin of the Seismological Society of America 84(4): 974-1002.

Wesnousky SG 2008. Displacement and geometrical characteristics of earthquake surface ruptures: Issues and implications for seismic-hazard analysis and the process of earthquake rupture. Bulletin of the Seismological Society of America 98(4): 1609.

Yetton MD 2000. The Probability and Consequences of the Next Alpine Fault Earthquake, South Island, New Zealand. Unpublished Ph.D thesis, University of Canterbury, Christchurch.

Appendix A: Differential GPS Contours and Data

Mt Noble Contour

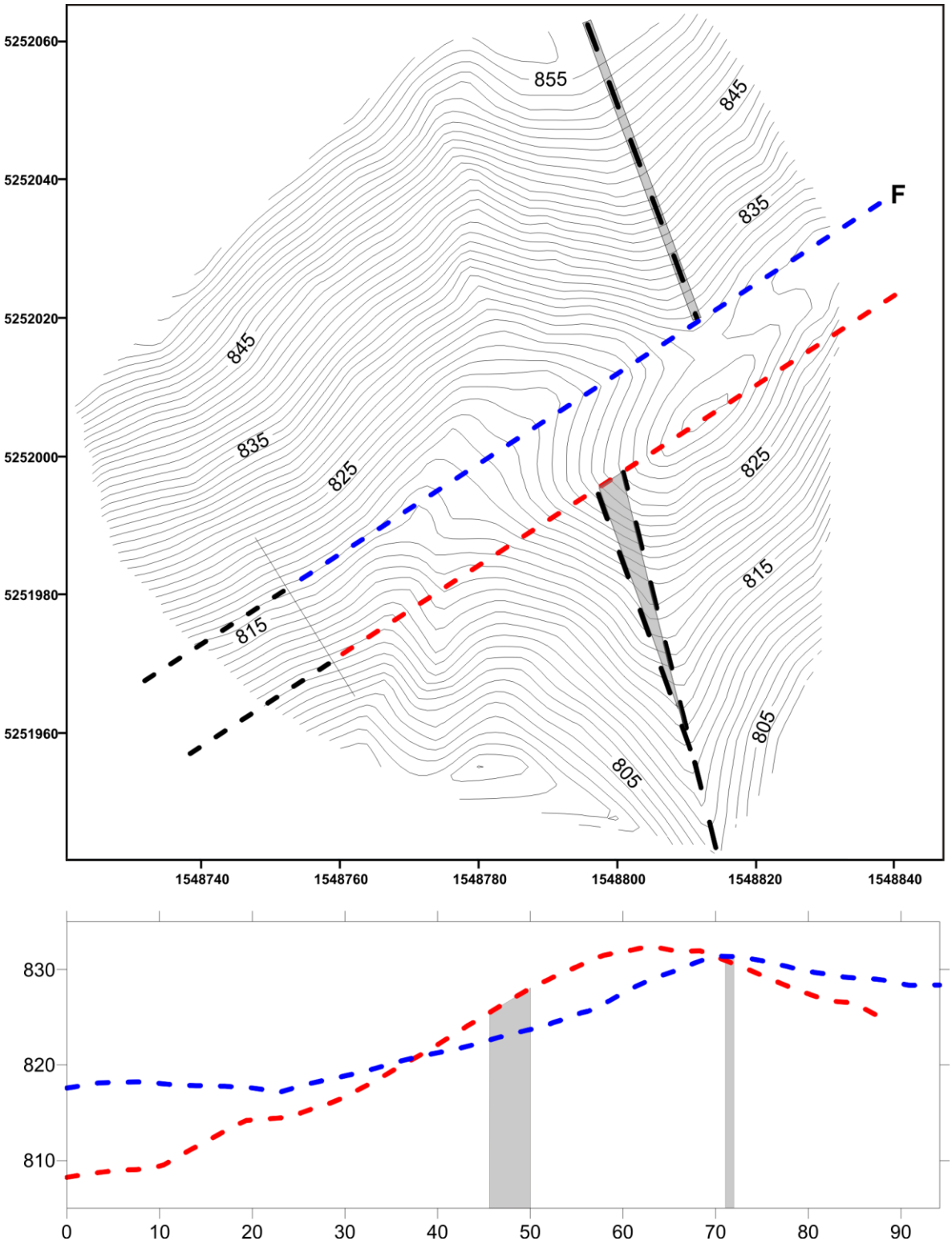

Mt Noble GPS Points

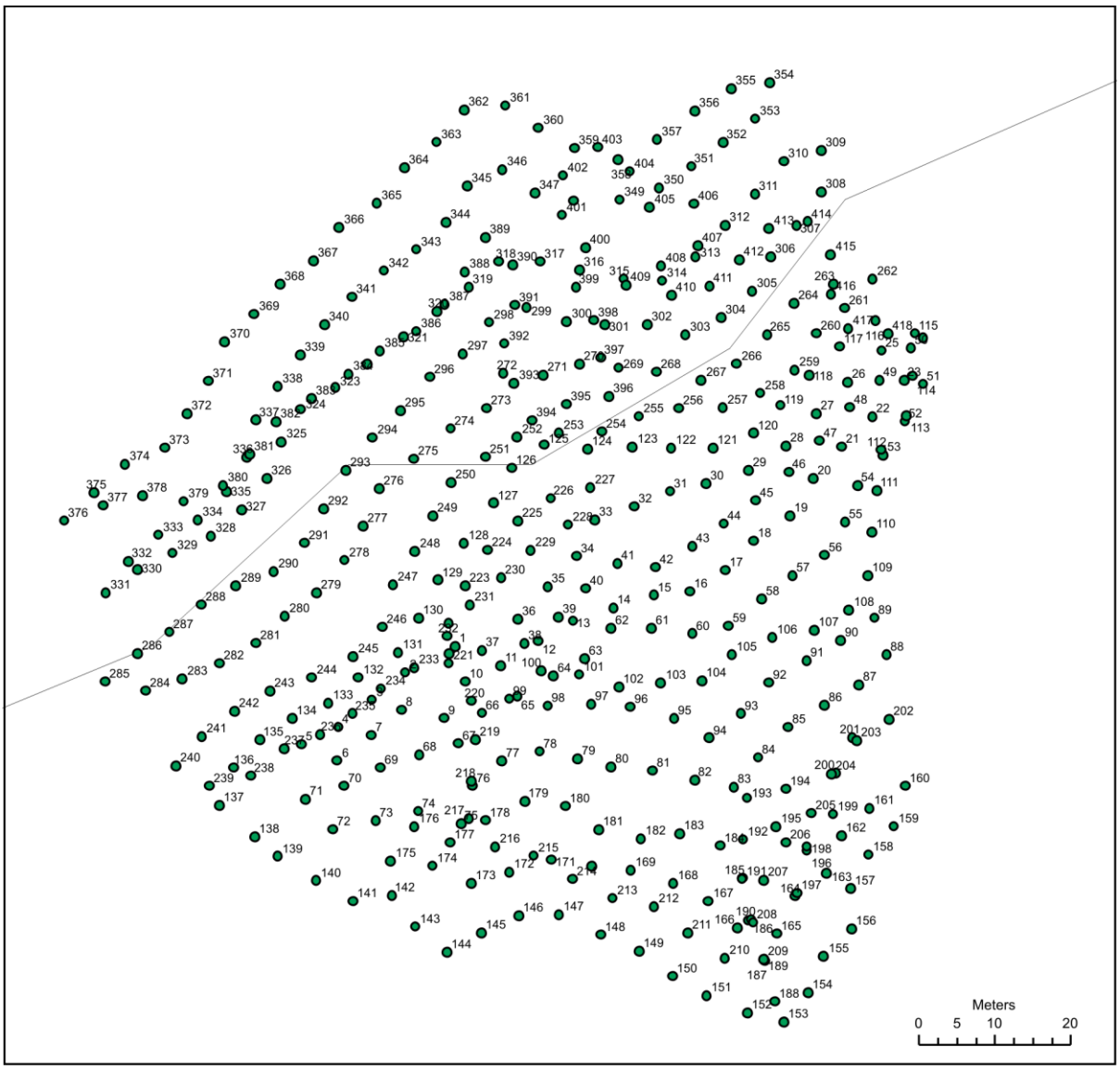

Mt Noble GPS Data

ID	Easting	Northing	Elevation	Vert Precision	Horz Precision	MaxPDOP	MaxHDOP
1	2458771.861	5813815.395	815.859	0.9	0.7	3.2	1.8
2	2458765.228	5813811.965	816.209	0.4	0.3	2.5	1.6
3	2458760.837	5813808.418	816.259	0.5	0.3	2.5	1.6
4	2458756.412	5813804.773	816.149	0.4	0.3	2.5	1.6
5	2458751.563	5813802.525	815.898	0.4	0.3	2.5	1.6
6	2458756.275	5813800.366	813.136	0.4	0.2	2.5	1.6
7	2458760.752	5813803.68	813.785	0.4	0.3	2.5	1.6
8	2458764.769	5813807.011	813.369	0.4	0.3	2.5	1.6
9	2458770.361	5813805.967	812.184	0.4	0.3	2.5	1.6
10	2458773.19	5813810.792	816.095	0.4	0.3	2.5	1.6
11	2458777.831	5813812.85	817.16	0.4	0.3	2.5	1.6
12	2458782.815	5813816.128	818.644	0.4	0.3	3.3	1.7
13	2458787.36	5813818.761	821.065	0.4	0.2	3.3	1.7
14	2458792.751	5813820.504	823.931	0.4	0.3	3.3	1.7
15	2458798.066	5813822.177	827.022	0.4	0.2	3.3	1.7
16	2458802.795	5813822.699	829.185	0.4	0.2	2.6	1.6
17	2458807.497	5813825.443	831.682	0.4	0.2	2.6	1.6
18	2458811.22	5813829.346	832.743	0.4	0.2	2.6	1.6
19	2458816.025	5813832.562	832.28	0.4	0.2	2.6	1.6
20	2458819.078	5813837.541	831.716	0.4	0.2	2.6	1.6
21	2458822.804	5813841.774	830.651	0.4	0.2	2.6	1.6
22	2458826.874	5813845.717	829.747	0.4	0.2	2.6	1.6
23	2458831.068	5813850.456	828.476	0.3	0.2	2.6	1.6
24	2458833.565	5813856.081	827.826	0.2	0.1	3.4	1.7
25	2458828.089	5813854.424	828.223	0.4	0.2	3.4	1.7
26	2458823.676	5813850.263	828.596	0.4	0.2	3.4	1.7
27	2458819.469	5813846.093	829.043	0.4	0.2	3.4	1.7
28	2458815.526	5813841.861	829.848	0.4	0.2	2.6	1.6
29	2458810.516	5813838.586	829.79	0.3	0.2	2.6	1.6
30	2458804.953	5813836.842	828.212	0.3	0.2	2.6	1.6
31	2458800.208	5813835.893	825.736	0.3	0.2	3.4	1.7
32	2458795.457	5813833.862	823.959	0.3	0.2	3.4	1.7
33	2458790.295	5813832.033	822.424	0.3	0.2	3.4	1.7
34	2458787.864	5813827.326	821.491	0.3	0.2	3.4	1.7
35	2458784.069	5813823.304	820.314	0.3	0.2	3.4	1.7
36	2458780.09	5813819.003	818.773	0.3	0.2	3.4	1.7
37	2458775.394	5813814.864	817.977	0.5	0.3	3.4	1.7
38	2458780.976	5813815.826	818.183	0.3	0.2	3.4	1.7
39	2458785.482	5813819.271	820.284	0.3	0.2	3.4	1.7
40	2458789.034	5813823.043	822.235	0.3	0.2	3.4	1.7
41	2458793.284	5813826.312	824.179	0.3	0.2	3.4	1.7
42	2458798.274	5813825.871	826.857	0.3	0.2	3.4	1.7
43	2458803.168	5813828.641	829.148	0.3	0.2	3.4	1.7
44	2458807.271	5813831.594	830.391	0.3	0.2	3.4	1.7
45	2458811.473	5813834.684	830.973	0.3	0.2	2.8	1.4
46	2458815.859	5813838.44	830.698	0.3	0.2	3.5	1.7
47	2458819.917	5813842.584	829.851	0.3	0.2	3.5	1.7
48	2458823.906	5813846.972	829.185	0.3	0.2	3.5	1.7
49	2458827.838	5813850.473	828.739	0.3	0.2	3.5	1.7
50	2458831.942	5813854.755	828.209	0.3	0.2	3.5	1.7
51	2458833.583	5813850.03	827.624	0.3	0.2	3.5	1.7
52	2458831.164	5813845.106	827.837	0.3	0.2	3.5	1.7
53	2458828.337	5813840.592	826.889	0.3	0.2	3.5	1.7
54	2458824.927	5813836.631	827.472	0.3	0.2	3.5	1.7
55	2458823.309	5813831.813	827.267	0.3	0.2	3.5	1.7
56	2458820.561	5813827.471	827.241	0.3	0.2	3.5	1.7
57	2458816.327	5813824.771	828.152	0.3	0.2	3.5	1.7
58	2458812.287	5813821.639	827.399	0.3	0.2	2.8	1.4
59	2458807.873	5813818.116	827.564	0.3	0.2	2.8	1.4
60	2458803.104	5813817.091	826.786	0.3	0.2	2.8	1.4
61	2458797.692	5813817.808	824.877	0.3	0.2	2.8	1.4
62	2458792.394	5813817.777	822.788	0.3	0.2	2.8	1.4
63	2458788.905	5813813.808	819.558	0.3	0.2	2.8	1.4
64	2458784.802	5813811.489	817.079	0.3	0.2	3.6	1.7
65	2458780.061	5813808.852	815.202	0.3	0.2	3.6	1.7
66	2458775.36	5813806.659	814.675	0.3	0.2	3.6	1.7
67	2458772.27	5813802.62	812.288	0.3	0.2	3.6	1.7
68	2458767.11	5813801.094	809.538	0.3	0.2	3.6	1.7
69	2458761.985	5813799.414	810.408	0.3	0.2	3.6	1.7
70	2458757.16	5813797.053	810.231	0.3	0.2	3.6	1.7
71	2458752.105	5813795.257	810.201	0.3	0.2	3.6	1.7
72	2458755.693	5813791.273	806.17	0.3	0.2	3.6	1.7
73	2458761.378	5813792.404	805.764	0.3	0.2	3.6	1.7
74	2458766.945	5813793.668	805.223	0.3	0.2	3.6	1.7
75	2458772.618	5813792	808.409	0.3	0.2	2.8	1.4
76	2458774.099	5813797.012	811.78	0.3	0.2	2.8	1.4
77	2458778.001	5813800.326	811.212	0.3	0.2	2.8	1.4
78	2458782.963	5813801.579	810.61	0.3	0.2	2.8	1.4
79	2458788.009	5813800.605	810.642	0.3	0.2	2.8	1.4
80	2458792.417	5813799.498	810.63	0.3	0.2	3.7	1.8
81	2458797.903	5813799.054	813.068	0.3	0.2	3.7	1.8
82	2458803.426	5813797.767	816.115	0.3	0.2	2.8	1.4
83	2458808.611	5813796.829	816.82	0.3	0.2	2.8	1.4
84	2458811.829	5813800.808	816.349	0.3	0.2	2.8	1.4
85	2458815.734	5813804.783	815.763	0.3	0.2	2.8	1.4
86	2458820.579	5813807.691	815.244	0.3	0.2	2.8	1.4
87	2458825.079	5813810.282	814.24	0.3	0.2	2.8	1.4
88	2458828.75	5813814.323	814.854	0.3	0.2	2.8	1.4
89	2458827.168	5813819.188	818.459	0.3	0.2	2.8	1.4
90	2458822.729	5813816.22	819.323	0.4	0.2	2.8	1.4
91	2458818.195	5813813.49	819.731	0.3	0.2	2.8	1.4
92	2458813.268	5813810.626	820.139	0.3	0.2	2.8	1.4
93	2458809.535	5813806.555	819.63	0.3	0.2	2.8	1.4
94	2458805.319	5813803.345	819.294	0.3	0.2	2.8	1.4
95	2458800.754	5813805.903	817.899	0.3	0.2	2.8	1.4
96	2458794.959	5813807.419	816.647	0.3	0.2	2.8	1.4
97	2458789.819	5813807.789	815.778	0.3	0.2	2.8	1.4
98	2458784.096	5813807.599	814.41	0.3	0.2	2.8	1.4
99	2458779.01	5813808.509	814.724	0.3	0.2	2.8	1.4
100	2458783.176	5813812.155	816.897	0.3	0.2	2.8	1.4
101	2458788.171	5813811.684	817.658	0.3	0.2	2.8	1.4
102	2458793.431	5813810.087	817.938	0.3	0.2	2.8	1.4
103	2458798.974	5813810.584	820.463	0.3	0.2	2.8	1.4
104	2458804.372	5813810.868	822.652	0.3	0.2	2.8	1.4
105	2458808.379	5813814.315	824.786	0.3	0.2	2.8	1.4
106	2458813.687	5813816.608	823.798	0.3	0.2	2.8	1.4
107	2458819.175	5813817.57	822.228	0.3	0.2	2.8	1.4
108	2458823.795	5813820.188	820.958	0.3	0.2	2.8	1.4
109	2458826.28	5813824.714	821.754	0.3	0.2	2.8	1.4
110	2458826.83	5813830.502	823.803	0.3	0.2	2.8	1.4
111	2458827.492	5813835.944	825.33	0.3	0.2	2.8	1.4
112	2458828.071	5813841.35	826.818	0.3	0.2	2.8	1.4
113	2458831.4	5813845.817	827.768	0.3	0.2	2.8	1.4
114	2458832.153	5813851.107	828.753	0.3	0.2	2.8	1.4
115	2458832.477	5813856.694	827.883	0.3	0.2	2.8	1.4
116	2458827.325	5813858.361	830.119	0.3	0.2	2.8	1.4
117	2458822.571	5813854.998	830.46	0.3	0.2	2.8	1.4
118	2458818.523	5813851.174	830.524	0.3	0.2	2.8	1.4
119	2458814.765	5813847.221	831.323	0.3	0.2	2.8	1.4
120	2458811.2	5813843.536	831.358	0.3	0.2	2.8	1.4
121	2458805.881	5813841.573	829.689	0.3	0.2	2.8	1.4
122	2458800.34	5813841.519	827.88	0.3	0.2	4.0	1.8
123	2458795.241	5813841.708	827.615	0.3	0.2	4.0	1.8
124	2458789.34	5813841.406	827.365	0.3	0.2	4.0	1.8
125	2458783.597	5813842.014	826.603	0.3	0.2	4.0	1.8
126	2458779.337	5813838.952	825.382	0.3	0.2	4.0	1.8
127	2458776.921	5813834.299	822.859	0.3	0.2	4.0	1.8
128	2458772.968	5813829.035	821.858	0.3	0.2	3.0	1.3
129	2458769.543	5813824.17	820.74	0.3	0.2	3.0	1.3
130	2458767.057	5813819.147	819.396	0.3	0.2	3.0	1.3
131	2458764.322	5813814.639	818.857	0.3	0.2	3.0	1.3
132	2458759.083	5813811.28	819.224	0.3	0.2	3.0	1.3
133	2458755.138	5813807.877	818.487	0.3	0.2	3.0	1.3
134	2458750.34	5813805.905	818.361	0.3	0.2	4.1	1.8
135	2458746.128	5813803.135	818.11	0.3	0.2	4.1	1.8
136	2458742.576	5813799.473	816.64	0.3	0.2	4.1	1.8
137	2458740.77	5813794.462	813.895	0.3	0.2	4.1	1.8
138	2458745.415	5813790.287	809.377	0.3	0.2	3.0	1.3
139	2458748.415	5813787.724	806.73	0.3	0.2	4.1	1.9
140	2458753.474	5813784.508	802.352	0.3	0.1	3.0	1.3
141	2458758.385	5813781.799	798.868	0.3	0.2	3.0	1.3
142	2458763.482	5813782.522	798.57	0.3	0.2	3.0	1.3
143	2458766.596	5813778.478	798.847	0.3	0.2	3.0	1.3
144	2458770.777	5813775.096	799.85	0.3	0.1	3.0	1.3
145	2458775.276	5813777.602	798.883	0.3	0.1	3.0	1.3
146	2458780.206	5813779.863	797.793	0.3	0.1	3.0	1.3
147	2458785.507	5813780.012	798.198	0.3	0.1	3.0	1.3
148	2458791.023	5813777.399	799.908	0.3	0.1	3.0	1.3
149	2458796.135	5813775.206	800.641	0.2	0.1	3.0	1.3
150	2458800.54	5813771.977	800.816	0.2	0.1	3.0	1.3
151	2458805.048	5813769.353	802.196	0.3	0.1	3.0	1.3
152	2458810.399	5813767.032	804.96	0.3	0.1	3.0	1.3
153	2458815.21	5813765.885	807.045	0.3	0.1	3.0	1.3
154	2458818.416	5813769.76	805.29	0.3	0.1	3.0	1.3
155	2458820.465	5813774.552	804.055	0.2	0.1	3.0	1.3
156	2458824.174	5813778.164	801.908	0.2	0.1	3.0	1.3
157	2458824.014	5813783.464	802.619	0.3	0.1	3.0	1.3
158	2458826.371	5813787.976	802.513	0.3	0.1	3.0	1.3
159	2458829.735	5813791.695	801.569	0.3	0.1	3.0	1.3
160	2458831.25	5813797.006	803.559	0.3	0.2	3.0	1.3
161	2458826.514	5813794.005	804.358	0.3	0.2	3.0	1.3
162	2458822.833	5813790.452	805.6	0.3	0.2	3.0	1.3
163	2458820.861	5813785.478	804.98	0.3	0.2	3.0	1.3
164	2458816.718	5813782.502	807.467	0.3	0.1	3.0	1.3
165	2458814.279	5813777.559	808.51	0.3	0.1	3.0	1.3
166	2458809.051	5813778.288	809.191	0.3	0.1	3.0	1.3
167	2458805.234	5813781.817	808.597	0.3	0.1	3.0	1.3
168	2458800.596	5813784.142	806.985	0.3	0.1	3.0	1.3
169	2458795.023	5813785.879	805.188	0.3	0.1	3.0	1.3
170	2458789.881	5813786.419	804.059	0.3	0.1	3.0	1.3
171	2458784.499	5813787.311	802.373	0.3	0.1	3.0	1.3
172	2458778.988	5813785.581	802.183	0.3	0.1	3.0	1.3
173	2458773.942	5813784.181	803.65	0.3	0.1	3.0	1.3
174	2458768.867	5813786.475	803.171	0.3	0.1	3.0	1.3
175	2458763.341	5813787.144	800.896	0.3	0.1	3.0	1.3
176	2458766.452	5813791.62	803.408	0.3	0.1	3.0	1.3
177	2458771.164	5813789.571	805.995	0.3	0.2	3.0	1.3
178	2458775.805	5813792.484	808.163	0.3	0.2	3.0	1.3
179	2458781.069	5813794.978	806.771	0.3	0.2	3.0	1.3
180	2458786.382	5813794.361	806.238	0.3	0.2	3.0	1.3
181	2458790.799	5813791.207	806.87	0.3	0.2	3.0	1.3
182	2458796.34	5813790.018	808.24	0.3	0.2	3.0	1.3
183	2458801.467	5813790.698	811.083	0.3	0.2	3.0	1.3
184	2458806.812	5813789.153	812.596	0.3	0.2	3.0	1.3
185	2458809.697	5813784.907	812.128	0.3	0.2	3.0	1.3
186	2458810.472	5813779.289	810.42	0.3	0.1	3.0	1.3
187	2458812.713	5813773.963	809.328	0.3	0.1	3.0	1.3
188	2458814.034	5813768.589	807.729	0.3	0.1	3.0	1.3
189	2458812.591	5813774.198	809.253	0.3	0.1	3.0	1.3
190	2458810.896	5813779.381	810.363	0.3	0.1	3.0	1.3
191	2458809.677	5813784.766	811.937	0.3	0.1	3.0	1.3
192	2458809.816	5813789.93	813.883	0.3	0.1	3.0	1.3
193	2458810.372	5813795.42	815.069	0.3	0.1	3.0	1.3
194	2458815.499	5813796.649	812.226	0.3	0.2	3.0	1.3
195	2458814.187	5813791.604	811.637	0.3	0.2	3.0	1.3
196	2458818.231	5813788.474	808.183	0.3	0.1	3.0	1.3
197	2458816.937	5813782.909	807.242	0.3	0.2	3.0	1.3
198	2458818.227	5813789.044	808.25	0.3	0.1	3.0	1.3
199	2458821.687	5813793.3	807.17	0.3	0.1	3.0	1.3
200	2458822.068	5813798.703	809.024	0.3	0.1	3.0	1.3
201	2458824.229	5813803.407	810.641	0.3	0.1	3.0	1.3
202	2458829.084	5813805.815	810.029	0.3	0.2	3.0	1.3
203	2458824.784	5813802.981	810.25	0.3	0.2	3.0	1.3
204	2458821.468	5813798.596	809.401	0.3	0.2	3.0	1.3
205	2458818.855	5813793.416	808.925	0.3	0.2	3.0	1.3
206	2458815.518	5813789.551	810.349	0.3	0.2	3.0	1.3
207	2458812.502	5813784.541	810.695	0.3	0.2	3.0	1.3
208	2458811.114	5813779.002	810.31	0.3	0.2	3.0	1.3
209	2458812.569	5813774.109	809.235	0.3	0.2	3.0	1.3
210	2458807.441	5813774.262	806.302	0.3	0.2	3.0	1.3
211	2458802.51	5813777.633	804.899	0.3	0.2	3.0	1.3
212	2458798.074	5813781.085	804.363	0.3	0.2	3.0	1.3
213	2458792.626	5813782.207	802.813	0.3	0.2	3.0	1.3
214	2458787.344	5813784.767	802.191	0.3	0.2	3.0	1.3
215	2458782.172	5813787.808	802.086	0.3	0.2	3.0	1.3
216	2458777.13	5813789.015	804.829	0.3	0.2	3.0	1.3
217	2458773.61	5813792.647	809.123	0.3	0.2	3.0	1.3
218	2458774.008	5813797.667	811.785	0.3	0.2	3.0	1.3
219	2458774.525	5813803.115	813.493	0.3	0.2	3.0	1.3
220	2458773.969	5813808.232	815.438	0.3	0.2	3.0	1.3
221	2458770.983	5813813.215	816.388	0.3	0.2	3.0	1.3
222	2458770.979	5813818.468	817.272	0.3	0.2	3.0	1.3
223	2458773.171	5813823.435	818.642	0.3	0.2	3.0	1.3
224	2458776.1	5813828.151	819.731	0.3	0.2	3.0	1.3
225	2458780.08	5813831.93	821.448	0.3	0.2	3.0	1.3
226	2458784.43	5813834.989	823.242	0.3	0.2	3.0	1.3
227	2458789.651	5813836.322	823.387	0.3	0.2	3.0	1.3
228	2458786.715	5813831.466	822.32	0.3	0.2	2.4	1.3
229	2458781.821	5813828.11	821.072	0.3	0.2	3.4	1.3
230	2458777.887	5813824.439	819.399	0.3	0.2	2.4	1.3
231	2458773.792	5813820.908	818.157	0.3	0.2	2.4	1.3
232	2458770.761	5813816.773	817.086	0.3	0.2	4.6	2.1
233	2458766.476	5813812.603	816.45	0.3	0.2	3.4	1.3
234	2458762.018	5813809.837	816.43	0.3	0.2	3.4	1.3
235	2458758.278	5813806.557	816.273	0.3	0.2	3.4	1.3
236	2458754.039	5813803.763	815.941	0.3	0.2	3.4	1.3
237	2458749.307	5813801.894	815.688	0.3	0.2	3.4	1.3

ID	Easting	Northing	Elevation	Vert Precision	Horz Precision	MaxPDOP	MaxHDOP
238	2458744.906	5813798.338	815.379	0.3	0.2	3.4	1.3
239	2458739.428	5813797.069	815.46	0.3	0.2	3.4	1.3
240	2458734.971	5813799.629	819.03	0.3	0.2	3.4	1.3
241	2458738.439	5813803.52	821.25	0.3	0.2	3.4	1.3
242	2458742.783	5813806.879	822.403	0.3	0.2	3.4	1.3
243	2458747.442	5813809.559	821.987	0.3	0.2	3.4	1.3
244	2458752.939	5813811.287	821.567	0.3	0.2	3.4	1.3
245	2458758.421	5813814.019	821.269	0.3	0.2	3.4	1.3
246	2458762.264	5813818.017	821.88	0.3	0.2	3.4	1.3
247	2458763.637	5813823.501	824.053	0.3	0.2	2.4	1.3
248	2458766.562	5813827.947	824.849	0.3	0.2	2.4	1.3
249	2458768.893	5813832.588	826.329	0.3	0.2	2.4	1.3
250	2458771.333	5813836.999	827.46	0.3	0.2	2.4	1.3
251	2458775.856	5813840.408	827.715	0.3	0.2	2.4	1.3
252	2458780.016	5813842.997	827.579	0.3	0.2	2.4	1.3
253	2458785.511	5813843.568	827.618	0.3	0.2	2.4	1.3
254	2458791.192	5813843.746	829.201	0.3	0.2	2.4	1.3
255	2458796.073	5813845.73	830.353	0.3	0.2	2.4	1.3
256	2458801.323	5813846.826	832.374	0.3	0.2	2.4	1.3
257	2458807.134	5813846.939	834.013	0.3	0.2	2.4	1.3
258	2458812.088	5813848.824	833.659	0.3	0.2	2.4	1.3
259	2458816.618	5813851.853	832.285	0.3	0.2	2.4	1.3
260	2458819.456	5813856.698	832.944	0.3	0.2	2.4	1.3
261	2458823.247	5813860.047	833.013	0.3	0.2	2.4	1.3
262	2458826.926	5813863.798	833.473	0.3	0.2	2.4	1.3
263	2458821.731	5813863.189	836.116	0.3	0.2	2.4	1.3
264	2458816.539	5813860.661	836.916	0.3	0.2	2.4	1.3
265	2458812.991	5813856.505	836.812	0.3	0.2	2.4	1.3
266	2458808.98	5813852.696	837.112	0.3	0.1	2.4	1.3
267	2458804.3	5813850.52	836.433	0.3	0.1	2.4	1.3
268	2458798.403	5813851.595	836.105	0.3	0.1	2.4	1.3
269	2458793.408	5813852.188	836.146	0.3	0.1	2.4	1.3
270	2458788.253	5813852.622	835.857	0.3	0.1	2.4	1.3
271	2458783.464	5813851.156	833.436	0.3	0.2	2.4	1.3
272	2458778.192	5813851.437	832.505	0.3	0.2	2.4	1.3
273	2458775.992	5813846.861	832.267	0.3	0.2	2.4	1.3
274	2458771.212	5813844.17	832.414	0.3	0.2	2.4	1.3
275	2458766.325	5813840.194	832.574	0.3	0.2	2.4	1.3
276	2458761.847	5813836.217	832.025	0.3	0.2	2.4	1.3
277	2458759.668	5813831.279	830.997	0.3	0.2	2.4	1.3
278	2458757.246	5813826.779	830.157	0.3	0.2	2.4	1.3
279	2458753.53	5813822.49	829.993	0.3	0.2	2.4	1.3
280	2458749.35	5813819.427	828.868	0.3	0.2	2.4	1.3
281	2458745.54	5813815.851	827.581	0.3	0.1	2.4	1.3
282	2458740.76	5813813.197	827.203	0.3	0.1	2.4	1.3
283	2458735.844	5813811.099	827.697	0.3	0.1	3.5	1.4
284	2458731.006	5813809.571	827.813	0.3	0.1	3.5	1.4
285	2458725.683	5813810.8	829.463	0.5	0.2	3.5	1.4
286	2458729.94	5813814.459	831.48	0.5	0.2	3.5	1.4
287	2458734.114	5813817.305	832.894	0.5	0.3	3.5	1.4
288	2458738.362	5813820.935	835.484	0.5	0.3	2.6	1.3
289	2458742.931	5813823.373	834.758	0.4	0.3	2.6	1.3
290	2458747.88	5813825.255	833.958	0.5	0.3	2.6	1.3
291	2458751.953	5813829.054	835.389	0.5	0.3	2.6	1.3
292	2458754.502	5813833.513	836.199	0.5	0.3	2.6	1.3
293	2458757.445	5813838.589	836.946	0.4	0.2	2.6	1.3
294	2458760.947	5813842.946	837.212	0.4	0.2	2.6	1.3
295	2458764.656	5813846.494	837.211	0.4	0.2	2.6	1.3
296	2458768.513	5813850.954	838.694	0.4	0.2	2.6	1.3
297	2458772.854	5813853.957	838.622	0.4	0.2	3.5	1.4
298	2458776.305	5813858.167	838.648	0.4	0.2	2.6	1.3
299	2458781.258	5813860.119	839.312	0.4	0.2	2.6	1.3
300	2458786.577	5813858.21	840.135	0.4	0.2	2.6	1.3
301	2458791.619	5813857.872	840.421	0.4	0.2	2.6	1.3
302	2458797.214	5813857.827	840.94	0.4	0.2	2.6	1.3
303	2458802.21	5813856.473	840.931	0.3	0.2	2.6	1.3
304	2458806.929	5813858.769	841.593	0.3	0.2	2.6	1.3
305	2458811.005	5813862.235	840.973	0.3	0.2	2.6	1.3
306	2458813.481	5813866.777	841.877	0.3	0.2	2.6	1.3
307	2458816.854	5813870.869	842.721	0.3	0.2	2.6	1.3
308	2458820.11	5813875.362	842.928	0.3	0.2	2.6	1.3
309	2458820.142	5813880.784	844.826	0.3	0.2	2.6	1.3
310	2458815.184	5813879.405	847.295	0.3	0.2	2.6	1.3
311	2458811.414	5813875.056	847.274	0.3	0.2	2.6	1.3
312	2458807.456	5813870.905	847.035	0.3	0.2	2.6	1.3
313	2458803.551	5813866.812	846.7	0.3	0.2	2.6	1.3
314	2458799.149	5813863.633	845.807	0.3	0.2	2.6	1.3
315	2458794.105	5813863.924	845.303	0.3	0.2	2.6	1.3
316	2458788.25	5813865.033	845.391	0.3	0.2	2.6	1.3
317	2458783.074	5813866.157	845.04	0.3	0.2	2.6	1.3
318	2458777.557	5813866.183	843.247	0.3	0.2	2.6	1.3
319	2458773.618	5813862.744	843.411	0.3	0.2	2.6	1.3
320	2458769.463	5813859.567	843.868	0.3	0.2	2.6	1.3
321	2458765.073	5813856.231	843.651	0.3	0.2	2.6	1.3
322	2458760.204	5813852.619	843.638	0.3	0.2	2.6	1.3
323	2458756.039	5813849.518	843.2	0.3	0.2	2.6	1.3
324	2458751.463	5813846.694	844.619	0.3	0.1	2.6	1.3
325	2458748.941	5813842.319	843.962	0.3	0.1	2.6	1.3
326	2458747.009	5813837.54	843.2	0.3	0.1	2.6	1.3
327	2458743.709	5813833.429	842.193	0.3	0.1	2.6	1.3
328	2458739.622	5813829.98	841.624	0.3	0.1	2.6	1.3
329	2458734.58	5813827.74	841.252	0.3	0.1	2.6	1.3
330	2458729.96	5813825.584	840.703	0.3	0.1	2.6	1.3
331	2458725.742	5813822.495	839.09	0.3	0.1	2.6	1.3
332	2458728.763	5813826.588	842.273	0.3	0.2	2.6	1.3
333	2458732.717	5813830.134	843.535	0.3	0.2	2.6	1.3
334	2458737.918	5813832.029	844.059	0.3	0.2	2.6	1.3
335	2458741.635	5813835.823	844.866	0.3	0.2	2.6	1.3
336	2458744.398	5813840.344	846.13	0.3	0.2	2.6	1.3
337	2458745.556	5813845.243	847.504	0.3	0.2	2.6	1.3
338	2458748.448	5813849.689	848.384	0.3	0.2	2.6	1.3
339	2458751.449	5813853.824	849.454	0.3	0.2	2.6	1.3
340	2458754.659	5813857.845	850.772	0.3	0.2	2.6	1.3
341	2458758.237	5813861.476	851.118	0.3	0.2	2.6	1.3
342	2458762.425	5813864.982	851.197	0.3	0.2	2.6	1.3
343	2458766.723	5813867.753	851.977	0.3	0.2	2.6	1.3
344	2458770.597	5813871.34	851.816	0.3	0.2	2.6	1.3
345	2458773.44	5813876.152	851.561	0.3	0.2	2.6	1.3
346	2458778.048	5813878.311	851.523	0.3	0.2	2.6	1.3
347	2458782.407	5813875.175	852.035	0.3	0.2	2.6	1.3
348	2458787.458	5813874.172	852.771	0.3	0.2	2.6	1.3
349	2458793.528	5813874.337	852.903	0.3	0.2	2.6	1.3
350	2458798.739	5813875.863	852.718	0.3	0.2	2.6	1.3
351	2458802.977	5813878.729	852.547	0.3	0.2	2.6	1.3
352	2458807.237	5813881.88	852.308	0.3	0.2	2.6	1.3
353	2458811.406	5813885.004	852.014	0.3	0.2	2.6	1.3
354	2458813.354	5813889.766	852.607	0.3	0.2	2.6	1.3
355	2458808.25	5813888.936	855.069	0.3	0.2	2.6	1.3
356	2458803.463	5813886.007	855.374	0.3	0.2	2.6	1.3
357	2458798.469	5813882.267	855.261	0.3	0.2	2.6	1.3
358	2458793.327	5813879.611	855.252	0.3	0.2	2.6	1.3
359	2458787.594	5813881.132	855.818	0.3	0.2	2.6	1.3
360	2458782.83	5813883.842	856.661	0.3	0.2	2.6	1.3
361	2458778.481	5813886.761	856.515	0.3	0.2	2.6	1.3
362	2458773.006	5813886.156	857.737	0.3	0.2	2.6	1.3
363	2458769.39	5813881.937	857.644	0.3	0.2	2.6	1.3
364	2458765.188	5813878.525	858.43	0.3	0.2	2.6	1.3
365	2458761.52	5813873.87	858.416	0.3	0.2	2.6	1.3
366	2458756.547	5813870.648	858.459	0.3	0.2	2.6	1.3
367	2458753.171	5813866.213	857.4	0.3	0.2	2.6	1.3
368	2458748.739	5813863.199	857.381	0.3	0.2	2.6	1.3
369	2458745.323	5813859.228	856.872	0.3	0.2	2.6	1.3
370	2458741.465	5813855.587	857.425	0.3	0.2	2.6	1.3
371	2458739.238	5813850.425	855.973	0.3	0.2	2.6	1.3
372	2458736.507	5813846.1	854.259	0.3	0.2	2.6	1.3
373	2458733.53	5813841.591	853.815	0.3	0.2	2.6	1.3
374	2458728.276	5813839.423	852.596	0.3	0.2	2.6	1.3
375	2458724.192	5813835.65	850.89	0.3	0.2	2.6	1.3
376	2458720.237	5813832.016	850.964	0.3	0.2	2.6	1.3
377	2458725.404	5813834.01	849.312	0.3	0.2	2.6	1.3
378	2458730.589	5813835.27	848.602	0.4	0.2	2.6	1.3
379	2458736.056	5813834.539	846.62	0.4	0.2	2.6	1.3
380	2458741.217	5813836.622	845.77	0.3	0.2	2.6	1.3
381	2458744.737	5813840.786	846.282	0.3	0.2	2.6	1.3
382	2458748.209	5813845.023	845.691	0.3	0.2	2.6	1.3
383	2458752.897	5813848.091	844.509	0.3	0.2	2.6	1.3
384	2458757.766	5813851.273	843.992	0.4	0.2	2.6	1.3
385	2458761.899	5813854.386	843.751	0.4	0.2	2.6	1.3
386	2458766.692	5813856.982	843.681	0.4	0.2	2.6	1.3
387	2458770.435	5813860.534	843.848	0.3	0.2	2.6	1.3
388	2458773.118	5813864.799	845.448	0.3	0.2	2.6	1.3
389	2458775.84	5813869.352	846.1	0.3	0.2	2.6	1.3
390	2458779.468	5813865.672	842.512	0.3	0.2	2.6	1.3
391	2458779.724	5813860.445	838.846	0.3	0.2	2.6	1.3
392	2458778.355	5813855.378	835.795	0.3	0.2	2.6	1.3
393	2458779.61	5813850.098	831.259	0.3	0.2	2.6	1.3
394	2458781.953	5813845.203	828.455	0.3	0.2	2.6	1.3
395	2458786.529	5813847.354	830.979	0.3	0.2	2.6	1.3
396	2458792.095	5813848.345	832.986	0.3	0.1	2.6	1.3
397	2458791.095	5813853.529	836.225	0.6	0.3	2.6	1.3
398	2458790.109	5813858.436	840.061	0.6	0.3	2.6	1.3
399	2458787.776	5813862.783	844.092	1.2	0.5	2.6	1.3
400	2458789.031	5813867.991	848.036	0.8	0.4	2.6	1.3
401	2458785.95	5813872.331	851.016	0.8	0.4	2.6	1.3
402	2458786.056	5813877.53	854.363	0.8	0.4	2.6	1.3
403	2458790.654	5813881.27	856.13	0.7	0.4	2.6	1.3
404	2458794.844	5813878.055	854.558	0.7	0.4	2.6	1.3
405	2458797.525	5813873.33	851.877	0.7	0.4	2.6	1.3
406	2458803.303	5813873.783	850.249	0.7	0.3	2.6	1.3
407	2458803.863	5813868.237	847.439	0.7	0.3	2.6	1.3
408	2458799.022	5813865.615	847.178	0.6	0.3	2.6	1.3
409	2458794.425	5813863.081	844.984	0.6	0.3	2.6	1.3
410	2458800.405	5813861.703	844.939	0.6	0.3	2.6	1.3
411	2458805.405	5813862.924	844.83	0.6	0.3	2.6	1.3
412	2458809.362	5813866.383	844.247	0.6	0.3	2.6	1.3
413	2458813.257	5813870.491	843.96	0.6	0.3	2.6	1.3
414	2458818.327	5813871.398	842.856	0.6	0.3	2.6	1.3
415	2458821.402	5813867.025	839.056	0.5	0.3	2.6	1.3
416	2458821.417	5813861.836	835.434	0.5	0.2	2.6	1.3
417	2458823.709	5813857.334	831.333	0.3	0.2	2.6	1.3
418	2458828.951	5813856.629	828.631	0.4	0.2	2.6	1.3
419	2458771.02	5813814.482	816.633	0.5	0.3	3.2	1.8

Whistling Creek Contour

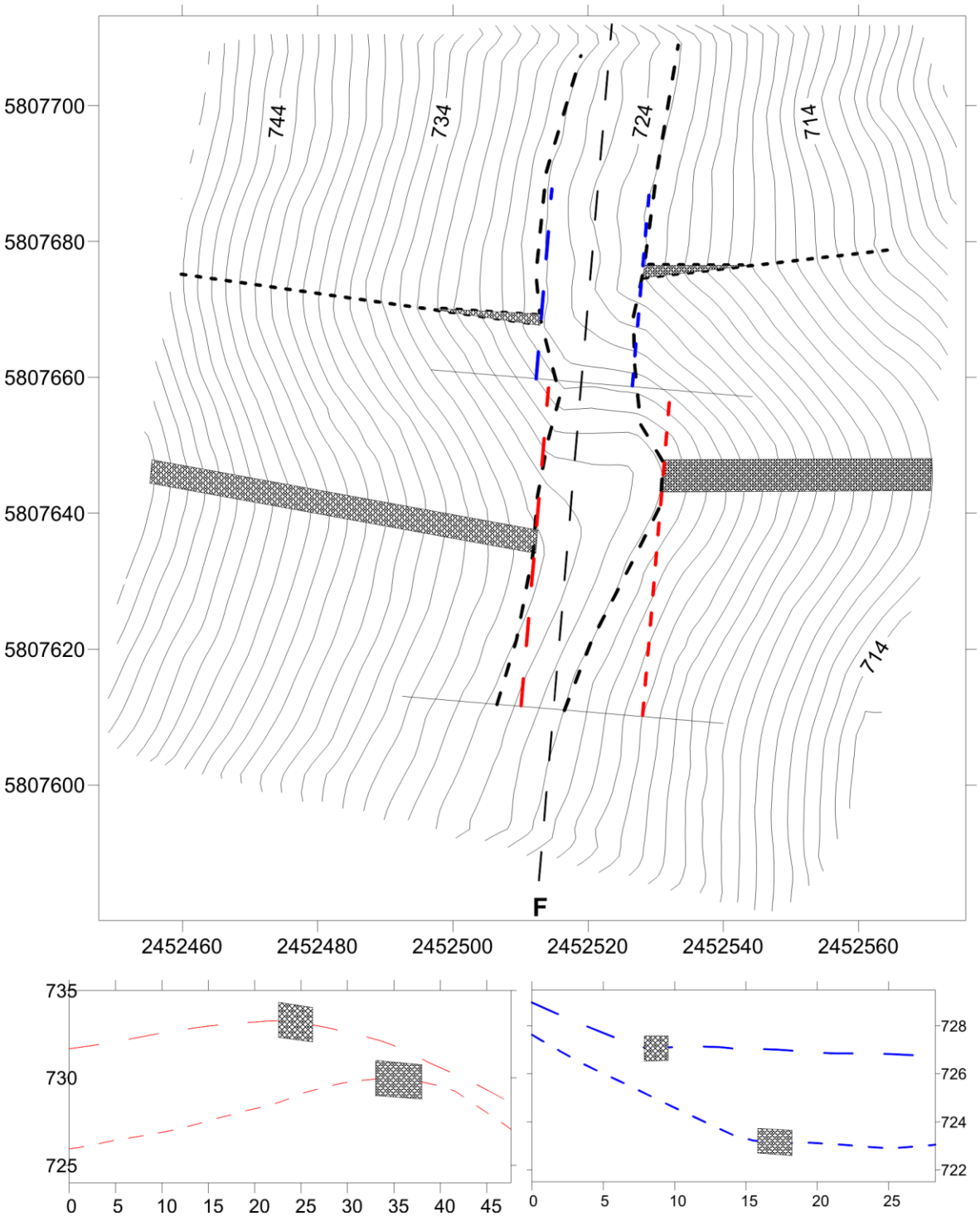

Whistling Creek GPS Points

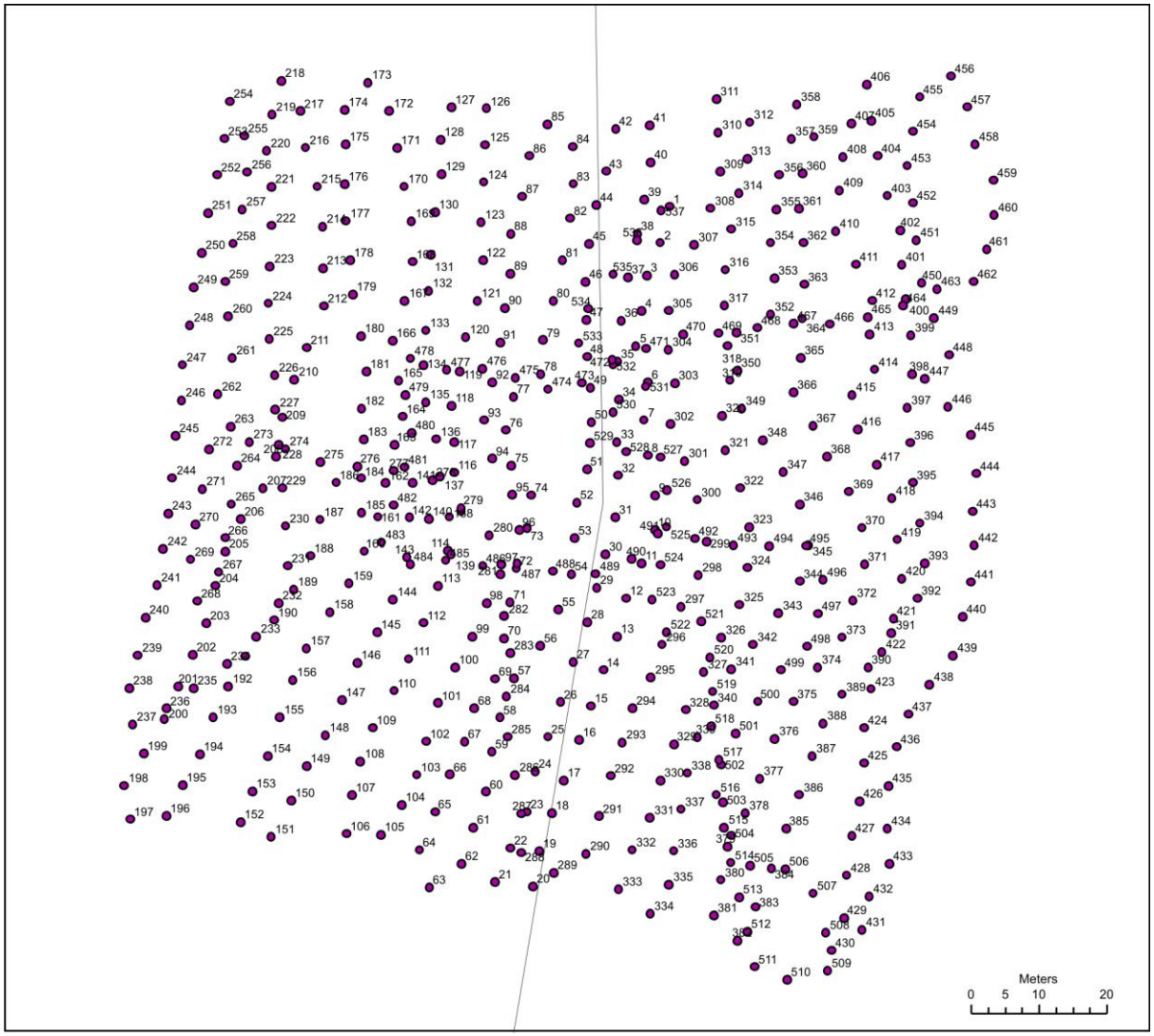

Whistling Creek GPS Data

ID	Easting	Northing	Elevation	Vert Precision	Horz Precision	Max PDOP	Max HDOP
1	2452528.061	5807693.975	723.811	0.4	0.3	2.8	1.5
2	2452526.634	5807688.636	723.714	0.3	0.3	2.8	1.5
3	2452524.697	5807683.802	723.831	0.4	0.3	2.8	1.5
4	2452523.872	5807678.571	724.266	0.4	0.3	2.8	1.5
5	2452523.059	5807673.351	724.295	0.4	0.3	2.8	1.5
6	2452524.837	5807668.086	724.943	0.3	0.3	2.8	1.5
7	2452524.256	5807662.521	726.524	0.3	0.2	2.8	1.5
8	2452524.817	5807657.316	728.178	0.3	0.2	2.8	1.5
9	2452525.869	5807651.35	730.2	0.3	0.2	2.8	1.5
10	2452525.86	5807646.337	731.163	0.3	0.2	2.8	1.5
11	2452523.901	5807641.399	731.569	0.3	0.2	2.8	1.5
12	2452521.686	5807636.242	731.406	0.3	0.2	2.6	1.4
13	2452520.303	5807630.583	731.291	0.3	0.2	2.6	1.4
14	2452518.278	5807625.681	731.256	0.3	0.2	2.6	1.4
15	2452516.481	5807620.362	731.022	0.3	0.2	2.6	1.4
16	2452514.731	5807615.353	730.886	0.3	0.2	2.6	1.4
17	2452512.422	5807609.402	730.898	0.2	0.2	2.6	1.4
18	2452510.747	5807604.61	730.794	0.2	0.2	2.6	1.4
19	2452508.854	5807598.935	731.033	0.2	0.1	2.6	1.4
20	2452507.889	5807593.764	731.181	0.2	0.1	2	1.2
21	2452502.288	5807594.419	731.992	0.2	0.1	2	1.2
22	2452504.592	5807599.413	731.988	0.2	0.1	2	1.2
23	2452507.026	5807604.774	732.018	0.2	0.1	2	1.2
24	2452508.224	5807610.71	732.138	0.2	0.1	2	1.2
25	2452510.105	5807615.815	732.133	0.2	0.1	2	1.2
26	2452511.954	5807620.919	732.328	0.2	0.1	2	1.2
27	2452513.825	5807626.826	732.527	0.2	0.1	2	1.2
28	2452515.894	5807632.714	732.48	0.2	0.1	2	1.2
29	2452517.276	5807637.806	732.418	0.2	0.1	2	1.2
30	2452518.585	5807642.684	731.814	0.2	0.1	2	1.2
31	2452520.054	5807648.133	730.858	0.2	0.2	2.1	1.2
32	2452520.446	5807654.356	729.361	0.2	0.2	2	1.2
33	2452520.282	5807659.287	727.818	0.2	0.2	2.1	1.2
34	2452520.554	5807665.55	726.229	0.2	0.1	2.1	1.2
35	2452520.348	5807671.157	725.526	0.2	0.1	2.1	1.2
36	2452520.915	5807677.07	725.353	0.2	0.1	2.1	1.2
37	2452521.936	5807683.515	724.839	0.2	0.1	2.1	1.2
38	2452523.297	5807689.901	724.6	0.2	0.1	2.1	1.2
39	2452524.312	5807695.003	724.821	0.2	0.1	2.1	1.2
40	2452525.266	5807700.46	724.973	0.2	0.1	2.1	1.2
41	2452525.122	5807705.963	724.883	0.2	0.2	2.1	1.2
42	2452520.103	5807705.356	726.47	0.2	0.2	2.1	1.2
43	2452518.693	5807699.14	726.291	0.2	0.2	2.1	1.2
44	2452517.233	5807694.169	726.621	0.2	0.2	2.1	1.2
45	2452516.176	5807688.47	726.336	0.2	0.2	2.1	1.2
46	2452515.665	5807682.819	726.535	0.2	0.2	2.1	1.2
47	2452515.759	5807677.229	726.608	0.2	0.1	2.1	1.2
48	2452515.882	5807671.84	726.681	0.2	0.2	2.1	1.2
49	2452516.361	5807667.254	726.414	0.2	0.2	4	2.5
50	2452516.529	5807662.167	727.069	0.2	0.2	4	2.5
51	2452515.873	5807655.231	728.988	0.2	0.1	2.2	1.2
52	2452514.355	5807650.307	730.511	0.2	0.1	2.2	1.2
53	2452514.063	5807645.076	731.844	0.2	0.1	2.1	1.2
54	2452513.534	5807639.758	732.658	0.2	0.1	2.1	1.2
55	2452511.63	5807634.573	733.397	0.2	0.1	2.1	1.2
56	2452508.954	5807629.225	733.721	0.2	0.1	2.1	1.2
57	2452505.131	5807624.427	734.312	0.2	0.1	2.1	1.2
58	2452503.012	5807618.683	734.306	0.2	0.1	2.1	1.2
59	2452501.825	5807613.62	733.883	0.2	0.1	2.1	1.2
60	2452500.962	5807607.746	733.48	0.2	0.1	2.1	1.2
61	2452499.066	5807602.48	733.405	0.2	0.1	2.1	1.2
62	2452497.378	5807597.077	733.18	0.2	0.1	2.1	1.2
63	2452492.612	5807593.62	734.057	0.2	0.1	2.1	1.2
64	2452491.178	5807599.177	735.108	0.2	0.1	2.1	1.2
65	2452493.464	5807604.756	735.341	0.2	0.1	2.1	1.2
66	2452495.606	5807610.27	735.109	0.2	0.1	2.1	1.2
67	2452497.808	5807615.106	735.297	0.2	0.1	2.1	1.2
68	2452499.241	5807620.055	735.549	0.2	0.1	2.1	1.2
69	2452502.344	5807624.399	735.03	0.2	0.1	2.1	1.2
70	2452503.671	5807630.319	735.388	0.2	0.1	2.1	1.2
71	2452504.545	5807635.649	735.159	0.2	0.1	2.1	1.2
72	2452505.419	5807640.605	734.881	0.2	0.1	2.1	1.2
73	2452507.063	5807646.542	733.645	0.2	0.1	2.1	1.2
74	2452507.609	5807651.441	732.623	0.2	0.1	2.2	1.2
75	2452504.738	5807655.792	732.651	0.2	0.1	2.2	1.2
76	2452503.863	5807661.025	731.597	0.2	0.1	2.2	1.2
77	2452505.007	5807665.897	730.454	0.2	0.1	2.2	1.2
78	2452509.031	5807669.242	728.496	0.2	0.1	2.2	1.2
79	2452509.363	5807674.258	728.348	0.2	0.1	2.2	1.2
80	2452510.9	5807680.055	727.7	0.2	0.1	2.2	1.2
81	2452512.244	5807686.026	727.527	0.2	0.1	2.2	1.2
82	2452513.37	5807692.255	727.381	0.2	0.1	2.2	1.2
83	2452513.839	5807697.279	727.932	0.2	0.1	2.2	1.2
84	2452513.813	5807702.782	728.357	0.2	0.1	2.2	1.2
85	2452510.023	5807706.089	729.928	0.2	0.1	2.2	1.2
86	2452507.37	5807701.438	730.816	0.2	0.1	2.2	1.2
87	2452506.323	5807695.474	730.724	0.2	0.1	2.2	1.2
88	2452504.648	5807689.906	730.824	0.2	0.1	2	1.2
89	2452504.608	5807684.095	730.488	0.2	0.1	2	1.2
90	2452503.816	5807678.962	730.174	0.2	0.1	2.2	1.2
91	2452503.071	5807673.869	730.266	0.2	0.1	2.2	1.2
92	2452501.921	5807668.024	730.771	0.2	0.1	2.2	1.2
93	2452500.705	5807662.477	732.587	0.2	0.1	2.2	1.2
94	2452501.875	5807656.819	733.398	0.2	0.1	2.2	1.2
95	2452504.842	5807651.479	733.408	0.2	0.1	2.2	1.2
96	2452505.871	5807646.313	733.948	0.2	0.1	2.2	1.2
97	2452503.281	5807641.205	735.426	0.2	0.1	2.1	1.1
98	2452501.078	5807635.491	736.202	0.2	0.1	2.1	1.1
99	2452498.985	5807630.57	736.542	0.2	0.1	2.1	1.1
100	2452496.443	5807626.064	736.984	0.2	0.1	2.1	1.1
101	2452493.888	5807620.797	737.002	0.2	0.1	2.1	1.1
102	2452492.164	5807615.155	736.737	0.2	0.1	2.1	1.1
103	2452490.741	5807610.241	736.746	0.2	0.1	2.1	1.1
104	2452488.531	5807605.737	736.525	0.2	0.1	2.1	1.1
105	2452485.441	5807601.357	736.799	0.2	0.1	2.1	1.1
106	2452480.403	5807601.587	738.242	0.2	0.1	2.1	1.1
107	2452481.2	5807607.246	739.435	0.2	0.1	2.1	1.1
108	2452482.466	5807612.143	739.599	0.2	0.1	2.1	1.1
109	2452484.294	5807617.18	739.715	0.2	0.1	2.1	1.1
110	2452487.392	5807622.648	739.656	0.2	0.1	2.1	1.1
111	2452489.566	5807627.335	739.407	0.2	0.1	2.1	1.1
112	2452491.747	5807632.639	738.858	0.2	0.1	2.1	1.1
113	2452493.868	5807638.002	738.665	0.2	0.1	2.1	1.1
114	2452495.361	5807643.253	738.109	0.2	0.1	2.1	1.1
115	2452497.278	5807649.026	736.656	0.2	0.1	2.1	1.2
116	2452496.3	5807654.773	735.664	0.2	0.1	2.1	1.2
117	2452496.333	5807659.225	734.485	0.2	0.1	2.2	1.2
118	2452495.888	5807664.591	733.553	0.2	0.1	2.2	1.2
119	2452497.086	5807669.622	732.273	0.2	0.1	2.2	1.2
120	2452497.995	5807674.699	731.986	0.2	0.1	2.2	1.2
121	2452499.69	5807680.041	731.747	0.2	0.1	2.2	1.2
122	2452500.604	5807686.031	731.917	0.2	0.1	2.2	1.2
123	2452500.261	5807691.626	732.572	0.2	0.1	2.2	1.2
124	2452500.627	5807697.581	733.178	0.2	0.1	2.2	1.2
125	2452500.887	5807703.053	733.211	0.2	0.1	2.1	1.2
126	2452501.035	5807708.411	733.461	0.2	0.1	2.1	1.2
127	2452495.893	5807708.594	735.533	0.2	0.1	2.1	1.2
128	2452494.266	5807703.748	736.392	0.2	0.2	2.1	1.2
129	2452494.405	5807698.683	735.875	0.2	0.1	2.1	1.2
130	2452493.51	5807693.122	735.729	0.2	0.1	2.4	1.3
131	2452492.802	5807686.862	735.175	0.2	0.1	2.1	1.2
132	2452492.492	5807681.533	734.782	0.2	0.1	2.1	1.2
133	2452492.088	5807675.713	734.144	0.2	0.1	2.2	1.2
134	2452491.759	5807670.522	734.144	0.2	0.1	2.2	1.2
135	2452492.097	5807665.083	734.819	0.2	0.1	2.2	1.2
136	2452493.68	5807659.712	735.339	0.2	0.1	2.2	1.2
137	2452494.208	5807654.175	736.434	0.2	0.1	2.1	1.1
138	2452495.603	5807648.235	737.37	0.2	0.1	2.1	1.1
139	2452495.831	5807642.742	737.948	0.2	0.1	2.1	1.1
140	2452492.552	5807647.923	738.527	0.2	0.1	2.1	1.1
141	2452490.191	5807653.232	738.414	0.2	0.1	2.1	1.1
142	2452489.675	5807648.178	739.719	0.2	0.1	2.1	1.1
143	2452489.266	5807642.277	740.451	0.2	0.1	2.1	1.1
144	2452487.265	5807636.03	740.86	0.2	0.1	2	1.1
145	2452484.918	5807631.228	741.216	0.2	0.1	2	1.1
146	2452482.039	5807626.705	741.6	0.2	0.1	2	1.1
147	2452479.788	5807621.262	741.824	0.2	0.1	2	1.1
148	2452477.29	5807616.033	741.835	0.2	0.1	2	1.1
149	2452474.509	5807611.545	742.131	0.2	0.1	2	1.1
150	2452472.285	5807606.422	741.887	0.2	0.1	2	1.1
151	2452469.274	5807601.151	741.681	0.2	0.1	2	1.1
152	2452464.825	5807603.252	743.535	0.2	0.1	2	1.1
153	2452466.561	5807607.797	744.147	0.2	0.2	2	1.1
154	2452468.784	5807612.966	744.323	0.2	0.2	2	1.1
155	2452470.58	5807618.688	744.652	0.2	0.1	2.1	1.1
156	2452472.474	5807624.157	744.667	0.2	0.1	2.1	1.1
157	2452474.495	5807628.864	744.585	0.2	0.1	2.1	1.1
158	2452477.955	5807634.189	743.917	0.2	0.2	2.1	1.1
159	2452480.765	5807638.423	743.365	0.2	0.1	2.1	1.1
160	2452483.013	5807643.167	742.478	0.2	0.1	2	1.1
161	2452485.004	5807648.208	741.307	0.2	0.1	2.1	1.1
162	2452486.158	5807653.269	739.877	0.2	0.1	2.1	1.1
163	2452487.515	5807658.823	737.921	0.2	0.1	2.1	1.1
164	2452488.66	5807663.052	736.648	0.2	0.1	2.3	1.2
165	2452488.123	5807668.342	736.005	0.2	0.1	2.3	1.2
166	2452487.227	5807674.201	735.93	0.2	0.1	2.3	1.2
167	2452488.993	5807680.013	735.995	0.2	0.1	2.3	1.2
168	2452490.121	5807685.829	736.275	0.2	0.1	2.3	1.2
169	2452489.974	5807691.793	737.013	0.2	0.1	2.1	1.1
170	2452488.889	5807696.924	738.3	0.2	0.1	2.1	1.1
171	2452487.919	5807702.566	738.717	0.2	0.1	2.1	1.1
172	2452486.737	5807708.009	739.372	0.2	0.1	2.1	1.1
173	2452483.581	5807712.187	740.55	0.2	0.1	2.1	1.1
174	2452480.173	5807708.171	741.996	0.2	0.1	2.1	1.1
175	2452480.31	5807703.13	741.672	0.2	0.1	2.1	1.1
176	2452480.175	5807697.223	741.838	0.2	0.1	2.1	1.1
177	2452480.338	5807691.851	741.272	0.2	0.1	2.1	1.1
178	2452480.929	5807686.055	740.024	0.2	0.1	2.1	1.1
179	2452481.347	5807680.996	739.199	0.2	0.1	2.1	1.1
180	2452482.552	5807674.848	738.164	0.2	0.1	2.3	1.2
181	2452483.346	5807669.596	737.485	0.2	0.1	2.3	1.2
182	2452482.608	5807664.174	738.598	0.2	0.1	2.3	1.2
183	2452482.936	5807659.589	739.288	0.2	0.1	2.1	1.1
184	2452482.593	5807653.996	740.605	0.2	0.1	2.3	1.2
185	2452482.654	5807648.84	741.896	0.2	0.1	2.1	1.1
186	2452478.86	5807653.29	742.345	0.2	0.1	2.1	1.1
187	2452476.491	5807647.861	744.174	0.2	0.1	2.1	1.1
188	2452475.127	5807642.519	745.42	0.2	0.1	2.1	1.1
189	2452472.618	5807637.525	746.022	0.2	0.1	2.1	1.1
190	2452469.715	5807633.073	746.615	0.2	0.1	2.1	1.1
191	2452465.504	5807627.733	747.479	0.2	0.1	2.1	1.1
192	2452462.985	5807623.199	747.98	0.2	0.1	2.1	1.1
193	2452460.758	5807618.702	747.763	0.2	0.1	2.1	1.1
194	2452458.845	5807613.267	747.741	0.2	0.1	2.1	1.1
195	2452456.277	5807608.715	748.037	0.2	0.1	2.1	1.1
196	2452453.902	5807604.169	747.839	0.2	0.1	2.4	1.3
197	2452448.557	5807603.692	748.893	0.2	0.1	2.4	1.3
198	2452447.647	5807608.677	750.725	0.2	0.1	2.4	1.3
199	2452450.555	5807613.362	750.55	0.2	0.1	2.4	1.3
200	2452453.536	5807618.459	750.243	0.2	0.1	2.4	1.3
201	2452455.621	5807623.268	750.463	0.2	0.1	2.4	1.3
202	2452457.715	5807627.934	750.289	0.2	0.1	2.4	1.3
203	2452459.717	5807632.612	750.365	0.2	0.1	2.4	1.3
204	2452461.051	5807638.111	750.407	0.2	0.1	2.4	1.3
205	2452462.536	5807643.147	750.376	0.2	0.1	2.4	1.3
206	2452464.837	5807647.909	749.111	0.2	0.1	2.4	1.3
207	2452468.12	5807652.408	747.006	0.2	0.1	2.4	1.3
208	2452470.039	5807657.083	745.274	0.2	0.1	2.4	1.3
209	2452470.938	5807662.913	743.913	0.2	0.1	2.3	1.2
210	2452472.737	5807668.423	742.249	0.2	0.1	2.1	1.1
211	2452474.571	5807673.188	741.355	0.2	0.1	2.1	1.1
212	2452477.068	5807679.325	740.891	0.2	0.1	2.1	1.1
213	2452476.972	5807684.836	741.314	0.2	0.1	2.1	1.1
214	2452476.901	5807690.965	742.528	0.2	0.1	2.1	1.1
215	2452476.121	5807696.903	743.19	0.2	0.1	2.1	1.1
216	2452474.366	5807702.637	744.073	0.2	0.1	2.1	1.1
217	2452473.643	5807708.002	744.911	0.2	0.1	2.1	1.1
218	2452470.848	5807712.458	745.869	0.2	0.1	2.1	1.1
219	2452469.462	5807707.479	746.454	0.2	0.1	2.1	1.1
220	2452468.613	5807702.2	746.53	0.2	0.1	2.1	1.1
221	2452469.35	5807696.848	745.98	0.2	0.1	2.1	1.1
222	2452469.416	5807691.14	745.609	0.2	0.1	2.1	1.1
223	2452469.128	5807685.105	744.712	0.2	0.1	2.1	1.1
224	2452468.923	5807679.693	744.138	0.2	0.1	2.1	1.1
225	2452469.039	5807674.41	743.712	0.2	0.1	2.1	1.1
226	2452469.839	5807669.089	743.465	0.2	0.1	2.1	1.1
227	2452469.937	5807664.014	744.03	0.2	0.1	2.1	1.1
228	2452470.414	5807658.854	744.702	0.2	0.1	2.1	1.1
229	2452470.958	5807652.543	745.638	0.2	0.1	2.1	1.1
230	2452471.416	5807646.927	746.203	0.1	0.1	2.1	1.1
231	2452471.766	5807641.055	746.656	0.2	0.1	2.1	1.1
232	2452470.444	5807635.514	746.588	0.2	0.1	2.1	1.1
233	2452467.14	5807630.582	747.251	0.2	0.1	2.1	1.1
234	2452462.838	5807626.572	748.546	0.2	0.1	2.1	1.1
235	2452457.887	5807623.003	749.546	0.2	0.1	2.1	1.1
236	2452453.852	5807619.983	750.449	0.2	0.1	2.1	1.1
237	2452448.875	5807617.611	751.972	0.2	0.1	2.1	1.1
238	2452448.393	5807622.979	753.193	0.2	0.1	2.1	1.1
239	2452449.651	5807627.84	753.449	0.2	0.1	2.1	1.1
240	2452450.779	5807633.342	753.768	0.2	0.1	2.1	1.1
241	2452452.502	5807638.16	753.796	0.2	0.1	2.1	1.1
242	2452453.391	5807643.518	754.015	0.2	0.1	2.1	1.1
243	2452454.105	5807648.707	753.679	0.2	0.1	2.1	1.1
244	2452454.743	5807653.957	752.821	0.2	0.1	2.1	1.1
245	2452455.245	5807660.205	751.722	0.2	0.1	2.1	1.1
246	2452456.089	5807665.42	750.444	0.2	0.1	2.1	1.1
247	2452456.249	5807670.599	750.013	0.2	0.1	2.1	1.1
248	2452457.29	5807676.464	749.296	0.2	0.1	2.1	1.1
249	2452457.911	5807682.025	749.267	0.2	0.1	2.1	1.1
250	2452459.074	5807687.077	749.446	0.2	0.1	2.1	1.1
251	2452460	5807692.967	749.611	0.2	0.1	2.1	1.1
252	2452461.359	5807698.619	749.584	0.2	0.1	2.1	1.1

253	2452462.394	5807704.016	749.525	0.2	0.1	2.1	1.1
254	2452463.229	5807709.44	749.417	0.2	0.1	2.1	1.1
255	2452465.34	5807704.348	748.289	0.2	0.1	2.1	1.1
256	2452465.785	5807699.028	747.9	0.2	0.1	2.1	1.1
257	2452465.042	5807693.504	747.639	0.2	0.1	2.1	1.1
258	2452463.66	5807688.523	747.663	0.2	0.1	2.1	1.1
259	2452462.53	5807682.894	747.257	0.2	0.1	2.1	1.1
260	2452462.989	5807677.774	746.742	0.2	0.1	2.1	1.1
261	2452463.564	5807671.644	746.35	0.2	0.1	2.1	1.1
262	2452461.444	5807666.303	748.037	0.2	0.1	2.1	1.1
263	2452463.368	5807661.512	747.478	0.2	0.1	2.1	1.1
264	2452464.297	5807655.77	748.27	0.2	0.1	2.1	1.1
265	2452463.41	5807650.134	749.285	0.2	0.1	2.1	1.1
266	2452462.567	5807645.183	750.374	0.2	0.1	2.1	1.1
267	2452461.545	5807640.116	750.547	0.2	0.1	2.1	1.1
268	2452458.448	5807635.862	751.302	0.2	0.1	2.1	1.1
269	2452457.435	5807642	752.204	0.2	0.1	2.1	1.1
270	2452458.125	5807647.08	752.105	0.2	0.1	2.1	1.1
271	2452459.155	5807652.316	751.14	0.2	0.1	2.1	1.1
272	2452460.117	5807658.125	749.729	0.2	0.1	2.1	1.1
273	2452466.128	5807659.272	746.675	0.2	0.1	2.1	1.1
274	2452471.441	5807658.251	744.624	0.2	0.1	2.1	1.1
275	2452476.558	5807656.278	742.778	0.2	0.1	2.1	1.1
276	2452482.064	5807655.625	740.759	0.2	0.1	2.1	1.1
277	2452487.332	5807655.039	739.007	0.2	0.1	2.1	1.1
278	2452493.117	5807653.669	737.579	0.2	0.1	2.1	1.1
279	2452497.276	5807649.536	736.67	0.2	0.1	2.1	1.1
280	2452501.441	5807645.546	735.81	0.2	0.1	2.1	1.1
281	2452503.071	5807639.766	735.829	0.2	0.1	2.1	1.1
282	2452503.676	5807633.605	735.483	0.2	0.1	2.1	1.1
283	2452504.553	5807628.148	734.934	0.2	0.1	2.1	1.1
284	2452503.979	5807621.793	734.215	0.2	0.1	2.1	1.1
285	2452504.168	5807615.825	733.693	0.2	0.1	2.1	1.1
286	2452505.275	5807610.15	732.659	0.2	0.1	2.1	1.1
287	2452506.203	5807604.513	732.056	0.2	0.1	2.1	1.1
288	2452506.176	5807598.783	731.745	0.2	0.1	2.1	1.1
289	2452510.945	5807595.803	730.412	0.2	0.1	2.1	1.1
290	2452515.712	5807598.589	729.393	0.2	0.1	2.1	1.1
291	2452517.605	5807604.129	729.253	0.2	0.1	2.1	1.1
292	2452519.397	5807610.09	729.112	0.2	0.1	2.1	1.1
293	2452521.051	5807614.977	728.867	0.2	0.1	2.1	1.1
294	2452522.551	5807619.996	729.3	0.2	0.1	2.1	1.1
295	2452525.28	5807624.588	729.052	0.2	0.1	2.1	1.1
296	2452526.932	5807629.427	729.378	0.2	0.1	2.1	1.1
297	2452529.728	5807634.963	729.315	0.2	0.1	2.1	1.1
298	2452532.24	5807639.593	729.389	0.2	0.1	2.1	1.1
299	2452533.481	5807644.602	729.503	0.2	0.1	2.1	1.1
300	2452532.118	5807650.761	729.318	0.2	0.1	2.1	1.1
301	2452530.219	5807656.434	727.921	0.2	0.1	2.1	1.1
302	2452528.136	5807661.863	726.481	0.2	0.1	2.1	1.1
303	2452528.838	5807667.884	724.738	0.2	0.1	2.1	1.1
304	2452527.87	5807672.814	723.455	0.2	0.1	2.1	1.1
305	2452527.933	5807678.64	723.256	0.2	0.1	2.1	1.1
306	2452528.779	5807683.916	722.867	0.2	0.1	2.1	1.1
307	2452531.694	5807688.358	722.483	0.2	0.1	2.1	1.1
308	2452534.081	5807693.694	722.079	0.2	0.1	2.1	1.1
309	2452535.531	5807699.13	722.077	0.2	0.1	2.1	1.1
310	2452535.186	5807704.824	722.584	0.2	0.1	2.1	1.1
311	2452535.013	5807709.819	722.727	0.2	0.1	2.1	1.1
312	2452539.869	5807706.362	720.565	0.2	0.1	2.1	1.1
313	2452539.518	5807700.984	720.346	0.2	0.1	2.1	1.1
314	2452538.281	5807695.951	720.607	0.2	0.1	2.1	1.1
315	2452537.14	5807690.634	720.354	0.2	0.1	2.1	1.1
316	2452536.24	5807684.651	720.694	0.2	0.1	2.1	1.1
317	2452536.1	5807679.413	720.639	0.2	0.1	2.1	1.1
318	2452536.581	5807673.445	720.822	0.2	0.1	2.1	1.1
319	2452536.923	5807668.364	722.35	0.2	0.1	2.1	1.1
320	2452535.733	5807663.118	723.969	0.2	0.1	2.1	1.1
321	2452536.221	5807658.003	725.656	0.2	0.1	2.1	1.1
322	2452538.43	5807652.505	726.649	0.2	0.1	2.1	1.1
323	2452539.766	5807646.699	727.23	0.2	0.1	2.1	1.1
324	2452539.491	5807640.761	727.313	0.2	0.1	2.1	1.1
325	2452538.351	5807635.311	726.751	0.2	0.1	2.1	1.1
326	2452535.674	5807630.469	726.392	0.2	0.1	2.1	1.1
327	2452533.034	5807625.364	726.221	0.2	0.1	2.1	1.1
328	2452530.411	5807619.821	726.311	0.2	0.1	2.1	1.1
329	2452528.724	5807614.726	726.383	0.2	0.1	2.1	1.1
330	2452526.68	5807609.364	726.423	0.2	0.1	2.1	1.1
331	2452525.137	5807603.955	726.915	0.2	0.1	2.1	1.1
332	2452522.499	5807599.182	727.42	0.2	0.1	2.1	1.1
333	2452520.518	5807593.361	727.102	0.2	0.1	2.1	1.1
334	2452525.191	5807589.792	725.897	0.2	0.1	2.1	1.1
335	2452527.942	5807594.012	725.216	0.2	0.1	2.1	1.1
336	2452528.647	5807599.022	725.137	0.2	0.1	2.1	1.1
337	2452529.698	5807605.147	725.168	0.2	0.1	2.1	1.1
338	2452530.648	5807610.535	725.021	0.2	0.1	2.1	1.1
339	2452532.076	5807615.75	725.146	0.2	0.1	2.1	1.1
340	2452534.607	5807620.495	724.991	0.2	0.1	2.1	1.1
341	2452537.136	5807625.76	725.199	0.2	0.2	2.1	1.1
342	2452540.36	5807629.421	724.69	0.2	0.1	2.1	1.1
343	2452544.095	5807634.035	724.243	0.2	0.1	2.1	1.1
344	2452547.233	5807638.778	724.166	0.2	0.1	2.1	1.1
345	2452548.474	5807644.017	724.179	0.2	0.1	2.1	1.1
346	2452547.223	5807650.003	724.194	0.2	0.1	2.1	1.1
347	2452544.795	5807654.809	723.826	0.2	0.1	2.1	1.1
348	2452541.814	5807659.537	723.341	0.2	0.1	2.1	1.1
349	2452538.648	5807664.173	722.981	0.2	0.1	2.1	1.1
350	2452538.054	5807669.768	721.627	0.2	0.1	2.1	1.1
351	2452537.92	5807675.383	719.895	0.2	0.1	2.1	1.1
352	2452542.894	5807678.042	718.423	0.2	0.1	2.1	1.1
353	2452543.518	5807683.4	718.333	0.2	0.1	2.1	1.1
354	2452542.894	5807688.612	718.55	0.2	0.1	2.1	1.1
355	2452543.805	5807693.556	718.198	0.2	0.1	2.1	1.1
356	2452544.209	5807698.647	718.097	0.2	0.1	2.1	1.1
357	2452546.017	5807703.874	717.744	0.2	0.1	2.1	1.1
358	2452546.821	5807709.006	717.569	0.2	0.1	2.1	1.1
359	2452549.329	5807704.227	716.044	0.2	0.1	2.1	1.1
360	2452547.645	5807698.828	716.323	0.2	0.1	2.1	1.1
361	2452547.086	5807693.671	716.902	0.2	0.1	2.1	1.1
362	2452547.74	5807688.61	716.969	0.2	0.1	2.1	1.1
363	2452547.93	5807682.488	716.94	0.2	0.1	2.1	1.1
364	2452547.587	5807677.464	717.068	0.2	0.1	2.1	1.1
365	2452547.367	5807671.673	718.17	0.2	0.1	2.1	1.1
366	2452546.276	5807666.563	719.583	0.2	0.1	2.1	1.1
367	2452549.157	5807661.634	720.242	0.2	0.1	2.1	1.1
368	2452551.246	5807657.073	720.922	0.2	0.1	2.1	1.1
369	2452554.513	5807651.974	721.11	0.2	0.1	2.1	1.1
370	2452556.353	5807646.621	721.127	0.2	0.1	2.1	1.1
371	2452556.762	5807641.241	720.871	0.2	0.1	2.1	1.1
372	2452555.082	5807635.929	720.737	0.2	0.1	2.1	1.1
373	2452553.439	5807630.492	720.113	0.2	0.1	2.1	1.1
374	2452549.863	5807626.017	720.11	0.2	0.1	2.1	1.1
375	2452546.339	5807621.073	720.506	0.2	0.1	2.1	1.1
376	2452543.574	5807615.514	720.699	0.2	0.1	2.1	1.1
377	2452541.309	5807609.645	720.821	0.2	0.1	2.1	1.1
378	2452539.176	5807604.608	721.241	0.2	0.1	2.1	1.1
379	2452536.582	5807599.692	722.254	0.2	0.1	2.1	1.1
380	2452535.598	5807594.811	722.574	0.2	0.1	2.1	1.1
381	2452534.558	5807589.477	722.971	0.2	0.1	2.1	1.1
382	2452538.054	5807585.789	721.853	0.2	0.1	2.1	1.1
383	2452540.724	5807590.756	720.712	0.2	0.1	2.1	1.1
384	2452543.009	5807596.48	719.757	0.2	0.1	2.1	1.1
385	2452545.264	5807602.297	718.908	0.2	0.1	2.1	1.1
386	2452547.145	5807607.306	718.388	0.2	0.1	2.1	1.1
387	2452549.038	5807613.01	718.262	0.2	0.1	2.1	1.1
388	2452550.657	5807617.806	718.432	0.2	0.1	2.1	1.1
389	2452553.473	5807622.103	718.081	0.2	0.1	2.1	1.1
390	2452557.292	5807626.02	717.579	0.2	0.1	2.1	1.1
391	2452560.772	5807631.095	717.692	0.2	0.1	2.1	1.1
392	2452564.595	5807636.223	717.523	0.2	0.1	2.1	1.1
393	2452565.626	5807641.363	717.744	0.2	0.1	2.1	1.1
394	2452564.931	5807647.263	718.132	0.2	0.1	2.1	1.1
395	2452563.875	5807653.311	717.733	0.2	0.1	2.1	1.1
396	2452563.523	5807659.188	716.705	0.2	0.1	2.1	1.1
397	2452563.067	5807664.28	715.305	0.2	0.1	2.1	1.1
398	2452563.764	5807669.267	713.753	0.2	0.1	2.1	1.1
399	2452563.603	5807674.961	712.287	0.2	0.1	2.1	1.1
400	2452562.845	5807680.32	711.924	0.2	0.1	2.1	1.1
401	2452562.268	5807685.378	712.001	0.2	0.1	2.1	1.1
402	2452562.086	5807690.414	711.727	0.2	0.1	2.1	1.1
403	2452560.149	5807695.599	711.523	0.2	0.1	2.1	1.1
404	2452558.707	5807701.436	711.311	0.2	0.1	2.1	1.1
405	2452557.791	5807706.559	712.536	0.2	0.1	2.1	1.1
406	2452557.086	5807711.874	713.111	0.2	0.1	2.1	1.1
407	2452554.856	5807706.189	713.543	0.2	0.1	2.1	1.1
408	2452553.606	5807701.254	713.333	0.2	0.1	2.1	1.1
409	2452553.028	5807696.323	713.85	0.2	0.1	2.1	1.1
410	2452552.515	5807690.284	714.931	0.2	0.1	2.1	1.1
411	2452555.506	5807685.42	714.296	0.2	0.1	2.1	1.1
412	2452557.911	5807680.117	713.462	0.2	0.1	2.1	1.1
413	2452557.542	5807675.144	714.101	0.2	0.1	2.1	1.1
414	2452558.284	5807669.963	715.109	0.2	0.1	2.1	1.1
415	2452554.895	5807666.185	717.08	0.2	0.1	2.1	1.1
416	2452555.738	5807661.121	718.178	0.2	0.1	2.1	1.1
417	2452558.588	5807655.923	718.664	0.2	0.1	2.1	1.1
418	2452560.799	5807650.947	719.061	0.2	0.1	2.1	1.1
419	2452561.592	5807644.932	719.245	0.2	0.1	2.1	1.1
420	2452562.263	5807639.058	718.673	0.2	0.1	2.1	1.1
421	2452561.03	5807633.258	718.073	0.2	0.1	2.1	1.1
422	2452559.331	5807628.313	717.366	0.2	0.1	2.1	1.1
423	2452557.762	5807622.882	716.491	0.2	0.1	2.1	1.1
424	2452556.73	5807617.196	715.624	0.2	0.1	2.1	1.1
425	2452556.704	5807611.958	715.01	0.2	0.1	2.1	1.1
426	2452556.064	5807606.286	714.479	0.1	0.1	2.1	1.1
427	2452554.881	5807601.238	714.861	0.1	0.1	2.1	1.1
428	2452554.121	5807595.429	715.05	0.1	0.1	2.1	1.1
429	2452553.8	5807589.089	715.067	0.2	0.1	2.1	1.1
430	2452551.882	5807584.386	716.351	0.2	0.1	2.1	1.1
431	2452556.422	5807587.413	714.385	0.2	0.1	2.1	1.1
432	2452557.477	5807592.284	713.767	0.2	0.1	2.1	1.1
433	2452560.42	5807597.072	712.141	0.2	0.1	2.1	1.1
434	2452560.135	5807602.336	712.559	0.2	0.1	2.1	1.1
435	2452560.339	5807608.568	712.761	0.2	0.1	2.1	1.1
436	2452561.516	5807614.36	713.302	0.2	0.1	2.1	1.1
437	2452563.266	5807619.147	713.745	0.2	0.1	2.1	1.1
438	2452566.369	5807623.554	713.728	0.2	0.1	2.1	1.1
439	2452569.819	5807627.768	714.062	0.2	0.1	2.1	1.1
440	2452571.271	5807633.54	715.126	0.2	0.1	2.1	1.1
441	2452572.483	5807638.675	715.202	0.2	0.1	2.1	1.1
442	2452572.956	5807644.03	715.321	0.2	0.1	2.1	1.1
443	2452572.723	5807649.026	715.301	0.2	0.1	2.1	1.1
444	2452573.259	5807654.659	714.915	0.2	0.1	2.1	1.1
445	2452572.411	5807660.331	714.229	0.2	0.1	2.1	1.1
446	2452569.033	5807664.428	714.048	0.1	0.1	2.1	1.1
447	2452565.676	5807668.568	713.515	0.1	0.1	2.1	1.1
448	2452569.258	5807672.139	711.906	0.1	0.1	2.1	1.1
449	2452567.017	5807677.495	710.927	0.1	0.1	2.1	1.1
450	2452565.195	5807682.736	710.853	0.1	0.1	2.1	1.1
451	2452564.386	5807689.002	710.818	0.1	0.1	2.1	1.1
452	2452563.904	5807694.497	710.443	0.1	0.1	2.1	1.1
453	2452563.082	5807699.968	708.893	0.1	0.1	2.1	1.1
454	2452563.887	5807705.051	709.058	0.1	0.1	2.1	1.1
455	2452564.885	5807710.109	709.55	0.1	0.1	2.1	1.1
456	2452569.544	5807713.199	707.296	0.2	0.1	2.1	1.1
457	2452571.911	5807708.642	705.633	0.2	0.1	2.1	1.1
458	2452573.09	5807703.113	704.642	0.2	0.1	2.1	1.1
459	2452575.746	5807697.804	704.681	0.2	0.1	2.1	1.1
460	2452575.843	5807692.74	705.7	0.2	0.1	2.1	1.1
461	2452574.764	5807687.635	706.269	0.2	0.1	2.1	1.1
462	2452572.872	5807682.893	707.958	0.2	0.1	2.1	1.1
463	2452567.456	5807681.78	709.994	0.2	0.1	2.1	1.1
464	2452562.438	5807679.4	711.916	0.2	0.1	2.1	1.1
465	2452557.222	5807677.669	713.999	0.2	0.1	2.1	1.1
466	2452551.686	5807676.64	715.685	0.2	0.1	2.1	1.1
467	2452546.265	5807676.708	717.197	0.2	0.1	2.1	1.1
468	2452540.951	5807676.089	718.853	0.2	0.1	2.1	1.1
469	2452535.229	5807675.286	720.516	0.1	0.1	2.1	1.1
470	2452530.075	5807675.127	722.368	0.1	0.1	2.1	1.1
471	2452524.562	5807673.007	723.843	0.1	0.1	2.1	1.1
472	2452519.716	5807670.691	725.341	0.1	0.1	2.1	1.1
473	2452515.095	5807667.961	726.361	0.2	0.1	2.1	1.1
474	2452510.112	5807667.04	728.076	0.2	0.1	2.1	1.1
475	2452505.318	5807668.674	729.671	0.2	0.1	2.1	1.1
476	2452500.47	5807670.069	730.865	0.2	0.1	2.1	1.1
477	2452495.186	5807669.939	732.797	0.2	0.1	2.1	1.1
478	2452489.826	5807671.554	734.756	0.2	0.1	2.1	1.1
479	2452489.105	5807666.179	735.731	0.2	0.1	2.1	1.1
480	2452490.044	5807660.58	736.571	0.2	0.1	1.9	0.9
481	2452488.983	5807655.567	738.192	0.2	0.1	1.9	0.9
482	2452487.373	5807649.963	739.9	0.2	0.1	1.9	0.9
483	2452485.545	5807644.528	741.544	0.2	0.1	1.9	0.9
484	2452489.797	5807641.225	740.263	0.2	0.1	1.9	0.9
485	2452495.047	5807641.816	738.332	0.2	0.1	1.9	0.9
486	2452500.518	5807641.011	736.523	0.2	0.1	1.9	0.9
487	2452505.57	5807641.342	734.767	0.2	0.1	1.9	0.9
488	2452510.866	5807640.233	733.056	0.2	0.1	1.9	0.9
489	2452517.135	5807639.856	732.043	0.2	0.1	1.9	0.9
490	2452522.397	5807642.043	731.661	0.2	0.1	1.9	0.9
491	2452526.311	5807645.783	731.124	0.2	0.1	1.9	0.9
492	2452531.757	5807645.029	729.882	0.2	0.1	1.9	0.9
493	2452537.469	5807644.051	728.036	0.2	0.1	1.9	0.9
494	2452542.74	5807643.923	726.149	0.2	0.1	1.9	0.9
495	2452548.199	5807643.995	724.198	0.2	0.1	1.9	0.9
496	2452550.672	5807639.006	722.595	0.2	0.1	1.9	0.9
497	2452549.904	5807633.987	721.976	0.2	0.1	1.9	0.9
498	2452548.306	5807629.18	721.461	0.2	0.1	1.9	0.9
499	2452544.434	5807625.711	722.358	0.2	0.1	1.9	0.9
500	2452541.028	5807621.025	722.541	0.2	0.1	1.9	0.9
501	2452537.782	5807616.3	722.805	0.2	0.1	1.9	0.9
502	2452535.618	5807611.719	722.903	0.2	0.1	1.9	0.9
503	2452535.939	5807606.199	722.579	0.2	0.1	1.9	0.9
504	2452537.111	5807601.298	722.21	0.2	0.1	1.9	0.9

505	2452539.915	5807596.858	721.043	0.2	0.1	1.9	0.9
506	2452545.117	5807596.358	718.775	0.2	0.1	1.9	0.9
507	2452549.222	5807592.771	717.139	0.2	0.1	1.9	0.9
508	2452551.057	5807586.975	716.728	0.2	0.1	1.9	0.9
509	2452551.331	5807581.386	716.382	0.2	0.1	1.9	0.9
510	2452545.384	5807580.077	718.633	0.2	0.1	1.9	0.9
511	2452540.559	5807581.957	720.622	0.2	0.1	1.9	0.9
512	2452539.505	5807587.102	721.048	0.2	0.1	1.9	0.9
513	2452538.335	5807592.194	721.378	0.2	0.1	1.9	0.9
514	2452537.048	5807597.337	721.834	0.2	0.1	1.9	0.9
515	2452536.089	5807602.42	722.662	0.2	0.1	1.9	0.9
516	2452534.944	5807607.306	723.146	0.2	0.1	1.9	0.9
517	2452535.322	5807612.459	723.179	0.2	0.1	1.9	0.9
518	2452534.154	5807617.394	724.279	0.2	0.1	1.9	0.9
519	2452534.37	5807622.505	725.186	0.2	0.1	1.9	0.9
520	2452534.024	5807627.486	726.203	0.2	0.1	1.9	0.9
521	2452532.717	5807632.867	727.73	0.2	0.1	1.9	0.9
522	2452527.579	5807631.24	729.186	0.2	0.1	1.9	0.9
523	2452525.475	5807636.044	730.511	0.2	0.1	1.9	0.9
524	2452526.688	5807641.204	730.805	0.2	0.1	1.9	0.9
525	2452527.575	5807646.74	730.751	0.2	0.1	1.9	0.9
526	2452527.662	5807652.143	729.867	0.2	0.1	1.9	0.9
527	2452526.738	5807657.059	728.3	0.2	0.1	1.9	0.9
528	2452521.618	5807657.848	728.232	0.2	0.1	1.9	0.9
529	2452516.289	5807659.056	727.753	0.2	0.1	1.9	0.9
530	2452519.686	5807663.617	726.285	0.2	0.1	1.9	0.9
531	2452524.518	5807667.43	725.217	0.1	0.1	1.9	0.9
532	2452519.58	5807671.363	725.185	0.1	0.1	1.9	0.9
533	2452514.647	5807673.845	726.73	0.1	0.1	1.9	0.9
534	2452516.021	5807678.895	726.365	0.1	0.1	1.9	0.9
535	2452519.681	5807684.008	725.008	0.2	0.1	1.9	0.9
536	2452523.229	5807688.988	724.37	0.1	0.1	1.9	0.9
537	2452526.78	5807693.328	724.155	0.2	0.1	1.9	0.9

Hurunui River Terraces Contour

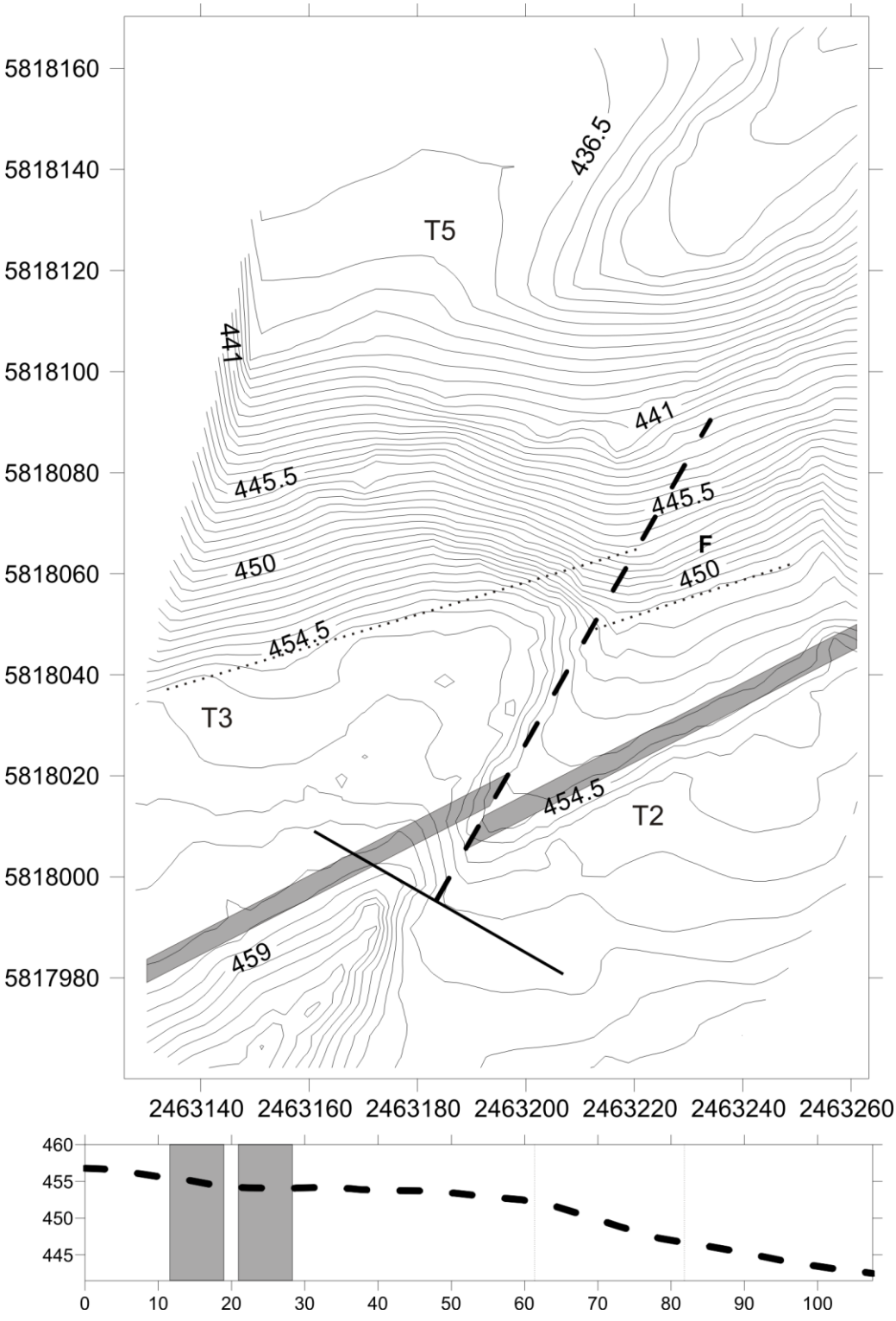

Hurunui River Terraces GPS Points

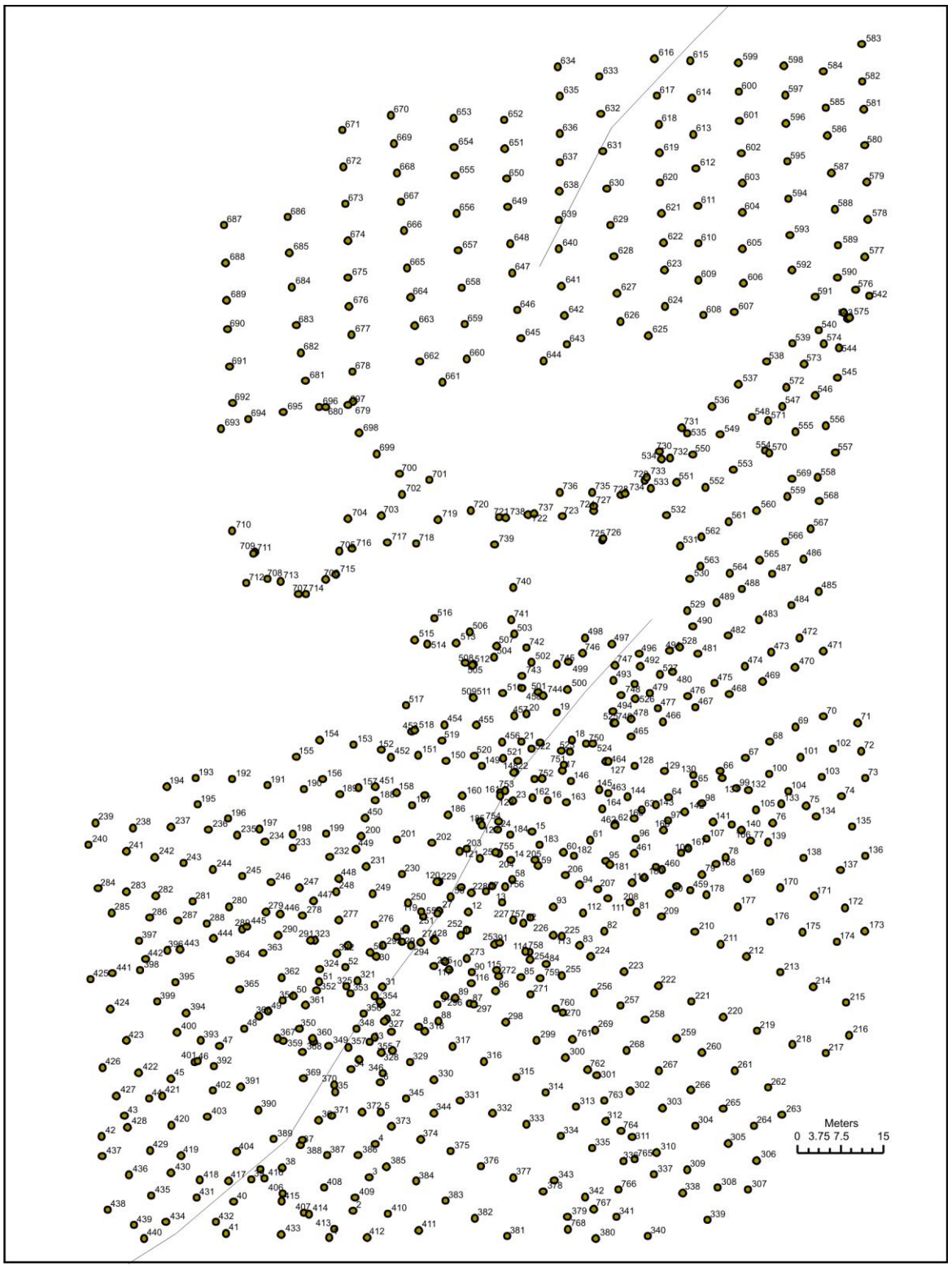

Hurunui River GPS Data

ID	Easting	Northing	Elevation	Vert Precision	Horz Precision	Max PDOP	Max HDOP
2	2463168.263	5817960.332	458.078	0.4	0.2	2.3	1.4
3	2463172.391	5817964.996	457.828	0.4	0.2	2.3	1.4
4	2463175.214	5817970.869	457.686	0.4	0.2	2.3	1.4
5	2463176.291	5817976.800	457.501	0.4	0.2	2.3	1.4
6	2463177.305	5817982.412	457.397	0.4	0.2	2.3	1.4
7	2463177.205	5817987.591	457.355	0.4	0.2	2.3	1.4
8	2463179.376	5817993.173	457.262	0.4	0.2	2.3	1.4
9	2463184.031	5817997.382	456.891	0.4	0.2	2.3	1.4
10	2463187.300	5818001.269	456.023	0.4	0.2	2.3	1.4
11	2463189.282	5818007.401	455.303	0.4	0.2	5.2	2.6
12	2463191.372	5818013.456	454.845	0.4	0.2	5.2	2.6
13	2463192.703	5818017.607	454.700	0.4	0.2	5.2	2.6
14	2463196.907	5818022.106	454.255	0.4	0.2	2.3	1.4
15	2463200.144	5818026.779	454.020	0.4	0.2	2.3	1.4
16	2463203.897	5818031.728	453.629	0.4	0.2	2.3	1.4
17	2463206.710	5818037.218	453.347	0.4	0.2	2.3	1.4
18	2463209.210	5818042.450	453.146	0.3	0.2	2.3	1.4
19	2463210.902	5818047.829	452.719	0.4	0.2	2.3	1.4
20	2463208.253	5818052.741	453.301	0.4	0.2	2.3	1.4
21	2463202.914	5818052.456	454.678	0.4	0.2	2.3	1.4
22	2463202.036	5818047.585	455.276	0.4	0.2	2.3	1.4
23	2463200.879	5818042.258	455.365	0.4	0.2	2.3	1.4
24	2463200.486	5818037.129	455.358	0.4	0.2	2.3	1.4
25	2463197.859	5818032.110	455.588	0.4	0.2	2.3	1.4
26	2463194.765	5818027.068	455.771	0.4	0.2	2.3	1.4
27	2463191.444	5818021.935	456.020	0.4	0.2	2.3	1.4
28	2463187.497	5818017.750	456.418	0.4	0.2	2.3	1.4
29	2463186.638	5818012.799	456.231	0.4	0.2	2.3	1.4
30	2463181.025	5818012.362	457.063	0.4	0.2	5.2	2.6
31	2463176.532	5818009.762	457.495	0.4	0.2	2.3	1.4
32	2463177.580	5818004.392	458.047	0.4	0.2	2.3	1.4
33	2463178.410	5817998.705	458.684	0.4	0.2	3.4	1.8
34	2463175.408	5817994.742	458.778	0.6	0.4	2.3	1.4
35	2463172.109	5817989.897	460.813	0.5	0.3	2.3	1.4
36	2463169.289	5817985.915	461.515	0.4	0.3	2.3	1.4
37	2463166.395	5817980.996	461.438	0.4	0.3	2.3	1.4
38	2463163.209	5817976.548	461.690	0.4	0.3	2.3	1.4
39	2463159.972	5817972.566	461.709	0.4	0.3	2.3	1.4
40	2463154.553	5817970.498	461.855	0.5	0.3	2.3	1.4
41	2463151.392	5817966.605	462.087	0.4	0.2	2.3	1.4
42	2463150.076	5817961.044	461.977	0.2	0.1	2.3	1.4
43	2463128.252	5817978.124	457.797	0.3	0.2	2.2	1.4
44	2463132.255	5817981.717	457.616	0.3	0.2	2.2	1.4
45	2463136.548	5817984.808	457.542	0.3	0.2	2.2	1.4
46	2463140.370	5817988.212	457.526	0.3	0.2	2.2	1.4
47	2463144.597	5817991.152	457.416	0.3	0.2	2.2	1.4
48	2463148.946	5817994.053	457.382	0.3	0.2	2.2	1.4
49	2463153.270	5817997.051	457.380	0.3	0.2	2.2	1.4
50	2463157.477	5818000.122	457.415	0.3	0.2	2.2	1.4
51	2463161.909	5818002.861	457.232	0.3	0.2	2.2	1.4
52	2463166.495	5818005.283	457.282	0.3	0.2	2.2	1.4
53	2463171.033	5818007.923	457.168	0.3	0.2	2.2	1.4
54	2463175.485	5818010.523	456.983	0.3	0.2	2.2	1.4
55	2463180.109	5818013.282	456.705	0.3	0.2	2.2	1.4
56	2463184.736	5818016.815	456.355	0.3	0.2	2.2	1.4
57	2463189.643	5818020.274	455.864	0.3	0.2	2.2	1.4
58	2463195.812	5818021.181	454.058	0.3	0.2	2.2	1.4
59	2463200.386	5818023.277	453.655	0.3	0.2	2.2	1.4
60	2463204.955	5818025.736	453.427	0.3	0.2	2.2	1.4
61	2463209.424	5818028.065	453.281	0.3	0.2	2.2	1.4
62	2463214.110	5818030.233	453.083	0.3	0.2	2.2	1.4
63	2463218.460	5818033.132	452.819	0.3	0.2	2.2	1.4
64	2463223.184	5818035.548	452.730	0.3	0.2	2.2	1.4
65	2463227.894	5818037.748	452.719	0.3	0.2	2.2	1.4
66	2463232.467	5818040.099	452.885	0.3	0.2	2.2	1.4
67	2463236.958	5818042.377	452.857	0.3	0.2	1.9	1.2
68	2463241.408	5818044.722	452.812	0.3	0.2	1.9	1.2
69	2463245.736	5818047.569	452.690	0.2	0.2	1.9	1.2
70	2463250.251	5818050.190	452.496	0.3	0.2	2.2	1.3
71	2463255.075	5818052.033	452.533	0.3	0.2	3.2	1.7
72	2463261.163	5818050.865	452.935	0.3	0.2	3.7	2.2
73	2463261.745	5818045.905	454.130	0.3	0.2	3.7	2.2
74	2463262.474	5818041.176	455.122	0.3	0.2	3.7	2.2
75	2463258.323	5818037.933	455.418	0.3	0.2	3.7	2.2
76	2463252.093	5818036.274	455.109	0.3	0.2	3.7	2.2
77	2463246.281	5818033.267	454.855	0.3	0.2	3.0	1.6
78	2463242.374	5818030.105	454.978	0.3	0.2	1.9	1.2
79	2463237.955	5818027.232	454.877	0.3	0.2	1.9	1.2
80	2463233.821	5818024.179	455.145	0.3	0.2	1.9	1.2
81	2463228.125	5818020.775	455.686	0.3	0.2	1.9	1.2
82	2463222.317	5818017.599	455.808	0.3	0.2	1.9	1.2
83	2463216.606	5818014.222	455.814	0.3	0.2	1.9	1.2
84	2463212.272	5818011.674	455.896	0.3	0.2	1.9	1.2
85	2463206.428	5818008.447	455.921	0.3	0.2	1.9	1.2
86	2463201.940	5818006.120	455.866	0.3	0.2	1.9	1.2
87	2463197.494	5818003.771	455.844	0.3	0.2	1.9	1.2
88	2463192.955	5818001.464	455.828	0.3	0.2	1.9	1.2
89	2463187.429	5817998.392	455.963	0.3	0.2	1.9	1.2
90	2463190.353	5818002.473	455.526	0.3	0.2	1.9	1.2
91	2463193.307	5818007.063	455.020	0.3	0.2	1.9	1.2
92	2463197.323	5818011.925	454.249	0.3	0.2	2.0	1.3
93	2463202.403	5818015.669	454.052	0.3	0.2	1.9	1.2
94	2463207.655	5818018.497	453.804	0.3	0.2	1.9	1.2
95	2463212.251	5818022.360	453.680	0.3	0.2	1.9	1.2
96	2463216.920	5818026.556	453.343	0.3	0.2	1.9	1.2
97	2463222.154	5818030.519	453.211	0.3	0.2	1.9	1.2
98	2463227.821	5818033.681	453.057	0.3	0.2	1.9	1.2
99	2463233.763	5818036.740	453.124	0.3	0.2	1.9	1.2
100	2463239.820	5818039.404	453.210	0.3	0.2	1.9	1.2
101	2463245.620	5818041.910	453.333	0.3	0.2	1.9	1.2
102	2463251.145	5818044.839	453.328	0.3	0.2	1.9	1.2
103	2463256.822	5818046.361	454.890	1.2	0.4	3.0	1.6
104	2463254.858	5818041.306	454.203	0.3	0.2	3.0	1.6
105	2463249.016	5818038.881	454.048	0.3	0.2	3.0	1.6
106	2463243.253	5818035.580	453.974	0.3	0.2	3.0	1.6
107	2463238.991	5818032.956	453.886	0.3	0.2	3.0	1.6
108	2463234.614	5818030.464	453.876	0.3	0.2	3.0	1.6
109	2463230.153	5818027.997	454.047	0.3	0.2	1.9	1.2
110	2463225.704	5818025.517	454.299	0.3	0.2	1.9	1.2
111	2463221.484	5818022.796	454.390	0.3	0.2	1.9	1.2
112	2463217.219	5818020.029	454.308	0.3	0.2	1.9	1.2
113	2463212.874	5818017.399	454.472	0.3	0.2	1.9	1.2
114	2463207.608	5818013.463	454.722	0.3	0.2	1.9	1.2
115	2463203.442	5818010.572	454.753	0.3	0.2	1.9	1.2
116	2463197.712	5818007.357	454.863	0.3	0.2	1.9	1.2
117	2463193.252	5818005.031	454.996	0.3	0.2	1.9	1.2
118	2463188.562	5818008.908	454.966	0.3	0.2	5.0	2.8
119	2463184.284	5818012.268	456.101	0.3	0.2	5.0	2.8
120	2463184.417	5818017.717	455.964	0.3	0.2	2.1	1.3
121	2463187.513	5818022.940	455.782	0.3	0.2	2.1	1.3
122	2463191.151	5818028.258	455.593	0.3	0.2	1.9	1.2
123	2463194.734	5818033.508	455.440	0.3	0.2	1.9	1.2
124	2463198.403	5818038.727	455.043	0.3	0.2	1.9	1.2
125	2463201.410	5818044.203	454.630	0.3	0.2	1.9	1.2
126	2463205.334	5818047.444	453.754	0.3	0.2	1.9	1.2
127	2463210.615	5818045.775	452.101	0.3	0.2	1.9	1.2
128	2463216.911	5818044.089	451.723	0.3	0.2	1.9	1.2
129	2463221.941	5818043.313	452.008	0.3	0.2	1.9	1.2
130	2463227.218	5818042.432	452.080	0.3	0.2	1.9	1.2
131	2463232.262	5818041.718	452.365	0.3	0.2	1.9	1.2
132	2463237.320	5818041.163	452.645	0.3	0.2	1.9	1.2
133	2463241.935	5818039.000	453.084	0.3	0.2	1.9	1.2
134	2463247.731	5818036.598	454.324	0.3	0.2	2.9	1.6
135	2463253.885	5818034.353	454.946	0.3	0.2	2.9	1.6
136	2463260.148	5818032.600	455.348	0.3	0.2	2.9	1.6
137	2463262.497	5818027.486	455.425	0.3	0.2	3.5	2.2
138	2463258.127	5818024.924	455.292	0.3	0.2	3.5	2.2
139	2463251.671	5818027.102	454.850	0.3	0.2	2.9	1.6
140	2463245.426	5818029.902	454.879	0.3	0.2	2.9	1.6
141	2463240.722	5818032.016	454.409	0.3	0.2	2.9	1.6
142	2463235.725	5818033.458	453.837	0.3	0.2	2.9	1.6
143	2463230.732	5818035.235	453.055	0.3	0.2	2.9	1.6
144	2463225.725	5818036.507	452.738	0.3	0.2	2.9	1.6
145	2463220.684	5818037.878	452.547	0.3	0.2	2.9	1.6
146	2463215.736	5818039.132	452.470	0.3	0.2	2.9	1.6
147	2463210.724	5818040.657	452.463	0.3	0.2	2.9	1.6
148	2463205.686	5818041.128	453.737	0.3	0.2	2.9	1.6
149	2463200.730	5818042.157	455.026	0.3	0.2	2.9	1.6
150	2463195.115	5818043.283	455.689	0.3	0.2	2.9	1.6
151	2463188.813	5818044.176	455.960	0.3	0.2	2.9	1.6
152	2463183.861	5818045.146	455.779	0.3	0.2	2.9	1.6
153	2463177.410	5818046.123	455.635	0.3	0.2	2.9	1.6
154	2463172.490	5818047.006	455.603	0.3	0.2	2.9	1.6
155	2463166.538	5818047.882	455.371	0.3	0.2	2.9	1.6
156	2463162.415	5818044.853	455.148	0.4	0.2	2.9	1.6
157	2463167.117	5818041.018	455.676	0.3	0.2	2.9	1.6
158	2463173.377	5818039.508	455.790	0.3	0.2	2.9	1.6
159	2463180.021	5818038.597	455.979	0.3	0.2	2.9	1.6
160	2463185.059	5818038.115	456.072	0.3	0.2	2.9	1.6
161	2463191.616	5818038.012	455.845	0.3	0.2	2.9	1.6
162	2463198.277	5818038.028	455.277	0.3	0.2	2.9	1.6
163	2463203.967	5818037.661	454.123	0.3	0.2	2.9	1.6
164	2463209.973	5818036.937	452.704	0.3	0.2	2.9	1.6
165	2463216.212	5818035.720	452.610	0.3	0.2	2.9	1.6
166	2463221.873	5818033.987	452.772	0.3	0.2	2.9	1.6
167	2463227.044	5818031.973	453.258	0.3	0.2	2.9	1.6
168	2463231.431	5818028.785	454.219	0.3	0.2	2.9	1.6
169	2463236.311	5818026.067	454.852	0.3	0.2	2.9	1.6
170	2463241.732	5818023.450	455.198	0.3	0.2	2.9	1.6
171	2463247.603	5818021.876	455.264	0.3	0.2	2.9	1.6
172	2463253.480	5818020.408	455.501	0.3	0.2	2.9	1.6
173	2463259.000	5818018.290	455.722	0.3	0.2	2.9	1.6
174	2463262.429	5818014.222	456.133	0.5	0.3	3.5	2.1
175	2463257.556	5818012.379	455.730	1.1	0.7	3.5	2.1
176	2463251.499	5818014.043	455.328	0.3	0.2	2.8	1.6
177	2463245.767	5818015.871	455.230	0.3	0.2	2.8	1.6
178	2463240.125	5818018.486	455.090	0.3	0.2	2.8	1.6
179	2463234.567	5818020.633	455.058	0.3	0.2	2.8	1.6
180	2463229.308	5818022.147	455.153	0.3	0.2	2.8	1.6
181	2463223.629	5818023.633	454.561	0.3	0.2	2.8	1.6
182	2463217.601	5818025.925	453.283	0.3	0.2	2.8	1.6
183	2463211.311	5818027.474	453.111	0.3	0.2	2.8	1.6
184	2463205.191	5818029.458	453.038	0.3	0.2	2.8	1.6
185	2463200.094	5818031.186	454.104	0.3	0.2	2.8	1.6
186	2463195.065	5818032.922	455.446	0.3	0.2	2.8	1.6
187	2463189.078	5818034.691	455.794	0.3	0.2	2.8	1.6
188	2463182.784	5818036.306	455.914	0.3	0.2	2.8	1.6
189	2463176.371	5818037.292	455.799	0.3	0.2	2.8	1.6
190	2463170.088	5818038.373	455.609	0.3	0.2	2.8	1.6
191	2463163.772	5818039.190	455.363	0.3	0.2	2.8	1.6
192	2463157.440	5818039.921	455.056	0.3	0.2	2.8	1.6
193	2463151.105	5818040.958	454.980	0.3	0.2	2.8	1.6
194	2463144.785	5818041.184	455.276	0.3	0.2	2.8	1.6
195	2463139.642	5818039.632	455.703	0.3	0.2	2.8	1.6
196	2463145.139	5818036.561	455.581	0.3	0.2	2.8	1.6
197	2463150.450	5818034.081	455.614	0.3	0.2	2.8	1.6
198	2463156.018	5818032.187	455.803	0.3	0.2	2.8	1.6
199	2463161.803	5818031.297	455.928	0.3	0.2	2.8	1.6
200	2463167.724	5818031.383	455.984	0.3	0.2	2.8	1.6
201	2463173.869	5818030.937	456.117	0.3	0.2	2.8	1.6
202	2463180.111	5818030.300	456.184	0.3	0.2	2.8	1.6
203	2463186.342	5818029.778	455.949	0.3	0.2	2.8	1.6
204	2463192.458	5818028.681	455.453	0.3	0.2	2.8	1.6
205	2463198.159	5818027.960	454.330	0.3	0.2	2.8	1.6
206	2463204.469	5818026.781	453.156	0.3	0.2	2.8	1.6
207	2463209.803	5818024.106	453.138	0.3	0.2	2.8	1.6
208	2463215.436	5818021.622	453.742	0.3	0.2	2.8	1.6
209	2463221.116	5818019.245	455.043	0.3	0.2	2.8	1.6
210	2463226.631	5818016.805	455.578	0.3	0.2	2.8	1.6
211	2463232.540	5818014.077	455.435	0.3	0.2	2.8	1.6
212	2463237.038	5818011.887	455.432	0.3	0.2	2.8	1.6
213	2463241.568	5818009.756	455.444	0.3	0.2	2.8	1.6
214	2463247.505	5818007.047	455.620	0.3	0.2	2.7	1.5
215	2463253.319	5818004.420	455.816	0.3	0.2	2.8	1.5
216	2463259.094	5818001.699	456.157	0.3	0.2	2.8	1.5
217	2463259.625	5817995.868	456.829	0.3	0.2	2.8	1.5
218	2463255.606	5817992.803	456.833	0.3	0.2	3.4	2.1
219	2463249.671	5817994.267	456.306	0.3	0.2	3.4	2.1
220	2463243.511	5817996.701	456.104	0.3	0.2	2.7	1.5
221	2463237.523	5817999.107	456.036	0.3	0.2	2.7	1.5
222	2463231.896	5818001.826	456.026	0.3	0.2	2.7	1.5
223	2463226.114	5818004.644	456.021	0.3	0.2	2.7	1.5
224	2463220.097	5818007.082	455.924	0.3	0.2	2.7	1.5
225	2463214.232	5818009.759	455.716	0.3	0.2	2.7	1.5
226	2463209.146	5818013.326	454.943	0.3	0.2	2.7	1.5
227	2463203.649	5818016.627	453.525	0.3	0.2	2.7	1.5
228	2463198.643	5818019.279	453.476	0.3	0.2	2.7	1.5
229	2463193.190	5818021.001	454.273	0.3	0.2	2.7	1.5
230	2463187.197	5818022.889	455.691	0.3	0.2	2.7	1.5
231	2463181.095	5818024.256	456.009	0.3	0.2	2.7	1.5
232	2463174.761	5818025.618	456.163	0.3	0.2	2.7	1.5
233	2463168.337	5818027.244	456.047	0.3	0.2	2.7	1.5
234	2463161.868	5818028.864	455.823	0.3	0.2	2.7	1.5
235	2463156.942	5818029.947	455.737	0.3	0.2	2.7	1.5
236	2463152.046	5818031.126	455.678	0.3	0.2	2.7	1.5
237	2463147.025	5818032.146	455.588	0.2	0.2	2.7	1.5
238	2463140.405	5818032.510	455.795	0.2	0.2	2.7	1.5
239	2463133.766	5818032.396	456.002	0.2	0.2	2.7	1.5
240	2463127.174	5818033.243	456.216	0.2	0.2	2.7	1.5
241	2463125.894	5818029.466	456.367	0.3	0.2	2.7	1.5
242	2463132.540	5818028.264	456.098	0.3	0.2	2.7	1.5
243	2463137.571	5818027.220	456.026	0.3	0.2	2.7	1.5
244	2463142.671	5818026.242	455.839	0.3	0.2	2.7	1.5
245	2463147.759	5818025.068	455.890	0.3	0.2	2.7	1.5
246	2463152.935	5818023.872	455.935	0.3	0.2	2.7	1.5
247	2463158.022	5818022.853	455.953	0.3	0.2	2.7	1.5
248	2463163.035	5818021.836	456.198	0.3	0.2	2.7	1.5
249	2463169.514	5818021.172	456.219	0.3	0.2	2.7	1.5
250	2463175.915	5818020.820	456.298	0.3	0.2	2.7	1.5
251	2463182.131	5818019.227	456.061	0.3	0.2	2.7	1.5
252	2463187.267	5818017.290	455.772	0.3	0.2	2.7	1.5

253	2463192.422	5818014.389	453.991	0.3	0.2	2.8	1.6
254	2463198.204	5818012.108	453.866	0.3	0.2	2.8	1.6
255	2463203.566	5818009.246	454.924	0.3	0.2	2.7	1.5
256	2463209.136	5818006.379	455.745	0.3	0.2	2.6	1.4
257	2463214.860	5818003.357	455.957	0.3	0.2	2.6	1.4
258	2463219.426	5818001.115	456.037	0.3	0.2	2.6	1.4
259	2463223.871	5817998.608	456.168	0.3	0.2	2.6	1.4
260	2463229.333	5817995.344	456.321	0.3	0.2	2.6	1.4
261	2463233.829	5817992.907	456.378	0.3	0.2	2.6	1.4
262	2463239.587	5817989.694	456.641	0.2	0.2	2.6	1.4
263	2463245.406	5817986.773	456.937	0.2	0.2	2.6	1.4
264	2463247.834	5817981.960	457.392	0.3	0.2	2.6	1.4
265	2463242.988	5817979.977	457.310	0.3	0.2	2.6	1.4
266	2463237.469	5817983.026	456.984	0.3	0.2	2.6	1.4
267	2463231.828	5817986.257	456.683	0.3	0.2	2.6	1.4
268	2463226.187	5817989.675	456.420	0.3	0.2	2.6	1.4
269	2463220.579	5817993.241	456.195	0.3	0.2	2.6	1.4
270	2463215.046	5817996.759	456.048	0.3	0.2	2.6	1.4
271	2463209.361	5817999.900	455.926	0.3	0.2	2.6	1.4
272	2463203.638	5818003.101	455.803	0.3	0.2	2.6	1.4
273	2463198.001	5818006.283	455.154	0.3	0.2	2.6	1.4
274	2463192.429	5818009.434	454.234	0.3	0.2	2.7	1.5
275	2463186.878	5818012.601	455.512	0.3	0.2	2.8	1.6
276	2463181.758	5818014.522	456.162	0.3	0.2	2.6	1.4
277	2463176.222	5818015.372	456.425	0.3	0.2	2.6	1.4
278	2463169.909	5818016.166	456.370	0.3	0.2	2.6	1.4
279	2463163.555	5818016.956	456.402	0.3	0.2	2.6	1.4
280	2463157.106	5818017.603	456.268	0.3	0.2	2.6	1.4
281	2463150.662	5818018.477	456.085	0.3	0.2	2.6	1.4
282	2463144.258	5818019.511	456.093	0.3	0.2	2.6	1.4
283	2463137.718	5818020.442	456.101	0.3	0.2	2.6	1.4
284	2463132.592	5818021.129	456.166	0.3	0.2	2.6	1.4
285	2463127.563	5818021.775	456.271	0.3	0.2	2.6	1.4
286	2463130.023	5818017.445	456.281	0.2	0.2	2.6	1.4
287	2463136.630	5818016.641	456.223	0.2	0.2	2.6	1.4
288	2463141.670	5818016.102	456.173	0.2	0.2	2.6	1.4
289	2463146.744	5818015.558	456.127	0.2	0.2	2.6	1.4
290	2463152.918	5818014.532	456.252	0.2	0.2	2.6	1.4
291	2463159.287	5818013.475	456.492	0.2	0.2	2.6	1.4
292	2463165.661	5818012.606	456.545	0.2	0.2	2.6	1.4
293	2463171.524	5818011.724	456.672	0.2	0.2	2.6	1.4
294	2463177.619	5818011.775	456.687	0.3	0.2	2.6	1.4
295	2463182.654	5818011.737	456.530	0.4	0.2	2.8	1.6
296	2463186.665	5818008.104	455.960	0.5	0.2	2.8	1.5
297	2463188.589	5818002.844	455.427	0.2	0.1	2.7	1.5
298	2463193.687	5818001.331	455.847	0.3	0.2	2.7	1.5
299	2463199.254	5817998.203	456.239	0.3	0.2	2.5	1.4
300	2463204.682	5817994.973	456.461	0.3	0.2	2.5	1.4
301	2463209.784	5817991.971	456.625	0.3	0.2	2.5	1.4
302	2463215.284	5817988.875	456.735	0.3	0.2	2.5	1.4
303	2463221.139	5817986.115	456.953	0.3	0.2	2.5	1.4
304	2463226.850	5817983.098	457.172	0.3	0.2	2.5	1.4
305	2463232.610	5817979.990	457.471	0.3	0.2	2.5	1.4
306	2463238.380	5817976.873	457.783	0.3	0.2	2.5	1.4
307	2463243.397	5817973.800	458.232	0.3	0.2	2.5	1.4
308	2463241.812	5817968.731	458.633	0.3	0.2	2.5	1.4
309	2463236.534	5817969.128	458.222	0.3	0.2	2.5	1.4
310	2463231.198	5817972.225	457.944	0.3	0.2	2.5	1.4
311	2463225.781	5817975.259	457.663	0.3	0.2	2.5	1.4
312	2463221.495	5817977.990	457.363	0.3	0.2	2.5	1.4
313	2463216.905	5817980.767	457.095	0.3	0.2	2.5	1.4
314	2463211.604	5817983.334	456.898	0.3	0.2	2.5	1.4
315	2463206.293	5817985.884	456.840	0.3	0.2	2.5	1.4
316	2463201.171	5817988.484	456.730	0.3	0.2	2.5	1.4
317	2463195.450	5817991.229	456.511	0.3	0.2	2.5	1.4
318	2463189.967	5817993.967	456.490	0.3	0.2	2.5	1.4
319	2463185.083	5817996.581	456.396	0.3	0.2	2.5	1.4
320	2463179.145	5817996.538	457.425	0.3	0.2	2.5	1.4
321	2463177.435	5818001.432	458.163	0.3	0.2	2.5	1.4
322	2463173.239	5818005.508	457.540	0.3	0.2	2.5	1.4
323	2463169.571	5818010.255	457.158	0.3	0.2	2.5	1.4
324	2463164.984	5818012.631	457.026	0.3	0.2	2.5	1.4
325	2463166.583	5818007.581	457.256	0.3	0.2	2.5	1.4
326	2463171.230	5818004.517	457.551	0.3	0.2	2.5	1.4
327	2463176.238	5818002.839	457.874	0.3	0.2	2.7	1.5
328	2463177.936	5817998.388	458.472	0.3	0.2	2.5	1.4
329	2463177.369	5817992.874	457.479	0.3	0.2	2.8	1.5
330	2463182.474	5817991.160	456.651	0.3	0.2	2.8	1.5
331	2463186.653	5817988.123	456.627	0.3	0.2	2.5	1.4
332	2463191.250	5817984.460	456.663	0.3	0.2	2.5	1.4
333	2463196.993	5817982.149	456.686	0.3	0.2	2.5	1.4
334	2463202.932	5817980.208	456.901	0.3	0.2	2.5	1.4
335	2463208.980	5817978.241	456.931	0.3	0.2	2.5	1.4
336	2463214.467	5817976.058	457.065	0.2	0.2	2.5	1.4
337	2463220.052	5817973.696	457.411	0.2	0.2	2.5	1.4
338	2463225.304	5817971.397	457.677	0.2	0.2	2.5	1.4
339	2463230.351	5817968.108	457.968	0.2	0.2	2.5	1.4
340	2463234.774	5817963.474	458.389	0.2	0.2	2.5	1.4
341	2463224.317	5817960.634	458.167	0.3	0.2	2.5	1.4
342	2463218.732	5817963.967	457.947	0.3	0.2	2.5	1.4
343	2463213.201	5817967.433	457.557	0.2	0.2	2.5	1.4
344	2463207.859	5817970.351	457.246	0.2	0.2	2.5	1.4
345	2463186.630	5817982.191	456.877	0.3	0.2	2.5	1.4
346	2463181.764	5817984.804	456.867	0.3	0.2	2.5	1.4
347	2463177.679	5817989.196	457.018	0.3	0.2	2.5	1.4
348	2463173.542	5817991.615	459.244	0.3	0.2	2.8	1.5
349	2463173.062	5817997.080	459.024	0.3	0.2	2.8	1.5
350	2463168.172	5817994.019	459.242	0.3	0.2	2.5	1.3
351	2463162.947	5817997.074	458.121	0.3	0.2	2.5	1.3
352	2463160.074	5818002.019	457.472	0.2	0.2	2.5	1.3
353	2463166.003	5818003.800	457.590	0.2	0.2	2.5	1.3
354	2463171.977	5818003.292	457.851	0.2	0.2	2.5	1.4
355	2463177.163	5818001.865	458.078	0.2	0.2	2.5	1.3
356	2463176.266	5817995.564	458.532	0.2	0.2	2.4	1.3
357	2463174.306	5817999.708	458.786	0.4	0.2	2.7	1.4
358	2463171.628	5817993.749	460.853	0.9	0.5	2.6	1.5
359	2463165.523	5817994.678	458.625	0.4	0.3	2.5	1.3
360	2463160.153	5817994.937	458.097	0.4	0.2	2.5	1.4
361	2463165.313	5817995.391	458.715	0.3	0.2	2.6	1.5
362	2463164.059	5818001.176	457.513	0.3	0.2	2.5	1.4
363	2463159.875	5818005.988	457.284	0.3	0.2	2.5	1.4
364	2463156.599	5818010.391	457.030	0.3	0.2	2.5	1.4
365	2463150.933	5818009.180	456.906	0.3	0.2	2.5	1.4
366	2463152.509	5818003.978	457.033	0.3	0.2	2.5	1.4
367	2463155.886	5817999.255	457.380	0.3	0.2	2.5	1.4
368	2463159.194	5817995.375	457.913	0.3	0.2	2.0	1.2
369	2463163.546	5817992.931	458.732	0.3	0.2	3.9	2.5
370	2463163.731	5817988.289	459.576	0.3	0.2	2.2	1.2
371	2463169.176	5817987.176	460.535	0.3	0.2	2.0	1.2
372	2463168.666	5817981.719	459.788	0.2	0.1	2.0	1.2
373	2463174.050	5817982.403	458.443	0.3	0.2	2.0	1.2
374	2463179.178	5817979.832	457.161	0.3	0.2	2.0	1.2
375	2463184.328	5817977.526	457.057	0.3	0.2	2.0	1.2
376	2463189.549	5817975.511	457.163	0.3	0.2	2.0	1.2
377	2463194.944	5817972.883	457.226	0.3	0.2	2.0	1.2
378	2463200.634	5817970.828	457.357	0.3	0.2	2.0	1.2
379	2463205.905	5817968.367	457.397	0.3	0.2	2.0	1.2
380	2463210.149	5817963.938	457.740	0.3	0.2	2.0	1.2
381	2463215.133	5817960.106	458.114	0.3	0.2	2.0	1.2
382	2463199.591	5817960.565	457.699	0.3	0.2	2.0	1.2
383	2463193.887	5817963.697	457.537	0.3	0.2	2.0	1.2
384	2463188.698	5817966.811	457.415	0.2	0.2	2.0	1.2
385	2463183.539	5817970.236	457.394	0.2	0.2	2.0	1.2
386	2463178.320	5817972.789	457.412	0.2	0.2	2.0	1.2
387	2463173.329	5817974.775	458.099	0.2	0.2	2.0	1.2
388	2463167.882	5817974.842	459.949	0.2	0.2	2.0	1.2
389	2463163.558	5817977.478	461.008	0.2	0.2	2.0	1.2
390	2463158.423	5817977.691	460.845	0.2	0.2	2.0	1.2
391	2463155.807	5817982.735	459.979	0.3	0.2	2.2	1.2
392	2463152.664	5817986.853	458.716	0.3	0.2	4.0	2.5
393	2463147.953	5817990.522	457.836	0.3	0.2	2.1	1.2
394	2463145.633	5817994.979	457.589	0.2	0.2	2.1	1.2
395	2463143.080	5817999.779	457.323	0.2	0.2	2.1	1.2
396	2463141.182	5818005.249	457.110	0.2	0.2	2.1	1.2
397	2463139.849	5818010.877	456.949	0.2	0.2	2.1	1.2
398	2463134.783	5818012.487	456.930	0.2	0.2	2.1	1.2
399	2463134.922	5818007.358	456.943	0.2	0.2	2.1	1.2
400	2463137.992	5818001.842	457.064	0.2	0.2	2.1	1.2
401	2463141.443	5817996.395	457.245	0.2	0.2	2.1	1.2
402	2463145.087	5817991.349	457.536	0.2	0.2	2.1	1.2
403	2463147.831	5817986.222	458.123	0.3	0.2	2.1	1.2
404	2463146.821	5817981.580	459.423	0.5	0.3	2.2	1.2
405	2463151.953	5817975.399	460.798	1.0	0.6	2.7	1.4
406	2463156.165	5817972.337	460.909	0.4	0.3	2.1	1.2
407	2463160.078	5817968.068	460.516	0.4	0.3	2.1	1.2
408	2463163.801	5817964.669	459.181	0.3	0.2	2.1	1.2
409	2463167.340	5817969.064	458.728	0.3	0.2	2.1	1.2
410	2463172.800	5817967.315	457.539	0.3	0.2	2.1	1.2
411	2463178.510	5817964.524	457.443	0.3	0.2	2.1	1.2
412	2463184.024	5817961.584	457.325	0.3	0.2	2.1	1.2
413	2463174.855	5817960.294	457.458	0.3	0.2	2.0	1.1
414	2463169.148	5817961.804	457.772	0.3	0.2	2.0	1.1
415	2463164.654	5817964.382	459.050	0.3	0.2	2.0	1.1
416	2463159.900	5817966.657	460.751	0.2	0.2	2.0	1.1
417	2463156.802	5817970.728	460.967	0.3	0.2	2.0	1.1
418	2463150.511	5817970.288	461.034	0.2	0.2	2.0	1.1
419	2463145.462	5817970.401	460.652	0.2	0.2	2.0	1.1
420	2463142.161	5817974.695	459.527	0.2	0.2	2.0	1.1
421	2463140.504	5817980.081	458.371	0.3	0.2	2.0	1.1
422	2463138.942	5817985.219	457.684	0.2	0.2	2.0	1.1
423	2463134.698	5817989.313	457.261	0.2	0.2	2.0	1.1
424	2463132.559	5817994.958	457.071	0.2	0.2	2.0	1.1
425	2463129.773	5818000.545	456.944	0.2	0.2	2.0	1.1
426	2463126.267	5818005.731	456.852	0.2	0.2	2.0	1.1
427	2463128.445	5817990.219	457.125	0.2	0.2	2.0	1.1
428	2463130.819	5817985.225	457.298	0.2	0.2	2.0	1.1
429	2463132.749	5817979.714	457.685	0.2	0.2	2.0	1.1
430	2463136.766	5817975.575	458.605	0.2	0.2	2.0	1.1
431	2463140.432	5817971.669	459.756	0.2	0.2	2.0	1.1
432	2463144.961	5817967.375	461.053	0.2	0.2	2.0	1.1
433	2463148.358	5817963.051	461.364	0.2	0.2	2.0	1.1
434	2463159.780	5817960.812	459.829	0.2	0.2	2.0	1.1
435	2463139.522	5817963.081	461.391	0.2	0.2	2.0	1.1
436	2463136.913	5817967.744	460.329	0.2	0.2	2.0	1.1
437	2463133.009	5817971.326	459.088	0.2	0.2	2.0	1.1
438	2463128.322	5817974.545	458.152	0.2	0.2	2.0	1.1
439	2463129.308	5817965.154	459.726	0.2	0.1	2.0	1.1
440	2463133.904	5817962.552	460.805	0.2	0.1	2.0	1.1
441	2463135.680	5817960.077	461.484	0.2	0.2	2.1	1.1
442	2463130.096	5818006.855	456.884	0.3	0.2	2.5	1.2
443	2463135.943	5818009.299	456.794	0.3	0.2	2.5	1.2
444	2463142.015	5818011.009	456.583	0.3	0.2	2.5	1.2
445	2463147.926	5818012.928	456.546	0.3	0.2	2.5	1.2
446	2463153.746	5818015.035	456.556	0.3	0.2	2.5	1.2
447	2463159.630	5818017.204	456.607	0.3	0.2	2.5	1.2
448	2463165.518	5818019.558	456.636	0.3	0.2	2.5	1.2
449	2463169.897	5818023.464	456.594	0.3	0.2	2.5	1.2
450	2463172.907	5818028.588	456.426	0.2	0.2	2.5	1.2
451	2463174.530	5818034.189	456.191	0.2	0.2	2.5	1.2
452	2463176.390	5818039.657	455.905	0.2	0.2	2.5	1.2
453	2463179.055	5818044.821	455.747	0.2	0.2	2.5	1.2
454	2463182.742	5818049.321	455.519	0.2	0.1	2.5	1.2
455	2463188.526	5818050.514	455.390	0.2	0.1	2.5	1.2
456	2463194.081	5818050.457	455.520	0.2	0.1	2.5	1.2
457	2463198.685	5818047.463	455.432	0.2	0.1	2.5	1.2
458	2463200.792	5818052.139	454.555	0.2	0.2	2.5	1.2
459	2463202.106	5818056.985	452.843	0.3	0.2	2.8	1.4
460	2463231.742	5818021.389	455.528	0.6	0.3	4.2	1.7
461	2463226.770	5818025.080	454.803	0.6	0.3	4.2	1.7
462	2463221.833	5818027.935	453.582	0.5	0.3	2.9	1.4
463	2463218.507	5818032.829	452.933	0.5	0.3	2.9	1.4
464	2463217.372	5818038.508	452.672	0.5	0.3	2.9	1.4
465	2463217.318	5818044.077	452.143	0.5	0.3	2.9	1.4
466	2463221.324	5818048.442	451.796	0.5	0.2	2.9	1.4
467	2463226.915	5818051.034	451.295	0.6	0.3	4.2	1.7
468	2463232.626	5818053.585	451.325	0.5	0.3	4.2	1.7
469	2463238.563	5818055.959	451.293	0.5	0.3	4.2	1.7
470	2463244.424	5818058.167	451.236	0.5	0.2	4.2	1.7
471	2463250.174	5818060.681	451.161	0.5	0.2	4.2	1.7
472	2463255.160	5818063.485	451.721	1.5	0.6	4.2	1.7
473	2463250.962	5818065.795	450.633	1.1	0.5	2.9	1.4
474	2463245.973	5818063.268	450.514	0.7	0.3	4.2	1.7
475	2463241.392	5818060.828	450.838	0.7	0.3	4.2	1.7
476	2463235.997	5818057.903	451.064	0.7	0.3	4.2	1.7
477	2463231.241	5818055.581	451.143	0.7	0.3	4.2	1.7
478	2463226.071	5818053.481	451.350	0.7	0.3	4.2	1.7
479	2463221.305	5818051.593	451.268	0.6	0.3	2.9	1.4
480	2463224.612	5818056.084	450.496	0.6	0.3	4.2	1.7
481	2463228.663	5818059.870	449.623	0.6	0.3	4.2	1.7
482	2463233.092	5818063.043	449.283	0.6	0.3	2.9	1.4
483	2463238.375	5818066.202	448.904	0.6	0.3	4.1	1.7
484	2463243.810	5818068.989	448.810	0.6	0.3	4.1	1.7
485	2463249.540	5818071.605	449.100	0.6	0.3	4.1	1.7
486	2463254.310	5818074.021	449.406	0.6	0.3	4.1	1.7
487	2463251.718	5818079.660	446.814	1.1	0.4	4.1	1.7
488	2463246.097	5818077.110	447.247	0.8	0.3	4.1	1.7
489	2463240.832	5818074.437	447.070	0.6	0.3	4.1	1.7
490	2463236.367	5818072.061	447.297	0.6	0.3	4.1	1.7
491	2463232.193	5818067.862	447.609	0.5	0.3	4.1	1.7
492	2463228.123	5818063.581	448.288	0.5	0.2	4.1	1.7
493	2463222.980	5818060.833	448.463	0.5	0.2	4.1	1.7
494	2463218.206	5818058.324	449.209	0.5	0.2	4.1	1.7
495	2463218.177	5818052.933	450.945	0.4	0.2	2.9	1.4
496	2463221.907	5818057.663	449.706	0.5	0.2	2.9	1.4
497	2463222.754	5818063.076	447.457	0.5	0.3	4.1	1.7
498	2463217.910	5818064.730	447.064	0.5	0.2	4.1	1.7
499	2463213.204	5818065.808	447.057	0.5	0.2	2.9	1.4
500	2463210.284	5818061.600	448.692	0.4	0.2	2.9	1.4
501	2463210.133	5818056.745	450.304	0.6	0.4	2.9	1.4
502	2463204.953	5818056.325	452.282	0.3	0.1	2.9	1.4
503	2463203.770	5818061.553	450.311	0.3	0.1	2.9	1.4
504	2463200.795	5818066.520	448.716	0.3	0.1	2.9	1.4

505	2463197.284	5818062.440	451.136	0.5	0.2	4.1	1.7
506	2463192.136	5818061.455	452.832	0.4	0.2	2.9	1.4
507	2463192.955	5818066.865	449.996	0.5	0.3	2.9	1.4
508	2463197.623	5818064.417	449.994	0.4	0.2	2.9	1.4
509	2463193.563	5818061.187	452.323	0.5	0.2	2.9	1.4
510	2463193.528	5818055.439	454.384	0.5	0.2	2.9	1.4
511	2463198.786	5818056.089	454.032	0.5	0.2	2.9	1.4
512	2463193.582	5818055.296	454.474	0.8	0.3	2.9	1.4
513	2463193.353	5818060.965	452.743	0.4	0.2	4.0	1.7
514	2463190.589	5818064.904	450.868	0.4	0.2	2.9	1.4
515	2463185.463	5818064.726	451.279	0.4	0.2	2.9	1.4
516	2463184.850	5818060.806	453.930	0.7	0.4	4.5	1.9
517	2463183.281	5818065.489	451.618	0.4	0.3	2.1	1.1
518	2463186.800	5818069.292	449.258	0.6	0.3	2.1	1.1
519	2463181.770	5818053.953	454.854	0.7	0.3	2.9	1.4
520	2463183.289	5818049.562	455.289	0.6	0.3	2.1	1.1
521	2463188.074	5818047.719	455.502	0.5	0.3	2.1	1.1
522	2463193.714	5818045.076	455.721	0.5	0.3	2.1	1.1
523	2463198.800	5818044.647	455.375	0.5	0.3	2.1	1.1
524	2463203.797	5818046.365	454.376	0.4	0.2	2.1	1.1
525	2463209.036	5818045.948	452.500	0.4	0.2	2.1	1.1
526	2463214.596	5818047.198	451.673	0.4	0.2	2.1	1.1
527	2463218.227	5818050.878	450.809	0.4	0.2	2.1	1.1
528	2463222.088	5818055.122	450.316	0.4	0.2	2.1	1.1
529	2463226.398	5818059.398	449.138	0.5	0.2	3.2	1.5
530	2463229.821	5818064.205	448.194	0.5	0.2	2.9	1.4
531	2463231.237	5818070.657	446.993	1.2	0.6	3.2	1.5
532	2463231.685	5818076.267	445.337	0.5	0.3	3.2	1.5
533	2463229.974	5818081.977	443.627	0.5	0.3	3.2	1.5
534	2463227.562	5818087.443	442.627	0.5	0.3	3.2	1.5
535	2463224.815	5818092.137	440.892	0.5	0.3	3.2	1.5
536	2463226.625	5818097.304	439.559	0.5	0.3	3.8	1.7
537	2463231.165	5818101.818	438.968	0.5	0.3	3.2	1.5
538	2463235.517	5818106.595	438.129	0.5	0.3	3.2	1.5
539	2463240.190	5818110.433	437.476	0.5	0.3	3.2	1.5
540	2463245.125	5818114.438	437.037	0.5	0.3	3.2	1.5
541	2463249.692	5818117.641	436.913	0.5	0.3	3.2	1.5
542	2463254.326	5818119.988	436.881	0.5	0.3	3.2	1.5
543	2463258.703	5818123.135	436.697	0.5	0.3	3.2	1.5
544	2463263.274	5818126.023	436.663	0.5	0.3	2.2	1.1
545	2463259.414	5818121.979	436.897	0.5	0.3	2.2	1.1
546	2463257.845	5818116.850	438.016	0.5	0.3	3.2	1.5
547	2463257.659	5818111.610	439.569	0.7	0.3	4.4	2.2
548	2463253.679	5818108.534	439.813	0.6	0.3	4.4	2.2
549	2463247.924	5818106.537	439.761	0.6	0.3	3.2	1.5
550	2463242.560	5818104.688	439.642	0.6	0.3	3.2	1.5
551	2463236.987	5818101.702	439.771	0.5	0.3	3.2	1.5
552	2463232.139	5818098.082	439.995	0.5	0.3	3.2	1.5
553	2463229.297	5818093.232	441.078	0.5	0.3	3.2	1.5
554	2463234.379	5818092.316	442.199	0.5	0.3	3.2	1.5
555	2463239.310	5818095.408	441.878	0.5	0.3	3.2	1.5
556	2463244.865	5818098.813	441.528	0.5	0.2	3.2	1.5
557	2463250.230	5818102.115	441.400	0.7	0.3	4.4	2.1
558	2463255.523	5818103.181	441.527	0.6	0.3	4.4	2.1
559	2463257.233	5818098.504	442.625	0.6	0.3	4.4	2.1
560	2463254.204	5818094.043	443.293	0.6	0.3	4.4	2.1
561	2463248.825	5818090.736	443.591	0.5	0.3	3.2	1.5
562	2463243.391	5818088.239	443.632	0.5	0.3	3.2	1.5
563	2463238.519	5818086.259	443.613	0.5	0.2	3.2	1.5
564	2463233.639	5818083.557	443.550	0.4	0.2	3.2	1.5
565	2463233.487	5818078.412	444.726	0.4	0.2	3.2	1.5
566	2463238.690	5818077.180	445.634	0.4	0.2	3.2	1.5
567	2463243.942	5818079.513	445.704	0.4	0.2	3.2	1.5
568	2463248.484	5818082.802	445.684	0.4	0.2	3.2	1.5
569	2463252.939	5818085.030	446.083	0.5	0.2	3.2	1.5
570	2463254.438	5818089.874	444.190	0.5	0.2	4.4	2.1
571	2463249.616	5818093.860	442.709	0.5	0.2	4.4	2.1
572	2463245.628	5818098.349	441.519	0.5	0.2	3.2	1.5
573	2463245.433	5818104.001	440.008	0.4	0.2	3.2	1.5
574	2463248.679	5818109.906	438.669	0.4	0.2	3.2	1.5
575	2463251.744	5818114.003	438.085	0.4	0.2	3.2	1.5
576	2463255.223	5818117.570	437.316	0.4	0.2	3.2	1.5
577	2463259.769	5818122.245	436.708	0.4	0.2	3.2	1.5
578	2463260.776	5818127.125	436.253	0.2	0.1	2.9	1.4
579	2463262.416	5818132.869	435.549	0.3	0.2	2.2	1.1
580	2463262.974	5818139.462	434.869	0.4	0.2	3.2	1.5
581	2463262.721	5818146.057	434.185	0.4	0.2	3.2	1.5
582	2463262.393	5818152.554	433.509	0.4	0.2	3.2	1.5
583	2463262.187	5818158.848	433.192	0.4	0.2	3.2	1.5
584	2463261.984	5818163.752	433.117	0.3	0.2	2.2	1.1
585	2463261.911	5818170.244	432.480	0.3	0.2	3.2	1.5
586	2463255.134	5818165.545	432.864	0.3	0.2	2.2	1.1
587	2463255.525	5818159.136	433.212	0.3	0.2	2.2	1.1
588	2463255.867	5818154.187	433.370	0.3	0.2	3.2	1.5
589	2463256.498	5818147.651	433.607	0.3	0.2	3.2	1.5
590	2463257.155	5818141.217	434.119	0.3	0.2	3.2	1.5
591	2463257.775	5818134.910	434.613	0.3	0.2	3.2	1.5
592	2463257.641	5818129.219	435.246	0.3	0.2	2.2	1.1
593	2463253.654	5818125.890	435.251	0.3	0.2	3.2	1.5
594	2463249.592	5818130.512	434.432	0.3	0.2	3.2	1.5
595	2463249.264	5818136.649	433.971	0.3	0.2	2.2	1.1
596	2463248.963	5818143.134	433.588	0.3	0.2	2.2	1.1
597	2463248.790	5818149.728	433.253	0.3	0.2	3.2	1.5
598	2463248.553	5818156.334	433.195	0.3	0.2	3.2	1.5
599	2463248.508	5818161.345	433.096	0.3	0.2	3.2	1.5
600	2463248.210	5818166.469	433.608	0.3	0.2	3.2	1.5
601	2463240.202	5818167.047	434.761	0.3	0.2	2.2	1.1
602	2463240.302	5818161.963	435.015	0.3	0.2	2.2	1.1
603	2463240.376	5818156.797	434.429	0.3	0.2	2.2	1.1
604	2463240.722	5818151.114	433.542	0.3	0.2	2.2	1.1
605	2463240.879	5818145.895	433.500	0.3	0.2	2.2	1.1
606	2463240.860	5818140.746	433.584	0.3	0.2	2.2	1.1
607	2463240.918	5818134.270	433.761	0.3	0.2	2.2	1.1
608	2463241.076	5818128.234	433.938	0.3	0.2	3.2	1.5
609	2463239.521	5818123.200	434.157	0.3	0.2	3.2	1.5
610	2463234.061	5818122.686	433.884	0.3	0.2	3.2	1.5
611	2463233.125	5818128.788	433.717	0.3	0.2	3.2	1.5
612	2463233.184	5818135.270	433.686	0.3	0.2	2.2	1.1
613	2463233.087	5818141.823	433.703	0.3	0.2	2.2	1.1
614	2463232.735	5818148.400	433.827	0.3	0.2	2.2	1.1
615	2463232.271	5818154.439	435.049	0.3	0.2	2.2	1.1
616	2463232.028	5818160.835	435.490	0.3	0.2	2.2	1.1
617	2463231.736	5818167.352	435.491	0.3	0.2	2.2	1.1
618	2463225.402	5818167.786	435.962	0.3	0.2	2.2	1.1
619	2463225.862	5818161.213	436.061	0.3	0.2	2.2	1.1
620	2463226.229	5818156.212	435.961	0.3	0.2	2.2	1.1
621	2463226.337	5818151.167	435.636	0.3	0.2	2.2	1.1
622	2463226.435	5818145.994	434.984	0.3	0.2	2.2	1.1
623	2463226.726	5818140.515	434.039	0.3	0.2	2.2	1.1
624	2463227.033	5818135.380	433.934	0.3	0.2	2.2	1.1
625	2463227.177	5818130.563	433.957	0.3	0.2	3.2	1.5
626	2463227.279	5818124.174	434.060	0.3	0.2	3.2	1.5
627	2463224.396	5818118.997	434.346	0.3	0.2	3.2	1.5
628	2463219.453	5818121.516	434.429	0.3	0.2	3.2	1.5
629	2463218.857	5818126.510	434.234	0.3	0.2	3.2	1.5
630	2463218.349	5818132.927	434.674	0.3	0.2	3.2	1.5
631	2463217.705	5818138.503	435.495	0.3	0.2	2.2	1.1
632	2463217.047	5818144.902	436.074	0.3	0.2	2.2	1.1
633	2463216.390	5818151.441	436.478	0.3	0.2	2.2	1.1
634	2463216.028	5818158.027	436.450	0.3	0.2	2.2	1.1
635	2463215.694	5818164.666	436.362	0.3	0.2	2.2	1.1
636	2463208.487	5818166.315	436.574	0.3	0.2	2.2	1.1
637	2463208.762	5818161.199	436.775	0.3	0.2	2.2	1.1
638	2463208.798	5818154.575	436.778	0.3	0.2	2.2	1.1
639	2463208.781	5818149.484	436.773	0.3	0.2	2.2	1.1
640	2463208.728	5818144.474	436.689	0.3	0.2	2.2	1.1
641	2463208.641	5818139.410	436.589	0.3	0.2	2.2	1.1
642	2463208.607	5818134.308	436.372	0.3	0.2	2.2	1.1
643	2463209.073	5818127.716	435.931	0.3	0.2	2.2	1.1
644	2463209.610	5818122.594	435.567	0.3	0.2	2.2	1.1
645	2463210.096	5818117.486	435.246	0.3	0.2	3.1	1.5
646	2463205.931	5818114.588	435.992	0.3	0.2	3.1	1.5
647	2463202.003	5818118.547	436.358	0.3	0.2	2.3	1.1
648	2463201.310	5818123.537	436.562	0.3	0.2	2.3	1.1
649	2463200.450	5818130.049	436.789	0.3	0.2	2.3	1.1
650	2463200.060	5818135.183	436.904	0.3	0.2	2.3	1.1
651	2463199.643	5818141.699	437.023	0.3	0.2	2.3	1.1
652	2463199.405	5818146.697	436.894	0.3	0.2	2.3	1.1
653	2463199.126	5818151.902	436.883	0.3	0.2	2.3	1.1
654	2463198.996	5818156.951	436.926	0.3	0.2	2.3	1.1
655	2463190.113	5818157.234	436.946	0.3	0.2	2.3	1.1
656	2463190.201	5818152.193	436.896	0.3	0.2	2.3	1.1
657	2463190.357	5818147.147	436.943	0.3	0.2	2.3	1.1
658	2463190.645	5818140.574	437.007	0.3	0.2	2.3	1.1
659	2463190.931	5818134.006	437.090	0.3	0.2	2.3	1.1
660	2463191.513	5818127.424	437.248	0.3	0.2	2.3	1.1
661	2463192.093	5818121.006	437.173	0.3	0.2	2.3	1.1
662	2463192.462	5818114.863	437.172	0.3	0.2	2.3	1.1
663	2463188.165	5818110.854	437.779	0.3	0.2	3.1	1.5
664	2463184.149	5818114.512	438.023	0.3	0.2	2.3	1.1
665	2463183.267	5818120.818	437.531	0.3	0.2	2.3	1.1
666	2463182.534	5818125.760	437.453	0.3	0.2	2.3	1.1
667	2463181.951	5818130.889	437.195	0.3	0.2	2.3	1.1
668	2463181.412	5818137.514	437.123	0.3	0.2	2.3	1.1
669	2463180.858	5818142.595	437.040	0.3	0.2	2.3	1.1
670	2463180.160	5818147.628	436.887	0.3	0.2	2.3	1.1
671	2463179.668	5818152.821	436.870	0.3	0.2	2.3	1.1
672	2463179.115	5818157.825	436.824	0.3	0.2	2.3	1.1
673	2463170.582	5818155.267	436.751	0.3	0.2	2.3	1.1
674	2463170.775	5818148.693	436.872	0.3	0.2	2.3	1.1
675	2463171.135	5818142.233	436.878	0.3	0.2	2.3	1.1
676	2463171.499	5818135.751	437.090	0.3	0.2	2.3	1.1
677	2463171.542	5818129.226	437.255	0.3	0.2	2.3	1.1
678	2463171.748	5818124.197	437.372	0.3	0.2	2.3	1.1
679	2463172.130	5818119.131	437.687	0.2	0.2	2.3	1.1
680	2463172.351	5818112.720	438.433	0.2	0.2	2.3	1.1
681	2463172.416	5818107.488	438.960	0.3	0.2	3.1	1.5
682	2463167.584	5818106.464	438.871	0.3	0.2	3.1	1.5
683	2463164.091	5818111.048	438.128	0.3	0.2	2.3	1.1
684	2463163.275	5818115.978	437.597	0.3	0.2	2.3	1.1
685	2463162.438	5818120.903	437.425	0.3	0.2	2.3	1.1
686	2463161.643	5818127.537	437.086	0.3	0.2	2.3	1.1
687	2463161.253	5818133.599	436.992	0.3	0.2	2.3	1.1
688	2463160.955	5818139.883	436.885	0.3	0.2	2.3	1.1
689	2463149.774	5818138.444	436.776	0.2	0.2	1.9	1.0
690	2463150.010	5818131.845	436.934	0.2	0.2	1.9	1.0
691	2463150.195	5818125.205	437.139	0.2	0.2	1.9	1.0
692	2463150.331	5818120.151	437.443	0.2	0.2	1.9	1.0
693	2463150.704	5818113.545	437.621	0.2	0.2	1.9	1.0
694	2463151.230	5818107.212	437.997	0.2	0.2	2.1	1.1
695	2463149.189	5818102.609	438.402	0.2	0.2	2.1	1.1
696	2463154.052	5818104.330	438.315	0.3	0.2	2.1	1.1
697	2463160.196	5818105.548	438.502	0.3	0.2	3.1	1.5
698	2463166.432	5818106.506	438.808	0.3	0.2	2.3	1.1
699	2463171.493	5818106.769	438.846	0.3	0.2	2.3	1.1
700	2463173.540	5818101.886	439.717	0.4	0.3	2.3	1.1
701	2463176.577	5818098.174	440.319	0.3	0.3	2.3	1.2
702	2463180.552	5818094.733	440.990	0.3	0.2	2.5	1.3
703	2463185.860	5818093.675	440.573	0.3	0.2	2.5	1.3
704	2463181.010	5818091.072	442.177	0.3	0.2	2.5	1.3
705	2463177.382	5818087.314	443.577	0.4	0.2	3.0	1.5
706	2463171.557	5818086.820	443.957	0.4	0.2	3.0	1.5
707	2463170.024	5818081.079	445.924	0.4	0.2	3.0	1.5
708	2463167.638	5818076.094	447.097	0.3	0.2	2.1	1.1
709	2463162.779	5818073.529	448.023	0.5	0.3	2.1	1.1
710	2463157.415	5818076.269	446.523	0.5	0.3	3.0	1.5
711	2463155.197	5818080.912	444.838	0.5	0.3	3.0	1.5
712	2463151.123	5818084.648	443.292	0.4	0.3	3.0	1.5
713	2463154.957	5818080.682	445.279	0.7	0.4	3.0	1.5
714	2463153.650	5818075.495	446.204	0.7	0.4	3.0	1.5
715	2463159.701	5818075.811	447.225	0.7	0.4	2.3	1.1
716	2463164.154	5818073.566	448.200	0.6	0.4	2.2	1.1
717	2463169.392	5818076.964	446.183	1.0	0.9	2.2	1.1
718	2463172.270	5818081.557	446.525	0.6	0.4	3.0	1.5
719	2463178.458	5818082.588	445.800	0.5	0.3	3.0	1.5
720	2463183.536	5818082.489	445.986	0.5	0.3	3.0	1.5
721	2463187.353	5818086.613	444.167	0.5	0.3	3.0	1.5
722	2463193.160	5818088.251	442.425	0.5	0.3	3.0	1.5
723	2463198.176	5818087.088	442.310	0.5	0.3	3.0	1.5
724	2463203.176	5818087.497	441.353	0.5	0.3	3.0	1.5
725	2463209.261	5818087.226	442.062	0.5	0.3	3.0	1.5
726	2463214.715	5818088.204	441.363	0.4	0.3	2.2	1.1
727	2463216.277	5818083.052	442.331	1.4	1.2	4.5	1.9
728	2463219.265	5818077.310	442.832	1.5	1.9	4.6	2.8
729	2463216.442	5818083.360	441.052	1.1	0.9	3.0	1.5
730	2463214.700	5818089.013	441.471	0.5	0.4	3.0	1.5
731	2463219.540	5818090.953	440.787	0.5	0.3	3.0	1.5
732	2463223.729	5818093.525	440.661	0.5	0.3	3.0	1.5
733	2463226.336	5818098.626	439.724	0.4	0.3	3.0	1.5
734	2463230.190	5818102.834	438.854	0.4	0.3	3.0	1.5
735	2463228.168	5818097.518	440.189	0.4	0.3	2.2	1.1
736	2463224.045	5818094.065	440.805	0.4	0.3	2.2	1.1
737	2463220.238	5818091.226	440.573	0.4	0.3	3.0	1.6
738	2463214.539	5818091.413	440.518	0.4	0.3	3.0	1.6
739	2463208.819	5818091.456	440.612	0.5	0.3	3.0	1.6
740	2463204.276	5818087.671	441.003	0.6	0.4	3.0	1.6
741	2463199.299	5818086.969	441.703	0.6	0.4	3.0	1.6
742	2463197.330	5818082.218	443.923	0.7	0.4	3.0	1.6
743	2463198.623	5818079.353	445.066	1.8	1.7	4.8	2.6
744	2463200.643	5818074.755	446.158	1.2	1.4	2.8	1.8
745	2463200.263	5818069.039	448.364	0.9	0.6	2.2	1.2
746	2463202.934	5818064.137	449.567	0.4	0.3	2.2	1.2
747	2463202.110	5818059.075	452.321	0.4	0.3	2.0	1.0
748	2463205.845	5818055.691	452.955	0.4	0.3	2.0	1.0
749	2463208.301	5818061.151	450.128	0.4	0.2	3.0	1.6
750	2463212.775	5818063.111	448.252	0.3	0.2	2.2	1.2
751	2463218.476	5818060.981	448.315	0.3	0.2	2.0	1.0
752	2463219.586	5818055.785	449.964	0.3	0.2	2.0	1.0
753	2463218.476	5818050.897	451.430	0.3	0.2	2.0	1.0
754	2463213.417	5818047.204	452.266	0.3	0.2	2.0	1.0
755	2463209.555	5818043.527	452.920	0.3	0.2	2.0	1.0
756	2463204.336	5818041.004	454.482	0.3	0.2	2.0	1.0

757	2463199.218	5818038.918	455.597	0.3	0.2	2.0	1.0
758	2463197.999	5818033.514	455.651	0.3	0.2	2.0	1.0
759	2463197.482	5818028.080	455.213	0.3	0.2	2.0	1.0
760	2463199.164	5818022.004	454.094	0.3	0.2	2.0	1.0
761	2463200.620	5818016.178	454.262	0.3	0.2	2.0	1.0
762	2463202.733	5818010.635	455.048	0.3	0.2	2.0	1.0
763	2463205.339	5818005.905	456.404	0.3	0.2	2.0	1.0
764	2463208.076	5818000.627	456.611	0.3	0.2	2.0	1.0
765	2463211.031	5817995.202	456.827	0.3	0.2	2.0	1.0
766	2463213.640	5817989.818	456.938	0.3	0.2	2.0	1.0
767	2463216.606	5817984.416	457.153	0.3	0.2	2.0	1.0
768	2463219.504	5817979.059	457.471	0.3	0.2	2.0	1.0
769	2463222.010	5817974.130	457.854	0.2	0.2	2.2	1.1
770	2463219.164	5817968.792	457.973	0.2	0.2	2.2	1.1
771	2463214.703	5817965.299	458.015	0.2	0.2	2.2	1.1
772	2463210.207	5817961.751	458.022	0.2	0.2	2.2	1.1

Appendix B: Historic Seismicity First Motion Focal Mechanisms

All recorded earthquakes occurring within 15 km of the NEF during the period January 2004 to May 3rd 2011 were processed at GNS Science using first motion data. The full list of earthquakes within this period can be down loaded from Geonets Quake search resource (http://magma.geonet.org.nz/resources/quakesearch/). Event numbers (CUSP Ids) correspond to reference numbers in Figures 3.10 and 3.11. Focal mechanisms are shown as upper hemisphere projections.

Two mechanisms derived from the microearthquake survey of Cowan (1992) are also included. These mechanisms are shown as lower hemisphere projections.

Event 2655520 : 2006 Nov 18 1447 42.99°S 172.10°E 5 km Mag 4.2

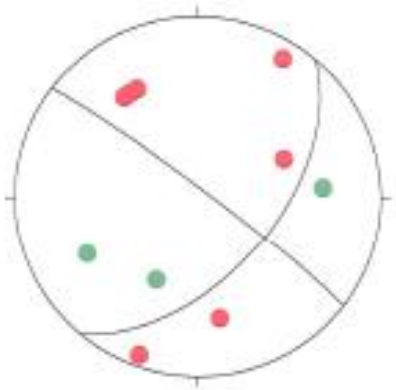

Upper Hemisphere Plots

strike, dip, rake =
220.0 55.0 185.0
127.1 85.9 324.9
resolution = 5.0
n wrong = 0 of 11
n best = 713 of 93312
quality = 0.38
az gap = 85

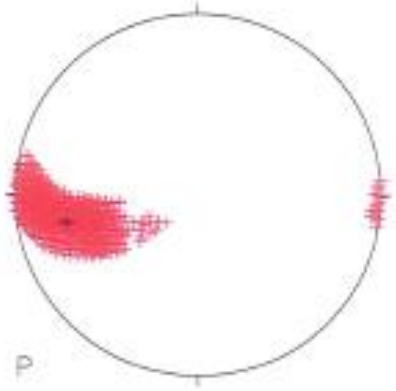

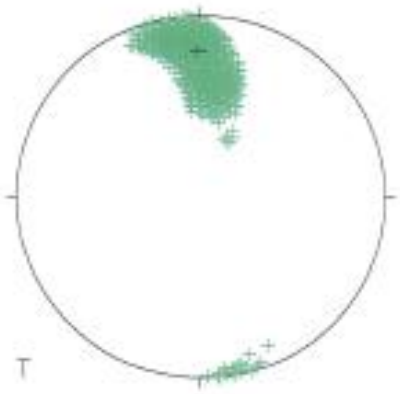

Event 2263205 : 2004 Jul 12 0610 42.82°S 172.44°E 9 km Mag 3.4

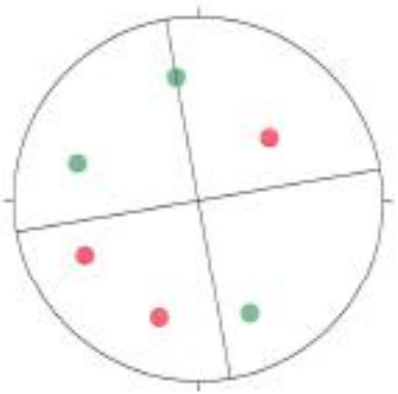

Upper Hemisphere Plots

strike, dip, rake =
80.0 90.0 180.0
170.0 90.0 0.0
resolution = 5.0
n wrong = 0 of 7
n best = 31 of 93312
quality = 0.67
az gap = 106

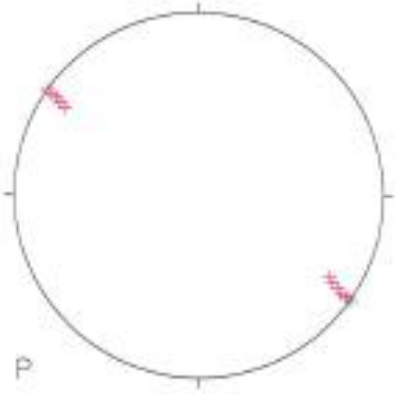

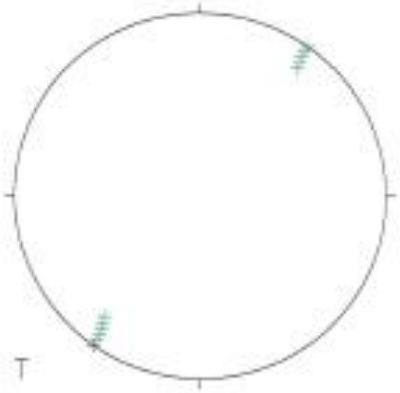

Event 2274769 : 2004 Aug 04 1043 42.83°S 172.44°E 8 km Mag 3.6

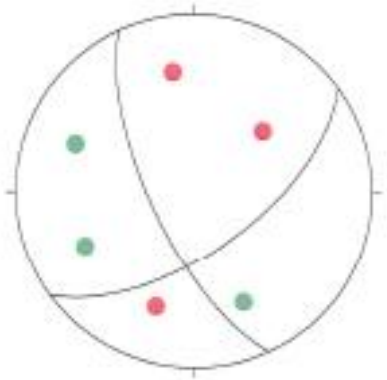

Upper Hemisphere Plots

strike, dip, rake =
335.0 70.0 30.0
233.8 62.0 157.2
resolution = 5.0
n wrong = 0 of 7
n best = 1367 of 93312
quality = 0.00
az gap = 107

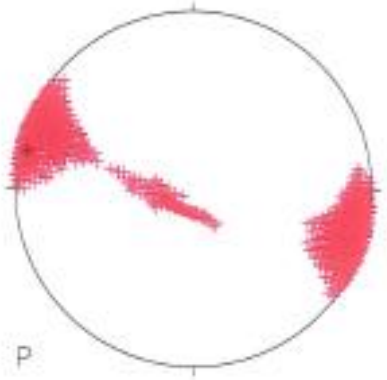

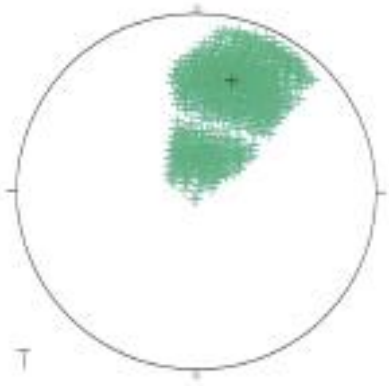

Event 3038001 : 2009 Jan 30 0826 42.74°S 172.38°E 8 km Mag 4.8

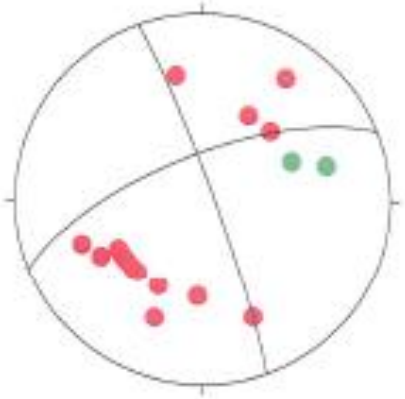

Upper Hemisphere Plots

strike, dip, rake =
160.0 85.0 20.0
68.2 70.1 174.7
resolution = 5.0
n wrong = 0 of 24
n best = 27 of 93312
quality = 0.96
az gap = 98

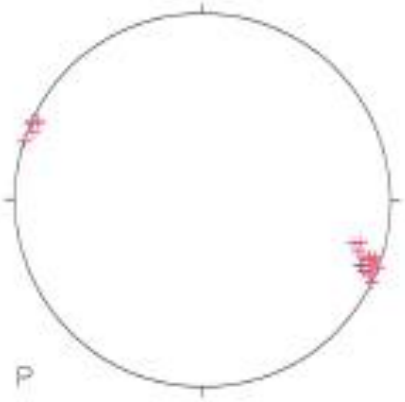

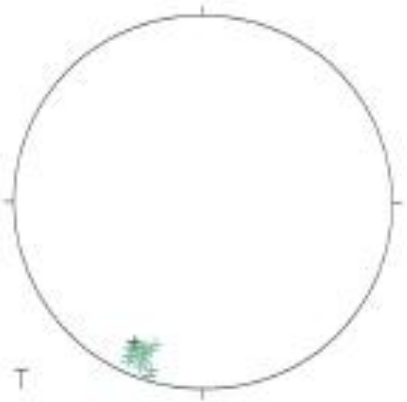

Event 2261397 : 2004 Jul 09 1608 42.82°S 172.48°E 5 km Mag 3.8

Upper Hemisphere Plots

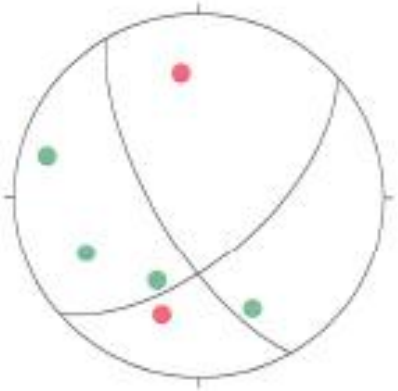

strike, dip, rake =
330.0 70.0 30.0
228.8 62.0 157.2
resolution = 5.0
n wrong = 0 of 7
n best = 734 of 93312
quality = 0.00
az gap = 113

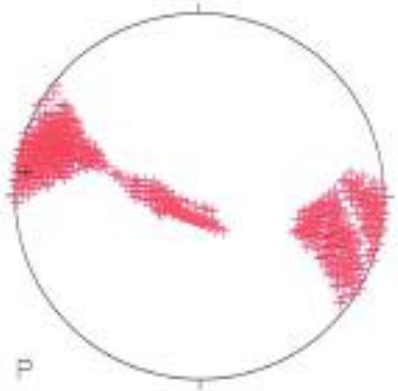

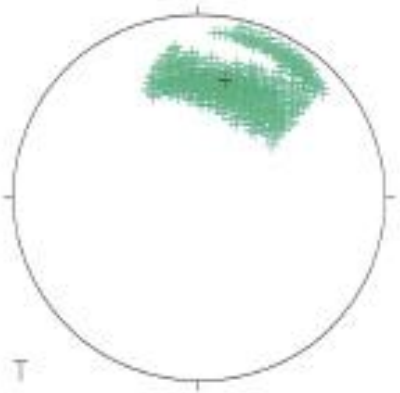

Event 2171148 : 2004 Jan 16 1534 42.97°S 172.39°E 5 km Mag 3.5

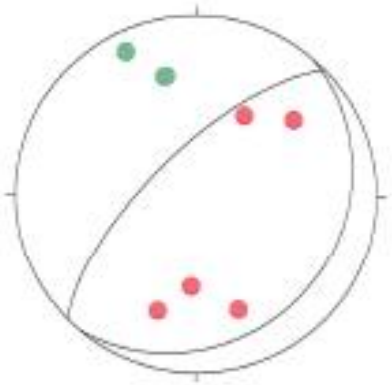

Upper Hemisphere Plots

strike, dip, rake =
220.0 20.0 85.0
45.3 70.1 91.8
resolution = 5.0
n wrong = 0 of 8
n best = 2953 of 93312
quality = 0.00
az gap = 147

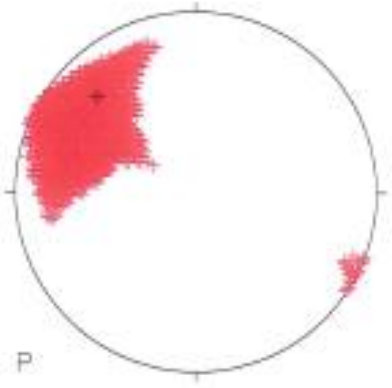

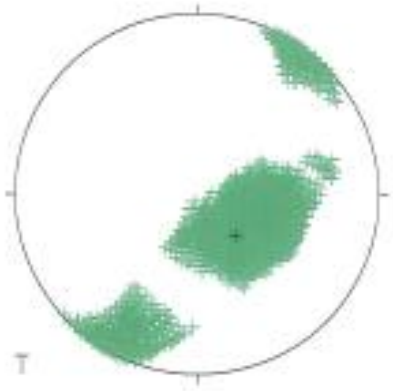

Event 3202903 : 2009 Dec 02 1715 42.96°S 172.44°E 5 km Mag 3.2

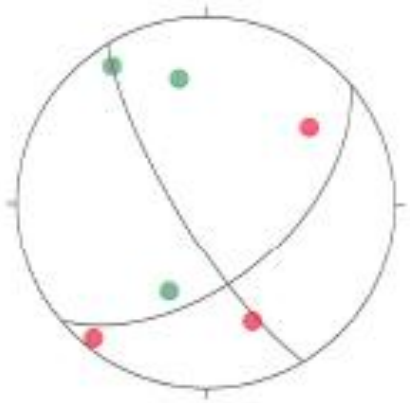

Upper Hemisphere Plots

strike, dip, rake =
230.0 55.0 165.0
328.7 77.8 35.9
resolution = 5.0
n wrong = 1 of 7
n best = 2114 of 93312
quality = 0.00
az gap = 146

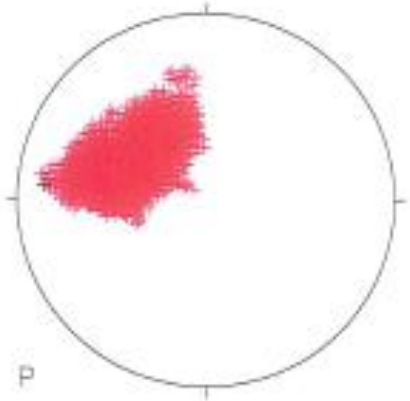

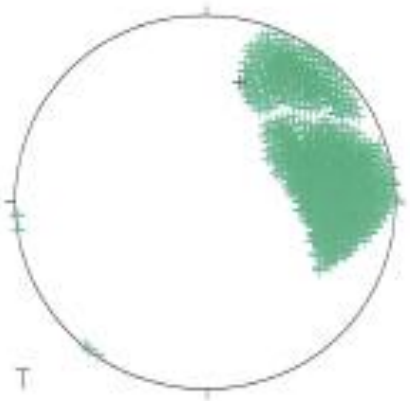

Event 2733209 : 2007 May 03 0000 42.74°S 172.52°E 5 km Mag 4.2

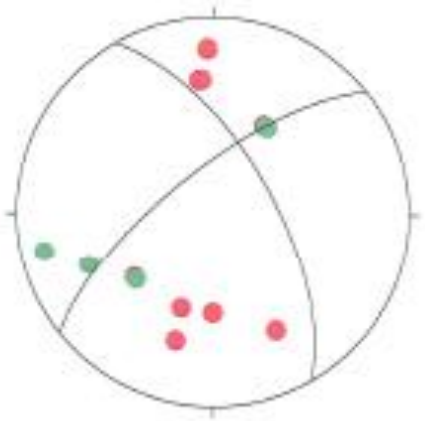

Upper Hemisphere Plots

strike, dip, rake =
150.0 65.0 20.0
51.3 71.9 153.6
resolution = 5.0
n wrong = 1 of 15
n best = 84 of 93312
quality = 0.24
az gap = 107

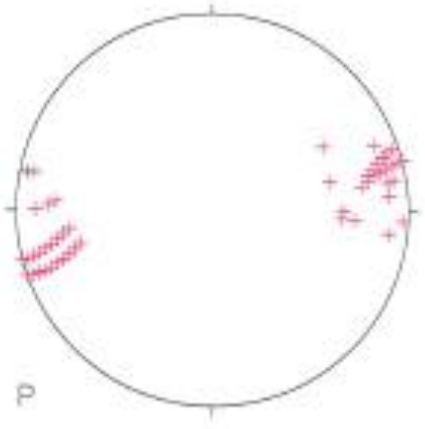

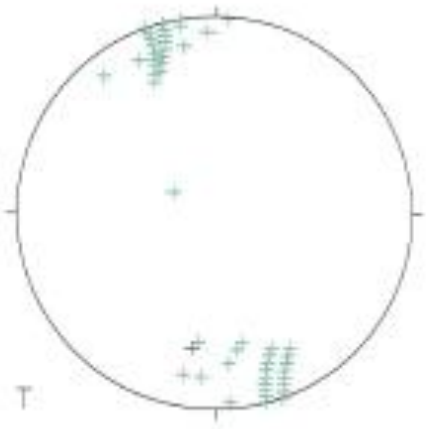

1990 10 4 22 48 56.30 sec -42.765 172.355 5.80 km 2.4

Solution No.12
Event No.112

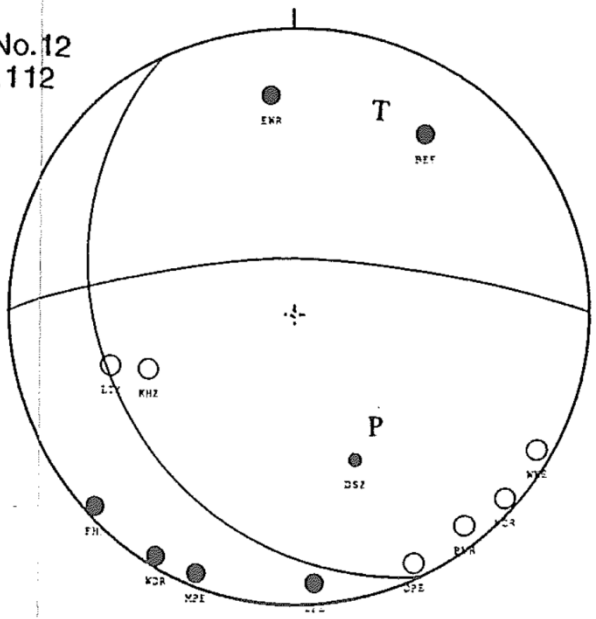

P-Axis 144/52
T-Axis 022/24

1990 11 7 9 4 7.48 sec -42.751 172.380 17.00 km 2.7

Solution No.47
Event No.189

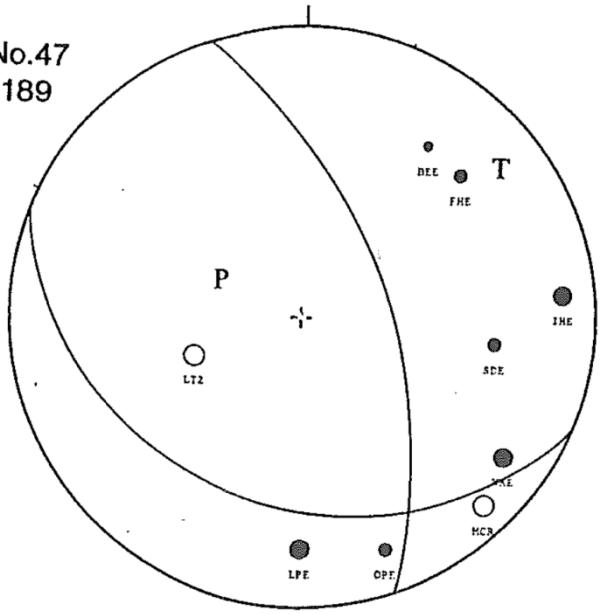

P-Axis 295/64
T-Axis 052/18

From Cowan (1992)

Appendix C – OSL and ^{14}C Results

1. **Luminescence Dating Technical Report**

    - **Summary**
    - **Experimental Work**
    - **Results**

2. **Accelerator Mass Spectrometry Results**

    - **DN-MN1-2010 Result**
    - **DN-MN1-2010 Calibration report**
    - **DN-EF1-2010 Result**
    - **DN-EF1-2010 Calibration report**

1. Luminescence Dating Report

Report No. 1-11-10

Luminescence Dating Technical Report

Ms. Ningsheng Wang (MSc)

Dr. Uwe Rieser

Luminescence Dating Laboratory

School of Geography, Environment and Earth Sciences

Victoria University of Wellington

Wellington

New Zealand

Reported by:	Ms. Ningsheng Wang
Date of Issue:	26-11-2010
Contact:	Room 414
	Cotton Building
	Victoria University of Wellington
	Ph: (04) 463 6127

1. SUMMARY

Seven samples (Field code: JM01, DN-T6-2010, JM02, DN-T2-2010, DN-T3-2010, DN-WW1-2010, DN-WE1-2010) were submitted for luminescence dating by Duncan Noble from Canterbury University. The laboratory codes of the samples are WLL895-WLL901.

Due to the sample being fine material, the fine grain (4-11um) preparation technique was used. The paleodose (the equivalent dose) of all samples was evaluated using the Multiple Aliquot Additive Dose method (MAAD) based on measurements of blue luminescence from the fine grain feldspar produced during infrared stimulation. The dose rate was determined on the basis of gamma spectrometry measurements.

2. EXPERIMENTAL WORK

A) Sample Preparation

Samples had their outer surfaces removed. "Fresh" sample material, that had outer surfaces removed earlier (unexposed light sample material), was treated in 10% HCl. This was carried out overnight until all carbonate was removed by the reaction. Following this treatment the sample was further reacted overnight with 10% H_2O_2 in order to remove organic matter. The next step involved 200ml CBD* solution being added to the sample for 12 hours to remove iron oxide coatings. Note, after every chemical treatment procedure distilled water was used to wash the sample several times. After chemical treatment, calgon solution (1g sodium hexametaphosphate per litre distilled water) was added to make thick slurry. This slurry was placed into an ultrasonic bath and mechanically agitated for an hour. The sample was then placed into a 1L measuring cylinder, filled with a certain amount of distilled water to separate out the 4-11μm grains according to Stokes' Law.
The 4-11μm grains were then rinsed with ethanol and acetone and a suspension of these grains were then deposited evenly onto 70 aluminium disks (diameter 9.8mm).

This removed outer scraping was then dried in an oven, milled, weighed and sealed in air tight perspex containers, then stored for at least four weeks before the gamma

spectrometer analysis. The storage time minimizes the loss of the short lived noble gas ^{222}Rn and allows ^{226}Ra to reach equilibrium with its daughters ^{214}Pb and ^{214}Bi.

A plastic cube was then filled with remaining scrapings in preparation for water content measuring.

*CBD solution: 71g sodium citrate, 8.5 g sodium bicarbonate, and 2g sodium dithionate per litre of distilled water

B) Measurements

Luminescence age was determined by two factors: the equivalent dose (De) and the dose rate. It involves measurements of luminescence for determination of De and concentrations of ^{238}U, ^{232}Th, ^{40}K and water contents (used to determine of dose rate).

Equivalent dose: obtained from the lab equivalents to the paleodose absorbed by samples during the burial time in the natural environment since their last exposure to the light.
Dose rate: amount dose received by the sample each year.

B1. Determination of Equivalent Dose (De)

De for all of these samples were obtained by using the *Multiple Aliquot Additive Dose Method (MAAD)*.

The test dose obtained from an initial test measurement was used for the MAAD. As luminescence vary between disks, all disks for MAAD need to be normalised before β irradiation. 0.1 second infrared measurements were taken before irradiation of all aliquots. Six groups (30 disks divided by five) were β irradiated up to five times of the test dose. Beta irradiation were done on the Riso TL-DA-15 ^{90}Sr/^{90}Y β irradiator, calibrated against ^{60}Co gamma source, SFU, Vancouver, Canada with about 3% uncertainty. Three groups (three disks per group) were α irradiated up to three times of the test dose. The α irradiation was carried out on a ^{241}Am irradiator, supplied and calibrated by ELSEC Littlemore, UK. The next step was that these 39

disks together with nine non-irradiated disks (total of 48 disks) were stored for four weeks to relax the crystal lattice after irradiation.

After storage, the 48 disks were preheated for five minutes at 230°C, then were measured using a Riso TL-DA-15 reader with infrared diodes at 880nm used to deliver a stimulated beam (30mW/cm^2)at the room temperature for 100s. Blue luminescence centred about 410nm emission from feldspar is then detected by an EMI 9235QA photomultiplier fixed behind three filters consisting of a Schott BG-39, Kopp 5-58 and GG40.

Luminescence growth curve (β induced luminescence intensity versus added dose) was constructed by using the initial the 10 seconds of the shine down curves and subtracting the average of the last 20 seconds, along with the so called late light which was thought to be a mixture of background and hardly bleachable components. Extrapolation of this growth curve to the dose axis was obtained the equivalent dose De which was used as a paleodose. The shine plateau was checked to be flat after this manipulation.

Measurement of a-value

A similar plot for the alpha irradiated disks allows for an estimation of α efficiency, a-value (a-value is measured by comparing the luminescence induced by alpha irradiation with that induced by beta or gamma irradiation). The a-value was for dose rate calculation.

B2: Determination of Dose Rate

Dose rate consisted of two parts.

(i) Dose rate from sample's burial environment

(ii) Dose rate from cosmic rays.

(I) *Dose rate from burial environment*

Dose rate from sample's burial environment was determined by radionuclide contents of ^{238}U, ^{232}Th and ^{40}K, a-value and water content.

Determination of Contents of U, Th and K by Gamma spectrometry

Gamma rays produced from sample material was counted for a minimum time of 24 hours by a high resolution and broad energy gamma spectrometer. The spectra were then analysed using GENIE2000 software. The contents of U, Th and K were obtained by comparison with standard samples. The dose rate calculation was based on the activity concentration of the nuclides ^{40}K, ^{208}TL, ^{212}Pb, ^{228}Ac, ^{214}Bi, ^{214}Pb, ^{226}Ra, using dose rate conversion factors published by Adamiec and Aitken (1998).

Measurement of Water Contents

Water content was measured as weight of water divided by dry weight of the sample taking into account a 10% uncertainty.

(ii) *Dose rate from cosmic rays*

Dose rate from cosmic rays were determined by the depth of sample below the surface along with its longitude, latitude and altitude, convention formula and factors published by Prescott, J.R. & Hutton, J.T. (1994).

3. RESULTS

Table 1 Cosmic dose rates

Table 2 Water contents, radionuclide contents

Table 3 a- Values, dose rates, equivalent doses and luminescence dating ages.

Table 1: Cosmic Dose Rates

Laboratory Code	Depth Below the Surface(m)	Cosmic Dose Rate (Gy/ka)	Field Code
[redacted]			
WLL896	0.46	0.2115±0.0106	DN-T6-2010
[redacted]			
WLL898	0.53	0.2104±0.0105	DN-T2-2010
WLL899	0.50	0.2113±0.0106	DN-T3-2010
WLL900	0.60	0.2125±0.0106	DN-WW1-2010
WLL901	0.50	0.2155±0.0108	DN-WE1-2010

Table 2: Water Contents, Radionuclide Contents

Laboratory Code	Water content %	U(ppm) from ^{234}Th	U(ppm) from ^{226}Ra, ^{214}Pb, ^{214}Bi	U(ppm) from ^{210}Pb	Th(ppm) From ^{208}Tl ^{212}Pb ^{228}Ac	K%	Field Code
[redacted]							
WLL896	21.75	3.20±0.37	3.28±0.23	2.77±0.29	13.14±0.18	2.07±0.05	DN-T6-2010
[redacted]							
WLL898	26.20	3.85±0.37	2.93±0.21	2.61±0.28	12.40±0.18	2.02±0.05	DN-T2-2010
WLL899	23.00	2.89±0.35	2.39±0.21	2.18±0.28	11.69±0.17	1.94±0.05	DN-T3-2010
WLL900	12.20	2.80±0.18	2.47±0.11	2.05±0.13	11.14±0.12	2.15±0.04	DN-WW1-2010
WLL901	19.75	2.68±0.33	3.26±0.20	2.51±0.27	12.28±0.17	2.23±0.05	DN-WE1-2010

Table 3: a-Values, Dose Rates, Equivalent Doses and Luminescence Dating Ages

Laboratory Code	a-value	De(Gy)	Dose rate(Gy/ka)	OSL age(ka)	Field Code
WLL896	0.055±0.002	23.78±1.48	4.00±0.11	**5.9±0.4**	DN-T6-2010
WLL898	0.069±0.012	42.97±4.92	3.78±0.17	**11.4±1.4**	DN-T2-2010
WLL899	0.077±0.009	38.70±3.52	3.67±0.13	**10.5±1.0**	DN-T3-2010
WLL900	0.052±0.018	121.43±6.32	3.99±0.20	**30.5±2.2**	DN-WW1-2010
WLL901	0.062±0.008	225.72±15.57	4.03±0.16	**56.0±4.4**	DN-WE1-2010

4. REFERENCES

Adamiec, G. & Aitken, M. 1998: Dose- rate conversion factors: update. Ancient TL, Vol.16, No.2, 37-50

Murry, A.S. & Wintle, A.G. 2000: Luminescence dating of quartz using an improved single aliquot regenerative dose protocol. Radiation Measurements 32, 57-73.

Prescott, J.R. & Hutton, J.T. 1994: Cosmic ray contributions to dose rates for luminescence and ESR dating: Large depths and long-term time variations. Radiation Measurements. Vol.23,Nos.2/3, 497-500.

2. Accelerator Mass Spectrometry Result

RAFTER
GNS SCIENCE

Accelerator Mass Spectrometry Result

This result for the sample submitted is for the exclusive use of the submitter.
All liability whatsoever to any third party is excluded.

NZA	**34441**
R	32468
Job No	102241
Measured	07-Jul-10
TW No	2525
Issued	09-Jul-10

Sample ID	DN-MN1-2010
Description	Charcoal
Fraction Dated	treated charcoal
Submitter	Mark Quigley Geological Sciences, University of Canterbury

* **Radiocarbon Age**		**5399 ± 20 BP**	$\delta^{13}C$ =	-24.3 ‰	
** **Per cent modern** =	50.69 ± 0.13	$\delta^{14}C$ =	-492.3 ± 1.3 ‰	$\Delta^{14}C$ =	-493.1 ± 1.3 ‰

* Reported age is the conventional radiocarbon age before present (BP)
** Per cent modern means absolute per cent modern relative to the NBS oxalic acid standard (HOxI) corrected for decay since 1950.
Age, $\Delta^{14}C$, $\delta^{14}C$ and absolute per cent modern are as defined by Stuiver Polach, Radiocarbon 19:355-363 (1977)

Sample Treatment Details

Sample consisted of wet, dark yellowish-brown (Munsell 10YR 4/4) soil with charcoal. Microscopic exam revealed black charcoal with small amount of yellow-brown soil. Charcoal has visible vascular structure. Picked out lumps of charcoal with tweezers. Washed them in ultrasonic bath, rinsed through sieve. Dried in vacuum oven. Ground in mortar and pestle. Treated with acid / alkali /acid process. Dried in vacuum oven.

Stored remainder

Comments

The reported errors comprise statistical errors in sample and standard determinations, combined in quadrature with a system error component based on the analysis of an ongoing series of measurements on an oxalic acid standard.
For the present result the system error component is conservatively estimated as 0% (= ± 0 radiocarbon years).

National Isotope Centre, Institute of Geological and Nuclear Sciences Ltd (GNS Science)
PO Box 31-312 Lower Hutt, New Zealand Fax +64 4 570 4657 Phone +64 4 570 4644
www.RafterRadiocarbon.co.nz

RAFTER RADIOCARBON LABORATORY

R32468

INSTITUTE OF GEOLOGICAL AND NUCLEAR SCIENCES LTD.
PO Box 31312, Lower Hutt, New Zealand
Phone (+64 4) 570 4671, Fax (+64 4) 570 4657

RADIOCARBON CALIBRATION REPORT

NZA 34441 CONVENTIONAL RADIOCARBON AGE 5399 ± 20 years BP

Southern Hemisphere Atmospheric data from McCormac et al (2004);
FG McCormac, AG Hogg, PG Blackwell, CE Buck, TFG Higham, and PJ Reimer (2004)
Radiocarbon 46, 1087-1092

CALIBRATED AGE in terms of confidence intervals (Smoothing parameter: 0, Offset: 0)

68% confidence interval is 4244 BC to 4223 BC 6193 BP to 6172 BP (11.4% of area)
plus 4205 BC to 4160 BC 6154 BP to 6109 BP (26.5% of area)
plus 4129 BC to 4069 BC 6078 BP to 6018 BP (30.1% of area)

95% confidence interval is 4315 BC to 4296 BC 6264 BP to 6245 BP (4.3% of area)
plus 4260 BC to 4050 BC 6209 BP to 5999 BP (90.6% of area)

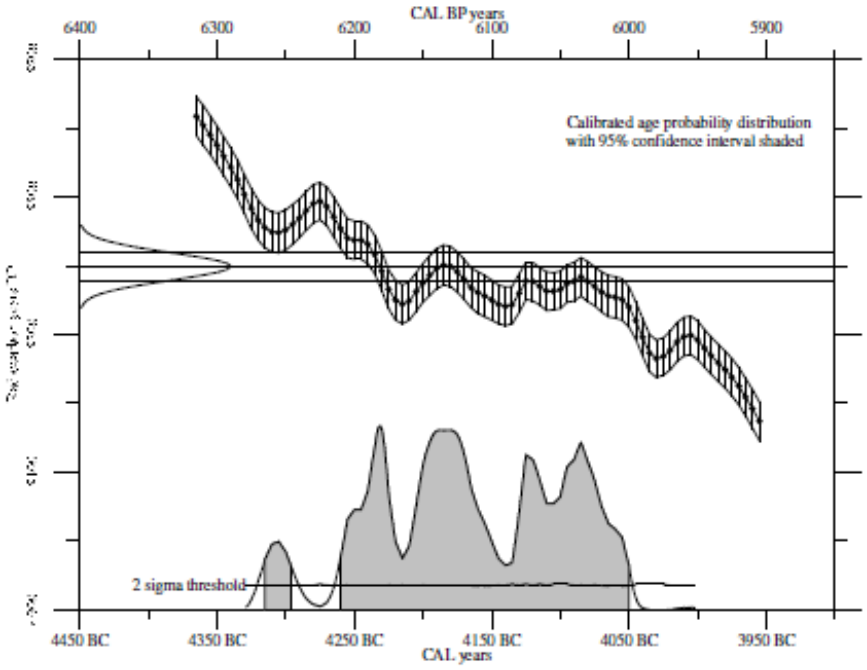

RAFTER
GNS SCIENCE

NZA	**37130**
R	32726
Job No	107252
Measured	26-Jul-11
TW No	2632
Issued	29-Jul-11

Accelerator Mass Spectrometry Result

Sample ID	EF-DN-01
Description	Charcoal
Fraction Dated	treated charcoal
Submitter	Mark Quigley Geological Sciences, University of Canterbury

* **Radiocarbon Age**		**778 ± 15 BP**		$\delta^{13}C$ =	-26.8 ‰
** **Per cent modern** =	90.11 ± 0.18	$\delta^{14}C$ =	-102.3 ± 1.8 ‰	$\Delta^{14}C$ =	-98.9 ± 1.8 ‰

* Reported age is the conventional radiocarbon age before present (BP)

** Per cent modern means absolute per cent modern relative to the NBS oxalic acid standard (HOxI) corrected for decay since 1950.

Age, $\Delta^{14}C$, $\delta^{14}C$ and absolute per cent modern are as defined by Stuiver & Polach, Radiocarbon 19:355-363 (1977)

Sample Treatment Details

Sample consisted of many fragments of charcoal along with soil. Examination under the microscope showed black shiny charcoal, with a few rootlets attached and some soil. Charcoal has visible vascular structure and is very light and brittle. Some roots throughout the sample. Used scalpel to remove attached rootlets and soil from charcoal. Crushed in mortar and pestle. Treated with acid/alkali/acid washes. Solution turned amber in alkali wash. Dried. Final product was black fine powder. Total weight loss in sample was 78% after treatment.

Stored remainder

Comments

The reported errors comprise statistical errors in sample and standard determinations, combined in quadrature with a system error component based on the analysis of an ongoing series of measurements on an oxalic acid standard.
For the present result the system error component is conservatively estimated as 0% (= ± 0 radiocarbon years).

National Isotope Centre, Institute of Geological and Nuclear Sciences Ltd (GNS Science)
PO Box 31-312 Lower Hutt, New Zealand Fax +64 4 570 4657 Phone +64 4 570 4644
www.RafterRadiocarbon.co.nz

RAFTER RADIOCARBON LABORATORY

R32726

INSTITUTE OF GEOLOGICAL AND NUCLEAR SCIENCES LTD.
PO Box 31312, Lower Hutt, New Zealand
Phone (+64 4) 570 4671, Fax (+64 4) 570 4657

RADIOCARBON CALIBRATION REPORT

NZA 37130 CONVENTIONAL RADIOCARBON AGE 778 ± 15 years BP

Southern Hemisphere Atmospheric data from McCormac et al (2004);
FG McCormac, AG Hogg, PG Blackwell, CE Buck, TFG Higham, and PJ Reimer (2004)
Radiocarbon 46, 1087-1092

CALIBRATED AGE in terms of confidence intervals (Smoothing parameter: 0, Offset: 0)

68% confidence interval is 1273 AD to 1286 AD	677 BP to 664 BP (69.1% of area)
95% confidence interval is 1234 AD to 1245 AD	716 BP to 705 BP (4.8% of area)
plus 1265 AD to 1294 AD	685 BP to 656 BP (90.2% of area)